AB INITIO CALCULATIONS OF ORGANIC MOLECULES; SUBSTITUTED ETHYLENES, AZOLES AND MEROCYANINE DYES

by

Allan Beveridge

Thesis Presented for the

Degree of Doctor of Philosophy

University of Edinburgh

November 1985

Acknowledgements

I would like to thank Dr. M.H. Palmer for his guidance during the course of this work. I would also like to thank Dr. G.A. Chamberlain (Shell Research, Thornton) for supplying the experimental results for Chapters 2 and 3 and supervising the work in Chapter 3.

I am grateful to Moira Bain and Annette Roper, who typed the bulk of this thesis, and Terry Jones who drew several of the figures in the text. I am especially grateful to Anne Grabinar (Wellcome Research) who corrected countless typing errors and also typed the text for Chapter 5.

Finally I would like to thank Wellcome Research for providing photocopying facilities.

Postgraduate Courses Attended

1.	Scientific German	(2 units)	German Department
2.	Fortran Programming Course	(2 units)	ERCC
3.	Pascal Programming Course	(2 units)	ERCC
4.	The Chemistry of Photographic Processes	(1 unit)	Dr. L.A. Williams
5.	Fourier Transform IR Spectroscopy	(1 unit)	Dr. S. Cradock
6.	Recent Advances in Electrochemistry	(1 unit)	Dr. Heath
7.	Current Topics in Organic Chemistry	(1 unit)	Dr. Tennant

Abstract

A correlation between photovoltaic activity and ionisation potential has been observed for merocyanine dyes. Ab initio SCF calculations using minimal basis sets have been performed on a range of merocyanines to investigate the effects of molecular tailoring on electronic structure.

A semi-empirical model based on the Onsager theory of geminate recombination has been used to predict the Applied Voltage/Photocurrent characteristics of some merocyanine solar cells. The agreement between theory and experiment was generally very good.

The electronic spectra of ethylene and some substituted ethylenes have been investigated using ab initio CI calculations. The basis set was relatively small; it was of double zeta quality supplemented with a set of diffuse Rydberg orbitals. Good general agreement between theory and experiment was obtained for most Rydberg states but the V state was poorly represented.

The photo-electron spectra of the azoles has been assigned with the aid of ab initio CI calculations. The calculated ionisation potentials were generally good but the present theoretical procedure invariably underestimated the IP for nitrogen lone pairs. Several hitherto undetected 'shake up' states were also predicted.

CONTENTS

CHAPTER I

Theoretical Background to Ab Initio Calculations

1) Historical Background

Historically, the development of modern quantum mechanics is indebted to the contributions of Planck and Einstein. Classical Physics had successfully explained most scientific phenomena, but the inability of the Rayleigh-Jeans law to predict the observed intensity distribution for black body radiation led Planck to propose the relation $E = h\upsilon$, and derive a formula which accounted for the experimental observations and avoided the so called 'ultra violet catastrophe'. Although Planck was unable to offer a theoretical justification for his constant, h, Einstein later demonstrated that the Planck relation, $E = h\upsilon$, could also be used to explain the photo-electric effect. The successes of Planck and Einstein gave birth to Modern Physics and led to the universal acceptance of the quantisation of energy and the wave/particle duality of matter.

Niels Bohr then combined the concept of quantisation with Rutherford's experimental picture of the atom to produce the first quantum mechanical model for the Hydrogen atom. Bohr envisaged the electron in planar orbit around the nucleus and restrained the possible values of the angular momentum of the electron, integrated around a circular path, to integral multiples of Planck's constant. Bohr then assumed that radiation was absorbed or emitted only when the electron changed orbits. By setting the energy change involved equal to $h\upsilon$ he derived the equation

$$\frac{1}{\lambda} = R\left(\frac{1}{n^2} - \frac{1}{m^2}\right)$$

where $R = 109737\ cm^{-1}$ (the Rydberg constant). This model then enabled Bohr to correctly predict the absorption and emission spectra of Hydrogen. Bohr's model survived over 10 years but was never successfully extended to predict the spectrum of Helium.

The failures of Bohr's model indicated the need for further refinement. In 1925 Heisenberg proposed his famous uncertainty principle, which stated that experimental observables such as momentum and position could not be determined independently. And in 1926 Schrödinger derived the Schrödinger equation for the hydrogen atom and solved it exactly. Molecular orbital theory was derived independently by Hund and Mulliken in the late 1920's and used to interpret the spectra of simple molecules. The foundations of molecular quantum mechanics had now been firmly established.

The Schrödinger Equation

The Schrödinger equation is central to molecular quantum mechanics, and in particular to the exact solutions one obtains when it is solved for hydrogenic systems.

The classical equation of motion of a particle in a potential is

$$E = \frac{p^2}{2m} + V(r) \tag{1}$$

To transform the above equation into its corresponding quantum mechanical equivalent one must:

i) replace E with the operator $ih\left(\frac{\partial}{\partial t}\right)$

and replace p with the operator $-ih\nabla$ where ∇ is the Laplace operator.

ii) apply the resulting operator equation to a wave function Ψ and solve for it.

Applying i) and ii) to equation (1) yields the Schrödinger equation

$$i\hbar \frac{\partial \Psi}{\partial t} = \frac{-\hbar^2}{2m}\nabla^2\Psi + V(r)\Psi \quad ; \quad \text{where } \hbar = h/2\pi \tag{2}$$

For the hydrogen atom the potential is given by Coulomb's Law:

$$V(r) = \frac{-e^2}{r} \tag{3}$$

Substituting this result into equation (2) yields

$$i\hbar \frac{\partial \Psi}{\partial t} = \left[\frac{-\hbar^2}{2m}\nabla^2 - \frac{e^2}{r}\right]\Psi \tag{4}$$

This is the Schrödinger equation for the hydrogen atom, which when solved produces complete agreement between the experimental and calculated energy levels.

Equation (4) can be rewritten

$$H\Psi = i\hbar \frac{\partial}{\partial t} \Psi \tag{5}$$

where $H = -\frac{\hbar^2}{2m}\nabla^2 - \frac{e^2}{r}$, is the Hamiltonion for this system.

Equation (5) is a partial differential equation in four variables, the three position coordinates x,y,z of the particles, and the time, and is separable whenever the potential energy function V is time independent. In such a case, to separate the time-dependent part of the differential equation, Ψ is expressed in the form

$$\Psi = u(x,y,z)v(t) \tag{6}$$

Substituting this into equation (2) and dividing through by $u(x,y,z)v(t)$ yields

$$\frac{1}{u(x,y,z)}\left[-\frac{\hbar^2}{2m}\nabla^2 + v(x,y,z)\right]u(x,y,z) = i\hbar \frac{1}{v(t)}\frac{\partial}{\partial t} v(t) \tag{7}$$

the left hand side of equation (7) is a function of the coordinates x,y and z, and the right hand side is a function only of the time t. Consequently, since these four variable are independent, each side of eqn. (7) must be equal to a constant, which shall be designated E, where E has the dimensions of energy.

Hence one may write

$$\frac{i\hbar}{\Psi}\frac{d\Psi}{dt} = E \text{ or } \Psi = \Psi_o e^{-iEt/\hbar} \tag{8}$$

and

$$Eu(r) = -\frac{\hbar^2}{2m}\nabla^2 u(r) + v(r)u(r) \tag{9}$$

Eqn. (9) is the time independent Schrödinger equation, and is more commonly written

$$H\Psi = E\Psi \tag{10}$$

where H is the Hamiltonian operator and the eigenvalues E, are the possible energy values of the system.

Analytical Solutions to the Schrödinger Eqn. of the H atom

The 3 dimensional Schrödinger eqn. for the H atom is

$$\left\{ \frac{\partial^2}{\partial x^2} + \frac{\partial^2}{\partial y^2} + \frac{\partial^2}{\partial z^2} \right\} \Psi = \frac{-8\pi^2 \mu}{h^2} (E-V) \Psi \qquad (10a)$$

where μ is the reduced mass of the system. Since an atom is a centrosymmetric system, it is much more convenient to represent the motion of the electrons about the nucleus by spherical polar coordinates, centred on the nucleus, than by cartesian coordinates.

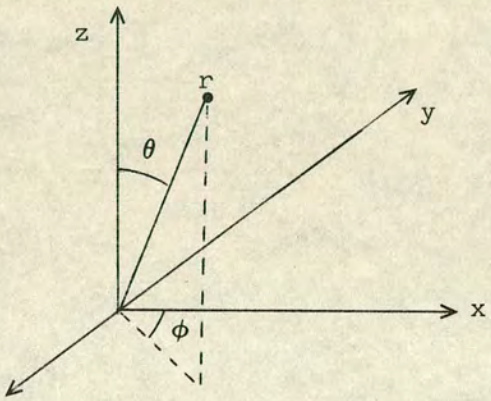

Figure 1

The cartesian coordinates of a point having polar coordinates r, θ and ϕ are given by

$x = r\sin\theta\cos\phi$

$y = r\sin\theta\sin\phi$

$z = r\cos\theta$

Equation (10) can be rewritten

$$\frac{1}{r^2} \frac{\partial}{\partial r} \left(r^2 \frac{\partial \Psi}{\partial r} \right) + \frac{1}{r^2 \sin^2\theta} \frac{\partial^2 \Psi}{\partial \phi^2} + \frac{1}{r^2 \sin^2\theta} \frac{\partial}{\partial \theta} \left(\sin\theta \frac{\partial \Psi}{\partial \theta} \right)$$

$$= \frac{-8\pi^2 \mu}{h^2} (E-V) \Psi \qquad (11)$$

Thus the Schrödinger equation can be separated into parts, each dependent on only one of the independent coordinates, and it is therefore possible to express the Schrödinger equation as a product of three functions: R(r) depending only on r; $\Theta(\theta)$ depending only on θ; and $\Phi(\phi)$ depending only on ϕ.

$$\Psi = (r, \theta, \phi) = R(r)\,\Theta(\theta)\,\Phi(\phi) \tag{12}$$

Substituting this into equation (11) produces

$$\frac{1}{r^2}\frac{d}{dr}\left(r^2\frac{dR}{dr}\right)\Theta\Phi + \frac{1}{r^2\sin^2\theta}\frac{d^2\Phi}{d\phi^2}\,R\,\Theta$$

$$+ \frac{1}{r^2\sin^2\theta}\frac{d}{d\theta}\left(\sin\theta\frac{d\Theta}{d\theta}\right)R\Phi + \frac{8\pi^2\mu}{h^2}[E-V(r)]\,R\Theta\Phi = 0 \tag{13}$$

Dividing eqn. (13) by $R\Theta\Phi$ yields

$$\frac{1}{R}\left[\frac{1}{r^2}\frac{d}{dr}\left(r^2\frac{dR}{dr}\right)\right] + \frac{1}{\Phi}\left[\frac{1}{r^2\sin^2\theta}\frac{d^2\Phi}{d\phi^2}\right]$$

$$+ \frac{1}{\Theta}\left[\frac{1}{r^2\sin\theta}\frac{d}{d\theta}\left(\sin\theta\frac{d\Theta}{d\theta}\right)\right] + \frac{8\pi^2\mu}{h^2}[E-V(r)] = 0 \tag{14}$$

multiplying by $r^2\sin^2\theta$ yields

$$\frac{\sin^2\theta}{R}\frac{d}{dr}\left(r^2\frac{dR}{dr}\right) + \frac{1}{\Phi}\frac{d^2\Phi}{d\phi^2} + \frac{\sin\theta}{\Theta}\frac{d}{d\theta}\left(\sin\theta\frac{d\Theta}{d\theta}\right)$$

$$+ \frac{8\pi^2\mu r^2\sin^2\theta}{h^2}[E-V(r)] = 0 \tag{15}$$

Now the second term is dependent only upon the variable ϕ, while the remaining terms are independent of ϕ, so eqn. (15) can be rearranged

$$\frac{1}{\Phi}\frac{d^2\Phi}{d\phi^2} = \text{terms independent of } \phi \tag{16}$$

Since all the variables are independent of one another eqn. (15) can only be satisfied if the terms independent of ϕ are equal to a

constant. If this constant is called m^2 then

$$\frac{1}{\Phi}\frac{d^2\Phi}{d\phi^2} = -m^2 \tag{17}$$

Substituting this into eqn. (14) yields

$$\frac{1}{R}\left[\frac{1}{r^2}\frac{d}{dr}\left(r^2\frac{dR}{dr}\right)\right]\frac{-m^2}{r^2\sin^2\theta} + \frac{1}{\Theta}\left[\frac{1}{r^2\sin\theta}\frac{d}{d\theta}\left(\sin\theta\frac{d\Theta}{d\theta}\right)\right]$$

$$+ \frac{8\pi^2\mu}{h^2}[E-V(r)] = 0 \tag{18}$$

Multiplying eqn. (18) by r^2 and rearranging yields

$$\frac{1}{R}\frac{d}{dr}\left(r^2\frac{dR}{dr}\right) + \frac{8\pi^2\mu r^2}{h^2}[E-V(r)]$$

$$= \frac{m^2}{\sin^2\theta} - \frac{1}{\Theta}\left[\frac{1}{\sin\theta}\frac{d}{d\theta}\left(\sin\theta\frac{d\Theta}{d\theta}\right)\right] \tag{19}$$

Now the left hand side of eqn. (19) is independent of θ, while the right hand side is independent of r, this can only be true if both sides are equal to a constant. If this constant is labelled β then a set of three second order differential equations are obtained from equations (17) and (19).

$$\frac{d^2\Phi}{d\Phi^2} = -m^2\Phi \tag{20}$$

$$\frac{1}{r^2}\frac{d}{dr}\left(r^2\frac{dR}{dr}\right) + \frac{8\pi^2\mu}{h^2}[E-V(r)]R - \frac{\beta R}{r^2} = 0 \tag{21}$$

$$\frac{1}{\sin\theta}\frac{d}{d\theta}\left(\sin\theta\frac{d\Theta}{d\theta}\right) - \frac{m^2}{\sin^2\theta}\Theta + \beta\Theta = 0 \tag{22}$$

An acceptable solution to eqn. (20) is

$$\Phi = Ne^{\pm im\phi} \tag{23}$$

where N is a normalising factor and m is limited to integer values by the requirement that $\Phi(o) = \Phi(2\pi)$.

N can be evaluated by normalising ϕ

i.e. $\int_0^{2\pi} \Phi^*\Phi d\phi = N^2 \int_0^{2\pi} e^{-im\phi}e^{im\phi}\, d\phi = 1$

Therefore $N = (2\pi)^{-\frac{1}{2}}$ and $\Phi = (2\pi)^{-\frac{1}{2}}e^{\pm im\phi}$ (24)

The solutions for equations (21) and (22), however, are non-trivial.

The formal solutions to eqns. (21) and (22) are in terms of what is known as the associated Legendre polynominal for eqn. (22) and the associated Laguerre polynomial for eqn. (21). The formal expression for the solutions of the Θ function, after normalisation, is

$$\Theta_{lm}(\theta) = \left\{\frac{(2l+1)(l-|m|)!}{2(l+|m|)!}\right\}^{\frac{1}{2}} P_l^{|m|}(\cos\theta) \qquad (25)$$

where $P_l^{|m|}(\cos\theta)$ has the form of an infinite series expansion. It can be shown that for this series to terminate the constant β in eqn. (22) must be equal to $l(l+1)$, where l must be an integer. The $P_l^{|m|}(\cos\theta)$ are the associated Legendre polynomials of degree l and order $|m|$. They are second order differential equations known as Legendre's equations.

Solutions to the radial function take the form

$$R(r) = \exp\left(-\sqrt{\frac{8\pi^2\mu E}{h^2}}\right) F(r) \qquad (26)$$

where $F(r)$ is known as the associated Laguerne polynomial. This again is an infinite series expansion, which for it to terminate, the integer n must be introduced. The final form of the radial function after normalisation is

$$R_{nl} = -\left(\frac{2z}{na_o}\right)^{3/2} \left\{\frac{(n-l-1)!}{2n\{(n+l)!\}^3}\right\}^{\frac{1}{2}} e^{-\rho/2}\rho^l L_{n+l}^{2l+1}(\rho) \qquad (27)$$

where $$a_o = \frac{h^2}{4\pi^2\mu e^2} \qquad (28)$$

$$\rho = \frac{2zr}{na_o} \qquad (29)$$

The integes n,l and m introduced in eqns. (24), (25) and (27) are the quantum numbers describing the atomic system.

Interpretation of the Quantum Numbers

The principle quantum number n, for 1 electron atoms in the absence of any perturbing external influences, is the only quantum number upon which the energy depends. The energy of a hydrogenic system is given by

$$E = \frac{-2\pi^2 \mu Z^2 e^4}{n^2 h^2} \tag{30}$$

where n may take any positive integer value. The azimuthal quantum number l is related to the angular momentum of the electron as it moves about the nucleus. The angular momentum is equal to

$$(h/2\pi)\sqrt{l(l+1)} \tag{31}$$

In one electron systems in the absence of a magnetic field, this offers no contribution to the overall energy of the system. However, electric charges moving in such a manner that there is a net angular momentum associated with them produce a magnetic moment. Therefore, in the presence of an external magnetic field, the interaction of these orbital magnetic moments with the magnetic field will affect the energy. The presence of other electrons, each with their own magnetic moments will also affect the energy through mutual interactions. The allowed values of l run from zero to n -1.

The magnetic quantum number, m, also has no affect on the energy of an isolated one electron atom. It refers to the orientation of the orbital angular momentum toward some external coordinate system. If this coordinate system is referred to an external magnetic field

then differing orientations of the orbital angular momentum will give rise to different energies. Therefore, when atoms are brought near each other in molecules or solids, perturbing fields provided by neighbouring atoms, can split the energies of orbitals of different m values.

The only remaining quantum number is the spin quantum number, m_s, which was introduced for empirical reasons. To explain certain properties of the spectra of the alkali metals and certain properties of other atoms when in a magnetic field, it was necessary to assume the electron itself had an intrinsic angular momentum, giving rise to a magnetic moment. The magnitude of this spin angular momentum is

$$(h/2\pi)\sqrt{S(S+1)} \tag{32}$$

where S is an integer. Since only the orientation with respect to an external field could be observed, the component of this momentum along an axis m_s was chosen as the quantum number rather than S itself. Only two possible values of m_s are allowed, $\pm\frac{1}{2}$.

Eigenfunctions of the Hydrogen Atom

Combining the previous results one can generalise the eigenfunctions of the hydrogen atom as:

$$U_{nlm} = \frac{1}{r} \exp[-(me^2/n\hbar^2)r] \sum_{o}^{n} C_k r^k Y_{lm} \tag{33}$$

where Y_{lm} are the spherical harmonics

$$Y_{lm} = N_{lm} e^{im\phi} P_l^{|m|}(\theta) \tag{34}$$

Table 1 contains all the eigenfunctions for Hydrogen up to n = 4.

Atomic Units

In SI units the Schrödinger equation for the hydrogen atom is

$$\left[-\frac{\hbar^2 \nabla^2}{2m_e} - \frac{e^2}{4\pi\varepsilon_o r} \right] \Psi = E\Psi \qquad (35)$$

Since it is rather cumbersome to work in SI units, one generally works in atomic units. The fundamental quantities of atomic units are:

the mass of the electron	as the unit of mass
the charge of the electron e	as the unit of charge
the Bohr radius a_o	as the unit of length
$e^2/4\pi\varepsilon_o a_o$	as the unit of energy

In these units Planck's constant h equals 2π and $\hbar = 1$, and $8\pi^2 m/h^2 = 2$.

Equation (35) can then be rewritten in the greatly simplified form

$$\left\{ -\tfrac{1}{2}\nabla^2 - \frac{1}{r} \right\} \Psi = E\Psi \qquad (36)$$

Polyelectron Systems and the Born Oppenheimer Approximation

In atomic units, the Hamiltonian for N electrons and M nuclei is

$$H = \sum_{i=1}^{N} \frac{1}{2}\nabla_i^2 - \sum_{A=1}^{M} \frac{1}{2M_A}\nabla_A^2 - \sum_{i=1}^{N}\sum_{A=1}^{M} \frac{Z_A}{r_{iA}} + \sum_{i=1}^{N}\sum_{j>i}^{M} \frac{1}{r_{ij}} + \sum_{A=1}^{M}\sum_{B>A}^{M} \frac{Z_A Z_B}{R_{AB}} \qquad (37)$$

where M_A is the ratio of the mass of nucleus A to the mass of an electron, Z_A is the atomic number of nucleus A, r_{iA} is the average distance between electron i and nucleus A, r_{ij} is the average distance between electrons i and j, and R_{AB} is the distance between nuclei A and B, see fig. (2). The Laplacian operators ∇_i^2 and ∇_A^2 involve differentiation with respect to the coordinates of the ith electron and the Ath nucleus. The first term in eqn. (37) is the operator for the kinetic energy of the electrons; the second term

is the operator for the kinetic energy of the nuclei; the third term represents the coulomb attraction between electrons and nuclei; the fourth and fifth terms represent the repulsion between electrons and between nuclei, respectively.

The problem of solving the Schrödinger equation for a polyelectron system can be simplified by using the Born-Oppenheimer approximation. Since nuclei are much heavier than electrons, they move more slowly. Therefore, to a good approximation, one can consider the electrons in a molecule to be moving in a field of fixed nuclei. Within this approximation, the second term of eqn. (37), the kinetic energy of the nuclei, can be neglected and the last term of eqn. (37), the repulsion between nuclei, can be considered to be a constant. Any constant added to an operator only adds to the operator eigenvalues and has no effect on the operator eigenfunctions. The remaining terms of eqn. (37) are called the electronic Hamiltonian.

$$H_{elec} = -\sum_{i=1}^{N} \frac{1}{2}\nabla_i^2 - \sum_{i=1}^{N}\sum_{A=1}^{M} \frac{Z_A}{r_{iA}} + \sum_{i=1}^{N}\sum_{j>i}^{N} \frac{1}{r_{ij}} \qquad (38)$$

The solution to the Schrödinger equation involving the electronic Hamiltonian

$$H_{elec}\ \Phi_{elec} = E_{elec}\ \Phi_{elec} \qquad (39)$$

is the electronic wave function

$$\Phi_{elec} = \Phi_{elec}\ (\{r_i\};\ \{R_A\}) \qquad (40)$$

which describes the motion of the electrons and depends on the electronic coordinates explicitly, but depends parametrically on the nuclear coordinates, as does the electronic energy,

$$E_{elec} = E_{elec}\ (\{R_A\}) \qquad (41)$$

To calculate the total energy one must also include the nuclear repulsion term.

$$E_{tot} = E_{elec} + \sum_{A=1}^{M} \sum_{B>A}^{M} \frac{Z_A Z_B}{R_{AB}} \qquad (42)$$

The total wavefunction is then calculated as a product of the electronic and nuclear wavefunctions.

$$\Phi(\{r_i\}; \{R_A\}) = \Phi_{elec}(\{r_i\}; \{R_A\}) \Phi_{nucl}(\{R_A\}) \qquad (43)$$

The Pauli Exclusion Principle

The electronic Hamiltonian in eqn. (38) depends only on the spatial coordinates of the electrons. For an electron to be described completely it is necessary to introduce electron spin. This is achieved by introducing two spin functions $\alpha(\omega)$ and $\beta(\omega)$ corresponding to spin up and spin down.

These functions are orthonormal, so that

$$\int \alpha^*(\omega)\alpha(\omega)d\omega = \int \beta^*(\omega)\beta(\omega)d\omega = 1 \qquad (44)$$

or using Dirac's notation

$$\langle\alpha|\alpha\rangle = \langle\beta|\beta\rangle = 1 \qquad (45)$$

and $$\int \alpha^*(\omega)\beta(\omega)d\omega = \int \beta^*(\omega)\alpha(\omega)d\omega = 0 \qquad (46)$$

or $$\langle\alpha|\beta\rangle = \langle\beta|\alpha\rangle = 0 \qquad (47)$$

An electron can thus be described completely in terms of the product of a spatial orbital and one of the above spin functions.

The Pauli Exclusion Principle states that: a many electron wave function must be antisymmetric with respect to interchange of coordinates of any two electrons. Correctly antisymmetrised wave

functions are obtained by using Slater determinants. For the ground state of Helium the Slater determinant is

$$\Psi_{He} = \frac{1}{\sqrt{2}} \begin{vmatrix} \phi_{1s}(1) & \bar{\phi}_{1s}(1) \\ \phi_{1s}(2) & \bar{\phi}_{1s}(2) \end{vmatrix} \qquad (48)$$

where a bar indicates β spin and no bar alpha spin.

Slater determinants are advantageous representations of the wavefunction for two reasons:

i) interchange of any two rows or columns inverts the sign but has no effect on the magnitude of the wavefunction

ii) if any two rows or columns are identical the determinant automatically vanishes and the Pauli Exclusion Principle is therefore satisfied.

The Hydrogen Molecule

From the point of view of theoretical chemistry it is desirable that one should be able to calculate good approximate wave functions for multi-electron molecules, the simplest of which is H_2. In order to attempt this, one has to decide how to describe the molecular orbitals of H_2. LCAO theory assumes that the molecular orbitals can be represented by linear combinations of the original atomic orbitals. Therefore combining the two 1s functions of each H atom produces two new molecular orbitals; one symmetric combination, which is bonding (denoted $1\phi_g$), and one antisymmetric combination, which is antibonding (denoted by $1\phi_u$). The ground state of H_2 can then be described by placing both electrons in the bonding $1\phi_g$ orbital. Therefore the Slater determinant for this system is

$$\Psi = ||1\phi_g \quad 1\bar{\phi}_g|| \qquad (49)$$

which is the shorthand of

$$\frac{1}{\sqrt{2}} \begin{vmatrix} 1\phi_g(1) & 1\bar{\phi}_g(1) \\ 1\phi_g(2) & 1\bar{\phi}_g(2) \end{vmatrix} \tag{50}$$

where the molecular orbital $1\phi_g$ could be expressed in LCAO form as

$$\left(\frac{1}{1+S}\right)\frac{1}{\sqrt{2}} \left(1S_{HA} + 1S_{HB} \right) \tag{51}$$

but quite often the inclusion of more terms would be used to improve accuracy.

The Hamiltonian for the H_2 system is

$$H^e_{1,2} = \left\{ -\frac{1}{2}\nabla_1^2 - \frac{1}{r_{1A}} - \frac{1}{r_{1B}} - \frac{1}{2}\nabla_2^2 - \frac{1}{r_{2A}} - \frac{1}{r_{2B}} + \frac{1}{r_{12}} \right\} \tag{52}$$

where subscripts 1 and 2 refer to the two electrons, and A and B refer to the nuclei.

The first three terms in eqn. (52) are associated with electron 1, and the second three with electron 2, and will hence forth be denoted by the 1-electron operators h_1 and h_2 respectively. The last term, representing the coulomb repulsion between electrons 1 and 2, will be replaced by the two electron operator $g_{1,2}$. Assuming the molecular orbitals are normalised, the energy of the ground state is then given by

$$E = \langle \Psi | h_1 + h_2 + g_{1,2} | \Psi \rangle \tag{53}$$

It should be noted that the Hamiltonian in eqn. (53) contains no spin operators and operates only on spatial functions, but since

$$1\phi_g(1) = 1\phi_g(1)\alpha(1) \tag{54}$$

$$1\bar{\phi}_g(2) = 1\phi_g(2)\beta(2) \tag{55}$$

the spin components can be treated separately.

Therefore,

$$E = \frac{1}{2}\langle [\,1\phi_g(1)1\bar{\phi}_g(2) - 1\phi_g(2)1\bar{\phi}_g(1)\,]^* | h_1 + h_2 + g_{1,2} |$$

$$1\phi_g(1)1\bar{\phi}_g(2) - 1\phi_g(2)1\bar{\phi}_g(1)\rangle \qquad (56)$$

Evaluation of the first term in eqn.(56) yields

$$\langle\Psi|h_1|\Psi\rangle = \frac{1}{2}\int d\tau_1 d\tau_2 [1\phi_g(1)1\bar{\phi}_g(2) - 1\phi_g(2)1\bar{\phi}_g(1)]^* | h_1 | 1\phi_g(1)1\bar{\phi}_g(2)$$

$$- 1\phi_g(2)1\bar{\phi}_g(1) \qquad (57)$$

$$= \frac{1}{2}\int d\tau_1 d\tau_2\; 1\phi_g^*(1)1\bar{\phi}_g^*(2) | h_1 | 1\phi_g(1)1\bar{\phi}_g(2)$$

$$+ \frac{1}{2}\int d\tau_1 d\tau_2 1\phi_g^*(2)1\bar{\phi}_g^*(1) | h_1 | 1\phi_g(2)1\bar{\phi}_g(1)$$

$$- \frac{1}{2}\int d\tau_1 d\tau_2\; 1\phi_g^*(1)1\bar{\phi}_g^*(2) | h_1 | 1\phi_g(2)1\bar{\phi}_g(1)$$

$$- \frac{1}{2}\int d\tau_1 d\tau_2 1\phi_g^*(2)1\bar{\phi}_g^*(1) | h_1 | 1\phi_g(1)1\bar{\phi}_g(2) \qquad (58)$$

The last two terms in eqn. (58) are zero by spin orthogonality. Therefore, after rearranging and noting that h_1 operates only on electron 1,

$$\langle\Psi|h_1|\Psi\rangle = \frac{1}{2}\int d\tau_1 1\phi_g^*(1) | h_1 | 1\phi_g(1) + \frac{1}{2}\int d\tau_1\; 1\bar{\phi}_g^*(1) | h_1 | 1\bar{\phi}_g(1) \qquad (59)$$

The second term of eqn. (56) equals the first term by symmetry, i.e.

$$\langle\Psi|h_1|\Psi\rangle = \langle\Psi|h_2|\Psi\rangle \qquad (60)$$

Integrating $\langle\Psi|g_{1,2}|\Psi\rangle$ yields

$$\frac{1}{2}\int d\tau_1 d\tau_2 [1\phi_g(1)1\bar{\phi}_g(2) - 1\phi_g(2)1\bar{\phi}_g(1)]^* | r_{12}^{-1} | 1\phi_g(1)1\bar{\phi}_g(2) - 1\phi_g(2)1\bar{\phi}_g(1) \qquad (61)$$

$$= \frac{1}{2}\int d\tau_1 d\tau_2 1\phi_g^*(1)\; 1\bar{\phi}_g^*(2) | r_{12}^{-1} | 1\phi_g(1)1\bar{\phi}_g(2) + \frac{1}{2}\int d\tau_1 d\tau_2 1\phi_g^*(2)1\bar{\phi}_g^*(1) | r_{12}^{-1} | 1\phi_g(2)1\bar{\phi}_g(1$$

$$- \frac{1}{2}\int d\tau_1 d\tau_2 1\phi_g^*(1)1\bar{\phi}_g^*(2) | r_{12}^{-1} | 1\phi_g(2)1\bar{\phi}_g(1) - \frac{1}{2}\int d\tau_1 d\tau_2 1\phi_g^*(2)1\bar{\phi}_g^*(1) | r_{12}^{-1} | 1\phi_g(1)1\bar{\phi}_g(2)$$

(62)

since $r_{12}^{-1} = r_{21}^{-1}$, the dummy variables of integration can be interchanged in eqn. (62) showing that the first and second terms are equal, as are the third and fourth, i.e.

$$\langle\Psi|g_{1,2}|\Psi\rangle = \int d\tau_1 d\tau_2 1\phi_g^*(1)1\bar{\phi}_g^*(2)|r_{12}^{-1}|1\phi_g(1)1\bar{\phi}_g(2) \qquad (63)$$

$$- \int d\tau_1 d\tau_2 1\phi_g^*(1)\ 1\bar{\phi}_g^*(2)|r_{12}^{-1}|1\phi_g(2)1\bar{\phi}_g(1)$$

The last term in eqn. (63) is zero by spin orthogonality therefore

$$\langle\Psi|g_{1,2}|\Psi\rangle = \int d\tau_1 d\tau_2 1\phi g(1)1\bar{\phi}g(2)|r_{12}^{-1}|1\phi g(2)1\bar{\phi}g(1) \qquad (63a)$$

and represents the coulombic repulsion between two electrons.

The ground state energy for H_2 is then given by

$$E = 2\langle\Psi\ |h_1|\Psi\rangle \quad + \quad \langle\Psi|g_{1,2}|\Psi\rangle \qquad (64)$$

$$E = 2\varepsilon_{1\phi g} + J_{1\phi g 1\bar{\phi} g} \qquad (65)$$

where J is the coulomb repulsion term.

Triplet H_2

The ground state of H_2 has the configuration $1\phi g^2$, if one of these electrons is excited to the $1\phi_u$ orbital and the two electrons have identical spin the triplet state of H_2 is produced. The Slater determinant for triplet H_2 is

$$\Psi = ||1\phi_g 1\phi_u|| \qquad (66)$$

The energy E is then given by

$$E=\frac{1}{2}\langle 1\phi_g(1)1\phi_u(2)-1\phi_g(2)1\phi_u(1)|\ h_1+h_2+r_{12}^{-1}|1\phi_g(1)1\phi_u(2)-1\phi_g(2)1\phi_u(1)\rangle \qquad (67)$$

This expression reduces to the same form as that given already for the ground state of H_2 with the exception that an additional term now arises, known as the exchange integral K, where

$$K_{1\phi_g 1\phi_u} = \int d\tau_1 d\tau_2 1\phi_g^*(1)1\phi_u^*(2)|r_{12}^{-1}|1\phi_g(1)1\phi_u(2) \qquad (68)$$

The complete energy is then given by

$$E = \varepsilon_{1\phi g} + \varepsilon_{1\phi u} + J_{1\phi g 1\phi u} - K_{1\phi g 1\phi u} \qquad (69)$$

The exchange integral, K, has no classical analogue, it is a product of the mathematics of quantum mechanics. The exchange integral can be considered to be an attractive interaction between electrons of the same spin.

The general mathematical definitions of coulomb and exchange integrals are as follows

$$J_{ij} = \int d\tau_1 d\tau_2 \phi_i^*(1)\phi_i(1) r_{12}^{-1} \phi_j^*(2)\phi_j(2) \qquad (70)$$

$$K_{ij} = \int d\tau_1 d\tau_2 \phi_i^*(1)\phi_j(1) r_{12}^{-1} \phi_j^*(2)\phi_i(2) \qquad (71)$$

The Variation Principle

Central to molecular quantum mechanics is the variation principle, which states that the energy evaluated from an approximate wave function will always be greater than the lowest eigenvalue of the Hamiltonian i.e. if Ψ is an approximate normalised wavefunction then

$$\langle \Psi | H | \Psi \rangle \geq E_o \qquad (72)$$

Proof

Given the operator H, there exists an infinite set of exact solutions to the Schrödinger equation.

$$H|\Phi_\alpha\rangle = E_\alpha |\Phi_\alpha\rangle \qquad \alpha = 0,1,2... \qquad (73)$$

where $E_o \leq E_1 \leq E_2 \leq ..... \leq E_\alpha \leq ...$

and the eigenvalues E_α are real and the corresponding eigenfunctions are orthonormal

$$\langle \Phi_\alpha | \Phi_\beta \rangle = \delta_{\alpha\beta} \qquad (74)$$

multiplying eqn. (73) by $\langle \Phi_\beta |$ on the left yields

$$\langle \Phi_\beta | H | \Phi_\alpha \rangle = E_\alpha \delta_{\alpha\beta} \qquad (75)$$

If the eigenfunctions of H form a complete set, then any function $|\Phi>$ that satisfies the same boundary conditions as the set $\{|\Phi_\alpha>\}$ can be written as a linear combination of $|\Phi_\alpha>$'s i.e.

$$|\Phi> = \sum_\alpha |\Phi_\alpha> C_\alpha = \sum_\alpha \Phi_\alpha <\Phi_\alpha|\Phi> \tag{76}$$

and

$$<\Phi| = \sum_\alpha C^*_\alpha <\Phi_\alpha| = \sum_\alpha <\Phi|\Phi_\alpha><\Phi_\alpha| \tag{77}$$

Then using eqns. (75, 76, 77) yields

$$<\Phi|H|\Phi> = \sum_{\alpha\beta} <\Phi|\Phi_\alpha><\Phi_\alpha|H|\Phi_\beta><\Phi_\beta|\Phi> = \sum_\alpha E_\alpha |<\Phi_\alpha|\Phi>|^2 \tag{78}$$

Finally since $E_\alpha \geq E_o$ for all α

$$<\Phi|H|\Phi> \geq \sum_\alpha E_o |<\Phi_\alpha|\Phi>|^2 = E_o \sum_\alpha |<\Phi_\alpha|\Phi>|^2 = E_o \tag{79}$$

The Hartree Fock Equations

Extending the previous results for the H_2 ground and triplet states, it can be shown that for a polyatomic molecule the electonic energy is a sum of one electron, coulomb and exchange energy terms.

$$E = \sum_i^N [\phi_i|h|\phi_i] + \frac{1}{2}\sum_{i=1}^N \sum_{j=1}^N [\phi_i\phi_i|\phi_j\phi_j] - [\phi_i\phi_j|\phi_j\phi_i] \tag{80}$$

where: h is the one electron operator

$$[\phi_i|h|\phi_i] = \int d\tau_1 \phi_i^*(1) h(1) \phi_i(1) \tag{81}$$

$$[\phi_i\phi_i|\phi_j\phi_j] = \int d\tau_1 d\tau_2 \phi_i^*(1)\phi_i(1) r_{12}^{-1} \phi_j^*(2)\phi_j(2) \tag{82}$$

$$[\phi_i\phi_j|\phi_j\phi_i] = \int d\tau_1 d\tau_2 \phi_i^*(1)\phi_j(1) r_{12}^{-1} \phi_j^*(2)\phi_i(2) \tag{83}$$

$E_o = <\Psi_o|H|\Psi_o>$ is a function of the spin orbitals $\{\phi_i\}$, therefore to derive the Hartree-Fock equations one needs to minimise $E_o[\{\phi_i\}]$ with respect to the spin orbitals, subject to the constraint that the spin orbitals remain orthonormal, i.e.

$$\int d\tau_1 \, \phi_i(1)\phi_j(1) = [\phi_i|\phi_j] = \delta_{ij}$$

Therefore the constraints are of the form

$$[\phi_i|\phi_j] - \delta_{ij} = 0 \tag{84}$$

Using Lagrange's method of undetermined multipliers, one needs to minimise

$$L[\{\phi_i\}] = E_o[\{\phi_i\}] - \sum_{i=1}^{N}\sum_{j=1}^{N} \varepsilon_{ji} \left([\phi_i|\phi_j] - \delta_{ij}\right) \tag{85}$$

where E_o, the expectation value of the single determinant $|\Psi_o\rangle$ is given by

$$E_o[\{\phi_i\}] = \sum_{i=1}^{N} [\phi_i|h|\phi_i] + \frac{1}{2}\sum_{i=1}^{N}\sum_{j=1}^{N} [\phi_i\phi_i|\phi_j\phi_j] - [\phi_i\phi_j|\phi_j\phi_i] \tag{86}$$

and the ε_{ji} constitute a set of Lagrange multipliers ($\varepsilon_{ji} = \varepsilon_{ij}^*$)

An infinitesimal change in L is achieved by varying the spin orbitals by a corresponding arbitrary infinitesimal amount, i.e. $\phi_i \rightarrow \phi_i + \delta\phi_i$.

Setting the first variation in L to equal zero,

$$\delta L = \delta E_o - \sum_{i=1}^{N}\sum_{j=1}^{N} \varepsilon_{ji}\, \delta[\phi_i|\phi_j] = 0 \tag{87}$$

$$\delta[\phi_i|\phi_j] = [\delta\phi_i|\phi_j] + [\phi_i|\delta\phi_j] \tag{88}$$

and

$$\begin{aligned}\delta E_o = {} & \sum_{i=1}^{N} [\delta\phi_i|h|\phi_i] + [\phi_i|h|\delta\phi_i] \\ & + \frac{1}{2}\sum_{i=1}^{N}\sum_{j=1}^{N} [\delta\phi_i\phi_i|\phi_j\phi_j] + [\phi_i\delta\phi_i|\phi_j\phi_j] + [\phi_i\phi_i|\delta\phi_j\phi_j] + [\phi_i\phi_i|\phi_j\delta\phi_j] \\ & - \frac{1}{2}\sum_{i=1}^{N}\sum_{j=1}^{N} [\delta\phi_i\phi_j|\phi_j\phi_i] + [\phi_i\delta\phi_j|\phi_j\phi_i] + [\phi_i\phi_j|\delta\phi_j\phi_i] + [\phi_i\phi_j|\phi_j\delta\phi_i]\end{aligned} \tag{89}$$

Also

$$\begin{aligned}\sum_{ij} \varepsilon_{ji}([\delta\phi_i|\phi_j] + [\phi_i|\delta\phi_j]) &= \sum_{ij} \varepsilon_{ji}[\delta\phi_i|\phi_j] + \sum_{ij} \varepsilon_{ij}[\phi_i|\delta\phi_j] \\ &= \sum_{ij} \varepsilon_{ji}[\delta\phi_i|\phi_j] + \sum_{ij} \varepsilon_{ji}^*[\delta\phi_i|\phi_j]^* \\ &= \sum_{ij} \varepsilon_{ji}[\delta\phi_i|\phi_j] + \text{complex conjugate}\end{aligned} \tag{90}$$

Therefore the first variation in L of eqn. (87) is

$$\begin{aligned}\delta L = {} & \sum_{i=1}^{N} [\delta\phi_i|h|\phi_i] + \sum_{i=1}^{N}\sum_{j=1}^{N} [\delta\phi_i\phi_i|\phi_j\phi_j] - [\delta\phi_i\phi_j|\phi_j\phi_i] \\ & - \sum_{i=1}^{N}\sum_{j=1}^{N} \varepsilon_{ji}[\delta\phi_i|\phi_j] + \text{complex conjugate}\end{aligned} \tag{91}$$

If one now defines an exchange operator $K_j(1)$, which operates on a spin orbital $\phi_i(1)$, as

$$K_j(1)\phi_i(1) = [\int d\tau_2 \phi_j^*(2) r_{12}^{-1} \phi_i(2)]\, \phi_j(1) \tag{92}$$

then the corresponding coulomb operator is

$$J_j(1)\phi_i(1) = [\int d\tau_2 \phi_j^*(2) r_{12}^{-1} \phi_j(2)]\, \phi_i(1) \tag{93}$$

and eqn. (91) can be rewritten as

$$dL = \sum_{i=1}^{N} \int d\tau_1 \delta\phi_i^*(1)[h(1)\phi_i(1) + \sum_{i=1}^{N} (J_j(1)-K_j(1))\phi_i(1) - \sum_{j=1}^{N} \varepsilon_{ji}\phi_j(1)] + \text{complex conjugate} \tag{94}$$

since $\delta\phi_i^*(1)$ is arbitrary, it must be the quantity in square brackets which is zero for all i. Therefore

$$[h(1)+\sum_{j=1}^{N} J_j(1)-K_j(1)]\phi_i(1) = \sum_{j=1}^{N} \varepsilon_{ji}\phi_j(1) \quad i = 1,2,\ldots N \tag{95}$$

The quantity in square brackets is generally referred to as the Fock operator; therefore eqn. (95) can be rewritten

$$f|\phi_i\rangle = \sum_{j=1}^{N} \varepsilon_{ji}|\phi_j\rangle \tag{96}$$

The result is not the canonical (standard) eigenvalue form one would normally expect. The reason is that any single determinant wavefunction $|\Psi\rangle$ formed from a set of spin orbitals $\{\phi_i\}$ retains a certain degree of flexibility in the spin orbitals, in that the spin orbitals can be mixed among themselves without changing the expectation value $E_o = \langle\Psi_o|H|\Psi_o\rangle$. In eqn. (96) ϕ_i is transformed into a sum of ϕ_j, it is however, possible to diagonalise this sum. A new set of spin orbitals $\{\phi_i'\}$ can be obtained from an old set $\{\phi_i\}$ by unitary transformation,

$$\phi_i' = \sum_j \phi_j U_{ji} \tag{97}$$

A unitary transformation, which satisfies the relation,

$$U^{\dagger} = U^{-1} \tag{98}$$

is one which preserves the orthonormailty property. That is, if A is a square matrix such that the wavefunction $|\Psi_o>$ is just the normalised determinant of this matrix.

$$|\Psi_o> = (N!)^{-\frac{1}{2}}\det(A) \tag{99}$$

then $A' = AU$ (100)

Therefore, since $\det(AB) = \det(A)\det(B)$ (101)

the determinant of the transformed spin orbitals is related to the determinant of the original spin orbitals by

$$\det(A') = \det(U)\det(A) \tag{102}$$

or

$$|\Psi_o'> = \det(U)|\Psi_o> \tag{103}$$

Because

$$U^{\dagger}U = 1$$

it follows that

$$\det(U^{\dagger}U) = \det(U^{\dagger})\det(U) = (\det(U))^{*}\det(U) = |\det(U)|^2 = 1 \tag{104}$$

Therefore $\det(U) = e^{i\phi}$ (105)

and the transformed single determinant $|\Psi_o'>$ of eqn. (103) can only differ from the original determinant $|\Psi_o>$ by a phase factor.

A unitary transformation also has no effect on the sum of the coulomb operators.

Proof

The transformed sum of the coulomb operators is

$$\sum_i J_i'(1) = \sum_i d\tau_2 \phi_i'^{*}(2) r_{12}^{-1} \phi_i'(2) \tag{106}$$

$$= \sum_{jk} \left[\sum_{i} U^{*}_{ji} U_{ki} \right] \int d\tau_2 \phi^{*}_{j}(2) r_{12}^{-1} \phi_k(2) \tag{107}$$

But $$\sum_{i} U^{*}_{ji} U_{ki} = (UU^{\dagger})_{kj} = \delta_{kj} \tag{108}$$

so that

$$\sum_{i} J_i'(1) = \sum_{j} \int d\tau_2 \phi^{*}_{j}(2) r_{12}^{-1} \phi_j(2) = \sum_{j} J_j(1) \tag{109}$$

In an identical way it is possible to prove that the same relationship is true for the exchange operators.

Therefore the Fock operator is invariant to an arbitrary unitary transformation of the spin orbitals, i.e.

$$f'(1) = f(1) \tag{110}$$

Multiplying eqn. (96) by $\langle \phi_k |$ shows that the Lagrange multipliers are matrix elements of the Fock operator.

$$\langle \phi_k | f | \phi_i \rangle = \sum_{j=1}^{N} \varepsilon_{ji} \langle \phi_k | \phi_j \rangle = \varepsilon_{ki} \tag{111}$$

Therefore

$$\varepsilon'_{ij} = \int d\tau_1 \phi'^{*}_{i}(1)\, f(1) \phi'_j(1) \tag{112}$$

$$= \sum_{kl} U^{*}_{ki} U_{lj} \int d\tau_1 \phi^{*}_{k}(1) f(1) \phi_l(1) \tag{113}$$

$$= \sum_{kl} U^{*}_{ki} \varepsilon_{kl} U_{lj} \tag{114}$$

or in matrix form

$$\varepsilon' = U^{\dagger} \varepsilon U \tag{115}$$

Hence it follows that it is always possible to find a unitary matrix transformation U such that the transformation of eqn. (115) diagonalises ε. There must also exist a set of spin orbitals $\{\phi_i'\}$ for which the matrix of Lagrange multipliers is diagonal.

$$f | \phi_i' \rangle = \varepsilon_i' | \phi_i' \rangle \tag{116}$$

Dropping the primes yields the canonical form of the Hartree-Fock equations

$$f|\phi_i> = \varepsilon_i|\phi_i> \tag{117}$$

Restricted Closed-Shell Hartree Fock: The Roothaan Equations

A restricted set of spin orbitals has the form

$$\phi_i(1) = \phi_i(1)\,\alpha(\omega) \tag{118}$$
$$\bar{\phi}_i(1) = \phi_i(1)\,\beta(\omega)$$

and the closed-shell restricted ground state is

$$|\Psi_o> = |\phi_1\bar{\phi}_1 \cdots\cdots \phi_a\bar{\phi}_a \cdots\cdots \phi_{N/2}\,\bar{\phi}_{N/2}> \tag{119}$$

It can be shown that for a closed-shell ground state wavefunction, composed of restricted spin orbitals, the general spin orbital Fock operator, f, becomes

$$f(1) = h(1) + \sum_i^{N/2} 2J_i - K_i(1) \tag{120}$$

and the closed shell spatial Hartree Fock equation is just

$$f(1)\phi_i(1) = \varepsilon_i\phi_i(1) \tag{121}$$

For the closed-shell determinant, eqn. (119), the energy, E_o, is given by

$$E_o = <\Psi_o|H|\Psi_o> = 2\sum_i [\phi_i|h|\phi_i] + \sum\sum_{ij} 2[\phi_i\phi_i|\phi_j\phi_j] - [\phi_i\phi_j|\phi_j\phi_i]$$

$$= 2\sum_i h_{ii} + \sum\sum_{ij} 2J_{ij} - K_{ij} \tag{122}$$

Now that spin has been eliminated, the calculation of molecular orbitals becomes equivalent to the problem of solving the spatial-integro-differential equation

$$f(1)\phi_i(1) = \varepsilon_i\phi_i(1) \tag{123}$$

Roothaan [1] demonstrated that by introducing a set of known spatial basis functions, the differential equation could be converted to a set of algebraic equations and solved by standard matrix techniques.

Therefore one can use a set of K known basis functions $\{\chi_u(r) \mid u = 1,2,\ldots, K\}$ and expand the unknown molecular orbitals in the linear expansion.

$$\phi_i = \sum_{u=1}^{k} C_{ui}\chi_u \qquad i = 1,2,\ldots, k \tag{124}$$

If the set $\{\chi_u\}$ was complete, this would result in an exact expansion and any complete set $\{\chi_u\}$ could be used. Unfortunately, for practical computational reasons, one is always limited to a finite set of K basis functions. Therefore it is important to choose a basis that will provide, as far as possible an accurate representation of the molecular orbitals $\{\phi_i\}$.

Substituting eqn.(124) into the Hartree Fock equation yields

$$f(1)\Sigma_v C_{vi}\chi_v(1) = \varepsilon_i \Sigma_v C_{vi}\chi_v(1) \tag{125}$$

Multiplying on the left by $\chi_u^*(1)$ and integrating turns the integro-differential equation into a matrix equation.

$$\Sigma_v C_{vi}\int d\tau_1 \chi_u(1) f(1)\chi_v(1) = \varepsilon_i \Sigma_v C_{vi}\int d\tau_1 \chi_u^*(1)\chi_v(1) \tag{126}$$

Eqn. (126) can be rewritten in a simplified matrix form

$$\Sigma_v F_{uv} C_{vi} = \varepsilon_i \Sigma_v S_{uv} C_{vi} \qquad i = 1,2,\ldots.K \tag{127}$$

or

$$FC = SC\varepsilon \quad \text{(the Roothaan Equations)} \tag{128}$$

where S, the overlap matrix, is a K x K Hermitian matrix (generally real and symmetric) and

$$S_{uv} = \int d\tau_1 \chi_u^*(1)\chi_v(1) \tag{129}$$

The Fock matrix, F, is also a K x K Hermitian matrix (generally real and symmetric), the elements being defined by

$$F_{uv} = \int d\tau_1 \chi_u^*(1) f(1) \chi_v(1) \tag{130}$$

C is a K x K square matrix of the expansion coefficients C_{ui} and ε is a diagonal matrix of the orbital energies ε_i.

Practical Considerations for Solving Roothaan's Equations

i) The density matrix

For an electron in a molecular orbital ϕ_i the probability distribution function (charge density) is $|\phi_i(r)|^2$. For a closed shell molecule described by a single determinant wavefunction the total charge density is

$$\rho(r) = 2\sum_{i}^{N/2} |\phi_i(r)|^2 \tag{131}$$

such that $\rho(r)dr$ is the probability of finding an electron (any electron) in dr at r. The integral of this charge density is the total number of electrons,

$$\int dr\rho(r) = 2\sum_{i}^{N/2} \int dr |\phi_i(r)|^2 = 2\sum_{i}^{N/2} 1 = N \tag{132}$$

If eqn. (132) is expanded in terms of the basis functions

$$\begin{aligned}
\rho(r) &= 2\sum_{i}^{N/2} \phi_i^*(r)\phi_i(r) \\
&= 2\sum_{i}^{N/2} \sum_{v} C_{vi}\chi_v^*(r) \sum_{u} C_{ui}\chi_u(r) \\
&= \sum_{uv} [2\sum_{i}^{N/2} C_{ui}C_{vi}^*]\chi_u(r)\chi_v^*(r) \\
&= \sum_{uv} P_{uv}\chi_u(r)\chi_v^*(r)
\end{aligned} \tag{133}$$

where P is the density matrix, such that

$$P_{uv} = 2\sum_{i}^{N/2} C_{ui}C_{vi}^* \tag{134}$$

The matrix P specifies completely the charge density $\rho(r)$ and is directly related to the expansion coefficients C by eqn. (134). Therefore the results of closed-shell Hartree Fock Calculations can be characterised by either the C_{ui} or by the P_{uv}.

ii) The Fock Matrix

The Fock Matrix, F, is the matrix representation of the Fock operator

$$f(1) = h(1) + \sum_{i}^{N/2} 2J_i(1) - K_i(1) \qquad (135)$$

expressed in the basis $\{\chi_u\}$.

$$F_{uv} = \int d\tau_1 \chi_u^*(1) f(1) \chi_v(1)$$

$$= \int d\tau_1 \chi_u^*(1) h(1) \chi_v(1) + \sum_{i}^{N/2} \int d\tau_1 \chi_v^* [2J_i(1) - K_i(1)] \chi_v(1)$$

$$= H_{uv}^{core} + \sum_{i}^{N/2} 2[uv|ii] - [ui|iv] \qquad (136)$$

where $H_{uv}^{core} = \int d\tau_1 \chi_v^*(1) h(1) \chi_v(1)$ (137)

The elements of the core Hamiltonian matrix are integrals involving the one-electron operator h(1), describing the kinetic energy and nuclear attraction of an electron.

$$h(1) = -\frac{1}{2}\nabla_1^2 - \sum_{A} \frac{Z_A}{|r - R_A|} \qquad (138)$$

The core Hamiltonian matrix thus involves kinetic energy integrals of the form

$$T_{uv} = \int d\tau_1 \chi_u^*(1) [-\tfrac{1}{2}\nabla_1^2] \chi_v(1) \qquad (139)$$

and nuclear attraction integrals

$$V_{uv}^{nucl} = \int d\tau_1 \chi_u^*(1) \left(-\sum_{A} \frac{Z_A}{|r_1 - R_A|} \right) \chi_v(1) \qquad (140)$$

$$H_{uv}^{core} = T_{uv} + V_{uv}^{nucl} \qquad (141)$$

Expanding the molecular orbitals in terms of $\{\chi_u\}$, the Fock matrix elements are

$$F_{uv} = H_{uv}^{core} + \sum_{i}^{N/2} \sum_{\lambda\sigma} C_{\lambda i} C_{\sigma i}^{*} \left(2[uv|\sigma\lambda] - [u\lambda|\sigma v]\right)$$

$$= H_{uv}^{core} + \sum_{\lambda\sigma} P_{\lambda\sigma} \left([uv|\sigma\lambda] - \tfrac{1}{2}[u\lambda|\sigma v]\right)$$

$$= H_{uv}^{core} + G_{uv} \qquad (142)$$

Where G_{uv} is the two electron part of the Fock matrix. The core Hamiltonian matrix need only be evaluated once as it remains constant throughout the calculation, but the G matrix depends on P, the density matrix, and a set of two electron integrals. Therefore the Fock matrix can be considered to be a function of the density matrix.

$$F = F(P) \qquad (143)$$

or the expansion coefficients

$$F = F(C) \qquad (144)$$

Therefore,

$$F(C)C = SC\varepsilon \qquad (145)$$

iii) Orthogonalisation of the Basis Functions

The basis functions $\{\chi_u\}$ used in M.O. calculations are normalised but are not orthogonal to each other, and this gives rise to the overlap matrix in Roothaan's equations

$$FC = SC\varepsilon \qquad (146)$$

However it is always possible to find a transformation matrix X (not unitary) such that the basis functions transformed by X form an orthonormal set i.e.

$$\chi_u' = \Sigma X_{vu} \chi_v \qquad (147)$$

then

$$\int d\tau \chi_u'^{*}(1)\chi_v'(1) = \delta_{uv} \tag{148}$$

$$= \int d\tau [\Sigma_\lambda X^{*}_{\lambda u}\chi^{*}_\lambda(1)][\Sigma_\sigma X_{\sigma v}\chi_\sigma(1)] \tag{149}$$

$$= \Sigma\Sigma_{\lambda\sigma} X^{*}_{\lambda u}\int d\tau \chi^{*}_\lambda(1)\chi_\sigma(1)X_{\sigma v} \tag{150}$$

$$= \Sigma\Sigma_{\lambda\sigma} X^{*}_{\lambda u} S_{\lambda\sigma} X_{\sigma v} \tag{151}$$

Eqn. (151) can be rewritten in matrix form

$$X^{\dagger} S\, X \quad = 1 \tag{152}$$

This defines the relation that matrix X must satisfy if the transformed orbitals are to form an orthonormal set.

Since S is Hermitian it can be diagonalised by a unitary matrix U,

$$U^{\dagger} S\, U \quad = \mathbf{s} \tag{153}$$

where s is a diagonal matrix of the eigenvalues of S.

Then if

$$X \equiv S^{-\frac{1}{2}} = U\, \mathbf{s}^{-\frac{1}{2}}\, U^{\dagger} \tag{154}$$

it follows that

$$S^{-\frac{1}{2}}\, S\, S^{-\frac{1}{2}} = S^{0} = 1 \tag{155}$$

Therefore $X = S^{-\frac{1}{2}}$ is a possible orthogonalising transformation,

$$FC = SC\varepsilon \tag{156}$$

substituting $C = XC'$ (157)

$$FXC' = SXC'\varepsilon \tag{158}$$

Multiplying on the left by $X^{\dagger}$ yields

$$(X^{\dagger}FX)C' = (X^{\dagger}SX)C'\varepsilon \tag{159}$$

If $F' = X^{\dagger}FX$ (160)

then, $F'C' = C'\varepsilon$ (161)

These are the transformed Roothaan equations, which can be solved for C' by diagonalising F'. Therefore given C', C can be obtained from eqn. (157), and equations (160) and (161) can be used to solve the Roothaan equations FC = SCE.

The SCF Procedure

Molecular wave functions are generally calculated with the aid of high speed computers using the SCF method.

1. Specify a molecule (nuclear coordinates $\{R_A\}$, atomic numbers $\{Z_A\}$, total number of electrons, and the basis set $\{\chi_u\}$).
2. Calculate all the required integrals, S_{uv}, H_{uv}^{core} and $[uv|\lambda\sigma]$.
3. Diagonalise S, the overlap matrix, and obtain a transformation matrix X.
4. Make a guess for P.
5. Calculate the G matrix of eqn. (142) from the P matrix and the two electron integrals $[uv|\lambda\sigma]$.
6. Form the Fock matrix from $F = H^{core} + G$.
7. Calculate the transformed Fock matrix $F' = X'FX$.
8. Diagonalise F' to obtain C' and ε.
9. Calculate $C = XC'$.
10. Form a new P matrix from C using eqn. (134).
11. Determine whether the energy has converged.

    If the energy has not converged return to step 5.

    If the energy has converged print the wave function. The wave-function can be used to calculate molecular properties such as dipole moment etc.

Expectation Values and Population Analysis

Once a molecular wavefunction has been evaluated it can be used to predict molecular properties such as dipole moment quadropole moment, diamagnetic susceptibility etc. Molecular properties are invariably described by sums of one-electron operators of the general form

$$\tilde{O}_1 = \sum_i^N h(i) \tag{162}$$

where h(i) is not necessarily the core-Hamiltonian, but any operator depending only on the coordinates of a single electron.

Expectation values for such operators will always have the general form

$$\langle \tilde{O}_1 \rangle = \langle \Psi_o | \tilde{O}_1 | \Psi_o \rangle = \sum_i^{N/2} [\phi_i | h | \phi_i] = \sum_{ij} P_{ij} [\phi_i | h | \phi_j] \tag{163}$$

so that in addition to the density matrix, only the set of one electron integrals $[\phi_i | h | \phi_j]$ are needed to calculate expectation values.

(i) Dipole Moment

The classical definition of the dipole moment of a collection of charges q_i with position vectors r_i is

$$\vec{\mu} = \sum_i q_i r_i \tag{164}$$

the corresponding quantum mechanical description for a molecule is

$$\vec{\mu} = \langle \Psi_o | - \sum_{i=1}^N r_i | \Psi_o \rangle + \sum_A Z_A R_A \tag{165}$$

The first term is the quantum mechanical contribution of the electrons and the second term is the classical contribution of the nuclei, of Z_A, to the dipole moment. Therefore eqn. (165) can be rewritten

$$\vec{\mu} = -\sum_i \sum_j P_{ij} [\phi_i | r | \phi_j] + \sum_A Z_A R_A \tag{166}$$

(ii) Mulliken Population Alanysis

The charge density is given by

$$\rho(r) = \sum_{ij}\sum P_{ij}\phi_i(r)\phi_j^*(r) \tag{167}$$

The total no. of electron is given by

$$N = 2\sum_{i}^{N/2} \int dr|\phi_i(r)|^2 \tag{168}$$

substituting the basis expansion of ϕ_i into eqn. (168) yields

$$N = \sum_{ij}\sum P_{ij}S_{ij} = \sum_{i}(PS)_{ii} = \text{tr } PS \tag{169}$$

therefore it is possible to interpret $(PS)_{ii}$ as the electron density associated with χ_i. Assuming the basis functions are centred on the atomic nuclei, summing over all basis function centred on a given nucleus and subtracting the nuclear charge yields the net charge associated with that atom, i.e.

$$q_A = Z_A - \sum_{i\epsilon A}(PS)_{ii} \tag{170}$$

This is called a Mulliken Population Analysis.

Koopmans' Theorum

$$f|\phi_j\rangle = \varepsilon_j|\phi_j\rangle \tag{171}$$

Multiplying eqn. (171) by $\langle\phi_i|$ demonstrates that the matrix representation of the Fock Operator in the basis of spin orbital eigenfunctions is diagonal with diagonal elements equal to the orbital energies.

$$\langle\phi_i|f|\phi_j\rangle = \varepsilon_j\langle\phi_i|\phi_j\rangle = \varepsilon_j\delta_{ij} \tag{172}$$

Since $f(1) = h(1) + \sum_i J_j(1) - K_j(1)$

the orbital energies can be expressed as

$$\varepsilon_i = \langle\phi_i|f|\phi_i\rangle = \langle\phi_i|h + \sum_j (J_j - K_j)|\phi_i\rangle$$

$$= \langle\phi_i|h|\phi_i\rangle + \sum_j \langle\phi_i|J_j|\phi_i\rangle - \langle\phi_i|K_j|\phi_i\rangle$$

$$= h_{ii} + \sum_j [\phi_i\phi_i|\phi_j\phi_j] - [\phi_i\phi_j|\phi_j\phi_i] \qquad (173)$$

The orbital energy ε_i represents the energy of an electron in the spin orbital $|\phi_i\rangle$. This energy represents the kinetic energy and attraction to the nuclei (h_{ii}) plus the coulomb and exchange interactions with each of the remaining electrons in the remaining spin orbitals.

Koopmans' Theorum states that given an N-electron Hartree Fock single determinant $|^N\Psi_o\rangle$ with occupied and virtual spin orbital energies ε_a and ε_r, the ionisation potentials are given by $-\varepsilon_r$ and the electron affinities by $-\varepsilon_a$.

Koopmans' Theorum results in a rather crude approximation to the ionisation potential for two reasons,

i) it neglects the fact that the electron density of the ion would be redistributed, therefore the assumption of Koopmans' theorum that the same set of spin orbitals $\{\phi_i\}$ can be used to describe the neutral and ionised species is invalid.

ii) the SCF procedure treats the inter-electronic interactions in an averaged way. In reality an electron in an atom will have instantaneous interactions with all the other electrons which will not be the same as the average interaction included in the SCF procedure. This neglect of electron correlation introduces another source of error into SCF calculations.

Neglecting the redistribution of electron density results in the prediction of an ionisation energy which is too high, while the neglect of correlation affects produces an ionisation energy which is too low. Therefore these two effects partially cancel one another and Koopmans' Theorum generally yields good qualitative agreement between theory and experimental. The electron affinities predicted by Koopmans' theorum are generally quite bad.

Configuration Interaction

Thr greatest inherent weakness of SCF calculations is the neglect of electron correlation effects. However it is possible to reintroduce electron correlation by a procedure known as configuration interaction.

If $\Phi(x_1)$ is an arbitrary function of a single variable it can be expanded exactly as

$$\Phi(x_1) = \sum_i a_i \phi_i(x_1) \qquad (174)$$

where a_i is an expansion coefficient. In a similar way, one can also expand a function of two variables

$$\Phi(x_1,x_2) = \sum_i a_i(x_2) \phi_i(x_1) \qquad (175)$$

where the expansion coefficients are now functions of x_2. Since $a_i(x_2)$ is itself a function of a single variable it too can be expanded in an analagous manner, i.e.

$$a_i(x_2) = \sum_j b_{ij} \phi_j(x_2) \qquad (176)$$

substituting this result into eqn. (175) yields

$$\Phi(x_1,x_2) = \sum_{ij} b_{ij} \phi_i(x_1) \phi_j(x_2) \qquad (177)$$

If Φ is required to be antisymmetric,

$$\Phi(x_1,x_2) = -\Phi(x_2,x_1) \tag{178}$$

then $b_{ij} = -b_{ji}$ and $b_{ii} = 0$, or

$$\Phi(x_1,x_2) = \sum_{ij>i}\sum b_{ij}[\phi_i(x_1)\phi_j(x_2) - \phi_j(x_1)\phi_i(x_2)]$$

$$= \sum_{ij} 2^{\frac{1}{2}} b_{ij}|\phi_i\phi_j> \tag{179}$$

Therefore an arbitrary antisymmetric function of two variables can be exactly expanded in terms of all unique determinants from a complete set of one-variable functions $\{\phi_i(x)\}$. This argument is easily extended to more than two variables. Therefore the exact function of the ground and excited states of an N-electron problem can be written as a linear combination of all possible N-electron Slater determinants formed from a complete set of spin orbitals $\{\phi_i\}$.

Since all possible determinants can be described by reference to the Hartree Fock determinant, the exact wave function for any state can be written as

$$|\Phi_o> = C_o|\Psi_o> + \sum_{ra} C_a^r|\Psi_a^r> + \sum_{\substack{a<b\\r<s}} C_{ab}^{rs}|\Psi_{ab}^{rs}> + \sum_{\substack{a<b<c\\r<s<t}} C_{abc}^{rst}|\Psi_{abc}^{rst}> + \ldots\ldots \tag{180}$$

where the subscripts a,b,c etc. refer to the spin orbitals from which an electron has been removed and the superscripts r,s,t etc. represent the spin orbitals that the corresponding electron has been excited into.

The correlation energy is defined as the difference between the exact non-relativistic energy of the system, ε_o, and the Hartree Fock energy, E_o, obtained in the limit that the basis set approached completeness.

$$E_{corr} = \varepsilon_o - E_o \tag{181}$$

In order to calculate the correlation energy one must expand the wavefunction as a linear combination of several N-electron Slater determinants as in eqn. (180). This is best illustrated by considering a closed shell singlet ground state. The exact non-relativistic ground state energy is then given by

$$H|\Phi_o\rangle = \varepsilon_o|\Phi_o\rangle \tag{182}$$

Subtracting $E_o|\Phi_o\rangle$ from both sides yields

$$(H-E_o)|\Phi_o\rangle = (\varepsilon_o-E_o)|\Phi_o\rangle = E_{corr}|\Phi_o\rangle \tag{183}$$

multiplying by $\langle\Psi_o|$ produces

$$\langle\Psi_o|H-E_o|\Phi_o\rangle = E_{corr}\langle\Psi_o|\Phi_o\rangle = E_{corr} \tag{184}$$

where use has been made of the fact that $|\Phi_o\rangle$ is an intermediately normalised wave function of the form given by eqn. (180) and therefore $\langle\Psi|\Phi_o\rangle = 1$.

Expanding $|\Phi_o\rangle$ then yields

$$\langle\Phi_o|H-E_o|\Phi_o\rangle = \langle\Psi_o|H-E_o(|\Phi_o\rangle+\sum_{ct} C_c^t|\Psi_c^t\rangle+\sum_{\substack{c<d\\t<u}} C_{cd}^{tu}|\Psi_{cd}^{tu}\rangle+....) \tag{185}$$

To evaluate eqn. (185) one needs to be able to evaluate the matrix elements between symmetry adapted configurations. Tables 2,3 and 4 contain the rules necessary to evaluate such matrix elements. Using these rules eqn. (185) simplifies to

$$E_{corr}=\langle\Psi_o|H-E_o|\Phi_o\rangle = \sum_{\substack{c<d\\t<u}} C_{cd}^{tu}\langle\Psi_o|H|\Psi_{cd}^{tu}\rangle \tag{186}$$

Eqn. 186 indicates that the correlation energy of a ground state singlet wavefunction is determined solely by the coefficients of the matrix elements involving doubly excited states and the ground state. However, this does not mean that only double excitations are needed

for an exact CI description of the ground state. The coefficients $\{C_{ab}^{rs}\}$ are affected by the presence of other excitations. This becomes obvious when eqn. (183) is multiplied by $\langle\Psi_a^r|$ yielding

$$\langle\Psi_a^r|H-E_o|\Phi_o\rangle = E_{corr}\langle\Psi_a^r|\Phi_o\rangle \tag{187}$$

again using the rules given in tables 1,2 and 3 this simplifies to

$$C_a^r E_{corr} = \sum_{ct} C_c^t \langle\Psi_a^r|H-E_o|\Psi_c^t\rangle + \sum_{\substack{c<d\\t<u}} C_{cd}^{tu}\langle\Psi_a^r|H|\Psi_{cd}^{tu}\rangle + \sum_{\substack{c<d<e\\t<u<v}} C_{cde}^{tuv}\langle\Psi_a^r|H|\Psi_{cde}^{tuv}\rangle \tag{188}$$

Hence, the singly excited states interact indirectly with the ground state. If eqn. (183) is repeatedly multiplied by $\langle\Psi_{ab}^{rs}|$, $\langle\Psi_{abc}^{rst}|$ etc., a complete set of equations, which must be solved simultaneously, is produced.

For a completely rigorous CI calculation one must compute the contribution for all possible configurations.

Given a set of 2K one-electron spin orbitals one can construct $\binom{2K}{N}$ different N-electron Slater determinants. For a moderate size molecule the number of possible configurations becomes impossibly large and one needs to reduce the problem to a more viable size. One way of doing this is to consider only the contributions from single and double excitations. For a ground state calculation the contribution to the energy by single excitations is negligible. Therefore to a good approximation the ground state wavefunction can be written as

$$|\Phi_{DCI}\rangle = |\Phi_o\rangle + \sum_{\substack{c<d\\t<u}} C_{cd}^{tu}|\Psi_{cd}^{tu}\rangle \tag{189}$$

The correlation energy is then obtained from

$$(H-E_o)\left(|\Psi_o\rangle + \sum_{\substack{c<d\\t<u}} C_{cd}^{tu}|\Psi_{cd}^{tu}\rangle\right) = E_{corr}\left(|\Psi_o\rangle + \sum_{\substack{c<d\\t<u}} C_{cd}^{tu}|\Psi_{cd}^{tu}\rangle\right) \tag{190}$$

by multiplying successively by $\langle\Psi_o|$ and $\langle\Psi_{ab}^{rs}|$ yielding

$$\sum_{\substack{c<d \\ t<u}} C_{cd}^{tu}\langle\Psi_o|H|\Psi_{cd}^{tu}\rangle = E_{corr} \tag{191}$$

$$\langle\Psi_{ab}^{rs}|H|\Psi_o\rangle + \sum_{\substack{c<d \\ t<u}} C_{cd}^{tu}\langle\Psi_{ab}^{rs}|H-E_o|\Psi_{cd}^{tu}\rangle = C_{ab}^{rs}E_{corr} \tag{192}$$

Defining the matrices

$$(B)_{rasb} = \langle\Psi_{ab}^{rs}|H|\Psi_o\rangle \tag{193}$$

$$(D)_{rasb,tcud} = \langle\Psi_{ab}^{rs}|H-E_o|\Psi_{cd}^{tu}\rangle \tag{194}$$

$$(C)_{rasb} = C_{ab}^{rs} \tag{195}$$

equations (191) and (192) can be rewritten as

$$B^{\dagger}C = E_{corr} \tag{196}$$

$$B + Dc = cE_{corr} \tag{197}$$

or in matrix form

$$\begin{pmatrix} 0 & B^{\dagger} \\ B & D \end{pmatrix} \begin{pmatrix} 1 \\ c \end{pmatrix} = E_{corr} \begin{pmatrix} 1 \\ c \end{pmatrix}$$

The correlation energy is then given by the lowest eigenvalue of the CI matrix.

$$\begin{pmatrix} 0 & B^{\dagger} \\ B & D \end{pmatrix}$$

Even for DCI (CI involving only double excitations) it is invariably not feasible to include all possible double excitations, and therefore to reduce the required computational effort one uses only the most important configurations. Solving eqn. (196) for C produces

$$C = -(D-1E_{corr})^{-1}B \tag{198}$$

then substituting this result into eqn. (197) yields

$$E_{corr} = -B^{\dagger}(D-1E_{corr})^{-1}B \tag{199}$$

Solving this matrix equation for E_{corr} is completely equivalent to finding the lowest eigenvalue of the CI matrix. Since E_{corr} appears on both sides of the equation an iterative procedure must be used. The correlation energy is small compared to the difference between the energy of a doubly excited configuration and E_o (i.e. the diagonal elements of D); therefore one can set $E_{corr} = 0$ on the right hand side of eqn. (199) to obtain the approximation

$$E'_{corr} = -B^{\dagger}D^{-1}B \tag{200}$$

This value can then be used in the right side of eqn. (199) to obtain E''_{corr} and the correlation energy can be found iteratively.

When the matrix D is very large, its inverse cannot be computed and must be simplified. The largest elements of D generally occur on its diagonal, then assuming D is diagonal, its inverse can be computed from.

$$(D^{-1})_{rasb,tcud} = \frac{\delta_{ac}\delta_{bd}\delta_{rt}\delta_{su}}{\langle\Psi^{rs}_{ab}|H-E_o|\Psi^{rs}_{ab}\rangle}$$

the correlation energy can then be approximated as

$$E_{corr} \cong -\sum_{\substack{a<b\\ r<s}} \frac{\langle\Psi_o|H|\Psi^{rs}_{ab}\rangle\langle\Psi^{rs}_{ab}|H|\Psi_o\rangle}{\langle\Psi^{rs}_{ab}|H-E_o|\Psi^{rs}_{ab}\rangle} = \sum_{\substack{a<b\\ r<s}} E_{corr}\begin{pmatrix} rs \\ ab \end{pmatrix} \tag{201}$$

where $E_{corr}\begin{pmatrix} rs \\ ab \end{pmatrix}$ is the contribution of the double excitation $|\Psi^{rs}_{ab}\rangle$ to the approximate correlation energy. Since it can be easily computed, it can be used to identify the most important configurations to be used in the DCI expansion.

Although single excitations contribute negligibly to the energy of a closed shell ground state wave function, they do influence charge distributions and one electron properties such as dipole moments. Single excitations also play the primary role in the calculation of excited electronic states. Most CI computer programs use SDCI (CI involving only singly and doubly excited configurations) coupled with a configuration selection procedure which eliminates all but the most important configurations. The theory for DCI is easily extended to cover SDCI.

Evaluation of Molecular Integrals - Practical Considerations

The molecular orbitals in the SCF procedure are a linear combination of the basis functions which are generally centred on the nuclei

$$\phi_j = \sum_i \chi_i \qquad (202)$$

If one uses hydrogenic type orbitals (Slater type orbitals) for the basis functions problems arise over the evaluation of multicentre integrals of the type

$$\langle \chi_i \chi_j r_{12}^{-1} \chi_k \chi_l \rangle \quad \text{and} \quad \langle \chi_i | h | \chi_j \rangle$$

These basis functions have the general form

$$r^{\mu} \exp(-\zeta r) \times (\text{spherical harmonic})$$

and multicentre integrals involving these functions are difficult to compute.

An alternative approach is to use cartesian gaussian functions, which have the general form

$$x^l y^m z^n e^{-\alpha r^2}$$

where the product $x^l y^m z^n$ represents the angular distribution of the function and the coefficients l, m and n can have any integral value.

Multicentre integrals are then much easier to evaluate by the virtue of the following property: the product of two Gaussians G_a and G_b centred on different points a and b is itself a Guassian function centred at c somewhere on the line joining these two points. Or more specifically

$$G_i(r_A)G_j(r_B) = KG_k(r_C) \tag{203}$$

where: $G_i(r_A)$ is a gaussian centred on the point A and having the parameter α_i. It can also be written as a function of the coordinates of P(x,y,z)

$$G_i(r_A) = \exp\{-\alpha_i[(x-Ax)^2 + (y-Ay)^2 + (z-Az)^2]\} \tag{204}$$

K is a constant given by

$$K = \exp\left(\frac{-\alpha_i\alpha_j}{\alpha_i+\alpha_j}\overline{AB}^2\right) \tag{205}$$

and $$\alpha_k = \alpha_i + \alpha_j \tag{206}$$

$$Cx = \frac{\alpha_i Ax + \alpha_j Bx}{\alpha_i + \alpha_j}; \quad Cy = \frac{\alpha_i Ay + \alpha_j By}{\alpha_i + \alpha_j}; \quad Cz = \frac{\alpha_i Az + \alpha_j Bz}{\alpha_i + \alpha_j} \tag{207}$$

Proof

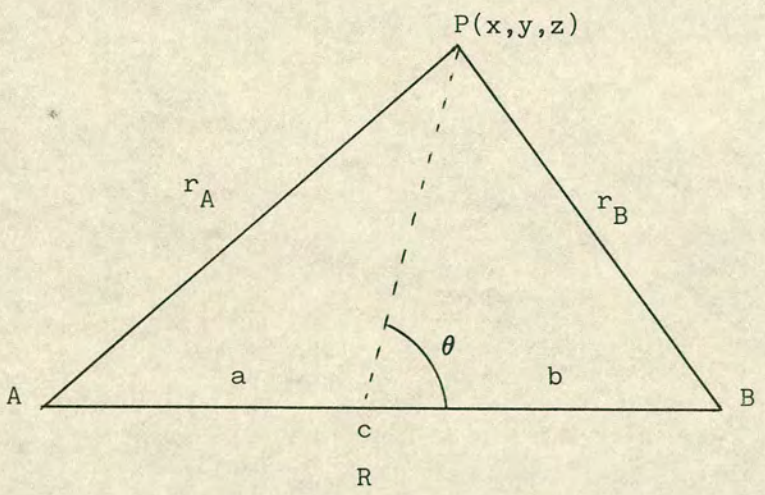

Figure 3 - definition of symbols

If the point C is placed in accordance with eqns. (207) then

$$a = \overline{AC} = \frac{\alpha_i}{\alpha_i + \alpha_j} R \tag{208}$$

$$b = \overline{CB} = \frac{\alpha_i}{\alpha_i + \alpha_j} R \tag{209}$$

where $R = \overline{AB}$.

Using the cosine law

$$r_A^2 = a^2 + r_c^2 + 2ar_c \cos\theta \tag{210}$$

$$r_B^2 = b^2 + r_c^2 - 2br_c \cos\theta \tag{211}$$

$$br_A^2 + ar_B^2 = a^2b + a^2b + (a + b)r_c^2 \tag{212}$$

$$= R(ab + r_c^2) \tag{213}$$

Substituting for a and b from eqns (208) and (209) and multiplying throughout by $(\alpha_i + \alpha_j)/R$, yields

$$\alpha_i R_A^2 + \alpha_j B^2 = \left(\frac{\alpha_i \alpha_j}{\alpha_i + \alpha_j}\right) R^2 + (\alpha_i + \alpha_j) r_c^2$$

from which the theorum follows directly. The use of Gaussians thereby reduces two centre integrals to one centre integrals, and three and four centre integrals to two centre integrals.

The main disadvantage of the Gaussian function is that it does not resemble the form of a real atomic orbital, see figure (4).

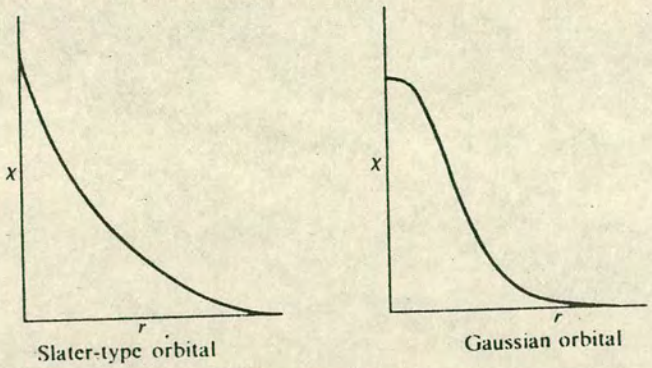

Slater-type orbital Gaussian orbital

Figure (4)

This defect can be overcome by using a linear combination of several Gaussian functions. However, this introduces difficulties in the solution of the Roothaan equations, and furthermore, makes convergence in the SCF procedure more difficult due to the large number of basis functions. However, these difficulties can beovercome, if instead of allowing all the coefficients of the basis function expansion to vary freely, certain coefficients are fixed relative to one another, thus forming groups of 'contracted Gaussians'.

The M.O. is then expressed as

$$\phi_i = \sum_k C_{ik} \gamma_k$$

where γ_k is a small contraction of gaussians of the same type on the same centre

e.g. $\gamma_1 = C_1' \beta_1 + C_2' \beta_2 + C_3 \beta_3'$

This approach is commonly implemented in quantum chemistry.

Table 1

State	n	l	m	u
$1s$	1	0	0	$A_n e^{-x}$
$2s$	2	0	0	$A_n e^{-x}(1-x)$
$2p$	2	1	0	$A_n e^{-x} x \cos\vartheta$
$2p$	2	1	± 1	$A_n \frac{e^{-x}}{\sqrt{2}} x \sin\vartheta e^{\pm i\varphi}$
$3s$	3	0	0	$A_n e^{-x}\left(1 - 2x + \frac{2x^2}{3}\right)$
$3p$	3	1	0	$A_n e^{-x}\sqrt{\frac{2}{3}} x(2-x)\cos\vartheta$
$3p$	3	1	± 1	$A_n e^{-x}\frac{1}{\sqrt{3}} x(2-x)\sin\vartheta e^{\pm i\varphi}$
$3d$	3	2	0	$A_n e^{-x}\frac{1}{3\sqrt{2}} x^2(3\cos^2\vartheta - 1)$
$3d$	3	2	± 1	$A_n e^{-x}\frac{x^2}{\sqrt{3}}\sin\vartheta\cos\vartheta e^{\pm i\varphi}$
$3d$	3	2	± 2	$A_n e^{-x}\frac{1}{2\sqrt{3}} x^2\sin^2\vartheta e^{\pm 2i\varphi}$
$4s$	4	0	0	$A_n e^{-x}\left(1 - 3x + 2x^2 - \frac{x^3}{3}\right)$
$4p$	4	1	0	$A_n e^{-x}\sqrt{5}x\left(1 - x + \frac{x^2}{5}\right)\cos\vartheta$
$4p$	4	1	± 1	$A_n e^{-x}\sqrt{\frac{5}{2}} x\left(1 - x + \frac{x^2}{5}\right)\sin\vartheta e^{\pm i\varphi}$
$4d$	4	2	0	$A_n e^{-x}\frac{1}{2} x^2\left(1 - \frac{x}{3}\right)(3\cos^2\vartheta - 1)$
$4d$	4	2	± 1	$A_n e^{-x}\sqrt{\frac{3}{2}} x^2\left(1 - \frac{x}{3}\right)\sin\vartheta\cos\vartheta e^{\pm i\varphi}$
$4d$	4	2	± 2	$A_n e^{-x}\sqrt{\frac{3}{8}} x^2\left(1 - \frac{x}{3}\right)\sin^2\vartheta e^{\pm 2i\varphi}$
$4f$	4	3	0	$A_n e^{-x}\frac{1}{6\sqrt{5}} x^3\cos\vartheta\,(5\cos^2\vartheta - 3)$
$4f$	4	3	± 1	$A_n e^{-x}\frac{1}{6}\sqrt{\frac{3}{20}} x^3\sin\vartheta\,(5\cos^2\vartheta - 1)e^{\pm i\varphi}$
$4f$	4	3	± 2	$A_n e^{-x}\frac{\sqrt{3}x^3}{6\sqrt{2}}\sin^2\vartheta\cos\vartheta e^{\pm 2i\varphi}$
$4f$	4	3	± 3	$A_n e^{-x}\frac{1}{12} x^3\sin^3\vartheta e^{\pm 3i\varphi}$

$$x = \frac{rme^2}{n\hbar^2} \qquad A_n = \frac{1}{\sqrt{\pi}}\left(\frac{me^2}{n\hbar^2}\right)^{3/2}$$

TABLE 2 MATRIX ELEMENTS BETWEEN DETERMINANTS FOR ONE-ELECTRON OPERATORS IN TERMS OF SPIN ORBITALS.

$\tilde{O}$	$\tilde{O}_1 = \sum_{i=1}^{N} h(i)$
Case 1: $\|K\rangle = \|\ldots mn \ldots\rangle$	$\langle K \|\tilde{O}_1\| K\rangle = \sum_m^N [m\|h\|m] = \sum_m^N \langle m\|h\|m\rangle$
Case 2: $\|K\rangle = \|\ldots mn \ldots\rangle$ $\|L\rangle = \|\ldots pn \ldots\rangle$	$\langle K \|\tilde{O}_1\| L\rangle = [m\|h\|p] = \langle m\|h\|p\rangle$
Case 3: $\|K\rangle = \|\ldots mn \ldots\rangle$ $\|L\rangle = \|\ldots pq \ldots\rangle$	$\langle K \|\tilde{O}_1\| L\rangle = 0$

TABLE 3 MATRIX ELEMENTS BETWEEN DETERMINANTS FOR TWO-ELECTRON OPERATORS IN TERMS OF SPIN ORBITALS

$$\tilde{O} = \sum_{i=1}^{N} \sum_{j>i}^{N} r_{ij}^{-1}$$

Case 1: $|K\rangle = |\ldots mn \ldots\rangle$

$$\langle K|\tilde{O}_2|K\rangle = \frac{1}{2}\sum_m^N \sum_n^N [mn|nn] - [mn|nm] = \frac{1}{2}\sum_m^N \sum_n^N \langle mn||mn\rangle$$

Case 2: $|K\rangle = |\ldots mn \ldots\rangle$

$|L\rangle = |\ldots pn \ldots\rangle$

$$\langle K|\tilde{O}_2|L\rangle = \sum_m^N [mp|nn] - [mn|np] = \sum_n^N \langle mn||pn\rangle$$

Case 3: $|K\rangle = |\ldots mn \ldots\rangle$

$|L\rangle = |\ldots pq \ldots\rangle$

$$\langle K|\tilde{O}_2|L\rangle = [mp|nq] - [mq|np] = \langle mn||pq\rangle$$

TABLE 4 SOME MATRIX ELEMENTS BETWEEN SINGLET SYMMETRY-ADAPTED CONFIGURATIONS CONSTRUCTED FROM REAL ORBITS

SINGLE EXCITATIONS

$$\langle \Psi_o | H | {}^1\Psi_a^r \rangle = 0$$

$$\langle {}^1\Psi_a^r | H - E_o | {}^1\Psi_b^s \rangle = (\varepsilon_r - \varepsilon_a)\delta_{rs}\delta_{ab} - (rs|ba) + 2(ra|bs)$$

DOUBLE EXCITATIONS

$$\langle \Psi_o | H | {}^1\Psi_{aa}^{rr} \rangle = K_{ra}$$

$$\langle \Psi_o | H | {}^1\Psi_{aa}^{rs} \rangle = 2^{\frac{1}{2}}(sa|ra)$$

$$\langle \Psi_o | H | {}^1\Psi_{ab}^{rr} \rangle = 2^{\frac{1}{2}}(rb|ra)$$

$$\langle \Psi_o | H | {}^A\Psi_{ab}^{rs} \rangle = 3^{\frac{1}{2}}((ra|sb) - (rb|sa))$$

$$\langle \Psi_o | H | {}^B\Psi_{ab}^{rs} \rangle = (ra|sb) + (rb|sa)$$

$$\langle {}^1\Psi_{aa}^{rr} | H - E_o | {}^1\Psi_{aa}^{rr} \rangle = 2(\varepsilon_r - \varepsilon_a) + J_{aa} + J_{rr} - 4J_{ra} + 2K_{ra}$$

$$\langle {}^1\Psi_{aa}^{rs} | H - E_o | {}^1\Psi_{aa}^{rs} \rangle = \varepsilon_r + \varepsilon_s - 2\varepsilon_a + J_{aa} + J_{rs} + K_{rs} - 2J_{ra} - 2J_{sa} + K_{sa} + K_{ra}$$

$$\langle {}^1\Psi_{ab}^{rr} | H - E_o | {}^1\Psi_{ab}^{rr} \rangle = 2\varepsilon_r - \varepsilon_a - \varepsilon_b + J_{rr} + J_{ab} + K_{ab} - 2J_{rb} - 2J_{ra} + K_{rb} + K_{ra}$$

$$\langle {}^A\Psi_{ab}^{rs} | H - E_o | {}^A\Psi_{ab}^{rs} \rangle = \varepsilon_r + \varepsilon_s - \varepsilon_a - \varepsilon_b + J_{ab} + J_{rs} - K_{ab} - K_{rs} - J_{sb} - J_{sa} - J_{rb} - J_{ra} + \frac{3}{2}(K_{sb} + K_{sa} + K_{rb} + K_{ra})$$

$$\langle {}^B\Psi_{ab}^{rs} | H - E_o | {}^B\Psi_{ab}^{rs} \rangle = \varepsilon_r + \varepsilon_s - \varepsilon_a - \varepsilon_b + J_{ab} + J_{rs} + K_{ab} + K_{rs} - J_{sb} - J_{sa} - J_{rb} - J_{ra} + \frac{1}{2}(K_{sb} + K_{sa} + K_{rb} + K_{ra})$$

$$\langle {}^A\Psi_{ab}^{rs} | H | {}^B\Psi_{ab}^{rs} \rangle = (3/4)^{\frac{1}{2}}(K_{sb} - K_{sa} - K_{rb} + K_{ra})$$

FIGURE 2

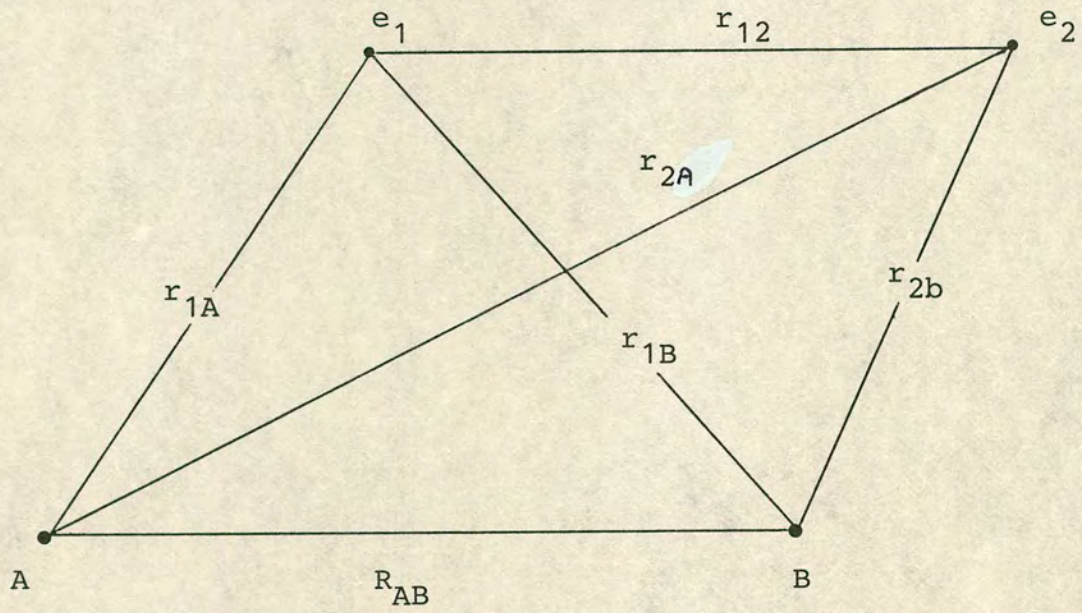

A=B=nucleus

e_1 e_2 electrons

R_{AB} = inter nuclear distance

REFERENCES

1. Roothaan, C., Rev.Mod.Phys., 23, 69 (1951)

2. Cook, D.B., Ab Initio Valence Calculations in Chemistry, Wiley, New York, 1974.

3. Szabo, A., Ostlund, N.S., Modern Quantum Chemistry: Introduction to Advanced Electronic Structure Theory, Macmillan Publishing Co. Inc., New York.

CHAPTER II

A THEORETICAL STUDY OF THE RELATIONSHIP BETWEEN IONISATION POTENTIAL AND PHOTOVOLTAIC ACTIVITY FOR SOME MEROCYANINE DYES

Introduction

During the last decade investigations of the photovoltaic behaviour of organic solar cells have resulted in improving sunlight conversion efficiency from 10^{-5}% to over 3% recently. Although organic solar cells cannot, at present, compete with fossil fuels, the possibility of molecular tailoring may lead to more viable organic cells in the future.

A typical organic solar cell consists of a low work function metal, an organic layer, and a high work function metal, or conducting glass, see Fig. 1. The organic layer invariably exhibits p-type semi-conduction and this is generally believed to be due to electron trapping impurities, which have yet to be identified, but O_2 is strongly suspected [1].

The low work function metal used is generally Aluminium (work function 4.2 eV), although occasionally Indium (work function 4.1 eV) is used. Aluminium has the advantage that it can readily be vacuum deposited onto clear substrates in thin layers thus ensuring that a large fraction of the incident solar energy is transmitted, and the conductivity of these thin layers is also high enough to ensure that resistance losses are negligible. The high work function metal is generally gold (although a conducting glass, Indium Tin Oxide, is sometimes used) and forms an ohmic contact with the organic layer.

Several organic compounds have been used in solar cells, and merocyanine dyes have proved to be amongst the most effective compounds to date. The dark conductivity and the photoconductivity

of these organic cells can be further enhanced by doping with molecular oxygen [2,3] and dopants with greater electonegativity, such as halogens and NO_2 result in even greater enhancement of photovoltaic behaviour [2,4].

The solid state photovoltaic cells are prepared by vacuum (10^{-6} torr) evaporation of thin layers in the order (a) Aluminium (b) merocyanine and (c) gold, onto a pyrex substrate with two indium contacts. The cell is then exposed to dopant vapour such as I_2[2].

By anology with the mechanism of Schottky barrier formation in inorganic semiconductor/metal junctions [5], a space charge layer is assumed to arise spontaneously in the organic semiconductor during equalisation of the Fermi energies of the metal and semiconductor. The situation is often complicated by the presence of oxide layers and surface states [6,7]. There is evidence, however, that surface states play a minor role in determining the interfacial characteristics of organic semiconductors [8], and if oxide layer formation is minimised, then the barrier width w is determined by the physics of an ideal Schottky contact, and to a good approximation W is given by equation (1).

$$W = \left[\frac{2\epsilon\epsilon_o(V_{bi} \pm V)}{eN_A}\right]^{\frac{1}{2}} \qquad (1)$$

where ϵ is the semiconductor permittivity, N_A is the density of ionised acceptors, V_{bi} is the built in diffusion potential (or band bending), and V is the applied field. The ± signs are for reverse and forward bias conditions respectively [9], see fig. 2 for a complete energy level diagram.

Charge carrier photogeneration in merocyanine dyes is believed to be a bulk phenomenon in which dye molecules absorb light, thus forming excitons, which then diffuse through the organic layer and dissociate at dopant sites producing charge carriers. There are two possible mechanisms to explain bulk charge carrier photogeneration [10].

1) $(M....dopant) \xrightarrow[\text{or } M^*]{h\upsilon} (M^+.....dopant^-) \xrightarrow[\text{separation in field}]{\text{charge}} M^+ + (dopant)^-$

   ground state complex; excited complex

or $M + dopant \xrightarrow[\text{or } M^*]{h\upsilon} (M^+.....dopant^-)$

   exciplex

here the function of the dopant is to form charge transfer complexes with the organic molecules in the thin film and excited complexes then dissociate in the built in field.

2) $M^* + (M....dopant) \xrightarrow[\text{transfer}]{e^-} M^+ (M....dopant^-)$

   exciton

with charge generation again being followed by charge separation in the field.

The two mechanisms have been differentiated by observing photocurrent as a function of field strength. Mechanism (1) predicts a quadratic dependence with field strength [11], while mechanism (2) predicts a linear dependence at low field strengths based on the theory of geminate recombination [12]. A low field linear dependence has been observed experimentally [9], and the following mechanism has been suggested.

$$D \xrightarrow{h\upsilon} D^{**} \longrightarrow D^{*} \xrightarrow{(D\text{-}Cl_2)} D^{+}.....Cl_2^{-}.....D$$

ground state	vibrationally "hot" exciton	relaxed exciton		encounter complex at dopant site

$$D^{+} + Cl_2^{-}.....D$$

"hole" "electron"

The above mechanism suggests that stability of the (M....dopant) complex is an important factor in determining the quantum yield for a given cell.

If K_d is the rate constant for electron transfer from an exciton to a (M....dopant) complex site, and Σk is the total rate constant for unimolecular disappearance of D* in the absence of dopant, then the quantum yield is proportional to equation (2)

$$\phi \alpha \frac{k_d[M....dopant]}{k_d[M....dopant] + \Sigma k} \qquad (2)$$

Therefore as the concentration of [M....dopant] increases, the quantum yield ϕ should also increase. The stability of a donor-acceptor complex in the ground state depends on its energy of formation ΔE_N and to a first approximation is proportional to $\Delta E_N/kT$. From the potential energy diagram of a typical charge transfer complex shown in Fig. 3, $\Delta E_N = W_N - I_S$, and therefore the stability of a series of complexes should increase as the I.P. of the donor is reduced assuming that W_N remains at the same energy for a series of complexes [10]. As the complex becomes more stable more dopant should be absorbed leading to an increase in the quantum yield. Thus molecular tailoring of merocyanine dyes offers a potential method of improving quantum yield. In summary, the photovotaic behaviour of merocyanine solar cells can be explained in terms of figures 2 and 3, and mechanism (2).

Merocyaninesare neutral polymethine dyes in which an electron donating group is attached to an electron accepting group via an unsaturated polymethine bridge, fig. (4).

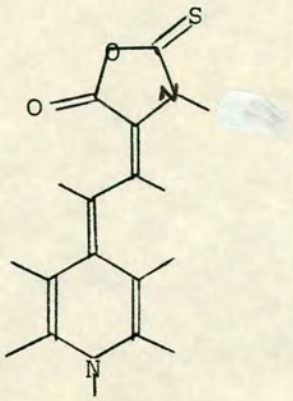

Figure (4) - a typical merocyanine dye

The effect of bridge length has been studied [4]; merocyanines of low I.P. with more than two bridging carbon atoms tend to decompose when evaporated, while solar cells constructed from merocyanines with the donor group directly attached to the acceptor exhibited no photvoltaic behaviour. The optimum bridge length has two carbon atoms, and the combination of a strong donor group with a weak acceptor leads to merocyanines with low I.P.s [2,4].

A reasonably good correlation between log of the quantum yield versus I.P. (as suggested by the complex stability argument) has been observed [10]. It has also been observed that the ability of a merocyanine dye to couple with Iodine appears to be related to the ground state polarity of the dye, the more polar dyes absorbing up to three times more dopant [2]. Therefore the purpose of this work has

been to study the effect of molecular tailoring on I.P. using theoretical methods.

Ab Initio M.O. calculations were carried out on a related series of merocyanine dyes using a (7s3p/3s) guassion orbital basis which was contracted to a (2s1p/1s) A.O. basis for (C,N/H) respectively (see appendix 1). Unfortunately no experimental structures were available for these molecules, so the structures were approximated by constructing them from several smaller molecules of known structure.

Geometries

The following small molecules have been used as partial structures.

Parabanic Acid	Ref. (13)	Fig. (5)
* Cyclopentadiene	Ref. (14)	Fig. (6)
* Rhodanine	Ref. (15)	Fig. (7)
* Isoxazoline	Ref. (16)	Fig. (8)
* Barbituric Acid	Ref. (17)	Fig. (9)
Merocyanine $C_{10}H_{12}S_3N_2O$	Ref. (18)	Fig.(10)
γ-pyridone	Ref. (19)	Fig.(11)
* 2-quinolinone	Ref. (20)	Fig.(12)

* No H data: therefore N-H = 1.03Å, C-H = 1.085Å, external angle bisected.

The unsaturated bridge was approximated by using standard C-C, C=C bond lengths and angles, see fig. (13).

Calculations were performed on several merocyanines in which 4-pyridone was used as the donor and the acceptor group was a five membered ring. Molecules PI - PV (fig. 14), were constructed from the structure of 4-pyridone (fig. 11) and parabanic acid (fig. 5). It was assumed that the substitution of O for NH would have a negligible effect on the structure of the five membered ring. In structures PII - PV the value used for the bond length of the thiocarbonyl group was 1.71Å, which is the literature value for ethylenethiourea, ref. (21).

Molecules PVI and PVII (fig. 15) were constructed from 4-pyridone and rhodanine (fig. 7). The bond length for the additional thio group in the thio-rhodanine structure PVII was assumed to be 1.64Å (C = S in rhodanine = 1.64Å). The thiazolidine thione structure, PVIII (fig. 15), was constructed from the structure given in fig. (10) ref. [18]. R_2 was replaced by H, R_1 by Oxygen and the carbonyl group was replaced by the unsaturated bridge connecting the pyridone group. In all three substitutions the external angles were bisected. Molecule PIX was constructed from the cyclopentadiene fragment (fig. 6), and PX was constructed from the barbituric acid fragment fig. (9), where the thiocarbonyl bond length used was 1.64Å. Structure PXI was constructed using the Isoxazoline fragment (fig. 8), where R_1 was replaced by H and R_2 by the bridge and donor unit.

Four quinoline compounds were also studied. The 1,4 dihydroquinoline structure being based upon the carbocyclic ring of 2-quinolinone, ref. (20) fig. (12ai, aii), which was fused onto the 4-pyridone fragment producing the structure in fig. (12bi, bii). The same acceptor groups as PI, PII, PV and PIX have been used to create structures

QI, QII, QV and QIX respectively (fig. 16).

A further two quinoline structures were studied in which an hydroxy group was added to the quinoline ring (fig. 16). The parameters used for the hydroxy group were based on phenol, ref. (22), C-O 1.364Å, O-H .956Å, <COH 109.0°.

Structural Effects on Ionisation Potentiais

Table 1 contains all the SCF results obtained for the neutral molecules and their respective sigma and pi ions. Tables 2 and 3 contain the first five I.P.'s by Koopman's Theorum and the first pi and sigma I.P.'s by ΔSCF methods. Tables 4, 5 and 6 indicate the effects of molecular tailoring on the ionisation potentials for molecules PI - PVIII, and the quinoline analogues, which all have related five membered acceptor rings.

The labelling system used in all these tables is indicated in fig. 17

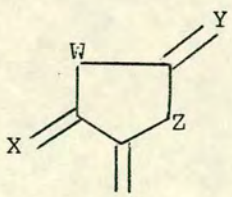

Figure (17)

Comparison of the structures QI, QII, QV and QIX with PI, PII, PV and PIX respectively indicates that the 4-pyridone group is a stronger donor than 1,4 dihydroquinolone, lowering the pi$I.P._1$ by 0.1 eV and the sigma $I.P._1$ by .09 eV on average (see tables 2 and 3, ΔSCF).

The hydroxy group in position (7) of the quinoline ring (HQIA) has little effect on I.P.$_1$, lowers I.P.$_2$ and I.P.$_4$, but increases I.P.$_3$ and I.P.$_5$, (see table 3, HQIA, HQI). Overall it appears that the hydroxy group in this position has a negligible effect. At first sight this result seems a little surprising when one considers that it is possible to draw resonance structures in which the OH group aquires a positive charge and the five membered ring a negative charge.

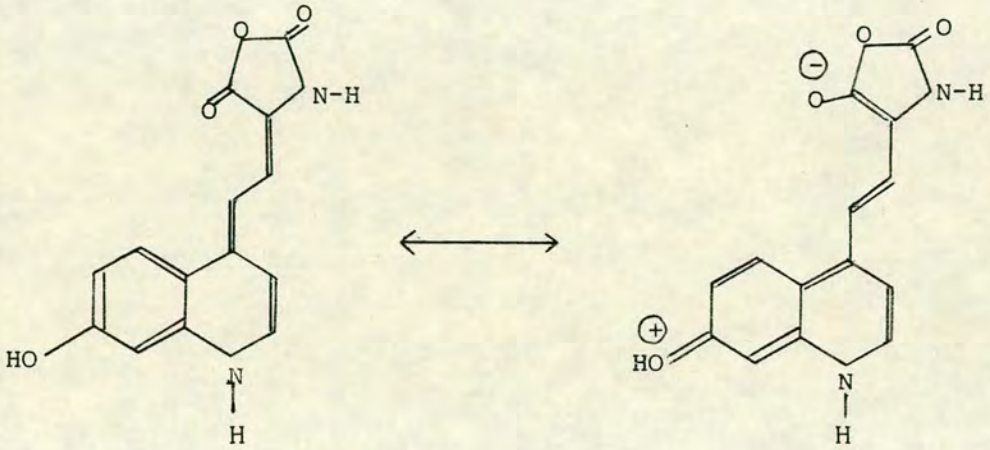

One would normally expect a resonance interaction such as this to lower the ionisation potential due to charge delocalisation. This, then suggests that the OH group is too distant from the five membered ring to have a strong resonance interaction.

The hydroxy group in position (8), (HQIB), increases I.P.$_1$ slightly, lowers I.P.$_3$, and increases I.P.$_4$ and I.P.$_5$, (table 3 HQIB, QI). Again it appears that the hydroxy group has a negligible effect. This, however, could have been anticipated because it is not possible for the OH group to interact with the five membered ring through the conjugative effects of the pi system. Consequently other substituents, such as alkyl groups, NH_2 etc. in positions 5,6,7,8 - are expected to have little effect overall, these substituents being too distant from the acceptor group to have strong electronic effects.

Table 4,5 and 6 indicate that for a five membered ring (fig. 17, page II.8) molecular tailoring has the following effects on the I.P.'s (as calculated using the ΔSCF approach).

π - $I.P._1$

position x	$S < 0$
position w	$HN<0<S$
position y	$S \approx 0$
position z	$HN < S$

(a<b: a has a lower I.P. than b).

σ - $I.P._1$

position x	$S < 0$
position w	$HN<S<0$
position y	$S < 0$
position z	$HN < S$

Using these qualitative theoretical observations the structure predicted to have the lowest $I.P._1$ is PIV, in agreement with the calculated values of tables 2 and 3. PIV is also predicted to have the lowest sigma $I.P._1$, again in agreement with the results of tables 2 and 3.

The structures for which experimental first I.P.'s have been determined (at the Shell Research Centre, Thornton) are illustrated in fig. 18. Table 7 contains the experimentally determined I.P.'s and the photocurrent quantum efficiencies of these structures, ref. (23). The experimental I.P.'s of the seven structures (SIV - SVIII, SX, SXI) in fig. 18 have been plotted against the theoretical I.P.'s (Pi ΔSCF, table 2) of the corresponding pyridine analogues (PIV - PVIII, PX, PXI) in fig. 19.

Ideally fig. 19 should produce a straight line at 45°. The main structural difference between the experimental (Shell) compounds and the theoretical structures (with the exception of the point corresponding to SXI/PXI) is in the donor; Ethyl quinoline instead of pyridine. Therefore the differences in the donor group should have a constant effect. However some pairs of structures (e.g. SVII/PVII) have additional structural differences such as N-Me, N-Et instead of N-H and therefore the scatter in fig. 19 may be attributable to these structural differences not being constant for each pair. An experimental error of $\pm$.15 eV will also contribute to the observed scatter.

The theoretical gas phase I.P.'s are related to the experimental solid state I.P.'s by

$$I_s = I_g + P \qquad (3)$$

where P is the polarisation energy of the crystal

$$P \simeq \left(1 - \frac{1}{n^2}\right) \frac{e}{4\pi\varepsilon_o 2R} \quad \text{(see Ref. (1))} \qquad (4)$$

and n is the optical refractive index, ε_o is the vacuum permittivity, and R is the effective radius of the molecule. Assigning $n^2 = 2.40 \pm .15$ and $R = 4.75\text{Å}$ as the average values for the dyes studied, eqn. (4) yields $P \simeq 0.9$ eV. Extrapolating the line of best fit in fig. 19 yields an intercept of approximately 0.9 eV. Since the major structural difference between the experimental compounds and the corresponding theoretical structures is the donor group, 0.1 eV should be added to the intercept (0.1 is the theoretically determined difference between pyridine and quinoline structures). Therefore the corrected intercept is ~1 eV, and is in good agreement with the value of .9 eV determined

by eqn. (4), thereby justifying the validity of ab initio SCF calculations to study the effects of molecular tailoring on I.P.

Other Attempted Correlations

Population analyses indicated that most of the excess negative charge on the acceptor ring is associated with the carbonyl/thiocarbonyl O/S atoms in positions X/Y, fig. 17. The theoretical charge densities of these atoms have been plotted against the experimental logarithmic values of the quantum yields for the following pairs of structures, PIV - PVIII/SIV - SVIII. It was assumed that the structural differences between comparative structures do not have a great effect, and since each pair of molecules have similar structural differences, the effect should be almost constant for each pair. See also Tables (8) and (9).

The following correlations were attempted,

Fig. 20	Log ϕ	vs	Charge density at X
Fig. 21	Log ϕ	vs	Sigma charge density at X
Fig. 22	Log ϕ	vs	pi charge density at X
Fig. 23	Log ϕ	vs	Charge density at Y
Fig. 24	Log ϕ	vs	Sigma charge density at Y
Fig. 25	Log ϕ	vs	pi charge density at Y

The plots indicate that there are no linear relationships between the above parameters.

Figures 26-33 illustrate further attempted correlations between charge density and I.P.

Fig. 26	Charge density at X vs I.P.$_{\pi 1}$
Fig. 27	pi charge density at X vs I.P.$_{\pi 1}$
Fig. 28	Charge density at X vs I.P.$_{\sigma 1}$
Fif. 29	Sigma charge density at X vs I.P.$_{\sigma 1}$

Fig. 30 Charge density at Y vs I.P.$_{\pi_1}$

Fig. 31 pi charge density at Y vs I.P.$_{\pi_1}$

Fig. 32 Charge density at Y vs I.P.$_{\sigma_1}$

Fig. 33 Sigma charge density at Y vs. I.P.$_{\sigma_1}$

Again there are no obvious linear relationships between any of these parameters, but these plots obviously suffer from the small number of points (5), so any potential relationship would be obscured by one or two anomolous points.

Table 10 contains the theoretical charge densities on the acceptor ring for the structures PI - PVIII, PX and PXI; again it appears that there are no trends, as the related molecules PI - PVIII differ over a range of only .09 in the total charge densities.

Dipole Moments

Table 11 contains the tabulated values of the ground state dipole moments for all the structures studied theoretically. In view of the possibility of several isomeric forms for each molecule no attempt has been made to include dipole moment in any previous or subsequent discussion, the table being added for completeness.

Relationship Between Log ϕ and I.P.$_1$ Revisited

Later experimental results from the Shell Research Centre at Thornton, Cheshire revealed that the quantum yield did not continue to increase with decreasing I.P. but passed a maximum at 5.3 eV after which molecules with lower I.P. produced poorer quantum yields fig. (34). This section is devoted to possible explanations, based on the theoretical calculations, to explain the non-linear dependence between log ϕ and I.P. when the experimental I.P. is less than 5.3 eV.

Fig. 35 is a plot of log quantum yield (experimental) against $I.P._{\pi 1}$ and $I.P._{\sigma 1}$ (theoretical, ΔSCF) for the following pairs of structures P_{IV} - P_{VIII}/S_{IV} - S_{VIII} and P_X/S_X (numerical values in tables 2 and 7). From fig. 35 and tables 2,3,4 and 5 it is obvious that molecular tailoring not only lowers $I.P._{\pi 1}$ but can have an even greater effect on $I.P._{\sigma 1}$. Therefore it is possible that the merocyanine $/I_2$ complexes might develop a greater degree of sigma bonding due to a decrease in the sigma I.P. If sigma bonding predominated as a result, then not only would the assumption that W_N remains constant for a series of dyes (see fig. 3) become invalid, but it would also mean that correlating log quantum yield with $I.P._1$ (pi) would also be invalid.

Furthermore, if one compares the thiazolidine thione structure PVIII with the rhodanine structure PVI, it is seen that these two structures, which have the same empirical formula and almost identical first I.P.'s (pi), differ substantially in their second I.P.'s (sigma). The thiazolidine thione structure has a lower sigma I.P. (7.18 vs 6.91 eV) and therefore it seems reasonable to assume that the complexes formed by SVIII and I_2 should exhibit a greater degree of sigma bonding than SVI and I_2.

Further examination of fig. 35 reveals that four of the six points representing the sigma I.P.'s form a straight line. The two remaining points could be considered anomolous. The barbituric acid derivative SX has a six membered ring instead of a five membered ring and is therefore not structurally related to the other compounds. The other anomolous point, the thiorhodanine derivative SVIII, has three

sulphur atoms and could therefore be expected to exhibit a heavy atom effect, thereby reducing the lifetime of the excited state (exciton), and consequently resulting in a poor quantum yield.

Therefore, one could, with speculation, suggest that the correlation between $\log \phi$ and $I.P._1$ is invalidated when a high degree of sigma bonding is present in the molecular complex. There is also some experimental X-ray photo-electron data which indicates that there is indeed a change in the bonding of merocyanine $/X_2$ complexes [23].

A much simpler explanation could be that the assumption of the complex stability argument, that W_N remains constant is invalid. Molecular tailoring could drastically affect the bonding in the complex, e.g. bonding may well become more localised/delocalised as a result of structural changes, without necessarily becoming predominantly sigma bound.

Another possible explanation is that both of the mechanisms suggested in the introduction are responsible for photovoltaic activity.

1) $\underset{\text{ground state complex}}{(M....\text{dopant})} \xrightarrow[\text{or } M^*]{h\upsilon} \underset{\substack{\text{excited complex} \\ \text{(exciplex)}}}{(M^+....\text{dopant}^-)} \xrightarrow[\text{in field}]{\text{charge separation}} M^+ + (\text{dopant}^-)$

or

$$M + \text{dopant} \xrightarrow[\text{or } M^*]{h\upsilon} (M^+....\text{dopant}^-)$$

2) $$M^* + (M....\text{dopant}) \xrightarrow[\text{transfer}]{e^-} M^+ + (M....\text{dopant}^-)$$

with charge generation again being followed by charge separation in the field.

Mechanism (2) predicts that the photocurrent should have a linear dependence on field strength at low fields, while mechanism (1) predicts a quadratic dependence at all field strengths. A low field linear dependence has been observed experimentally [9], but this does not, however, eliminate the possibility that both mechanisms operate at higher field strengths, since both mechanisms would exhibit a quadratic relationship between photocurrent and field strength.

Mechanism (1) involves separating the positive and negatively charged components of the exciplex in the presence of the built in field which arises during equalisation of the fermi levels, see introduction. Therefore if one assumes that the bonding of the ground state complex is similar to the bonding of the exciplex, then two competing affects are involved in generating a photocurrent,

i) increasing the concentration of molecular complexes, which requires a low I.P. (see introduction)

ii) avoiding geminate recombination of charge carriers.

Assuming W_N remains constant, reducing the I.P. of the dye stabilises the ground state complex. It could also be argued that the excited complex is also more stable thereby reducing the probability of it dissociating into charge carriers, and consequently reducing the quantum yield. Therefore one could explain the decrease in quantum yield on the basis of two competing effects, i.e. reducing the I.P. stabilises the ground state but reduces the probability of forming charge carriers.

It is also possible that the fermi energy of the dye decreases, thereby decreasing V_{bi} (fig. 2) resulting in a decrease in W. Charge carriers would then be generated over a smaller distance and the quantum yield would decrease.

Discussion

On the basis of the theoretical and experimental results available no clear conclusions can be made. From the theoretical point of view, several questions remain unanswered, notably the question of the type of bonding involved in the complex, sigma or pi? This could be approached theoretically by studying several complexes of merocyanines and Cl_2 and optimising the geometries of these complexes with an ab initio program such as HONDO or GAMESS. This would then enable one to determine whether pi or sigma bonding predominates and if molecular tailoring determines which type of bonding is dominant.

Experimentally, a measurement of the quantum yield from a solar cell using structure PI as the merocyanine would be interesting. PI has a low theoretical $I.P._{\pi}$ but a high $I.P._{\sigma}$, therefore the possibility of sigma bonding would be eliminated and this could perhaps explain if sigma bonding has a significant effect.

In summary, a better understanding of the bonding in these complexes is required before the effects of molecular tailoring can be fully understood.

References

1. H. Meier, Organic Semi Conductors, Verlag Chemie, Weinheim 1974.
2. G.A. Chamberlain and R.E. Malpas, J. Chem. Soc. Faraday Disc; 70 (1980) 299.
3. G.A. Chamberlain and P.J. Cooney, Chem. Phys. Lett., 66 (1979) 88.
4. G.A. Chamberlain and P.J. Cooney, Nature; 289 (1981) 45.
5. S.M. Sze, Physics of Semiconductor Devices (Wiley-Interscience, New York, 1969) p.370.
6. M.A. Green and J. Sewchum, J. Appl. Phys; 46 (1975) 5185.
7. J. Shewchum, R. Singh and M.A. Green, J. Appl. Phys; 48 (1977) 765.
8. N. Karl, Festor perprobleme XIV (1974) 261.
9. G.A. Chamberlain, J. Appl. Phys; 53(9) (1982) 6262.
10. G.A. Chamberlain, Solar Cells; 8 (1983) 47.
11. P. Petelenz, Chem. Phys. Lett; 65 (1979) 579.
12. L. Onsager, J. Chem. Phys; 2 (1934) 399.
13. B.M. Craven, R.K. McMullan, Acta. Cryst; B35, (1979) 934.
14. G. Liebling, R.E. Marsh, Acta Cryst; 19 (1965) 202.
15. D. Van der Helm, A.E. Lessor, L. Merritt Jr.; Acta. Cryst; 15 (1962) 1227.
16. J. Meunier-Piret, Piret, G. Germain, J.P. Putzeys and M. Van Meerssche; Acta Cryst., B28 (1972) 1308.
17. G.A. Jeffreys, S. Ghose, J.O. Warwicker, Acta Cryst; 14 (1961) 881.
18. G. Germain, P. Piret, M. Van Meerssche, Acta. Cryst; 15 (1962) 373.
19. M.H. Palmer, unpublished work.
20. B. Ribar, I. Janic, Cryst. Struct. Comm., 6 (1979) 677.
21. P.J. Wheatley, Acta. Cryst; 6 (1953) 369.
22. T. Pedersen, N. Wessel Larsen, L. Nygaard, J. Mol. Structure; 4 (1969) 59.
23. G.A. Chamberlain, unpublished work.

TABLE 1 SCF ENERGIES

Molecule	Neutral Molecule/A.U.	Pi Ion/A.U.	Sigma Ion/A.U.
PI	-714.7184500	-714.49247118	-714.38183176
PII	-1036.8989359	-1036.67230395	-1036.63091105
PIII	-1359.04733787	-1358.82310773	-1358.79662541
PIV	-1339.31533915	-1339.10099356	-1339.08129243
PV	-1017.1602578	-1016.9446858	-1016.9077315
PVI	-1359.0974737	-1358.86815586	-1358.83350327
PVII	-1681.24746439	-1681.0210809	-1680.9891350
PVIII	-1359.08732096	-1358.85847205	-1358.8332339
PIX	-513.83302877	-513.61771126	-513.43335423
PX	-1129.55380762	-1129.31391192	-1129.27944479
PXI	-640.047734711	-639.797914243	-639.746126787
QI	-867.00713789	-866.7771104	-866.66539237
QII	-1189.17502942	-1188.94539562	-1188.90450713
QV	-1169.43687613	-1169.21748465	-1169.18153207
QIX	-666.108534857	-665.88903879	-665.705262784
HQIA	-941.638161313	-	-
HQIB	-941.638034055	-	-

TABLE 2 CALCULATED IONISATION POTENTIALS

	KOOPMANS' THEORUM					ΔSCF	
Molecule	IP_5/eV	IP_4/eV	IP_3/eV	IP_2/eV	IP_1/eV	$\Delta SCFIP_{\pi 1}$/eV	$\Delta SCFIP_{\sigma 1}$/eV
PI	π 12.93	σ 12.16	π 11.04	π 10.20	π 6.84	6.15	9.16
PII	π 11.13	π 11.03	π 9.11	LP S_y 9.06	π 6.86	6.17	7.30
PIII	π 9.48	LP S_y 9.03	π 9.00	LP S_x 8.69	π 6.79	6.10	6.82
PIV	π 8.99	LP Sy 8.60	π 8.38	LP S_x 8.18	π 6.52	5.83	6.37
PVI	π 11.12	π 10.38	π 8.93	LP S_y 8.87	π 6.98	6.24	7.18
PVII	π 9.26	LP S_y 8.87	π 8.66	LP S_x 8.33	π 6.90	6.16	7.03
PVIII	π 11.17	π 10.44	π 8.79	LP S_y 8.64	π 6.92	6.23	6.91
PIX	σ 12.08	π 10.85	π 9.81	π 8.12	π 6.55	5.86	10.88
PX	π 11.25	π 11.14	π 8.98	8.92	π 7.33	6.53	7.47
PXI	π 12.81	π 11.48	σ 11.19	π 10.46	π 7.49	6.80	8.21

TABLE 3 CALCULATED IONISATION POTENTIALS

	Koopmans' Theorum					ΔSCF	
Molecule	IP_5/eV	IP_4/eV	IP_3/eV	IP_2/eV	IP_1/eV	$\Delta SCFIP_{\pi 1}$/eV	$\Delta SCFIP_{\sigma 1}$/eV
QI	σ 12.40	π 10.73	π 10.35	π 9.40	π 6.98	6.26	9.30
QII	π 10.45	π 9.76	LP S 9.16	π 9.03	π 6.97	6.25	7.36
QV	π 10.24	π 9.45	LP S 8.67	π 8.62	π 6.68	5.97	6.95
QIX	π 10.43	π 10.17	π 9.21	π 8.27	π 6.69	5.98	10.97
HQIA	σ 12.43	π 10.65	π 10.50	π 9.07	π 6.99	-	-
HQIB	σ 12.46	π 10.86	π 10.14	π 9.42	π 7.06	-	-

TABLE 4 STRUCTURAL EFFECTS ON 1ST Pi I.P.

Position	Molecules Compared	Structural Change	ΔSCF Result	ΔSCF I.P. lowering (eV)	KOOPMANS' THEORUM Result	KOOPMANS' THEORUM I.P. lowering (eV)
X	PII, PIII	S/O	S<O	.07	S<O	.07
X	PIV, PX	S/O	S<O	.04	S<O	.02
X	PVI, PVII	S/O	S<O	.08	S<O	.08
W	PV, PVIII	N/S	N<S	.36	N<S	.40
W	PII, PVIII	S/O	O<S	.06	O<S	.06
W	PII, PV	N/O	N<O	.30	N<O	.32
W	QII, QV	N/O	N<O	.28	N<O	.31
Y	PI, PII	S/O	O<S	.02	O<S	.02
Y	QI, QII	S/O	S<O	.01	S<O	.01
Z	PV, PVI	N/S	N<S	.37	N<S	.44

TABLE 5 STRUCTURAL EFFECTS ON 1ST SIGMA I.P.

Position	Molecules Compared	Structural Change	ΔSCF		KOOPMANS' THEORUM	
			Result	I.P. lowering (eV)	Result	I.P. lowering (eV)
X	PII, PIII	S/O	S<O	.48	S<O	.37
X	PIV, PV	S/O	S<O	.50	S<O	.38
X	PVI, PVII	S/O	S<O	.15	S<O	.52
W	PV, PVIII	N/S	N<S	.04	N<S	.10
W	PII, PVIII	S/O	S<O	.41	S<O	.42
W	PII, PV	N/O	N<O	.43	N<O	.50
W	QII, QV	N/O	N<O	.41	N<O	.49
Y	PI, PII	S/O	S<O	1.86	S<O	3.10
Y	QI, QII	S/O	S<O	1.94	S<O	3.24
Z	PV,PVI	N/S	N<S	.31	N<S	.31

TABLE 6 OVERALL MOLECULAR TAILORING EFFECTS ON 1ST FIVE I.P.'s (KOOPMANS') THEORUM

Position	Molecules Compared	Structural Change	Result
X	PII, PIII	S/0	S<0
X	PIV, PV	S/0	S<0
X	PVI, PVII	S/0	S<0
W	PV, PVIII	N/S	N<S
W	PII, PVIII	S/0	S<0
W	PII, PV	N/0	N<0
W	QII, QV	N/0	N<0
Y	PI, PII	S/0	S<0
Y	QI, QII	S/0	S<0
Z	PV, PVI	N/S	N<S

TABLE 7 EXPERIMENTAL QUANTUM YIELDS AND FIRST I.P.'s

Molecule	I.P. exp/eV	ϕ	log ϕ
SIV	5.2	1.7%	-1.77
SV	5.2	3.4%	-1.47
SVI	5.4	12%	-.92
SVII	5.2	1.7%	-1.77
SVIII	5.3	4.7%	-1.33
SX	5.9	2.1%	-1.68
SXI	6.1	.04%	-3.40

TABLE 8 CHARGE DENSITIES (TOTAL, Pi, SIGMA) ON ATOM X. CHARGE DENSITIES ON ATOM X FOR $HOMO_\sigma$ AND $HOMO_\pi$

Molecule	Charge density sigma	Charge density pi	Charge density total	Charge density $HOMO_\sigma$	Charge density $HOMO_\pi$	ϕ (exp)	IP_π (exp/eV)	IP_σ (exp/eV)
PI	-.129	-.344	-.437	-.453	-.018	-	-	-
PII	-.125	1.349	-.474	-.005	-.016	-	-	-
PIII	.211	-.420	-.209	-.685	-.054	-	-	-
PIV	.203	-.494	-.291	-.772	-.045	1.790	5.83	6.37
PV	-.136	-.379	-.515	-.005	-.013	3.4%	5.87	6.87
PVI	-.142	-.374	-.516	-.033	-.060	12%	6.24	7.18
PVII	.168	-.438	-.269	-.771	-.046	1.7%	6.16	7.03
PVIII	-.135	-.344	-.479	-.009	-.022	4.7%	6.23	6.91
PX*	.202	-.513	-.311	-.942	-.012	2.1%	6.53	7.47

TABLE 9 CHARGE DENSITIES ON ATOM Y (TOTAL SIGMA, PI). CHARGE DENSITIES ON ATOM Y FOR $HOMO_{\sigma}$ AND $HOMO_{\pi}$.

Molecule	Charge density sigma	Charge density pi	Charge density total	Charge density $HOMO_{\sigma}$	Charge density $HOMO_{\pi}$	Log ϕ (exp)
PI	-.093	-.046	-.499	-.033	-.018	-
PII	.259	-.517	-.257	-.955	-.078	-
PIII	.259	-.524	-.264	-.203	-.081	-
PIV	.237	-.573	-.336	-.111	-.089	-1.77
PV	.237	-.572	-.335	-.959	-.085	-1.47
PIII	.185	-.451	-.266	-.930	-.047	-.92
PVII	.185	-.453	-.268	-.083	-.046	-1.77
PVIII	.201	-.496	-.294	-.933	-.091	-1.33

TABLE 10 TOTAL CHARGES ON ACCEPTOR RINGS

Molecule	Sigma	Pi	Total
PI	-.0501	-.1375	-.1876
PII	-.0477	-.1732	-.2209
PIII	-.0297	-.2069	-.2366
PIV	-.0272	-.1832	-.2104
PV	-.0460	-.1371	-.1831
PVI	-.0228	-.2436	-.2691
PVII	-.0048	-.2684	-.2732
PVIII	-.0296	-.2297	-.2593
PX	-.0060	-.3874	-.3814
PXI	+.0049	-.3523	-.3464

TABLE 11 GROUND STATE DIPOLE MOMENTS

Molecule	Dipole(x)/A.U.	Dipole(y)/A.U.	Total Dipole/A.U.
PI	1.0097530	-4.3311	4.447273578
PII	.9525679	-4.5086182	4.608147531
PIII	.7836587	-4.7804265	4.844233527
PIV	.2703100	-3.5901443	3.596855479
PV	.2196207	-3.3523540	3.359540234
PVI	-.2222985	-3.7401443	3.74674472
PVII	-.3460545	-3.8970262	3.912360784
PVIII	.2449013	-4.3627645	4.36963279
PIX	.2541473	-2.6762028	2.68826843
PX	-.5712504	-3.7227032	3.766277488
PXI	.9614987	-5.3390071	5.424894151
QI	.9613427	-3.8105966	3.929990613
QII	.9379097	-4.0164590	4.124514212
QV	.2590549	-2.8401427	2.851932677
QIX	-.1945472	-2.1902966	2.198919691
HQIA	.3574774	-3.4773314	3.495657842
HQIB	.9684482	-3.0449553	3.195253462

Appendix 1: Minimal Basis Set for C,N,S,O,H.

Hydrogen

	coefficient	exponent
1s	0.07048000	7.37812000
	0.40789000	1.11692000
	0.64767000	0.24817000

Carbon

	coefficient	exponent
1s	0.00481300	1412.29000
	0.03726700	206.885000
	0.17240300	45.8498000
	0.45926100	12.3887000
	0.45618500	3.72337000
2s	0.52234200	0.58122600
	0.59418600	0.18127100
2p	0.11219400	4.74919000
	0.46622700	0.96685900
	0.62256900	0.22617700

Nitrogen

	coefficient	exponent
1s	0.00447900	2038.41000
	0.03458100	301.689000
	0.16426300	66.4630000
	0.45389800	17.8081000
	0.46897900	5.30452000
2s	0.51359800	0.71909300
	0.60572100	0.22035900
2p	0.11966400	6.25234100
	0.47462900	1.29458000
	0.61114200	0.30109000

Oxygen

	coefficient	exponent
1s	0.00432400	2714.89000
	0.03226500	415.725000
	0.15641000	91.9805000
	0.44781300	24.4515000
	0.48160200	7.22296000

2s	0.50470800	0.96745700
	0.61673400	0.29363800
2p	0.12937300	7.57741000
	0.48126900	1.58602000
	0.60448400	0.35663400

Sulphur

	coefficient	exponent
1s	0.00157500	25506.3000
	0.01221700	3812.82000
	0.06116600	860.556000
	0.21176100	242.940000
	0.45201300	79.0448000
	0.40019300	27.5705000
2s	0.38220400	6.49476000
	0.65779700	2.41078000
3s	0.46354500	0.41264400
	0.57956800	0.15229600
2p	0.02906900	129.088000
	0.17989300	29.6305000
	0.47817000	8.84715000
	0.49673600	2.85576000
3p	0.44103700	0.65036600
	0.66434400	0.18202200
1d	1.00000000	0.54100000

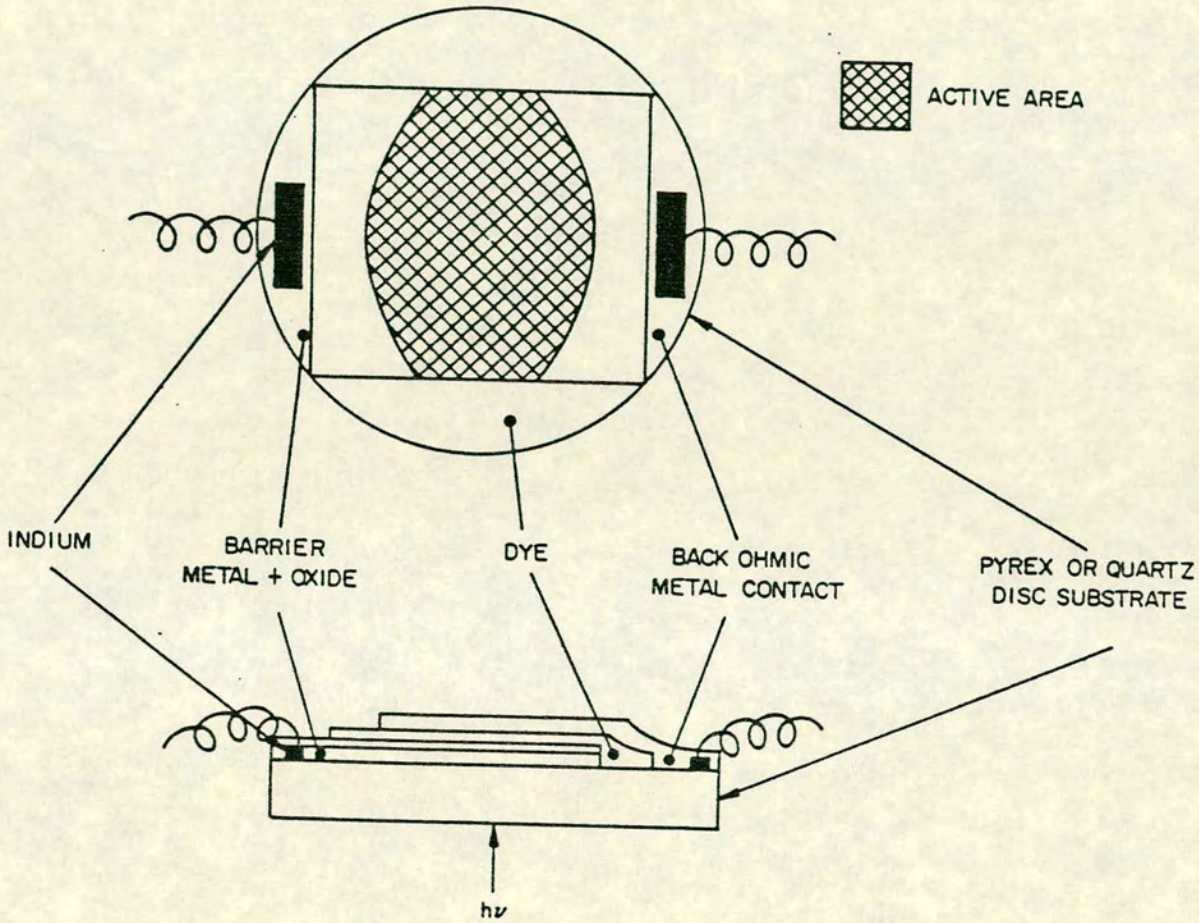

FIG. 1—A typical organic photovoltaic cell

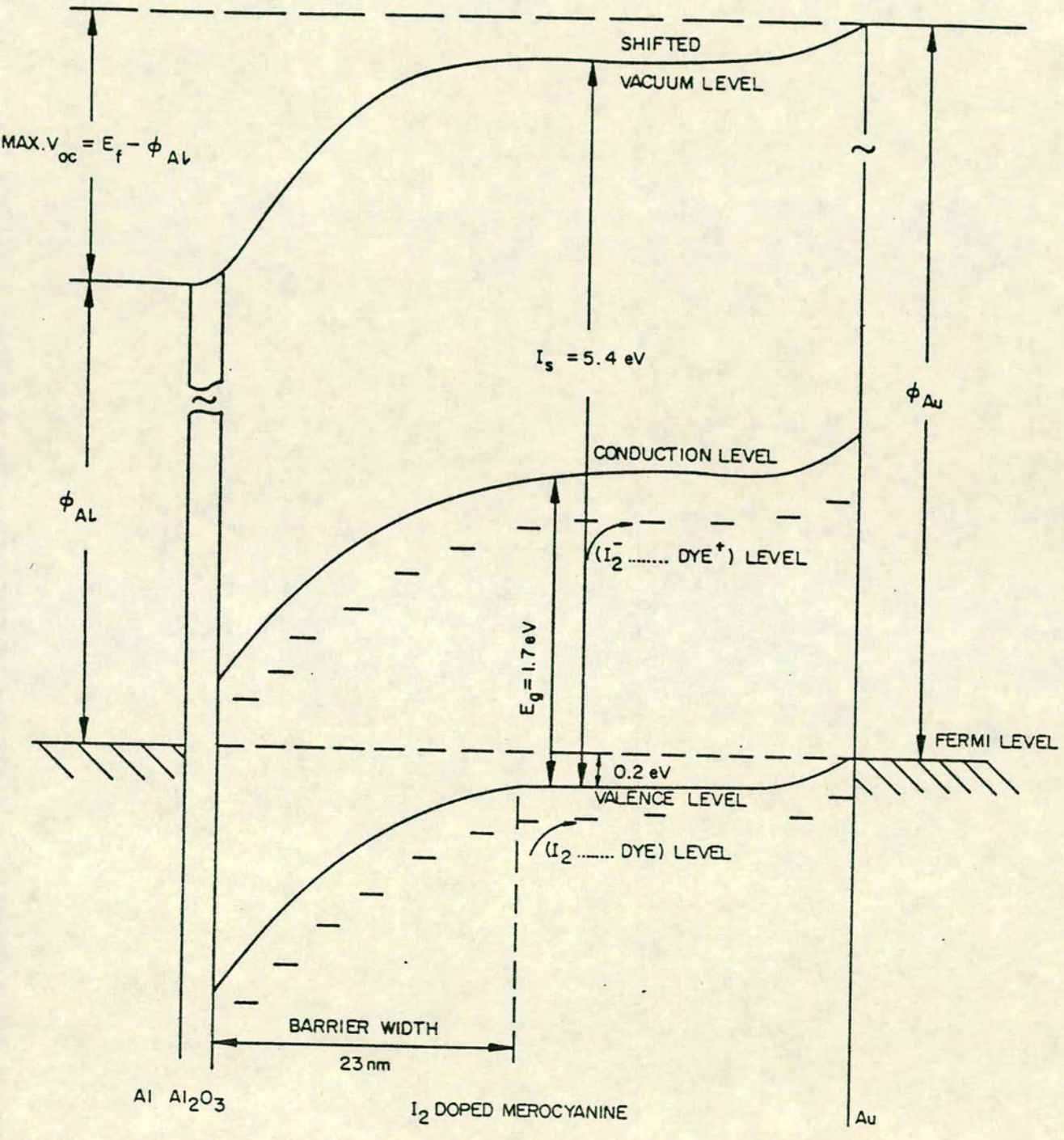

FIG. 2—Energy level diagram illustrating the photovoltaic effect in an iodine-doped merocyanine (No. 9 in Fig. 2) cell

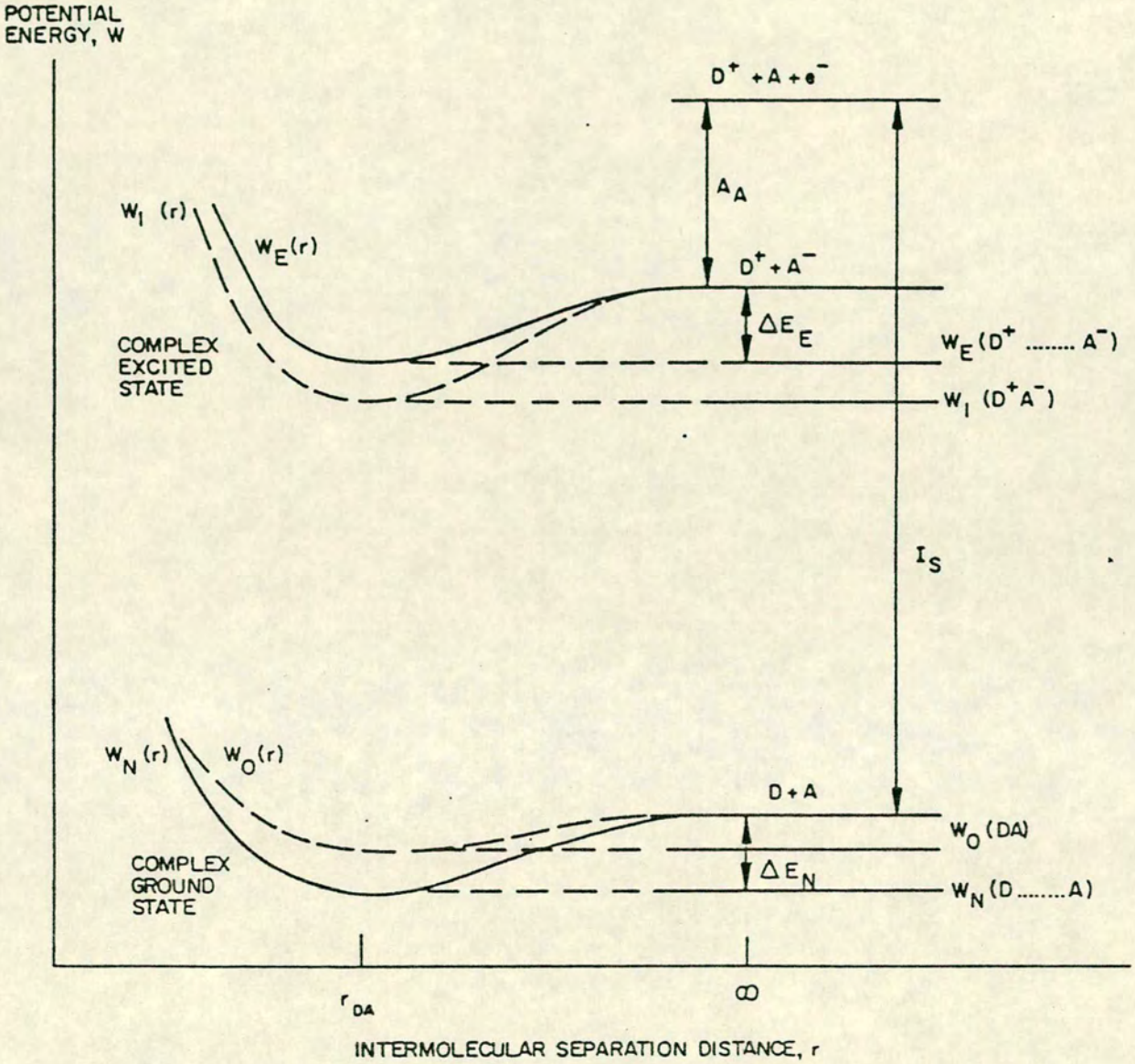

FIG 3—Schematic diagram of potential energy W of a DA complex against intermolecular separation distance r. $W_N(r)$ (D.....A) complex ground state, $W_E(r)$ (D^+.....A^-) complex excited state, $W_O(r)$ DA structure, $W_I(r)$ D^+A^- structure W_N, W_E, W_O, W_I potentials at equilibrium separation, r_{DA}. I_S donor ionisation potential, A_A acceptor electron affinity. Stability of (D.....A) complex $\propto \exp(W_N - I_S)/kT$

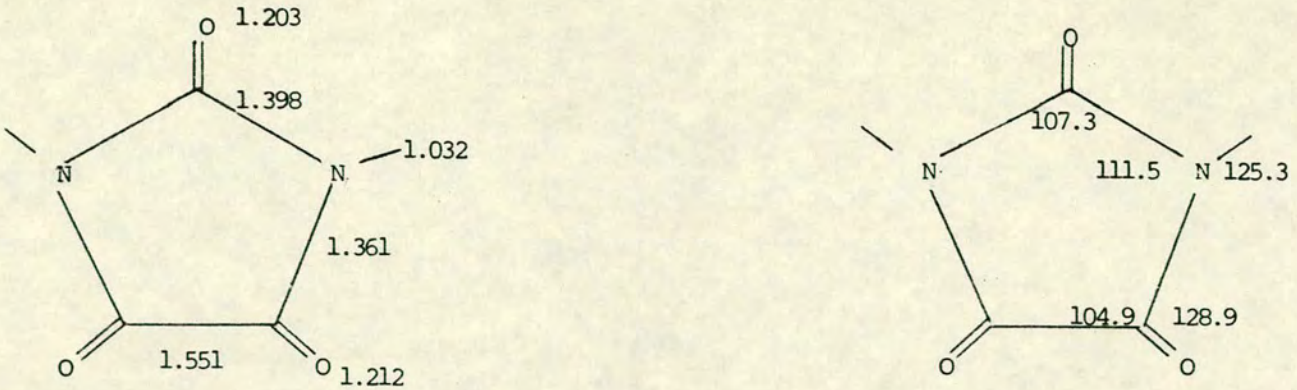

FIGURE 5

FIGURE 6

FIGURE 7

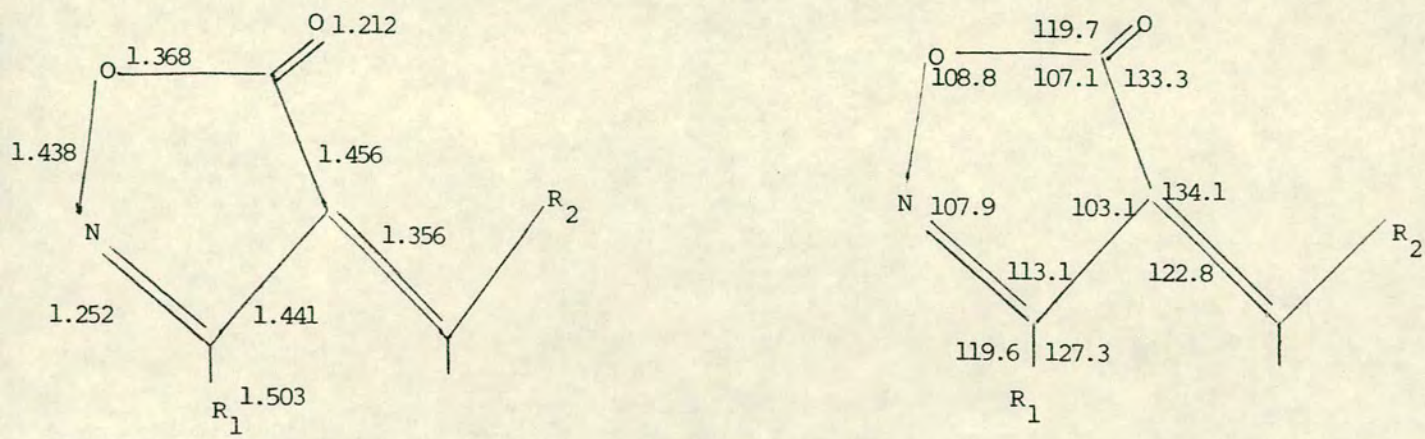

FIGURE 8

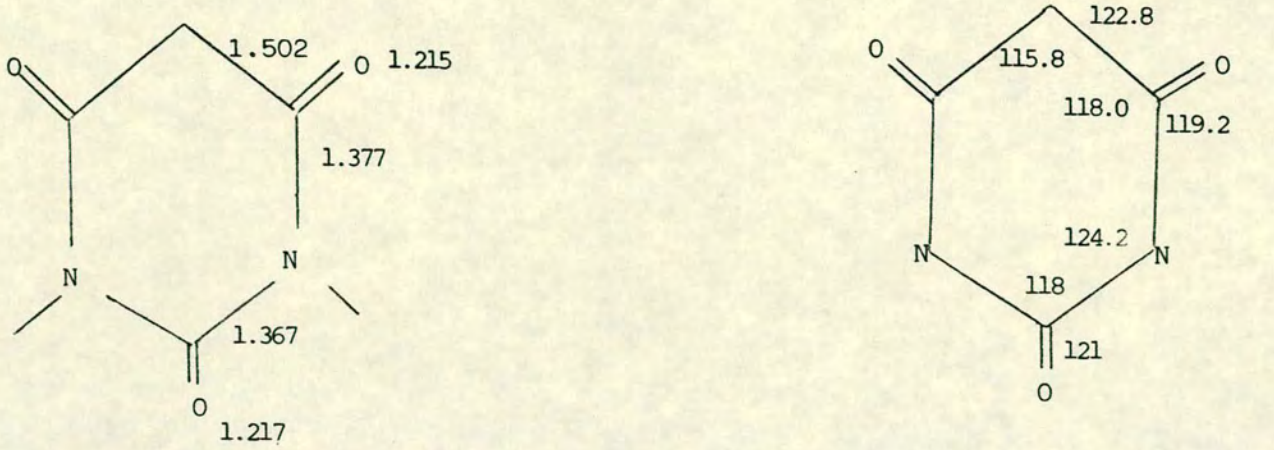

FIGURE 9

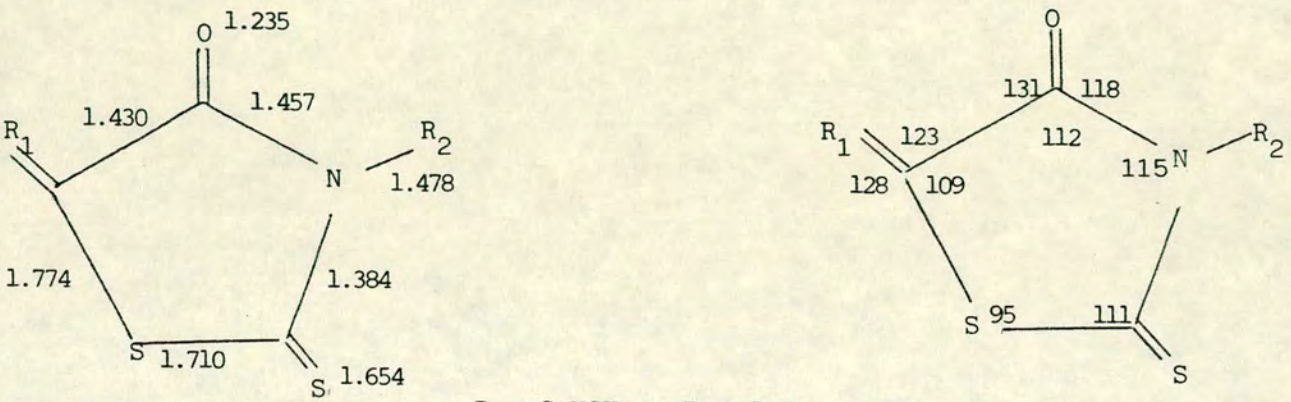

$R_1 = C_4NSH_7$, $R_2 = C_3H_5$

FIGURE 10

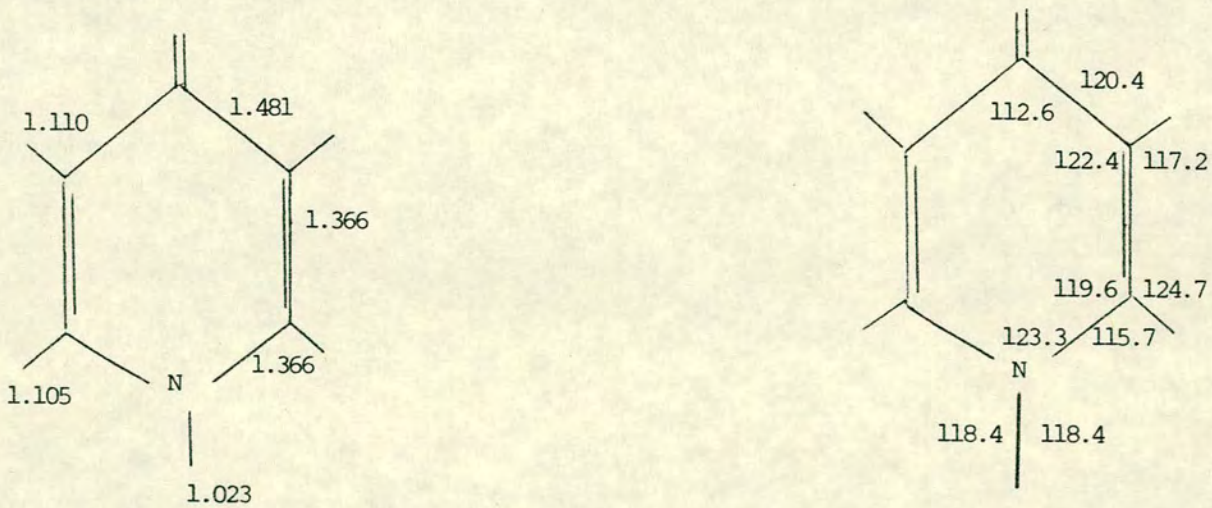

FIGURE 11

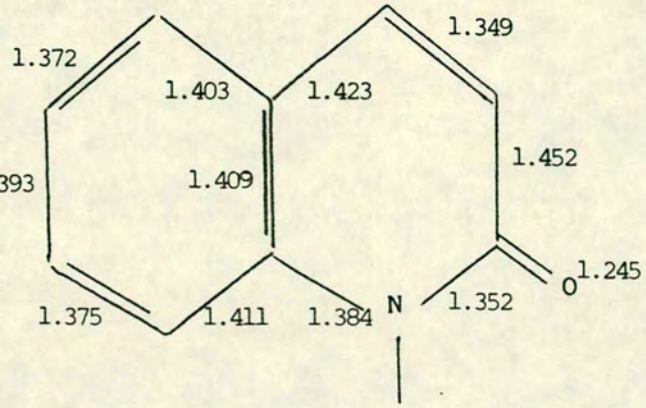

ai

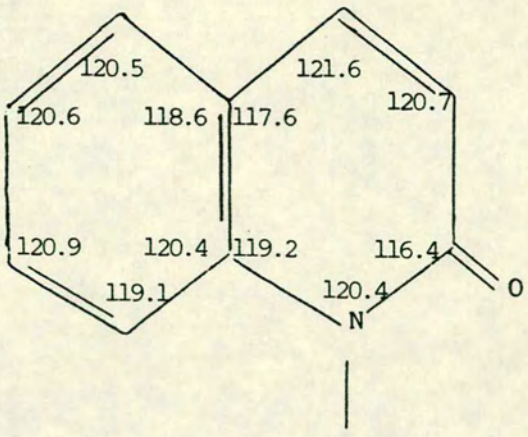

aii

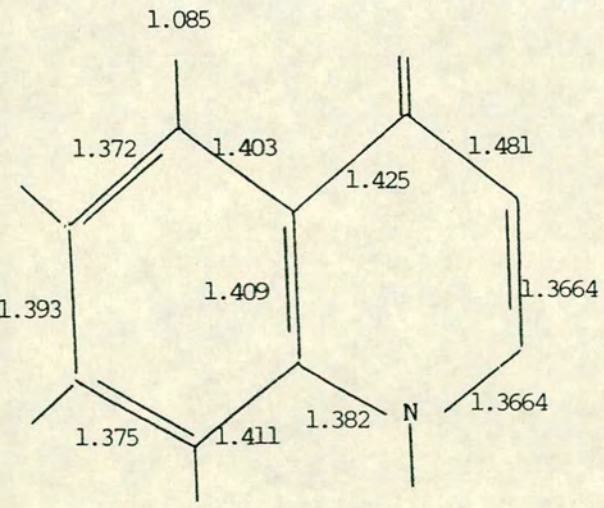

bi

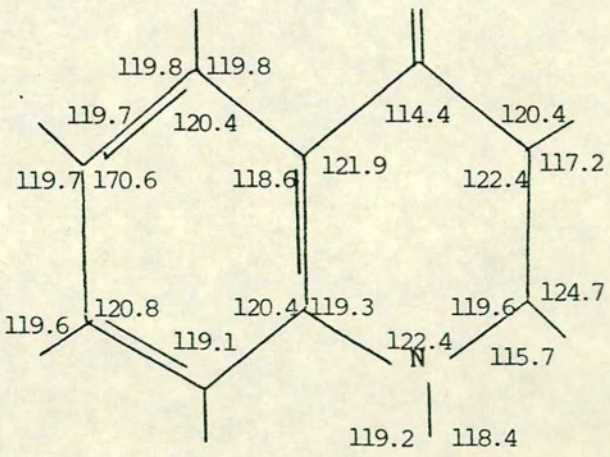

bii

FIGURE 12

FIGURE 13

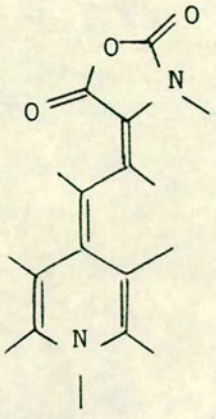

PI

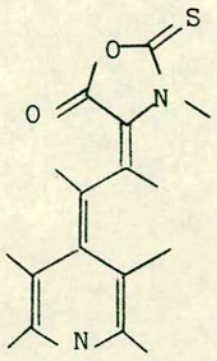

PII

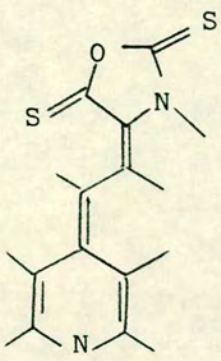

PIII

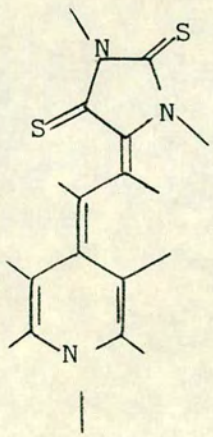

PIV

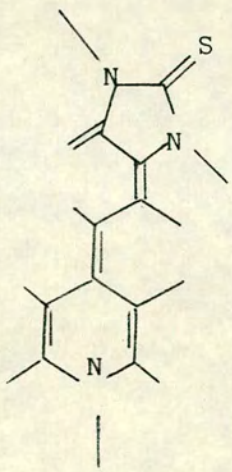

PV

FIGURE 14

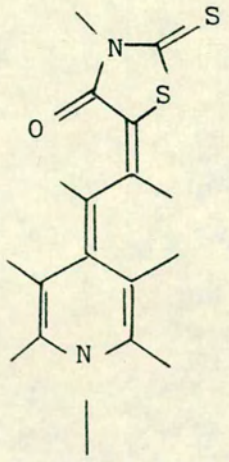

PVI

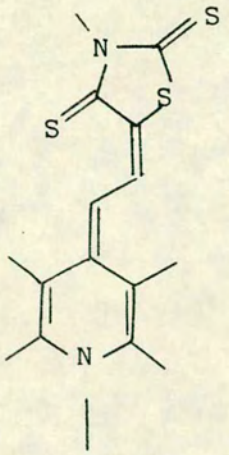

PVII

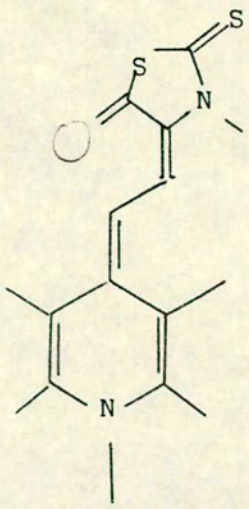

PVIII

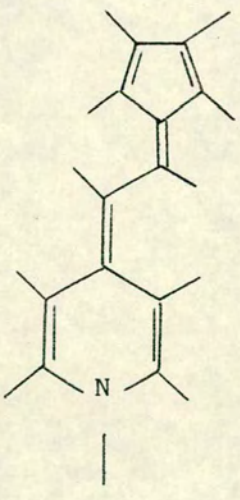

PIX

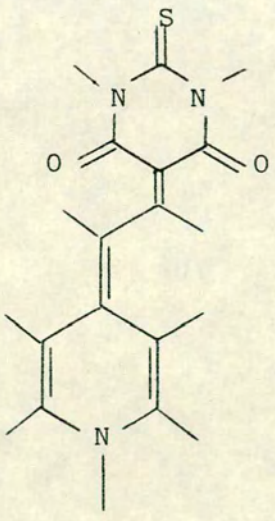

PX

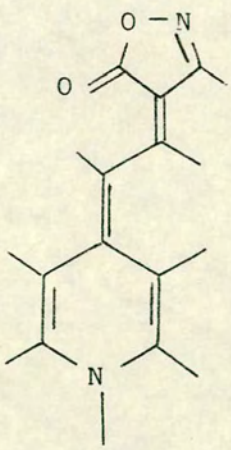

PXI

FIGURE 15

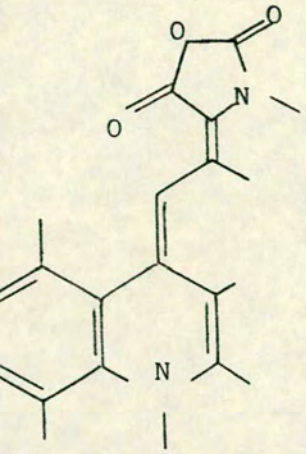

QI

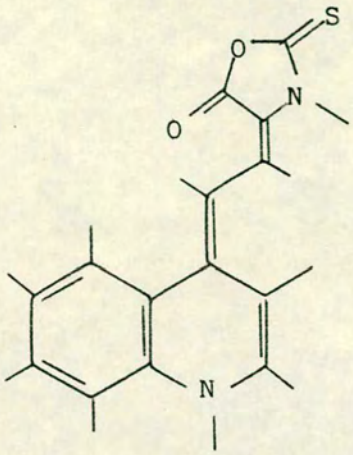

QII

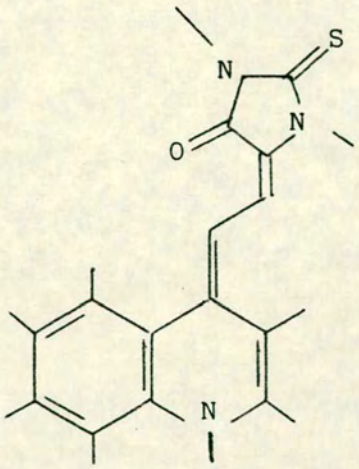

QV

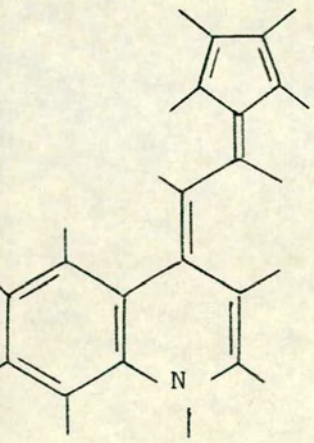

QIX

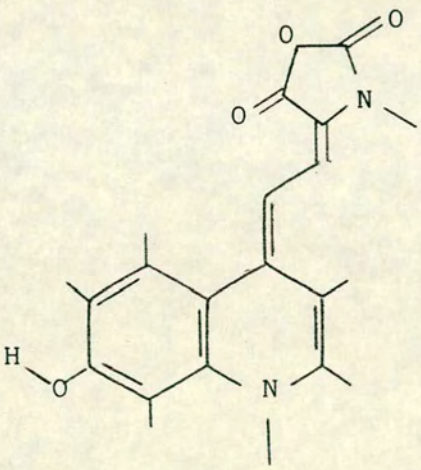

HQIA

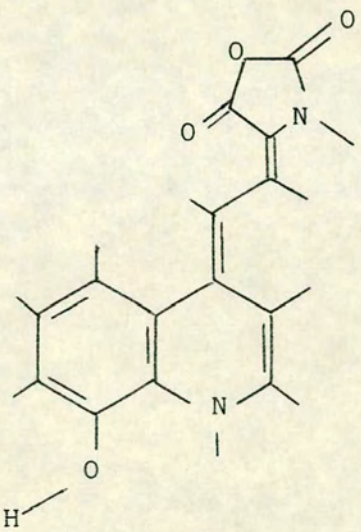

HQIB

FIGURE 16

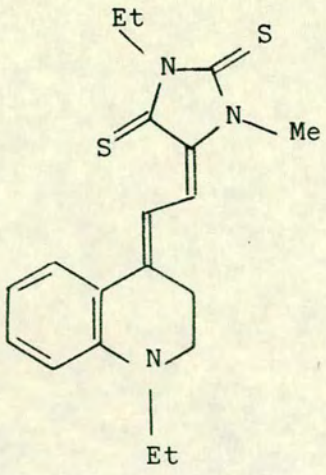

SIV

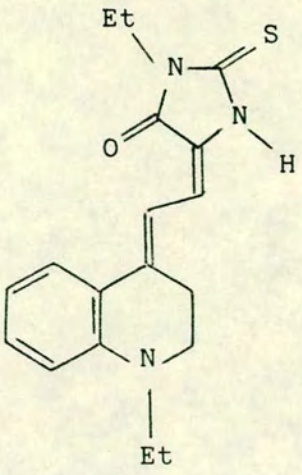

SV

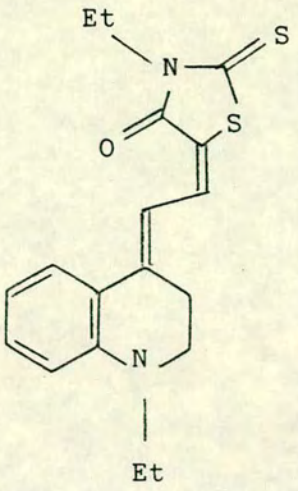

SVI

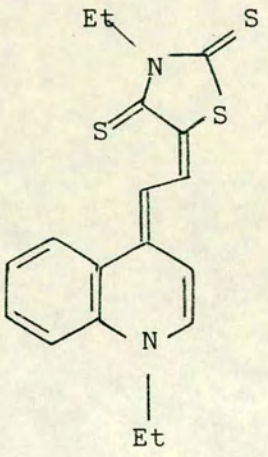

SVII

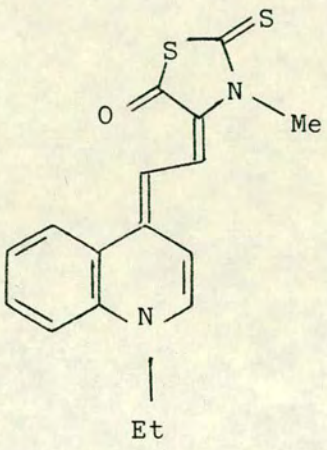

SVIII

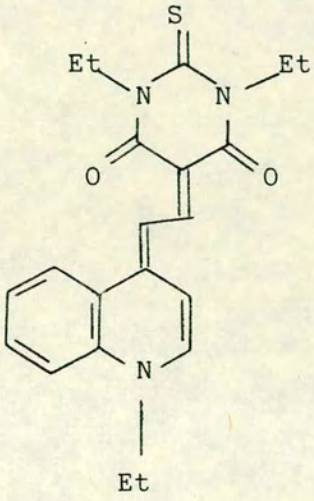

SX

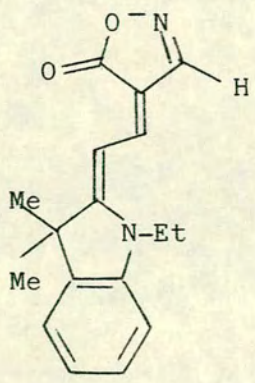

SX

FIGURE 18

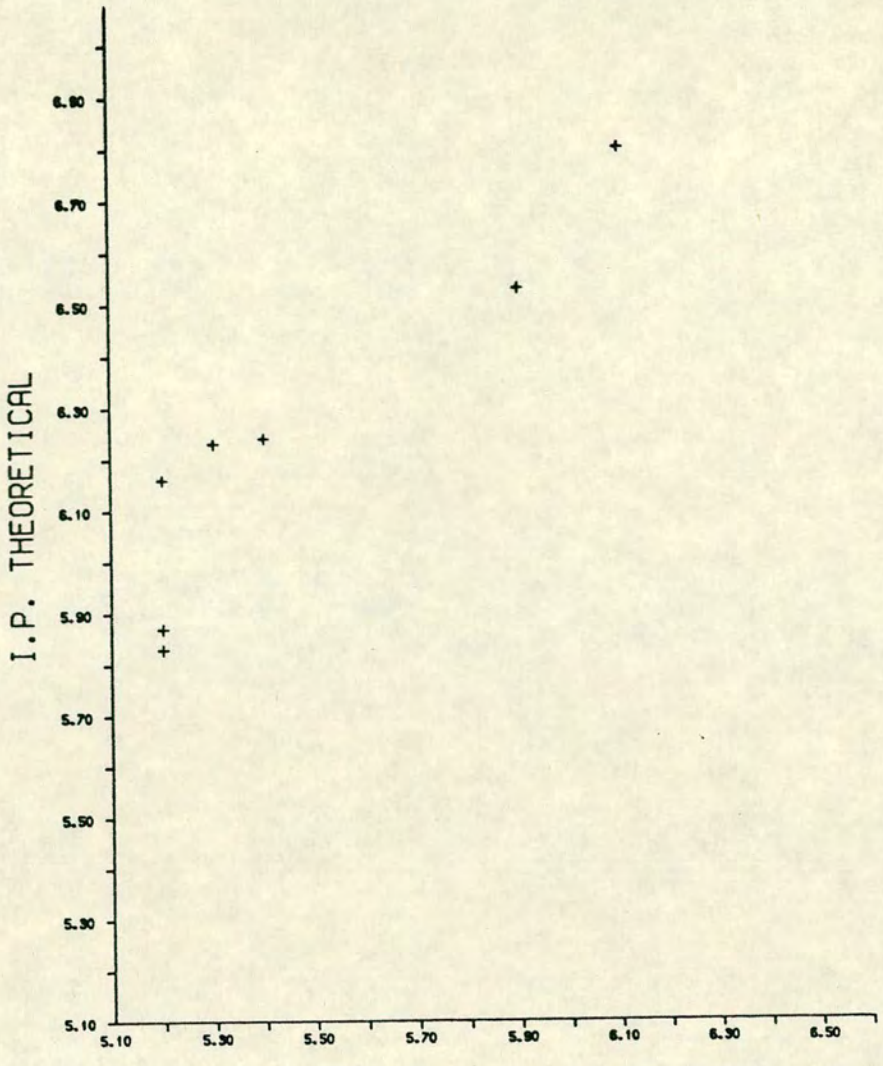

FIGURE 19 - THEORETICAL $I.P_1$ VS EXPERIMENTAL $I.P_1$

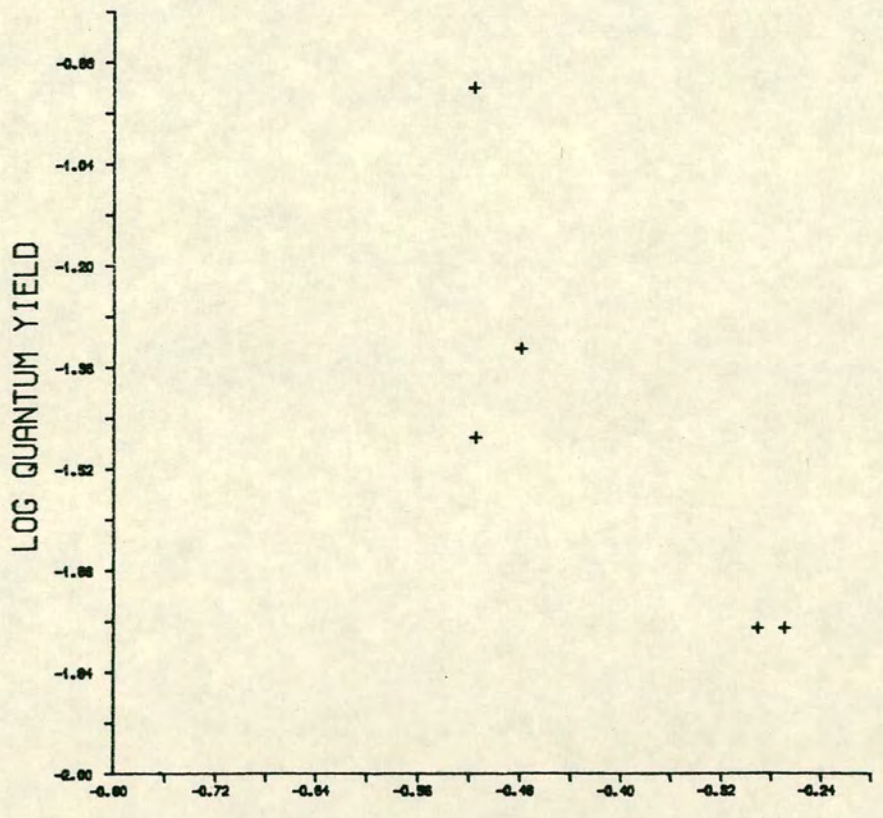

FIGURE 20

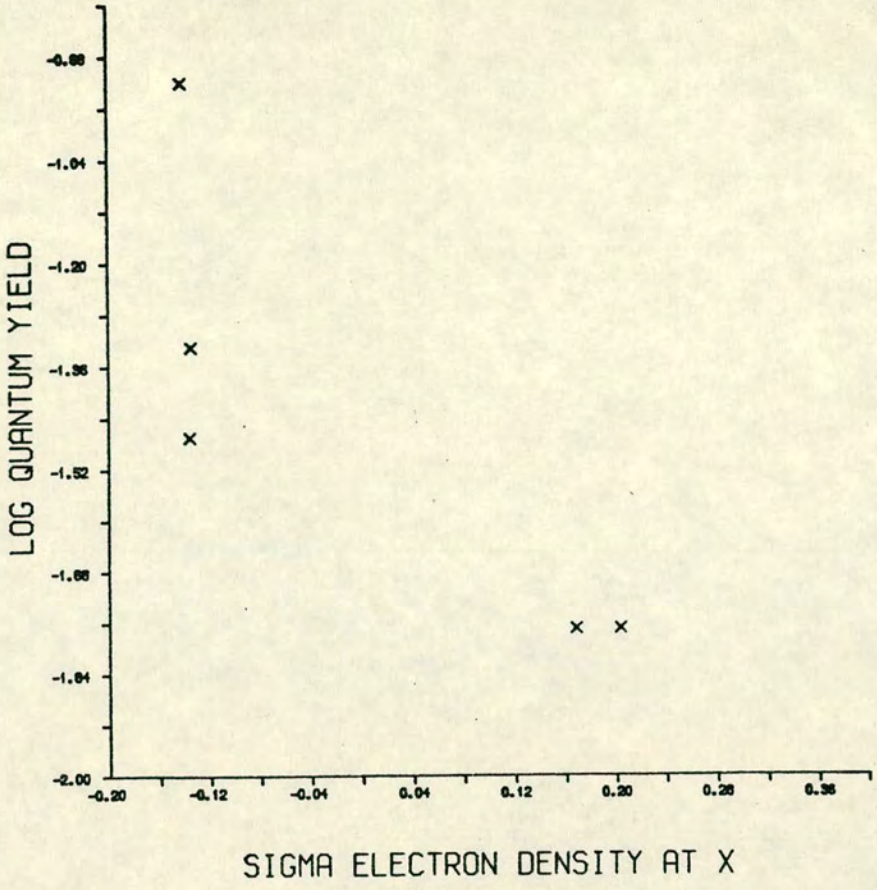

FIGURE 21

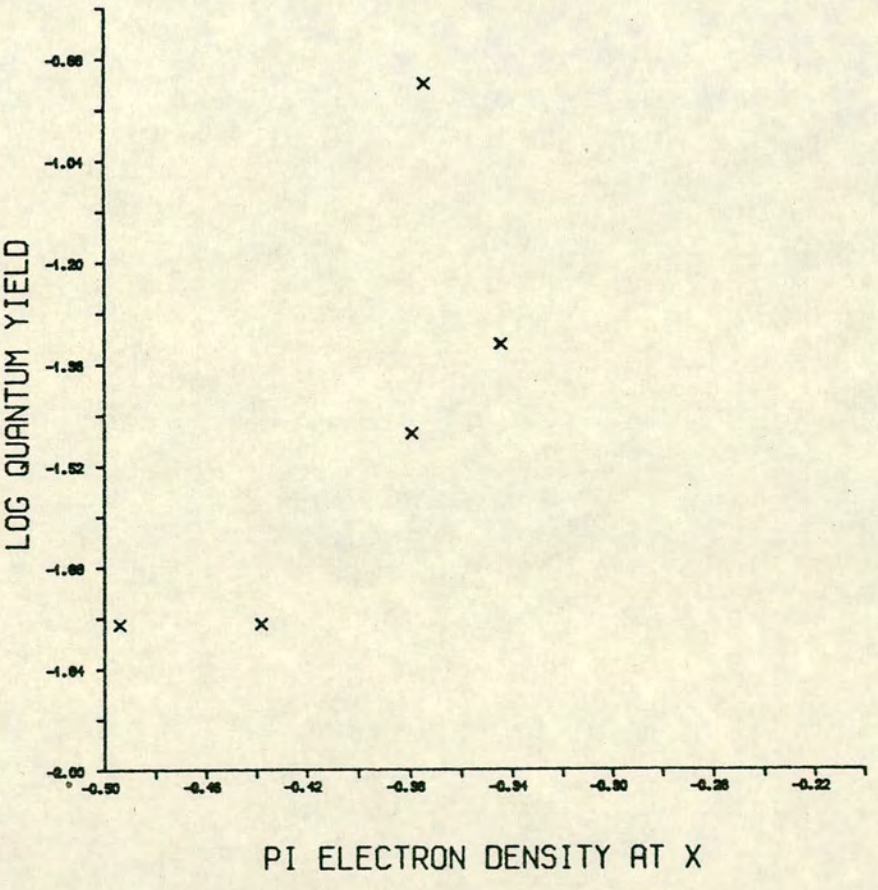

FIGURE 22

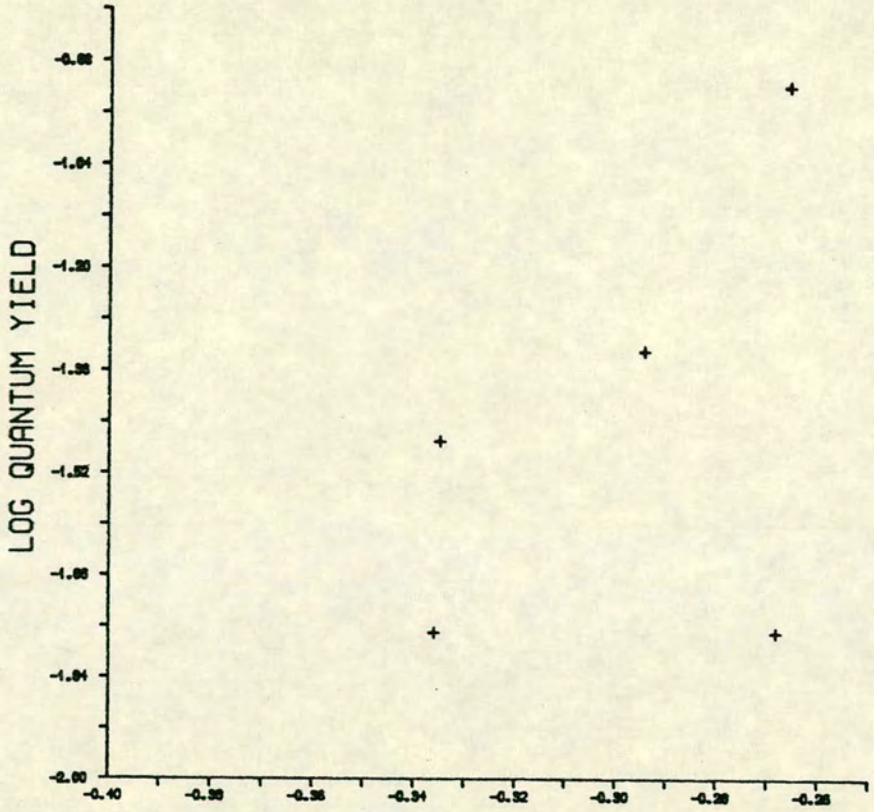

FIGURE 23

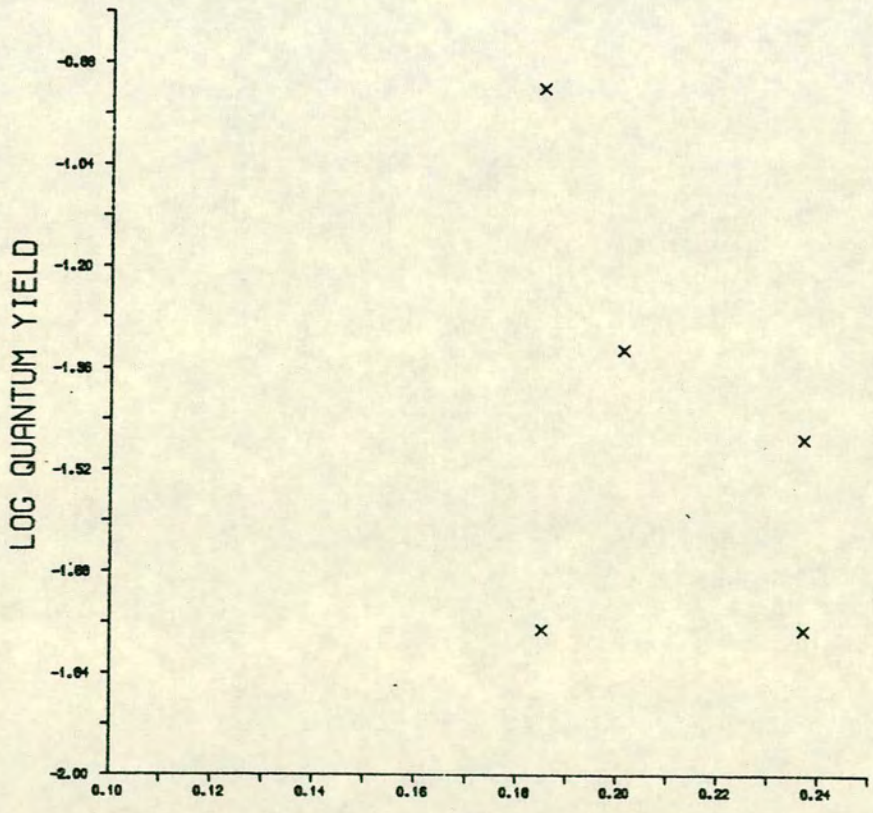

FIGURE 24

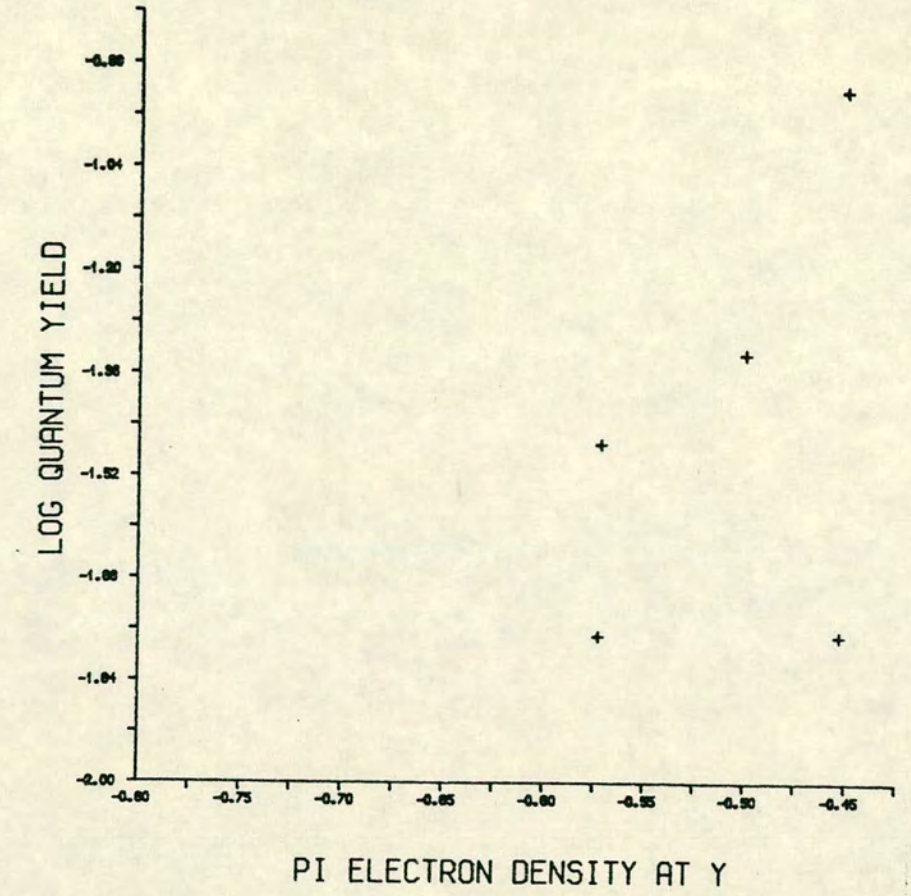

FIGURE 25

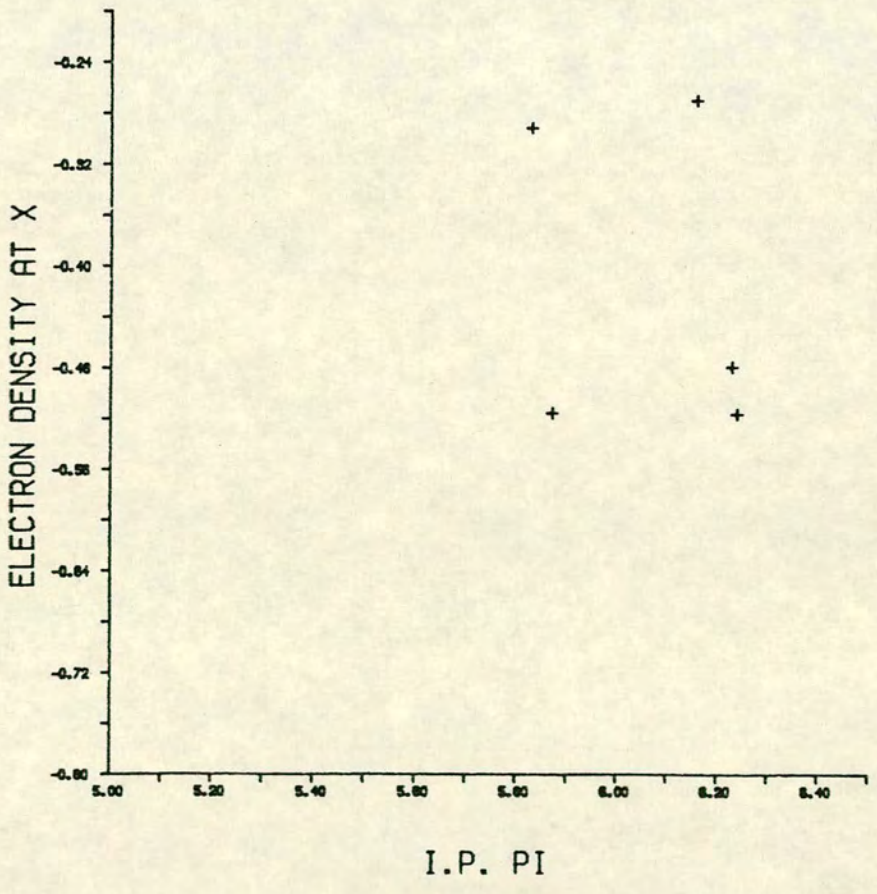

FIGURE 26

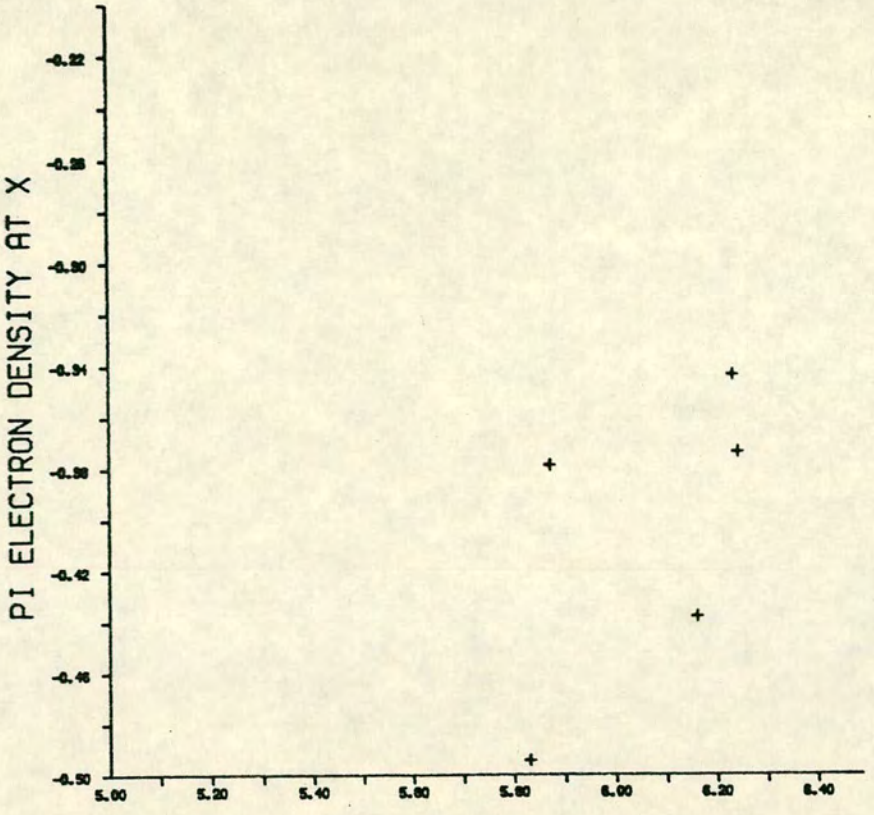

FIGURE 27

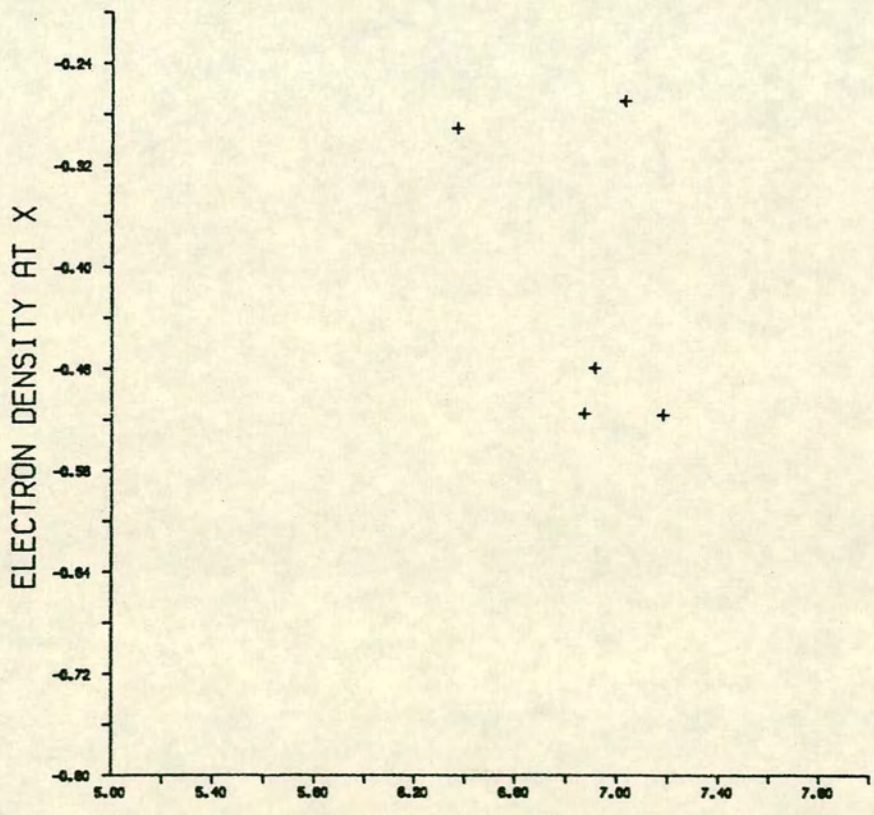

FIGURE 28

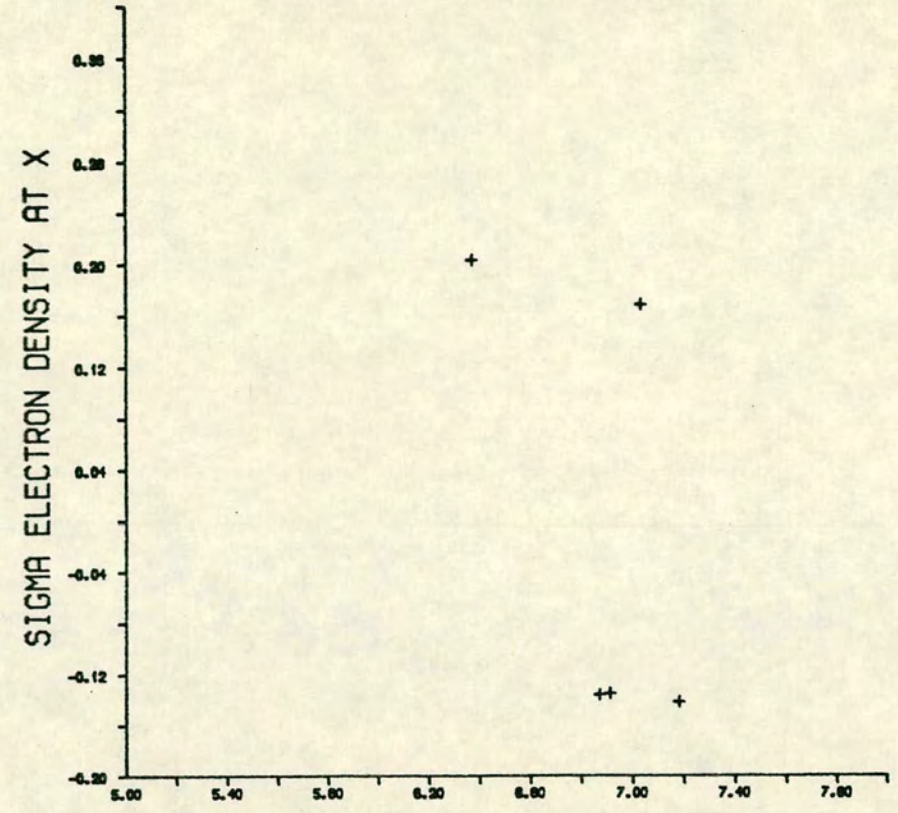

I.P. SIGMA

FIGURE 29

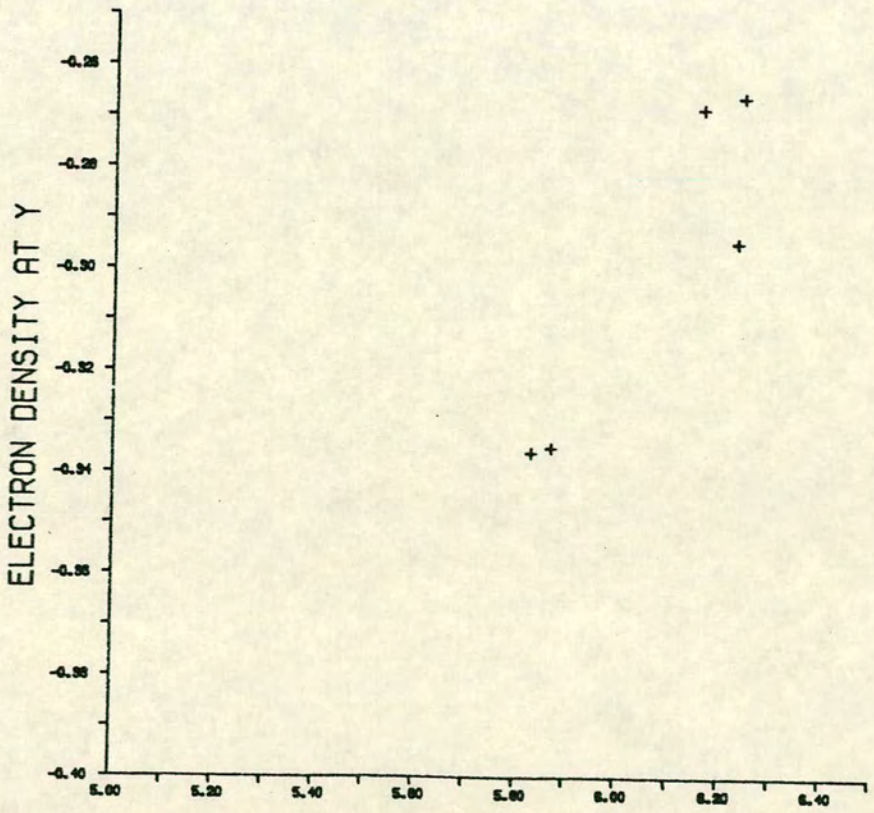

I.P. PI

FIGURE 30

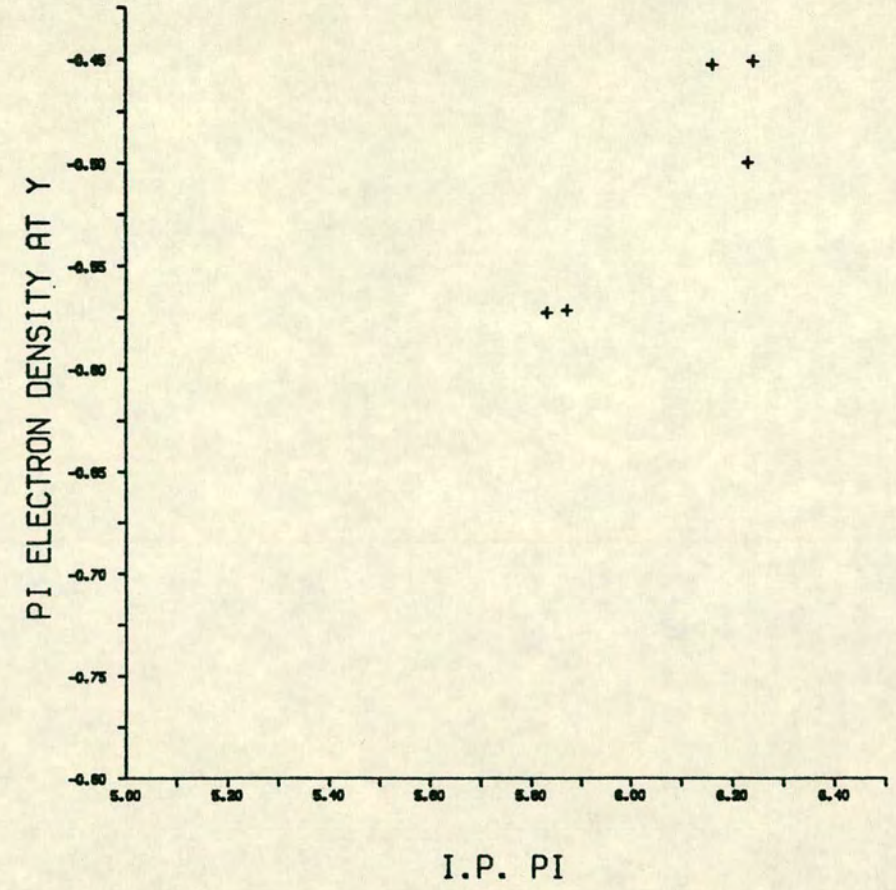

FIGURE 31

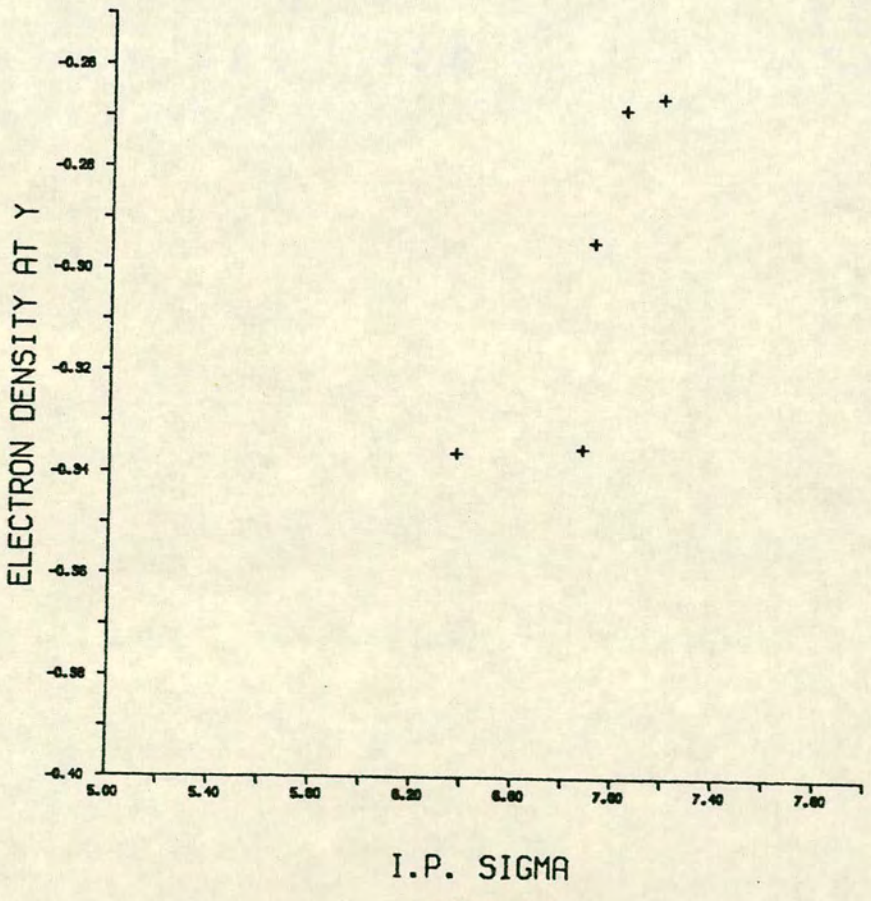

FIGURE 32

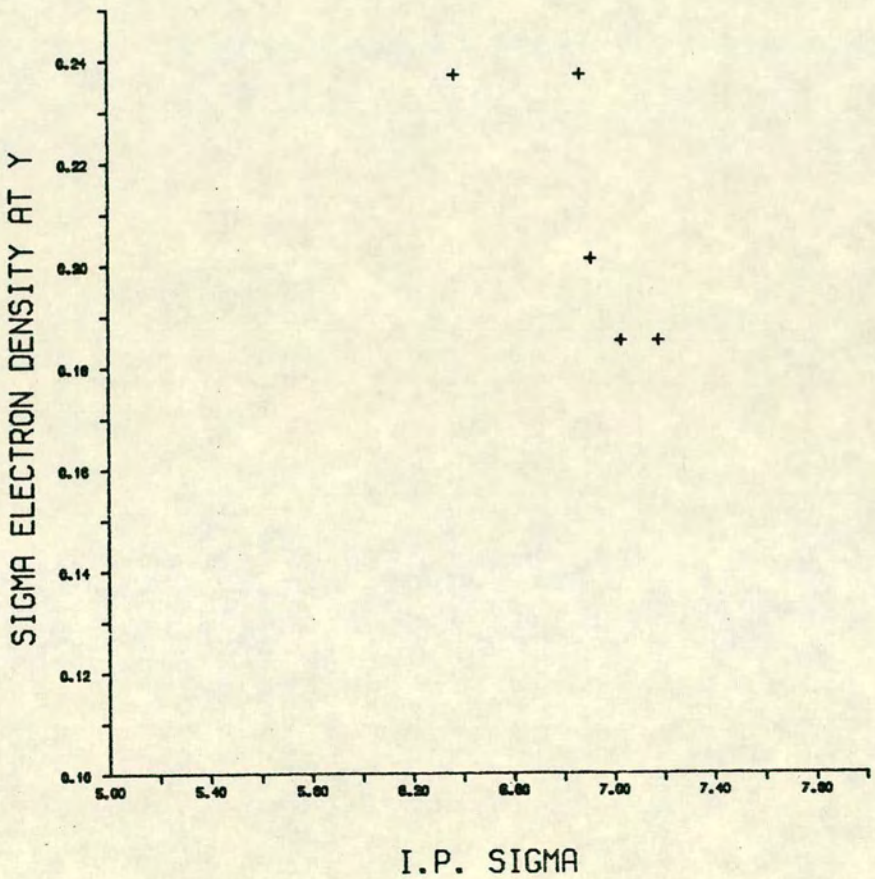
SIGMA ELECTRON DENSITY AT Y
0.24
0.22
0.20
0.18
0.16
0.14
0.12
0.10
5.00
5.40
5.80
6.20
6.60
7.00
7.40
7.80
I.P. SIGMA

FIGURE 33

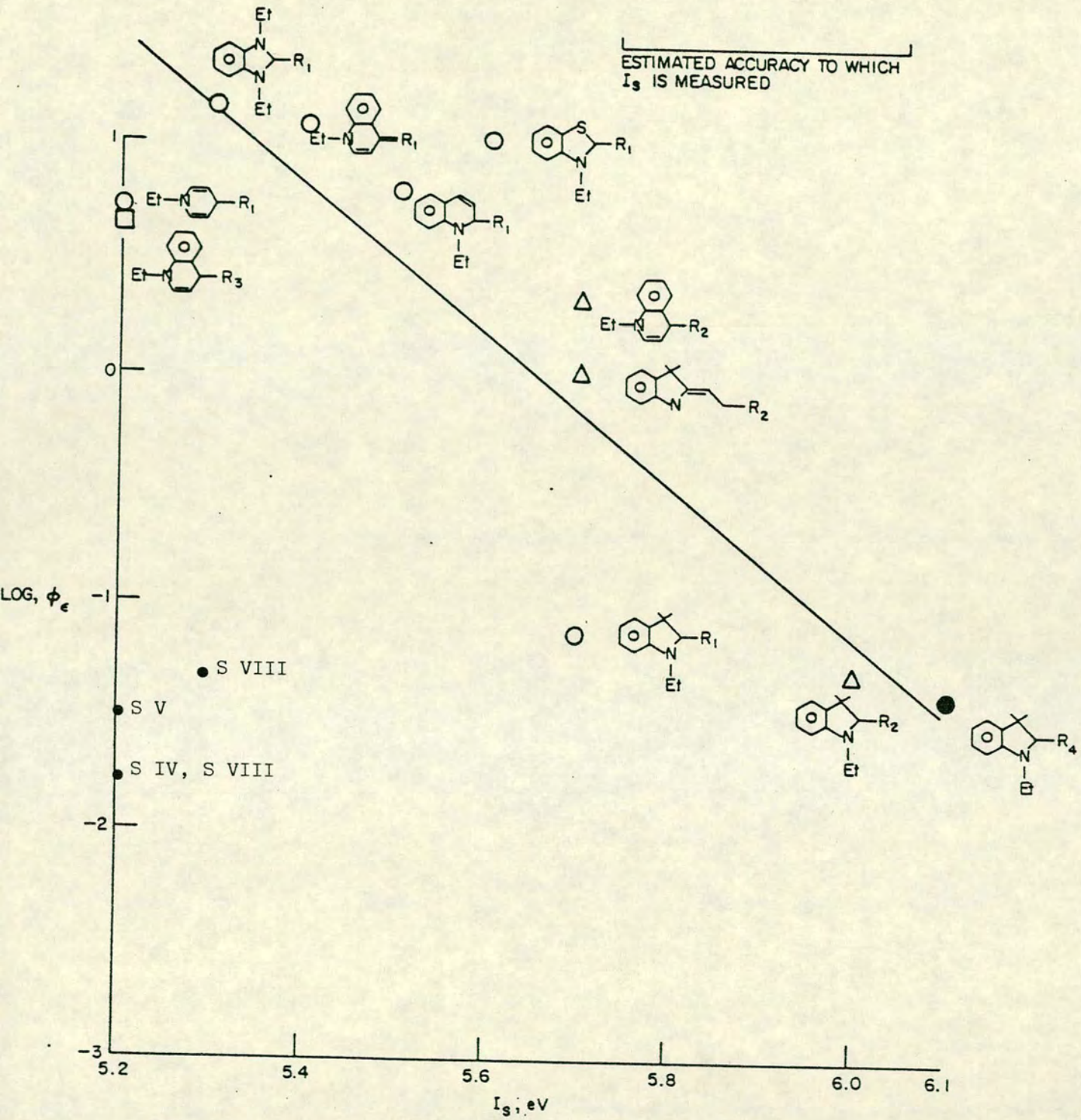

FIG. 34 —Relationship between quantum yield and ionisation potential For a series of merocyanine dyes.

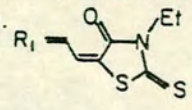

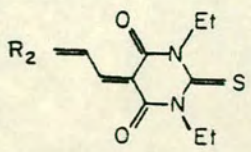

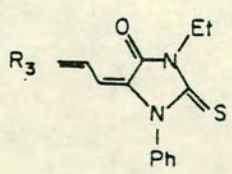

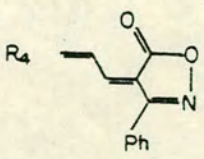

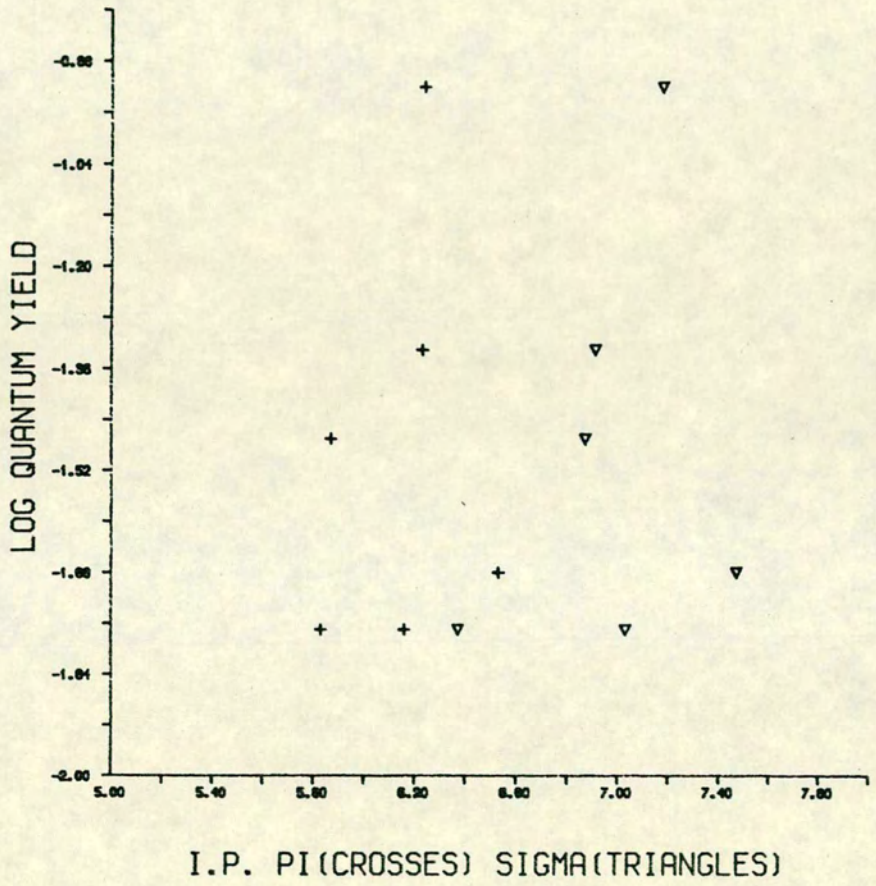
LOG QUANTUM YIELD
-0.88
-1.04
-1.20
-1.36
-1.52
-1.68
-1.84
-2.00
5.00
5.40
5.80
6.20
6.60
7.00
7.40
7.80
I.P. PI(CROSSES) SIGMA(TRIANGLES)

FIGURE 35

CHAPTER III

A SEMI-EMPIRICAL MODEL FOR THE APPLIED VOLTAGE/PHOTOCURRENT CHARACTERISTICS OF MEROCYANINE SOLAR CELLS

An understanding of the mechanism of photocurrent generation in organic photovoltaic cells is of central importance if practical cells are to be developed. The dominant mechanism of carrier photogeneration in molecularly doped organic cells is believed to be a bulk phenomenon in which excitons created by light absorption dissociate at the trapped dopant sites. In this process an electron is transferred from the exciton to the trap site. If the process occurs in the built-in field region (depletion layer) of the metal/organic semiconductor rectifying junction, then there is a possibility that the transferred electron and its counter charge (a hole) will escape their mutual coulombic attraction and drift to opposite electrodes giving rise to a photocurrent, (the mechanism for charge generation in merocyanines is given in Ch. 2, Introduction). The competing geminate recombination reaction leads to a loss of photogenerated carriers and a reduction in quantum efficiency.

Several models have been used to explain carrier recombination in low mobility materials. The most commonly used model is the Onsager theory of geminate recombination [1], which has been moderately successful in describing the photoactivity of organic semiconductors such as anthracene [2,3], napthalene [4], poly-n-vinylcarbazole [5], the poly-n-vinyl carbazole-trinitrofluorenone charge transfer complex [6] and poly 9,6 di(N-carbazoyl)-2,4 hexadiyne [7].

In this chapter the Onsager theory has been applied to merocyanines to produce a semi-empirical model which predicts the applied voltage/photocurrent characteristics of merocyanine solar cells.

Theory

Constant illumination of an organic cell gives rise to a steady state distribution of excitons given by

$$D \frac{d^2c}{dx^2} - kc + \alpha I_o \exp(-\alpha x) = 0 \qquad (1)$$

where D is the one dimensional diffusion coefficient of excitons at a given plane at a distance x from the Aluminium/dye interface (x = 0), k the total annihilation rate constant for excitons, α the absorption coefficient at wavelength λ, and I_o the flux density of unreflected monochromatic photons entering the organic film [8]. Since excitons are rapidly quenched at metal electrodes, the boundary conditions c = 0 at x = 0 and x = d (the total thickness of the organic layer) are used to obtain the exciton distribution.

$$C(x) = \frac{I_o\alpha}{k(1-\alpha^2L^2)}\left[\exp(-\alpha x) + \frac{\exp(x/L)}{\exp(d/L)-\exp(-d/L)}\left[\exp(-d/L)-\exp(-\alpha d)\right]\right.$$

$$\left. - \frac{\exp(-x/L)}{\exp(d/L)-\exp(-d/L)}\left[\exp(d/L)-\exp(-\alpha d)\right]\right] \qquad (2)$$

where L is the exciton diffusion length ($=\sqrt{D/k}$). If the excitons dissociate with rate constant k_d at dopant sites of uniform distribution and concentration N_d, the rate of exciton dissociation to charge carriers at x is $k_d N_d\, c(x)$.

However only a fraction of these carriers escape from their mutual coulombic attraction. The Onsager theory of geminate recombination assumes that the primary photogeneration step involves the absorption of a photon to produce a hot electron-hole pair separated by an initial distance, r_o. The photo-excited carrier pair then have an excess of kinetic energy given by $h\upsilon - \lambda_g + E_c(r)$, where $h\upsilon$ is the photon energy, λ_g is the band gap (threshold absorption energy), r is the pair separation

and $E_c(r) = e^2/4\pi\varepsilon\varepsilon_o r$ is the coulomb energy of the pair. If r_c is the distance at which $E_c \approx kT$, then production of charge carriers is only guaranteed when the electron-hole pair are separated by a distance greater than r_c before thermalisation. Otherwise geminate recombination is more likely than the creation of a free carrier pair.

The Onsager approach models geminate recombination on the basis of Brownian motion in the presence of a coulombic attraction and an applied field E [1]. For two charges, the relevant equation of Brownian motion is given by

$$\frac{\partial f}{\partial t} = \frac{kT}{e} (\mu_1 + \mu_2) \operatorname{div}(e^{-U/kT} \operatorname{grad} f e^{U/kT}) \qquad (3)$$

where μ_1 and μ_2 are the mobilities of the two charge carriers, and U is the coulomb potential modified by the applied electric field [1, 9]. Onsager showed that the probability $\rho(r,\theta,E)$, that an ion pair thermalised with an initial separation r and orientated at an angle θ with respect to the applied field E will escape initial recombination, is given by

$$\rho(r,\theta,E) = e^{-A} e^{-B} \sum_{n=0}^{\infty} \sum_{m=0}^{\infty} \frac{A^m}{m!} \frac{B^{m+n}}{(m+n)!} \qquad (4)$$

where $A = e^2/4\pi\varepsilon\varepsilon_o kTr$ and $B = (eEr/2kT)(1 + \cos\theta)$

Defining ϕ_o as the efficiency of production of thermalised ion pairs per adsorbed photon and $g(r,\theta)$ as the initial spatial distribution between ions of each pair, the overall generation efficiency is given by

$$\phi(E) = \phi_o \int \rho(r,\theta,E) g(r,\theta) d^3r \qquad (5)$$

where ϕ_o is assumed to be independent of the strength of the applied

field. If one assumes that the initial distribution of thermalised pairs is an isotropic δ function, then

$$g(r,\theta) = (1/4\pi r_o^2)\ \delta(r-r_o) \tag{6}$$

where r_o is a characteristic thermalisation length.

Substituting this result into eqn. (3) and integrating yields the following expression for the overall generation efficiency.

$$\phi(r_o,E) = \phi_o\ \phi_{esc}\ (r_o, E) \tag{7}$$

where

$$\phi_{esc}(r_o,E) = \frac{kT}{eEr_o}\ e^{-A} \sum_{m=o}^{\infty} \frac{A^m}{m!} \times \sum_{n=o}^{\infty}\left[1-e^{-eEr_o/kT} \sum_{\ell=o}^{m+n}\left(\frac{eEr_o}{kT}\right)^{\ell} \frac{1}{\ell!}\right] \tag{8}$$

which can be rewritten as

$$\phi_{esc}(r_o,E) = \frac{kT}{eEr_o}\ e^{-A}\ e^{-eEr_o/kT} \times \sum_{m=o}^{\infty}\frac{A^m}{m!} \sum_{n=o}^{\infty} \sum_{m+n+1}^{\infty}\left(\frac{eEr_o}{kT}\right)^{\ell} \frac{1}{\ell!} \tag{9}$$

where $A = e^2/4\pi\ \kappa\varepsilon\varepsilon_o kTr_o$, e is the electronic charge, ε is the dielectric constant, ε_o is the vacuum permitivitty and r_o is the thermalisation distance of the intially generated charge pairs [9]. Taking into consideration geminate recombination, the generation rate of carriers at x is given by

$$K_d\ N_d\ c(x)\phi_{esc}(r_o,E) \tag{10}$$

where K_d is the rate constant for exciton dissociation and N_d is the concentration of dopant sites.

During the fabrication of the cell a built-in field arises due to electron diffusion during equalisation of the Fermi energies at the barrier metal/organic semiconductor contact. The barrier width W is determined by the physics of an ideal Schottkey contact [8, 10] and

to a good approximation W is given by

$$W = \left[\frac{2\varepsilon\varepsilon_o}{eN_A} (V_{bi} \pm V)\right]^{\frac{1}{2}} \quad (11)$$

where ε is the semi-conductor permittivity, N_A the density of ionised acceptors, V_{bi} the built-in diffusion potential and V the applied field, see fig. (1). The field strength at x, by the depletion layer approximation, is given by

$$E(x) = \frac{eNa}{\varepsilon\varepsilon_o} (x - w) \quad (12)$$

and the potential drop across the depletion layer is given by

$$V_{bi} = \int_o^w E(x)dx = \left(\frac{eNa}{2\varepsilon\varepsilon_o}\right)w^2 \quad (13)$$

where N_a is the acceptor density responsible for the dark semiconductor of the p-type organic semiconductor [11]. If an external voltage, V, is applied to the cell, the depletion layer width varies according to

$$W = W_o\left(\frac{V_{bi} \pm V}{V_{bi}}\right)^{\frac{1}{2}} \quad (14)$$

where W_o is the depletion layer width at zero bias, and the ± signs are for reverse and forward bias conditions respectively.

Since the field strength varies within the depletion layer according to eqn. (12), eqn. (10) can be rewritten an

$$\text{Rate of carrier generation} = k_d N_d C(x)\phi_{esc}(r_o, E(x))$$
$$= k_d N_d C(x)\phi_{esc}(r_o, x) \quad (15)$$

Assuming that only charge carriers generated in the depletion region contribute to the photocurrent and that there is no 'non-geminate' recombination, the photocurrent J_{ph} is given by

$$J_{ph} = ek_d N_d \int_o^w \phi_{esc}(r_o, x)\, C(x)\, dx \quad (16)$$

where w is the width of the depletion layer [11]. The function C(x) contains constants α, I_o, L and k (the total annihilation rate constant for excitons) which can be written outside the integration, therefore eqn. (16) can be rewritten.

$$J_{ph} = \frac{ek_dN_dI_o\alpha}{k(1-\alpha^2L^2)} \int_o^w \left[\exp(-\alpha x) + \frac{\exp(x/L)}{\exp(d/L)-\exp(-d/L)}\left(\exp(-d/L)-\exp(-\alpha d)\right)\right.$$

$$\left. - \frac{\exp(-x/L)}{\exp(d/L)-\exp(-d/L)}\left(\exp(d/L)-\exp(-\alpha d)\right)\right]\phi_{esc}(r_o,x)dx \quad (17)$$

The quantum yield is then given by

$$\phi_i = J_{ph}/eI_o \quad (18)$$

Therefore the quantum yield can be calculated by the numerical integration of

$$\phi_i = \frac{k'\alpha}{(1-\alpha^2L^2)} \int_o^w \left[\exp(-\alpha x) + \frac{\exp(x/L)}{\exp(d/L)-\exp(-d/L)}\left(\exp(-d/L)-\exp(-\alpha d)\right)\right.$$

$$\left. - \frac{\exp(-x/L)}{\exp(d/L)-\exp(-d/L)}\left(\exp(d/L)-\exp(-\alpha d)\right)\right]\phi_{esc}(r_o,x)dx \quad (19)$$

$$\text{where } k' = \left(\frac{k_dN_d}{k}\right)^{-1} \quad (20)$$

Since k_d is the rate constant for exciton dissociation, N_d the concentration of dopant sites and k is the total annihilation rate constant for excitons, $(k')^{-1}$ is equivalent to ϕ_o in eqn. (5). Where ϕ_o is defined as the efficiency of production of thermalised ion pairs per adsorbed photon.

One would expect r_o, the thermalised distance, to be strongly wavelength-dependent since r_o is associated with the excess kinetic energy of the photo-excited carrier pair, and this is observed

experimentally for selenium [9]. However, the quantum efficiency of carrier generation in many organic thin films is independent of the wavelength of the incident radiation and the photoconductivity or photovoltaic threshold coincides with the absorption threshold [11]. These observations indicate that rapid relaxation in the excited state occurs before the carrier generation step, and therefore r_o is wavelength independent. A typical thermalisation distance for an organic film is about 30Å [12, 13].

Appendix 1 contains a new Fortran program which integrates eqn. (19) numerically (using a NAG routine, DØ1AJF). This program was used to calculate the theoretical quantum yields of a typical merocyanine cell.

The program requires ten data parameters:

i) α, absorption coefficient at wavelength λ (2.3×10^5 cm^{-1}).

ii) k', defined by eqn. (20) (value used = 1).

iii) L, exciton diffusion length (taken as about 30Å, which is a reasonable value for an amorphous organic film [8].)

iv) D, the thickness of the merocyanine layer (generally about 500Å [8]).

v) N_a, the acceptor density responsible for dark conductivity ($N_a = 1 \times 10^{18} cm^{-3}$ [8]).

vi) ε, the dielectric constant (4.5).

vii) kT, temperature (K) multiplied by Boltzmanns constant (kT=.026 eV).

viii) r_o, the thermalisation distance (30Å).

ix) E, the field strength at which r_o has the value given above. (1×10^5 Vcm^{-1})

x) W, the width of the depletion layer (this has been determined experimentally as 230Å for zero applied bias [8]).

The above values were used to calculate the quantum yield at zero applied bias, and Table 1 contains the program output. The program allows for the fact that r_o, the thermalisation distance, varies with the field strength E which is a function of x, E(x). Poole-Frenkel theory allows for the fact that the Coulomb potential of two charge carriers is lowered by an applied field [14]. The relationship between r_o and E is given by

$$\frac{h\nu_p^2}{D} r_o^2 = (h\upsilon - E_g) + \frac{e^2}{\varepsilon_o \varepsilon r_o} + eEr_o \qquad (21)$$

where υ_p is a phonon frequency, D is the diffusion coefficient and E_g is the band separation energy. If $h\upsilon_p^2$ is taken as a constant, the field dependence of r_o can be solved iteratively using eqn. (21), providing one knows r_o at a given field strength. Table 1 indicates that r_o is effectively constant in any case. Calculating $\phi_{esc}(r_o,x)$ involves summing over a series (eqn. (9)), the program terminates a series when the last contributing terms is less than 10^{-4} of the cumulative total.

Tables 2,3 and 4 contain calculated quantum yields using the parameter values given previously for parameters (i) to (ix). Parameter (x), the width of the depletion layer, was allowed to vary; the values of w are tabulated with the corresponding applied voltages (calculated from eqn. (14), W_o = 230Å). Tables 2,3 and 4 also contain the experimental photocurrents and dark currents from ref. [8, 15].

The tabulated quantum yields were calculated on the assumption that k' = 1, since $(k')^{-1}$ represents the probability of exciton dissociation., this is clearly invalid. There is no experimental data available to

estimate k'. However, the photocurrent is related to the quantum yield by eqn. (18) and since k' has been set to 1, inspection of eqns. (17), (18) and (19) indicate that the relationship between the observed photocurrent and the calculated quantum yield is given by

$$I_{ph(exp)} = \frac{\phi_{i(calc)}}{C} \tag{21}$$

where

$$C = \frac{k}{k_d N_d I_o 10^{-Al} e} \tag{21a}$$

and Al is the aluminium absorbance.

The total current is given by

$$I_{tot} = I_{ph} + I_{DARK} \tag{22}$$

At zero applied bias the dark photocurrent is zero. Therefore if one calculates C_o (where the subscript o indicates zero applied bias) from eqn. (21), C_o can be used as a 'fitting parameter'. Theoretical photocurrents at other applied voltages can then be calculated from

$$I(v)_{ph,theor} = \frac{\phi_i(v)_{calc}}{C_o} \tag{23}$$

The total theoretical current at voltage (V) is then obtained from

$$I(v)_{theor} = I(v)_{ph,theor} + I_{DARK} \tag{24}$$

where I_{DARK} has been obtained experimentally. Therefore, by determining C_o from eqn. (21), the photocurrent/voltage characteristics can be predicted using equations (23) and (24) and the theoretical quantum yields $\phi_{i(calc)}$. The theoretical photocurrents (triangles) and the experimental photocurrents (crosses) have been plotted against applied voltage for 3 different incident wavelengths in figures 2,3,4. The corresponding numerical values are tabulated in tables (2), (3), (4) and the experimental date is taken from ref. [8, 15].

The 'fitting parameter' C_o can then be used to predict other quantities such as k'. Taking the data for a cell irradiated by light, λ = 633 nm, the fitting parameter $C_{o,633}$ is given by $\phi_{i(calc)}/J_{ph(exp)}$ at zero applied bias (see table 2, ref [8, 15]).

$$C_{o,633} = \frac{.1195}{2.1.10^{-6}} = 5690.5$$

The exciton dissociation probability $\frac{k}{k_d N_d}$

can then be calculated from eqn. (21a). Therefore $\frac{k}{k_d N_d} = C_{o,633} s I_o x 10^{-A1} x e.$

Where $C_{o,633} = 56900.5$

$I_o = 6.375.10^{15}$

$10^{-A1} = 10^{-.5} = 0.3$

$e = 1.6.10^{-19}$

Using these values, the exciton dissociation probability is 0.57.

Conclusion

The semi-empirical model produces remarkably good agreement between theory and experiment. The 'fitting parameter' C_o also predicts a sensible exciton dissociation probability. The model has also been used to study the effects of diffusion length L, the absorption coefficient α, the thermalisation distance r_o and temperature on quantum yield. The results are indicated graphically in figures 5 → 8.

References

1. L. Onsager, J. Chem. Phys., 2 (1934) 599; Phys. Rev., 54 (1938) 554.
2. R.R. Chance and C.L. Brown, J. Chem. Phys., 64 (1976) 3573.
3. R.H. Batt, C.L. Brown and J.R. Horning, J. Chem. Phys., 49 (1967) 1967.
4. V.N. Joshi and M. Castillo, Chem. Phys. Lett., 46 (1977) 317.
5. G. Pfister and D.J. Williams, J. Chem. Phys., 61 (1974) 2416.
6. P.J. Melz, J. Chem. Phys., 57 (1972) 1694.
7. K. Lochner, H. Bassler, L. Sebastian, G. Weiser, G. Wegner and V. Enkelmann, Chem. Phys. Lett., 78 (1981) 366.
8. G.A. Chamberlain, J. Appl. Phys., 53 (1982) 6262.
9. D.M. Pai and R.C. Enck, Physical Review B, 11 (1975) 5163.
10. S.M. Sze, Physics of Semicondutor Devices (Wiley-Interscience, New York, 1969), p370.
11. G.A. Chamberlain, Sol. Cells, 8 (1983) 47.
12. G. Pfister and D.J. Williams, J. Chem. Phys., 61 (1974) 2416.
13. P.J. Melz, J. Chem. Phys., 57 (1972) 1694.
14. J.C. Knights and E. Davis, J. Phys. Chem. Solids; 35 (1974) 543-554.
15. G.A. Chamberlain, Private Communication.

APPENDIX 1

```
      REAL*8 A,EPSABS,EPSREL,RESULT,ABSERR
      REAL*8 E,ALPHA,K,L,D,W,NA,ES,E0,FK,FIELD,KT,R0,F0
      REAL*8 INC
      REAL*8 V(800)
      INTEGER IW(102)
      EXTERNAL CXESC
      COMMON ALPHA,K,L,D,W,FK,NA,ES,E0,KT,R0,F0
      DIMENSION SELECT(11)
      CHARACTER*6 SELECT
      CHARACTER*6 ANSWER
      CHARACTER*1 ANS
      SELECT(1)='ALPHA'
      SELECT(2)='K'
      SELECT(3)='L'
      SELECT(4)='D'
      SELECT(5)='W'
      SELECT(6)='????'
      SELECT(7)='NA'
      SELECT(8)='ES'
      SELECT(9)='????'
      SELECT(10)='KT'
       SELECT(11)='R0'
      E=-1.6D-19
      I=0
      NUMINC=1
      NINC=0
      WRITE(6,1005)
1005  FORMAT(' ','INPUT: ALPHA K L D W NA ES KT R0 FIELD FOR R0')
      READ(5,*) ALPHA,K,L,D,W,NA,ES,KT,R0,F0
      E0=8.854D-14
      FK=E*NA/(ES*E0)
      WRITE(6,2005)
2005  FORMAT(' ','    ALPHA       K       L       D      W')
      WRITE(6,3005) ALPHA,K,L,D,W
      WRITE(6,2006)
2006  FORMAT(' ','      NA         ES        KT        R0 AT      ',
     *'FIELD(V/CM)')
      WRITE(6,3005) NA,ES,KT,R0,F0
3005  FORMAT(5D14.4)
      A=0.0D0
      EPSABS=0.0D0
      EPSREL=1.0D-4
      IFAIL=0
      WRITE(6,43)
43    FORMAT(' ','DO YOU WISH ANY VARIABLE TO BE VARIED')
      READ(5,24) ANS
24    FORMAT(A1)
      IF(ANS.EQ.'Y') GO TO 98
99    WRITE(6,551)
551   FORMAT('1','       X      CXESC(X)       C(X)        ESC(X)      ',
     *'FIELD(X)       R0(CM)')
52    CALL D01AJF(CXESC,A,W,EPSABS,EPSREL,RESULT,ABSERR,V,800,IW,102,
     *IFAIL)
       WRITE(6,99998) A,W,EPSABS,EPSREL
99998 FORMAT('1','A ',D14.4,'W ',D14.4,' EPSABS ',F6.2,'EPSREL ',D14.4)
      WRITE(6,99999) RESULT,ABSERR,IW(1),IFAIL
99999 FORMAT(' ','RES ',D14.4,' AERR',F8.4,' IW(1)',I4,' IFAIL ',I2)
      IF (ANS.EQ.'N') GO TO 63
      CALL INCREMENT(I,INC)
      WRITE(10,54) RESULT
```

```
54    FORMAT(' ',D14.4)
      NINC=NINC+1
      IF (NINC.NE.NUMINC) GO TO 99
63    STOP
98    WRITE(6,92)
92    FORMAT(' ','TYPE IN VARIABLE TO BE VARIED')
      READ(5,103) ANSWER
103   FORMAT(A6)
      DO 101 J=1,11,1
      IF(ANSWER.EQ.SELECT(J)) I=J
101   CONTINUE
       WRITE(6,64)
64    FORMAT('TYPE IN NO. OF INCREMENTS & SIZE OF INC.')
      READ(5,*)NUMINC,INC
      GO TO 99
      END
      DOUBLE PRECISION FUNCTION CXESC  (XXX)
      REAL*8 PI,R10,R11
      REAL*8 RR1,R4,R5,R6,R7,R8,R12,A,B,C,R2,R3,R(1000)
      REAL*8 F0,DENOM,RSTORE,ROLD
      INTEGER X,Z,R9,R13,Y,R1
      PI=3.141592654D0
      REAL*8 ALPHA,K,L,D,ALPHA2,L2,P1,P2,PTOT1,PTOT2,PTOT3,CX,CXR1
      REAL*8 XXX,XX,FIELD,W,FK,NA,ES,E0,KT,R0,F0
      COMMON ALPHA,K,L,D,W,FK,NA,ES,E0,KT,R0,F0
      RR1=0.0D0
      XX=XXX
      FIELD=FK*(XX-W)
      PTOT1=DEXP(-ALPHA*XX)
      ALPHA2=ALPHA**2
      L2=L**2
      P1=DEXP(XX/L)/(DEXP(D/L)-DEXP(-D/L))
      P2=DEXP(-D/L)-DEXP(-ALPHA*D)
      PTOT2=P1*P2
      P1=DEXP(-XX/L)/(DEXP(D/L)-DEXP(-D/L))
      P2=DEXP(D/L)-DEXP(-ALPHA*D)
      PTOT3=P1*P2
      PTOT=PTOT1+PTOT2-PTOT3
      CX=ALPHA*PTOT/(K-K*ALPHA*L2)
405   FORMAT(' ','XXX=',F16.15)
      DENOM=DSQRT(2.56D-38/(ES*R0*E0)+1.6D-19*F0*R0+0.32D-19)
      RSTORE=R0
89     ROLD=DSQRT(2.56D-38/(ES*RSTORE*E0)+1.6D-19*FIELD*RSTORE+0.32D-19)
      ROLD=R0*ROLD/DENOM
       IF (DABS(ROLD-RSTORE).LE.1E-4*RSTORE) GO TO 79
       RSTORE=ROLD
       GO TO 89
79     R5=KT
       R6=FIELD
       R7=ROLD
       R4=ES
       R8=1.6E-19/(4*PI*R4*R5*8.854E-14)
       A=R8/R7
       B=R6*R7/R5
       IF (B.LE.0.0) GO TO 516
       R12=0.0D0
       X=0
3      Z=1
       Z=Z+X
        R9=Z
```

```
        R10=Z
       IF (Z.EQ.1) GO TO 1
2      Z=Z-1
       R11=Z*R10
       R10=R11
       IF (Z.GT.2) GO TO 2
1      Z=R9
       R2=Z*(B**Z)/R10
       R12=R12+R2
       IF (R2/R12.GT.0.0001) X=X+1
       IF (R2/R12.GT.0.0001) GO TO 3
       R(12)=R12
       R13=0.0D0
       R(13)=0.0D0
       Y=1
45     X=0
11     Z=1
       Z=Z+X
       R9=Z
       R10=Z+Y
       IF (Z+Y.EQ.1) GO TO 9
       R1=Z+Y-1
7      R11=R1*R10
       R10=R11
       IF (1.LE.R1) R1=R1-1
       IF (1.LE.R1) GO TO 7
9      Z=R9
       R3=(Z*B**(Z+Y))/R10
       R(13+Y-1)=R(13+Y-1)+R3
       IF (R3/R(13+Y-1).GT.0.0001) X=X+1
       IF (R3/R(13+Y-1).GT.0.0001) GO TO 11
12     Z=Y
       R9=Z
       R10=Z
       IF (Z.EQ.1) GO TO 20
30     Z=Z-1
       R11=Z*R10
       R10=R11
       IF (Z.GT.2) GO TO 30
20     Z=R9
       C=A**Z/R10
       R(13+Y-1)=R(13+Y-1)*C
       R(13+Y-1)=R(13+Y-1)+R(13+Y-2)
       IF (R(13+Y-2)/R(13+Y-1).GT.0.9999) GO TO 40
       Y=Y+1
       R(13+Y-1)=0.0D0
       GO TO 45
40     RR1=DEXP(-1.*A)*DEXP(-1.*B)*R(13+Y-1)/B
516    CXESC=CX*RR1
       CXR1=CX*RR1
       WRITE(6,351) XXX,CXR1,CX,RR1,FIELD,ROLD
351    FORMAT(' ',6D13.4)
       WRITE(7,357) XXX,RR1
357    FORMAT(' ',D14.4,' ',D14.4)
       WRITE(8,358) XXX,CX
358    FORMAT(' ',D14.4,' ',D14.4)
       WRITE(9,359) XXX,CXR1
359    FORMAT(' ',D14.4,' ',D14.4)
       RETURN
       END
```

```
      SUBROUTINE INCREMENT (I,INC)
      REAL*8 INC
      INTEGER I
      DIMENSION DUMMY(11)
      REAL*8 DUMMY
      COMMON DUMMY
      WRITE(10,34) DUMMY(I)
      DUMMY(I)=DUMMY(I)+INC
34    FORMAT(' ',D14.4)
      END
```

TABLE 1

ALPHA	K	L	D	W
0.2300D 06	0.1000D 01	0.3000D -06	0.5000D -05	0.2300D -05

NA	ES	KT	RO AT	FIELD(V/CM)
0.1000D 19	0.4500D 01	0.2600D -01	0.3000D -06	0.1000D 06

X	CXESC(X)	C(X)	ESC(X)	FIELD(X)	RO(CM)
0.1150D -05	0.6527D 05	0.1716D 06	0.3804D 00	0.4618D 06	0.3075D -06
0.4994D -08	0.2328D 04	0.3533D 04	0.6590D 00	0.9216D 06	0.3175D -06
0.2295D -05	0.2298D 04	0.1356D 06	0.1695D -01	0.2006D 04	0.2980D -06
0.3001D -07	0.1330D 05	0.2031D 05	0.6550D 00	0.9116D 06	0.3173D -06
0.2270D -05	0.2872D 04	0.1363D 06	0.2107D -01	0.1205D 05	0.1982D -06
0.8032D -07	0.3321D 05	0.4981D 05	0.6467D 00	0.8914D 06	0.3169D -06
0.2220D -05	0.4183D 04	0.1379D 06	0.3033D -01	0.3225D 05	0.2986D -06
0.1552D -06	0.5375D 05	0.8482D 05	0.6337D 00	0.8613D 06	0.3162D -06
0.2145D -05	0.6512D 04	0.1403D 06	0.4643D -01	0.6232D 05	0.2992D -06
0.2521D -06	0.7253D 05	0.1178D 06	0.6159D 00	0.8224D 06	0.3153D -06
0.2048D -05	0.1017D 05	0.1433D 06	0.7098D -01	0.1012D 06	0.3000D -06
0.3687D -06	0.8535D 05	0.1440D 06	0.5927D 00	0.7756D 06	0.3143D -06
0.1931D -05	0.1548D 05	0.1471D 06	0.1052D 00	0.1481D 06	0.3010D -06
0.5028D -06	0.9119D 05	0.1618D 06	0.5634D 00	0.7217D 06	0.3131D -06
0.1797D -05	0.2264D 05	0.1516D 06	0.1494D 00	0.2019D 06	0.3021D -06
0.6516D -06	0.9064D 05	0.1718D 06	0.5276D 00	0.6620D 06	0.3118D -06
0.1648D -05	0.3163D 05	0.1565S 06	0.2021D 00	0.2617D 06	0.3033D -06
0.8114D -06	0.8510D 05	0.1755D 06	0.4850D 00	0.5978D 06	0.3104D -06
0.1489D -05	0.4213D 05	0.1617D 06	0.2605D 00	0.3259D 06	0.3046D -06
0.9788D -06	0.7616D 05	0.1748D 06	0.4356D 00	0.5306D 06	0.3090D -06
0.1321D -05	0.5360D 05	0.1669D 06	0.3211D 00	0.3931D 06	0.3061D -06

A 0.0000D 00W 0.2300D -05 EPSABS 0.00EPSREL 0.1000D -03
RES 0.1190D 00 AERR 0.000 IW(1) 4 IFAIL 0

TABLE 2 λ = 633nm No Fitter $C_o = 5690.5\ A^{-1}$

Width of depletion layer	Q	Q/C_o (μA)	I_{DARK} (μA)	I_{THEOR} (μA)	I_{exp} (μA)	Applied voltage (volts)
176	.06847	12.03	-10.50	1.53	0	-.435
181	.07280	12.79	-9.00	3.79	2.75	-.4
194	.08450	14.85	-6.10	8.75	8.25	-.3
207	.09675	17.00	-3.75	13.25	13.00	-.2
219	.1085	19.07	-2.0	17.07	17.00	-.1
230	.1195	21.00	0	21.00	21.00	0
241	.1308	22.99	1.75	24.74	24.50	.1
251	.1412	24.82	3.75	28.57	28.75	.2
261	.1518	26.68	6.0	32.68	33.25	.3
270	.1614	28.37	8.75	37.12	37.75	.4
279	.1710	30.05	11.50	41.55	42.5	.5

TABLE 3 λ = 633nm 0.52 fitter $C_o = 1.116^{-1} \times 10^{4}\ A^{-1}$

Width of depletion layer	Q	Q/C_o (A)	I_{DARK} (A)	I_{THEOR} (A)	I_{exp} (A)	Applied voltage (volts)
176	.06847	6.16	-10.50	-4.34	-5.75	-.435
181	.07280	6.55	-9.00	-2.45	-3.00	-.4
194	.08450	7.60	-6.10	1.50	1.50	-.3
207	.09675	8.70	-3.75	4.95	5.00	-.2
219	.1085	9.76	-2.00	7.76	8.00	-.1
230	.1195	10.75	0	10.75	10.75	0
241	.1308	11.77	1.75	13.52	13.75	.1
251	.1412	12.70	3.75	16.45	16.75	.2
261	.1518	13.66	6.00	19.66	20.00	.3
270	.1614	14.52	8.75	23.37	24.00	.4
279	.1710	15.38	11.50	26.88	27.75	.5

TABLE 4 λ = 500nm No Fitter $C_o = 59750A^{-1}$

Width of depletion layer	Q	Q/C_o (A)	I_{DARK} (A)	I_{THEOR} (A)	I_{exp} (A)	Applied voltage (volts)
176	.06847	1.15	-10.50	-9.35	-8.8	-.435
181	.07280	1.22	-9.00	-7.78	-7.5	-.4
194	.08450	1.41	-6.10	-4.69	-4.6	-.3
207	.09675	1.62	-3.75	-2.13	-2.15	-.2
219	.1085	1.82	-2.0	-.18	0.1	-.1
230	.1195	2.00	0	2.00	2.0	0
241	.1308	2.19	1.75	3.94	4.1	.1
251	.1412	2.36	3.75	6.11	6.2	.2
261	.1518	2.54	6.0	8.54	8.5	.3
270	.1614	2.70	8.75	11.45	11.35	.4
279	.1710	2.86	11.50	14.36	14.35	.5

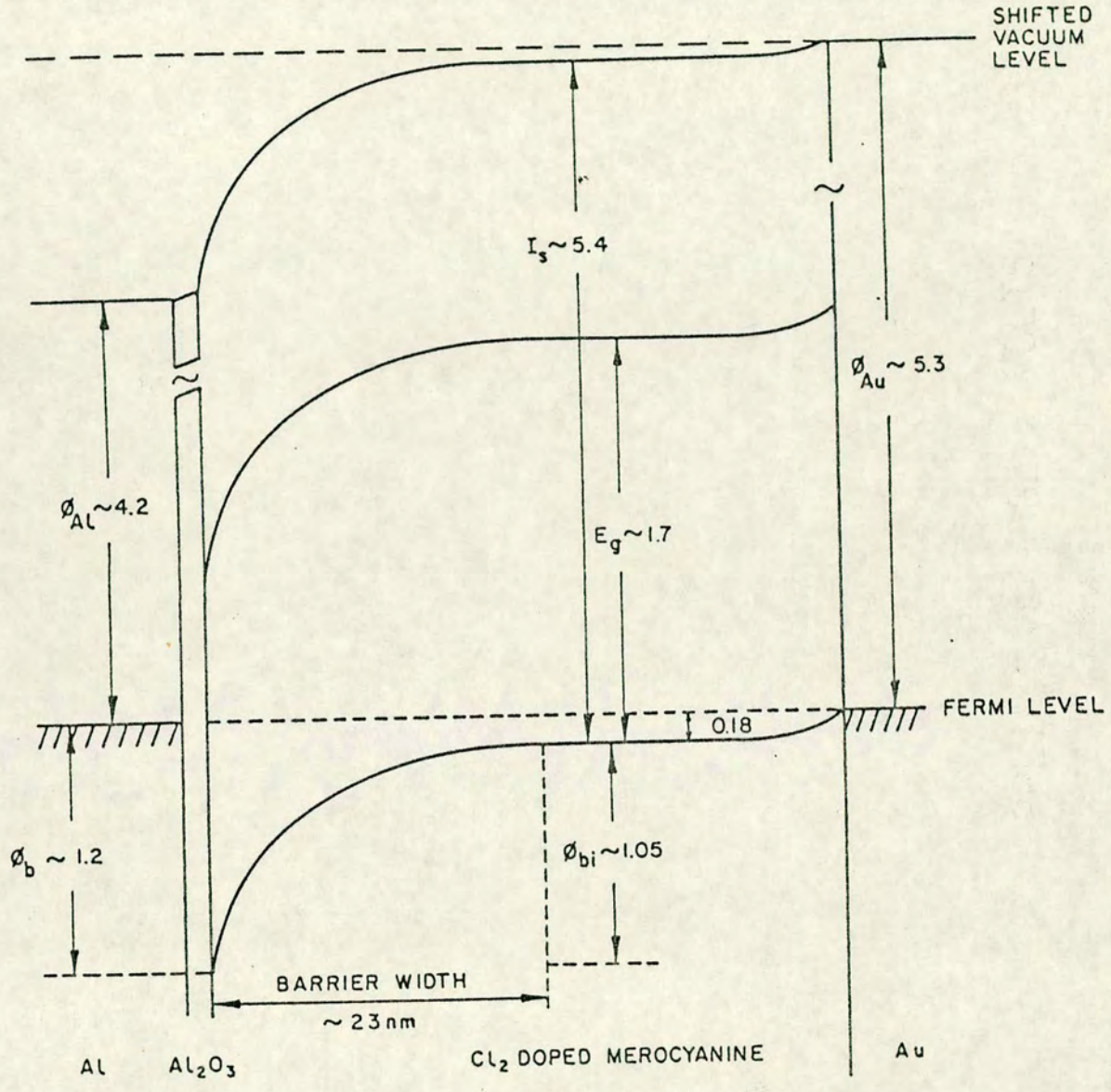

FIG. 1 - Energy level diagram for Al/Cl_2 doped merocyanine/Au photovoltaic cell. Energies are given in eV

PHOTO-CURRENT VS APPLIED VOLTAGE at 633 nm

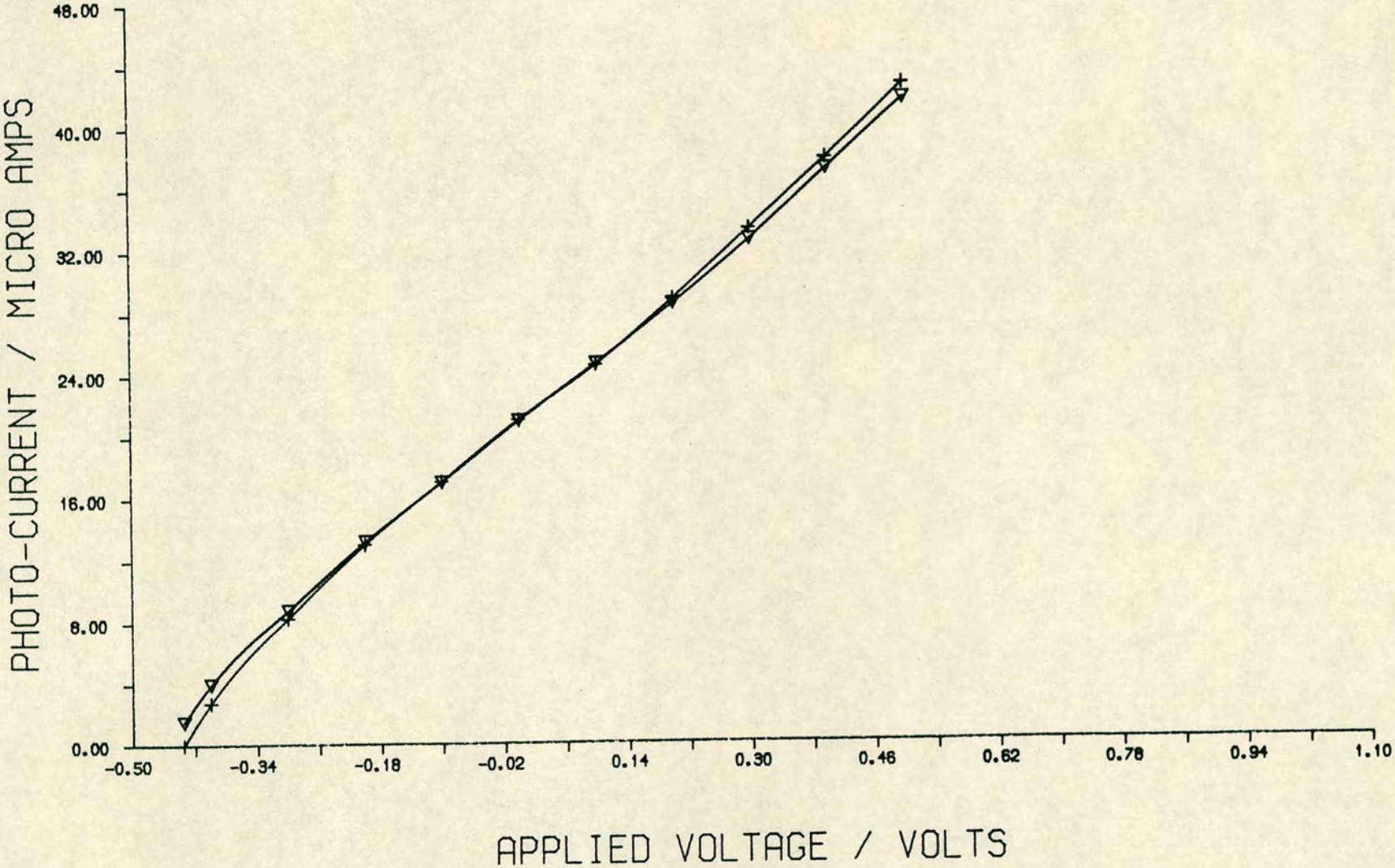

FIGURE 2

PHOTO-CURRENT VS APPLIED VOLTAGE at 633 nm 0.52 filter

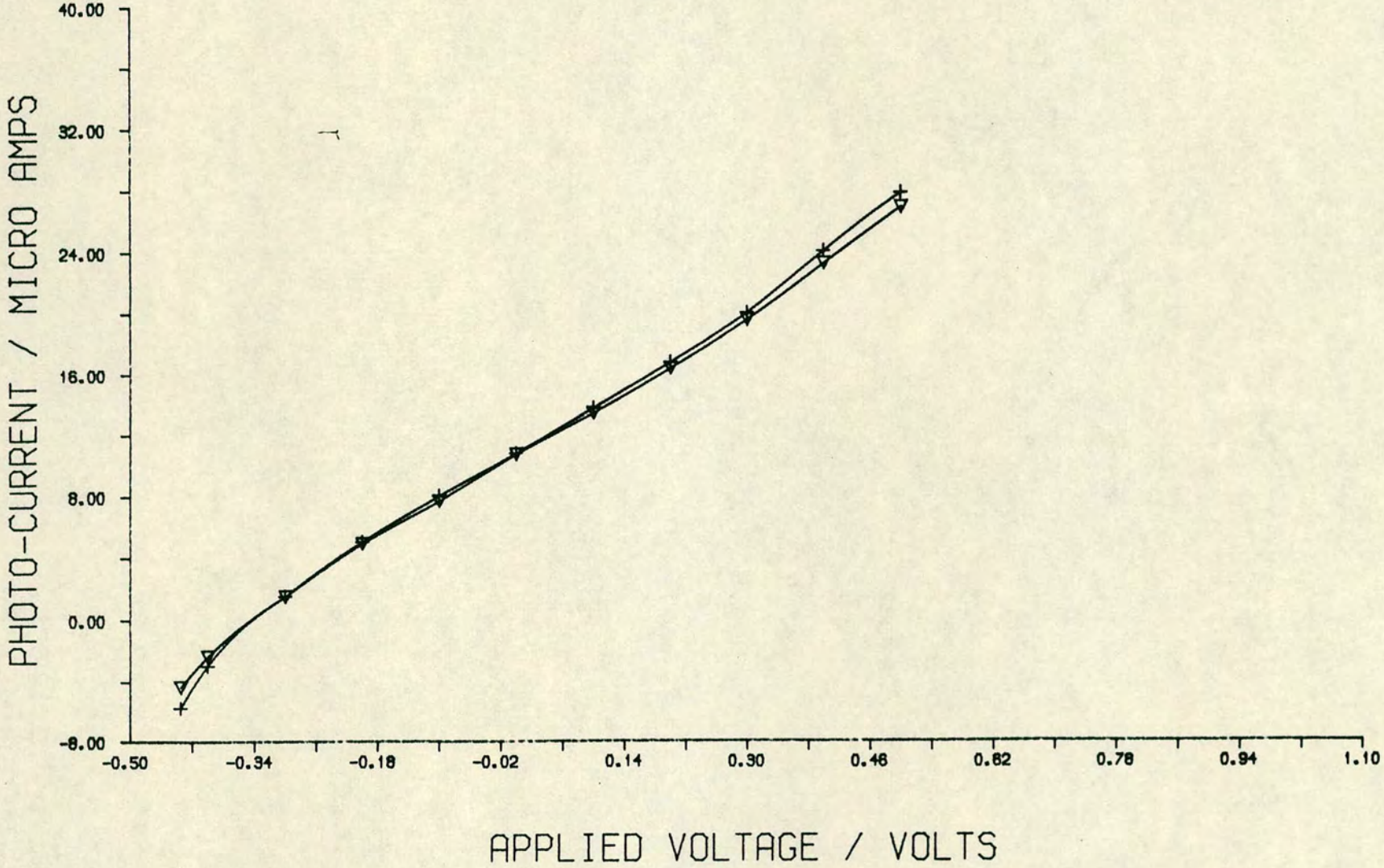

FIGURE 3

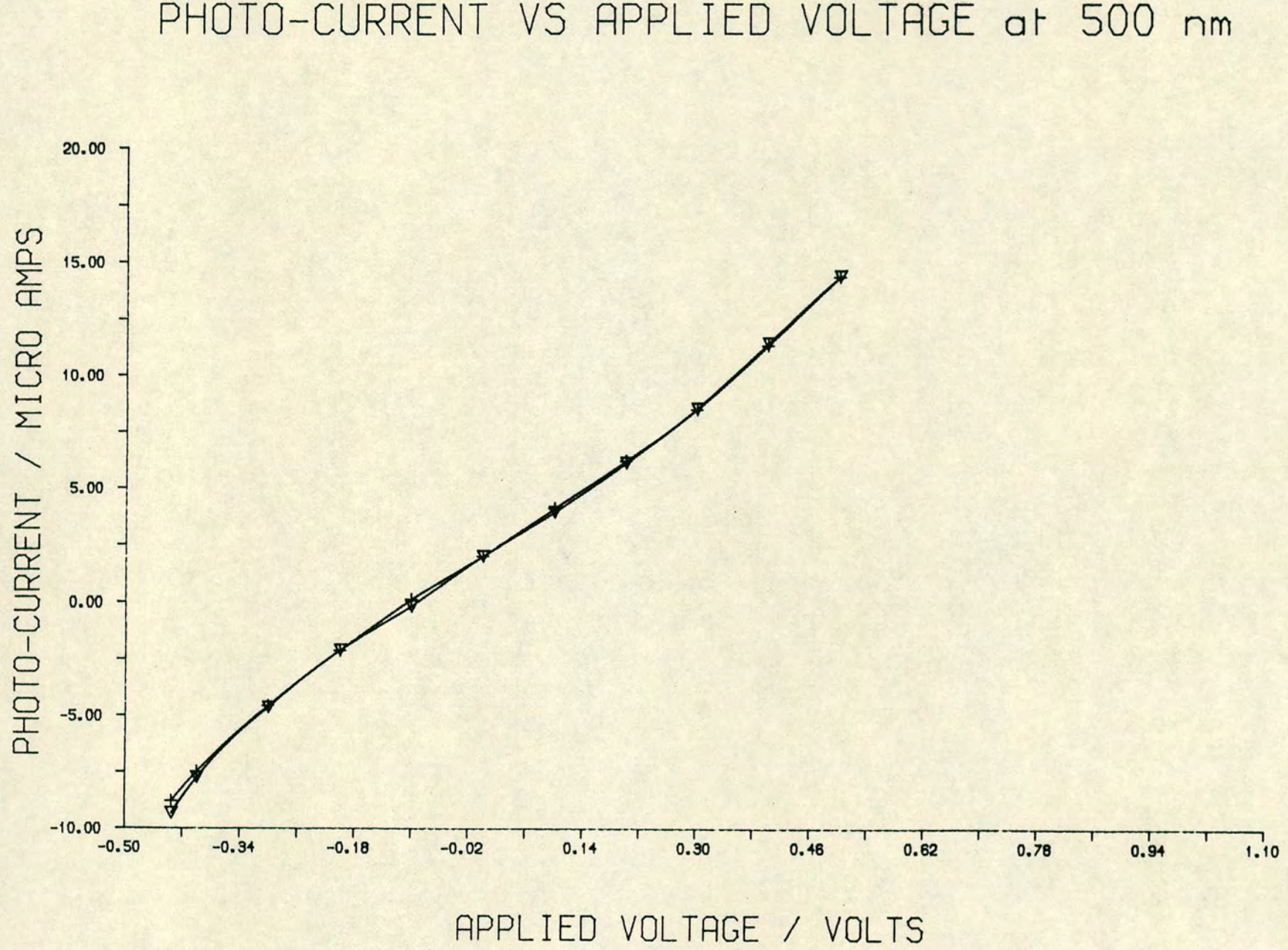
PHOTO-CURRENT VS APPLIED VOLTAGE at 500 nm
PHOTO-CURRENT / MICRO AMPS
20.00
15.00
10.00
5.00
0.00
-5.00
-10.00
-0.50
-0.34
-0.18
-0.02
0.14
0.30
0.46
0.62
0.78
0.94
1.10
APPLIED VOLTAGE / VOLTS

FIGURE 4

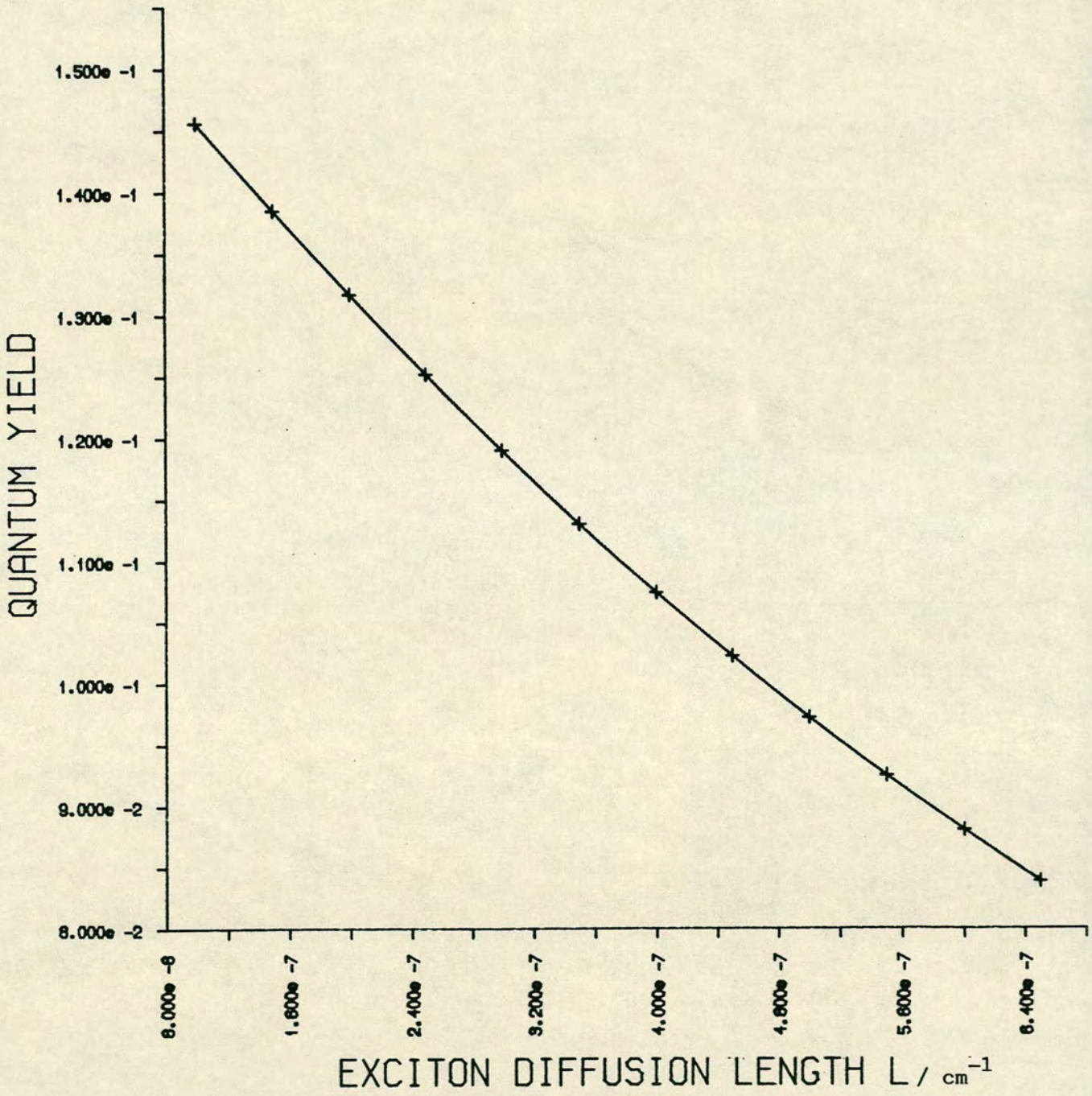

FIGURE 5

Exciton Diffusion Length v Quantum Yield

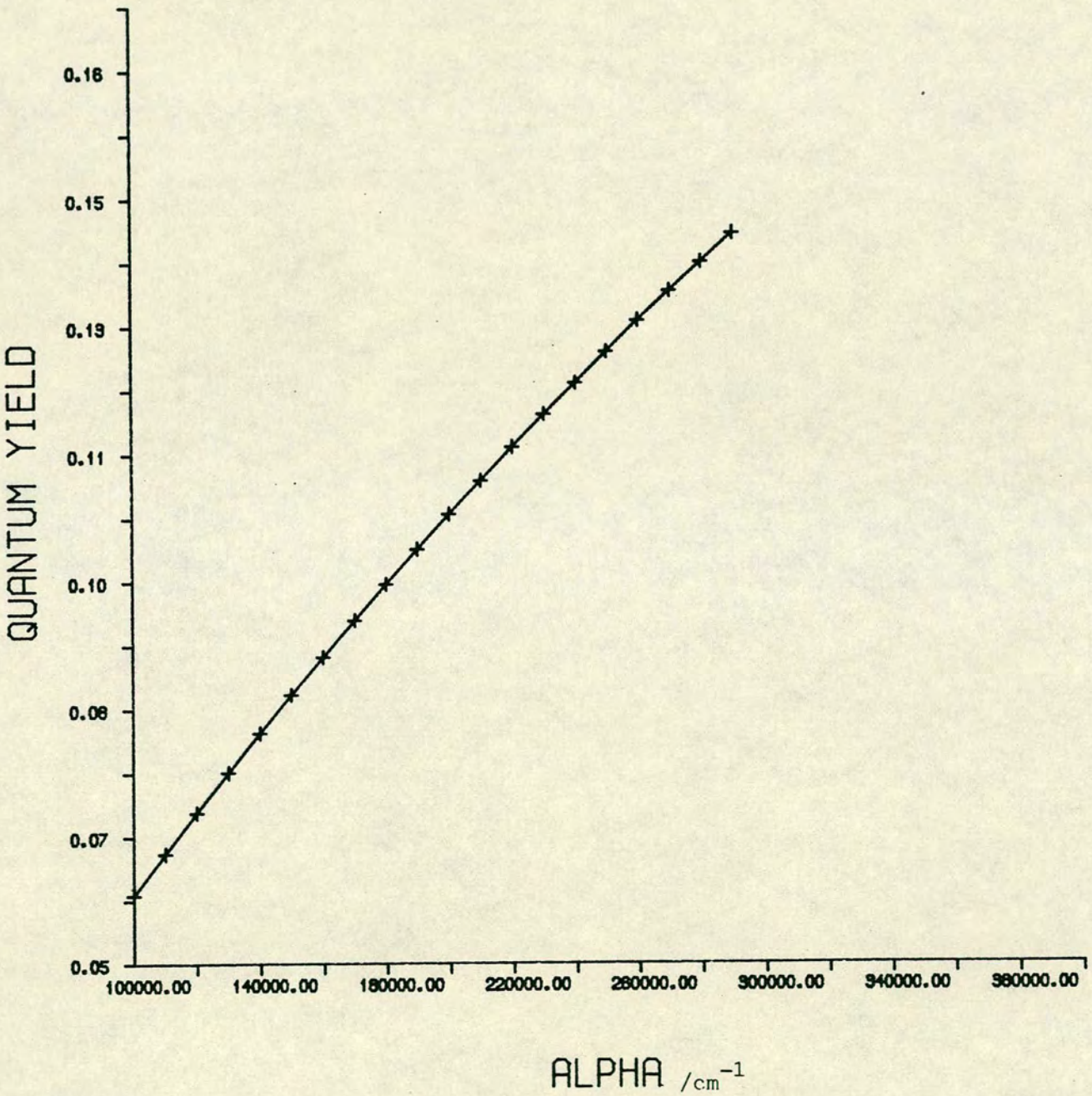

FIGURE 6

Quantum Yield v Absorption Coefficient α

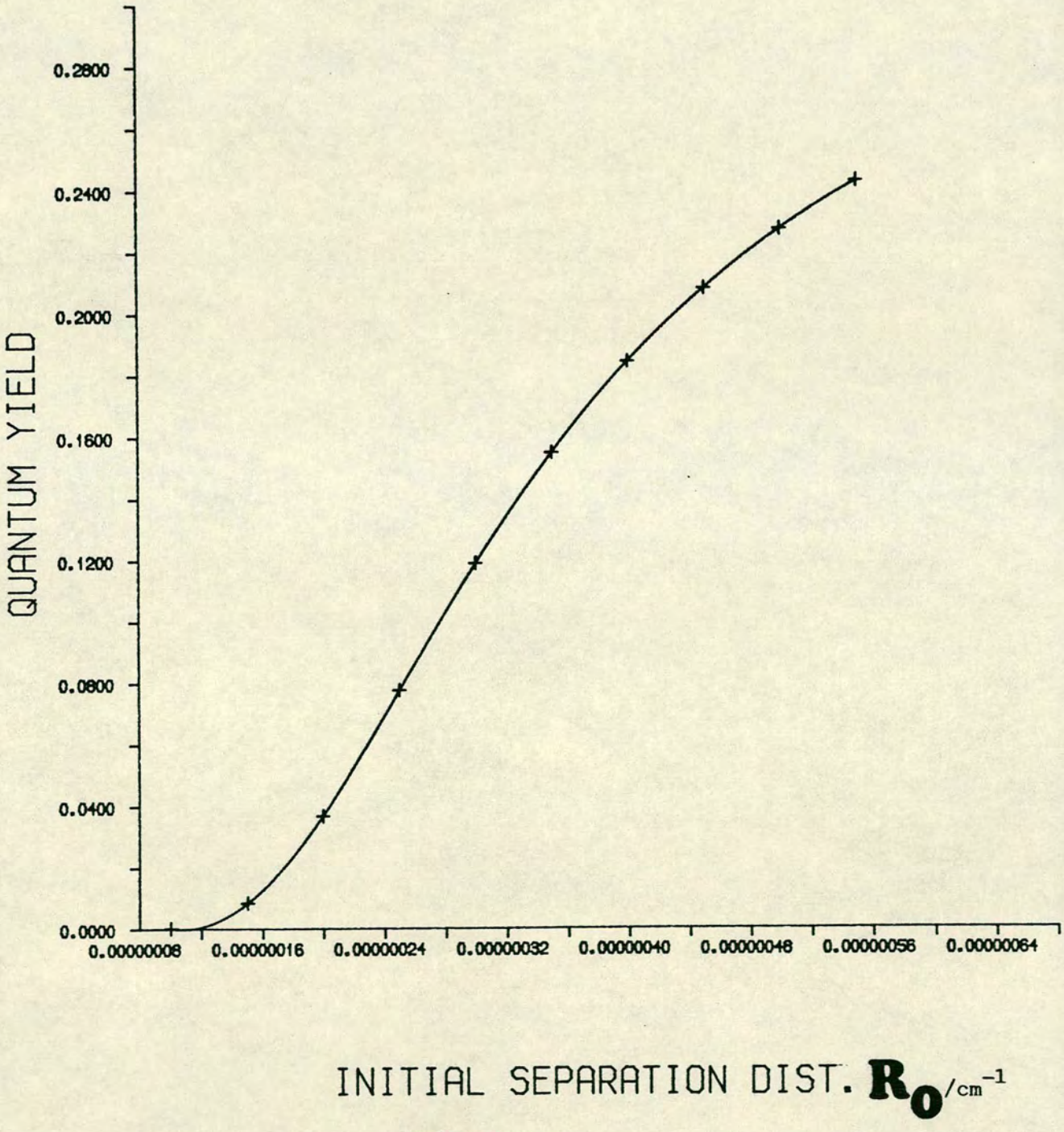

FIGURE 7

Quantum yield v thermalisation distance r_o

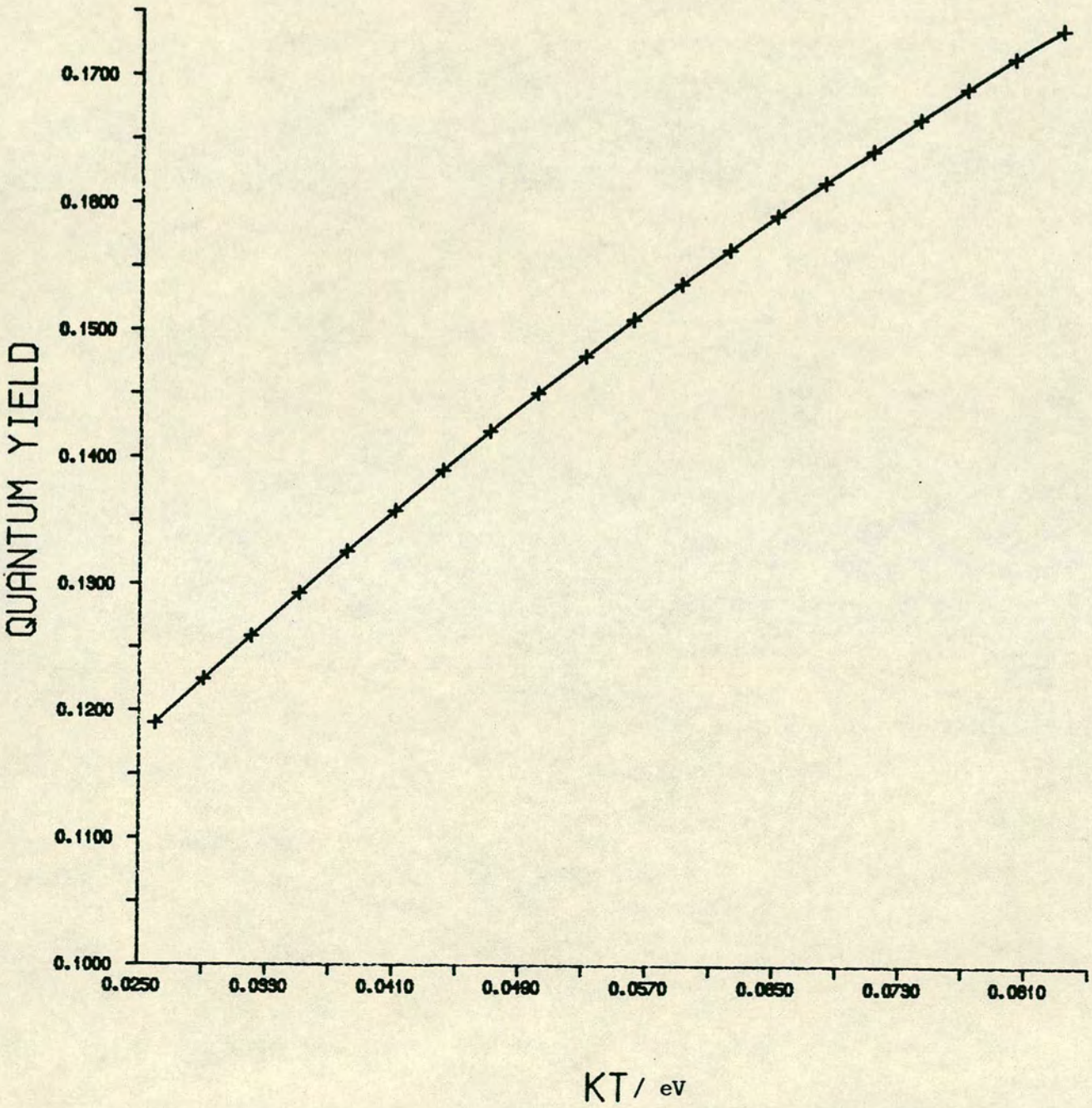

FIGURE 8

Quantum Yield v kT

CHAPTER IV

A THEORETICAL INVESTIGATION OF THE ELECTRONIC SPECTRUM OF ETHYLENE USING AB INITIO CI CALCULATIONS

I. Introduction

The electronic spectrum of ethylene has been studied extensively both theoretically and experimentally throughout the last few decades. Ethylene is the simplest olefinic compound and the interpretation of its spectrum provides valuable information on the nature of the olefinic double bond. The interpretation of the spectrum, however, is further complicated by the diffuse nature of the observed bands. The relatively small size of the ethylene molecule has permitted several comprehensive theoretical treatments to be undertaken with the aid of high speed computers, but even so, theoretical calculations have merely underlined the complexity of the interpretation of the spectrum.

II. The N,T,V,Z and Rydberg States

The electronic states of ethylene can be characterised as N,T,V,Z or Rydberg. The electronic ground state of ethylene is classified as the N state. Excitation of one of the pi electrons from the ground state (N) to the antibonding pi^* orbital creates one of two possible states, the triplet (T) and the singlet (V). Excitations of one pi electron from the ground state to a diffuse orbital creates a Rydberg state. A Rydberg state being one in which the united atom (UA) representation is a sufficiently good approximation to the orbital character of the terminating orbital, such that the state is found to be one of a series of transitions that fit the atom-like (hydrogenic) Rydberg formula

$$V_n = \text{I.P.} - 13.605/(n-\delta)^2 \qquad (1)$$

$$n = 3,4\ldots\infty \text{ for first row atoms}$$

Excitation of both pi electrons to the pi^* orbital produces the Z state.

III. MO Description of Ethylene

The molecular orbitals of planar ethylene are classified according to their behaviour under the symmetry operations of the point group D_{2h}. Table 1 contains a description of the orbitals of the ground state (the molecule being orientated in the yz plane, where z is the principal axis). If one CH_2 group is rotated such that the resulting dihedral angle lies between zero and ninety degrees, the symmetry is reduced to the point group D_2, while, if the dihedral angle equals ninety degrees the point group D_{2d} describes the symmetry of the molecule in this 'perpendicular' arrangement.

Table 2 indicates the MO correlations between planar, twisted and perpendicular ethylene, and illustrates how the electron configuration of the N state changes on twisting the molecule [1]. As the molecule is twisted from the planar to the perpendicular nuclear configuration, the energies of the $1b_2$ and $1b_3$ MO's become equal forming a predominately non-bonding degenerate pair, similarly, the $2b_2$ and $2b_3$ orbitals form another essentially non-bonding degenerate pair, both of which transform as the e representation of the point group D_{2d}.

If one now imagines the H atoms pushed into the C atoms, forming O atoms, the ethylene molecule is converted into the united molecule (UM) O_2. Table 2 also contains the corresponding MO description for O_2, as classified according to the point group $D_{\infty h}$, from which it is obvious that perpendicular ethylene (D_{2d}) is more closely correlated with O_2 than planar or twisted ethylene. This result is hardly surprising when one considers that the ground states of O_2 and perpendicular ethylene are both triplets.

At first sight it appears that perpendicular ethylene should be markedly unstable with respect to the planar form. However, hyperconjugation improves the stability of the perpendicular form. The orbital $2_{py} + [1s(H_a) - 1s(H_b)]$ associated with one CH_2 group interacts with the 2_{px} orbital on the remaining carbon atom, thereby providing some additional C-C bonding. Similarly, the $2_{px} + [1s(H_a) - 1s(H_b)]$ orbital mixing with the 2_{py} orbital on the other carbon has the same stabilising effect. On twisting planar ethylene the N- and Z- states mix increasingly, until at 90°, they are fully mixed; the N'Ag and Z'Ag states give rise to the $^1A_1$ and $^1B_1$ states of perpendicular ethylene, whose wavefunctions are each 50:50 mixtures of the wavefunctions for the N and Z states of planar ethylene.

If one now considers that part of the wavefunction associated with the π electrons as a Slater determinant, the N and Z states of planar ethylene can be represented as

$$\Psi = N \begin{vmatrix} (x + x)\alpha(1) & (x + x)\alpha(2) \\ (x + x)\beta(1) & (x + x)\beta(2) \end{vmatrix} \qquad N\,^1Ag$$

$$\Psi = N \begin{vmatrix} (x - x)\alpha(1) & (x - x)\alpha(2) \\ (x - x)\beta(1) & (x - x)\beta(2) \end{vmatrix} \qquad Z\,^1Ag$$

where $(x \pm x)$ represents $[2p\pi_x(a) \pm 2p\pi_x(b)]$.

These functions both transform according to the representation Ag of the point group D_{2h}. For perpendicular ethylene the $(x + x)$ and $(x - x)$ orbitals become degenerate and no longer transform individually according to any representation of the point group D_{2d}. Therefore to

get pure states, $N^1\,^1B_1$ and $Z^1\,^1A_1$ of perpendicular ethylene, linear combinations have to be taken

$$\Psi = N\begin{vmatrix}(x+x)\,(1) & (x-x)\,(2)\\ (x+x)\,(1) & (x-x)\,(2)\end{vmatrix} \pm N\begin{vmatrix}(x-x)\,(1) & (x-x)\,(2)\\ (x-x)\,(1) & (x-x)\,(2)\end{vmatrix}\begin{cases}Z^{11}A_1\\ N^{11}B_1\end{cases}$$

While the planar (N) state becomes destabilised upon twisting the T and V states, which both have an electron in the antibonding π^* orbital, become increasingly more stable as the dihedral angle between the two CH_2 groups is increased from zero to ninety degrees. An important stabilising effect in the case of the prependicular states is isovalent hyperconjugation, in which the bond pairs associated with the CH_2 groups are used to improve the stability of the C-C bond, see fig. (1).

Table 3 indicates the correlations between the planar states and their perpendicular counterparts.

IV. The N State (^1Ag) of Ethylene

The currently accepted structure of ethylene as determined by high resolution Raman and Infra-red spectroscopy is

$$r_o(C\text{-}C) = 1.338 \pm .003\text{Å}$$
$$r_o(H\text{-}C) = 1.086 \pm .002\text{Å}$$
$$\langle CCH = 121.3 \pm 0.5^\circ$$

for the zero point level.

The fundamental vibrations of C_2H_4 and C_2D_4 have been studied extensively by infra-red [2-8] and Raman spectroscopy [9-12], and their vibrational

frequencies are tabulated in table 4. From the point of view of the electronic spectrum, the most important frequencies are the C-C stretch, ν_2, and the twisting frequency, ν_4. The twisting vibration is inactive according to the selection rules [13], and cannot be observed directly by either Raman or infra-red spectroscopy. However, Arnett and Crawford [5] have calculated the frequencies of C_2H_4 and C_2D_4 by studying partially deuterated ethylenes. The lower symmetry relaxes the selection rules and by using theoretical relations between the frequencies of isotopic molecules, the frequencies of C_2H_4 and C_2D_4 have been calculated. Experimental studies on the absorption spectrum of matrix isolated ethylenes [7,8], for which the matrix environment also relaxes the selection rules, have confirmed the calculated frequencies. Twisting the ethylene molecule lengthens the C-C bond and therefore the twisting and stretching vibrations are expected to be strongly coupled.

V. The V and T States of Ethylene

The first UV absorption of ethylene is an exceedingly weak progression of diffuse bands in the region 2700 - 3500Å [14, 15], and has been assigned to the T-N absorption. The intervals in the band progression are about 990 cm^{-1} and change very little on deuteration, implying that these bands represent a progression in the upper state C-C stretching vibration, ν_2.

According to the rule $r_o^{2.88} w_o$ = constant (which fits the $B^3\Sigma_u^-$ and $X^3\Sigma_g^-$ states of O_2), the observed frequency implies a C-C bond length of about 1.58Å [16]. However, as in the V-N system, the bands are probably composed of overlapping stretching (ν_2) and twisting (ν_4)

bands. Since the T state is expected to have a perpendicular nuclear configuration, the observed bands are probably the most intense of an extensive system, the remaining bands being too weak to be observed (being doubly forbidden on account of the spin selection rule and the unfavourable Franck-Condon factors).

The steeply rising absorption near 2650Å in the T-N spectrum is apparently the beginning of the V-N system [16-23]. At 1744Å the V-N bands disappear under the intense bands of the first Rydberg transition, but the V-N system continues, reaching a broad flat maximum [21] at 1620Å. At shorter wavelengths the absorption decreases fairly steadily down to the next strong Rydberg transition [20, 24] which begins at 1393Å. In general V-N transitions are expected to be very intense, and ethylene is no exception, the measured oscillator strength for this transition being about 0.34[21].

Perhaps the most controversial issue of the ethylene spectrum is the constitution of the V state. Is it a purely valence state or does it possess some Rydberg character? Miron, Raz and Jortner [31] have studied ethylene in solid and liquid krypton and observed that the $^1(\pi,3s)$ state is blue shifted in the solid relative to the liquid, as expected for a Rydberg state. However, the $^1(\pi,\pi^*)$ state shows no such shift, indicating a valence description. A similar shift to higher energies accompanied with asymmetric line broadening are predicted for a molecule in the presence of moderate pressures of an inert gas. Robin and Kuebler [32] have observed such behaviour for the $^1(\pi, 3s)$ Rydberg state of ethylene in the presence of nitrogen, but not for the $^1(\pi,\pi^*)$ state.

These experimental observations, coupled with the high value for the oscillator strength, supported the view that the V-N transition is an intravalence one. However, the electron impact experiments of Krauss and Mielczarek [33] have shown that a minimum occurs in the generalised oscillator strength as a function of the momentum transfer (which is a characteristic feature of states with Rydberg character) with the $^1(\pi,\pi^*)$ state also. They concluded that the V state is not a purely intravalence one, but possesses some Rydberg character also.

Both the T and V states have been the subjects of extensive theoretical calculations, largely in the hope that the spectrum could be better understood. The earliest calculations based on the SCF procedure [25-27] predicted the excitation energies for the T and V states to be about 3.4 eV and 9.3-12.0 eV respectively; the accepted experimental values being 4.6 eV and 7.6 eV.

The low value for the T state was explained as a result of the neglect of correlation effects. However, the results for the V state implied that the V state has at least 1.7 eV more correlation energy than the ground state. This seems paradoxical since qualitative arguments suggest that the open shell states such as $^1(\pi,\pi^*)$ should have less correlation energy than the closed shell ground state.

The greatest inherent weakness of the earliest calculations was the assumption that the orbital exponent is the same for both π and π^* orbitals. In view of the V state being ionic [28] such an assumption was clearly invalid. If one considers a minimum basis set representation

of the π and π^* orbitals, then in terms of the atomic basis set $\{2p_a, 2p_b\}$, the spatial part of the wavefunctions are represented as

$$T : 2p_a(1)2p_b(2) - 2p_b(1)2p_a(2)$$

$$V : 2p_a(1)2p_a(2) - 2p_b(1)2p_b(2)$$

The triplet state is then just the anti-bonding state corresponding to the valence ground state and should therefore have a similar charge distribution to the ground state, thereby justifying the assumption of similar radial functions for π and π^*. The V state, on the other hand, is clearly poorly represented by such an assumption.

If the exponents of the basis functions in the π and π^* orbitals are different ($\zeta\pi^* \neq \zeta\pi$), then the wavefunction for the V state is a sum of two terms:

(i) a split shell ionic component,

$$[2p_a(1)2p_a'(2)+2p_a'(1)2p_a(2)]-[2p_b(1)2p_b'(2)+2p_b'(1)2p_b(2)]$$

and (ii) a covalent component,

$$[2p_a(1)2p_b'(2)-2p_b'(1)2p_a(2)]+[2p_a'(1)2p_b(2)-2p_b(1)2p_a'(2)]$$

Huzinaga [29] has optimised the exponents for the π^* orbital of the V state and the π orbital of the ground state, obtaining $\zeta_u = 1.6$ for the π orbital and $\zeta_g = 0.2$ for the π^* orbital, indicating a rather diffuse V state. This approach also produced a more satisfactory excitation energy of 6.97 eV. Huzinaga also optimised the orbital parameters for the T state, obtaining $\zeta_u = 1.4$, $\zeta_g = 1.2$ and a vertical excitation energy of 4.22 eV. This great difference in the spatial extension between the V and T states was contrary to most previous assumptions [27].

Dunning et al [30], using a double zeta basis set supplemented by 3 diffuse $2p_\pi$ functions on each carbon atom, calculated an excitation energy of 7.41 eV for the V state. They also calculated the expectation value for $\langle\pi^*/x^2/\pi^*\rangle$ to be 42.08 a_o^2 again indicating the diffuse nature of the π^* orbital.

The necessity of including diffuse functions in the basis set was also demonstrated by Hansen [34]. Hansen supplemented his basis set with additional $2p_\pi$ and $3d_\pi$ orbitals on each of the two carbon atoms and obtained a vertical excitation energy of 7.17 eV, and concluded that the V state had substantial Rydberg character.

Dunning [30] performed limited CI calculations on the ethylene V state, restricting the configuration subspace to the π orbitals. This approach yielded a satisfactory value for the T state (4.2 eV) but produced an unacceptably high excitation energy for the V state (8.28 eV). However, in view of the V state being ionic, the neglect of correlation between the sigma core and the pi electrons should have a substantial effect on the V state and Dunning's approach imposed a restrictive and artificial constraint on the CI calculation.

Basch and McKoy [35] also studied the planar V state of ethylene at the SCF level and succeeded in fitting the first three $^1B_{1u}$ states (7.43, 8.13, 8.64) to the Rydberg formula (1) based on their calculated ionisation potential, a quantum defect $\delta = 0.1$, and $n = 3,4,5$. They found that all three $^1B_{1u}$ states had considerable Rydberg character and that the oscillator strength of the first state

had a value of 0.075. They concluded, on the basis of these results, that Hartree-Fock theory is incapable of adequately describing the V state. They proposed that the V state in Hartree-Fock theory is calculated to be beyond the ionisation potential energy and is so heavily contaminated with spuriously calculated lower energy Rydberg components, as to render it unrecognisable as the true spectroscopic V state. Basch and McKoy suggest that the only way to adequately describe the V state is by configuration interaction involving not only $\pi \longrightarrow \pi^*$ transitions, but $\sigma \longrightarrow \sigma^*$ type transitions also. Mulliken [36] also emphasizes the need for $\sigma \longrightarrow \sigma^*$ and $\pi \longrightarrow \pi^*$ configuration interaction to describe the ethylene V state adequately.

Ryan and Whitten [37] have carried out configuration interaction calculations involving $\sigma \longrightarrow \sigma^*$ transitions for the V state and predicted an excitation energy of 8.02 eV compared to the experimental value of 7.65 eV. They also found that the inclusion of $\sigma \longrightarrow \sigma^*$ transitions reduces the expectation value of $\langle \pi^* / x^2 / \pi^* \rangle$ to a more acceptable value of 6.94 a_o^2 (in comparison to the value of 2.40 they obtain for the triplet).

They observed that the inclusion of diffuse d-functions was neccessary to adequately describe the V state, and concluded that the presence of the d functions allows for angular correlation effects and provides an important means of polarising the localised components of the π distribution toward opposite ends of the molecule.

While CI calculations produced better excitation energies for the V state, there was still a discrepancy of 0.4 eV unaccounted for, between the theoretical and experimental values. This led Buenker et al [38] to propose a substantially different interpretation of the spectrum. Their calculations indicated that a Rydberg transition $^1(\pi,3p_y)$ occurs at 7.52 eV. Calculations on twisted ethylene (D_2) indicated that the lowest energy state for planar ethylene which can be correlated with the most stable $^1B_1$ state for twisted ethylene, is not the $^1(\pi,\pi^*)$ transition, but the $^1(\pi,3p_y)$ excitation, to which transitions from the ground state are formally dipole forbidden. Buenker suggests that the higher energy $^1B_{1u}$ state, which is also quite diffuse, can be identified as the upper state in the 3R' Rydberg species assigned by Wilkinson [41].

These assignments require that the electronic transition moment for the most stable $^1B_1$ state necessarily vanish at 0° (and 90°) because of dipole selection rules and increase for larger values of the dihedral angle. This would then lead to non-vertical transitions of greater intensity, as is the case for certain nominally forbidden transitions of linear molecules [42, 43] such as C_2H_2 and HCN , and the planar molecule formaldehyde [44].

As the dihedral angle (θ) is increased, the 1^1B_1 state increases in energy and the 2^1B_1 state decreases in energy until an avoided crossing occurs, when the situation is reversed and the 1^1B_1 state decreases in energy, becoming rapidly more valence like as θ increases. Buenker argues that this behaviour could explain the maxima at 7.65 eV and

that the interaction between the two lowest $^1B_1$ states is responsible for the broad and diffuse nature of the spectrum in this region.

Buenker [45] extended the theoretical treatment and calculated vibrational ab initio wavefunctions involving CH_2 twisting and C-C stretching for several electronic states of ethylene. Electronic transition moments between the vibrational levels of the ground and excited electronic states were also calculated and enabled Buenker to predict an intensity maxima at 7.89 eV corresponding to a non vertical transition (0-0 transition 8.25 eV) thus supporting his earlier hypothesis that the experimental maxima at 7.65 eV corresponds to a non-vertical transition.

McMurchie and Davidson [47] succeeded in calculating a lower vertical transition energy of 7.96 eV for the V state using a double zeta basis set supplemented with polarisation functions ($p_{x,y,z}$ α = 1.2) on each hydrogen, a set of d orbitals (α = .45) on each carbon atom and two sets of diffuse d orbitals at the centre of inversion. Valence shell CI calculations were performed and they found it necessary to include excitations of the type $\sigma \longrightarrow \sigma^*$ to adequately describe the spatial extent of the V state. The individual contributions for each $\sigma \longrightarrow \sigma^*$ transition was found to be small but McMurchie and Davidson argue that the cumulative effect is significant and should not be neglected. Their calculated oscillator strengths, f(r) = .3569 and f(V) = .3583 are in good agreement with the experimental value of .34. The expectation values for $\langle \pi^* | x^2 | \pi^* \rangle$ and $\langle \chi | \Sigma x_i^2 | \chi \rangle$ were 8.8 au and 17.3 au respectively indicating a mostly valence state.

Buenker [46], however, using a basis set consisting of 84 basis functions performed valence shell SDCI calculations over 80 MO's and concluded that $\sigma \longrightarrow \sigma^*$ transition are unimportant with respect to both the energy and the spatial distribution of the V state. Buenker's results for $\langle\chi|\Sigma x_i^2|\chi\rangle$, the vertical transition energy and the oscillator strength were 20 a.u., 7.95 eV and 0.34 respectively in good agreement with Davidson and McMurchie.

While it is debatable how important $\sigma \longrightarrow \sigma^*$ transitions are in describing the V state all of the most recent CI calculations have confirmed the necessity of diffuse functions in the basis set in order to describe the V state adequately.

Currently, the most sophisticated calculations on the ethylene V state have been performed by Buenker et al [48]. Buenker has carried out ab initio SDCI calculations to investigate non adiabatic vibronic transitions involving the twisting mode ν_4 for the $N(\pi^2)$, $V^1(\pi,\pi^*)$ and $Ry^1(\pi,3p_y)$ electronic states and demonstrated qualitatively that his previous theory involving the $Ry^1(\pi,3p_y)$ and $V^1(\pi,\pi^*)$ states explains the broad diffuse nature of the V-N band system. Buenker concludes that the experimental intensity maximum at 7.65 eV involves a non-vertical transition.

VI. Rydberg States

The Rydberg orbitals of the ethylene molecule belong to the symmetry species $ns(a_g)$ $np(b_{1u}, b_{2u}, b_{3u})$ and $nd(a_g, b_{1g}, b_{2g}, b_{3g})$. Transitions involving promotion of the outer pi electron (b_{3u}) to the $ns(a_g)$ or

$nd(a_g, b_{1g}, \text{ or } b_{2g})$ orbitals are electric dipole allowed, and electric quadrupole forbidden. Exactly the opposite applies to transitions to the three np Rydberg orbitals, and the remaining transition, $\pi \longrightarrow nd(b_{3g})$ is forbidden for both electric dipole and quadrupole radiation. The assignment of all the Rydberg states of ethylene has proven to be an arduous task and the only state to be assigned with absolute certainty is the 2R level $^1(\pi,3s)$.

i) Rydberg ns States

The first observable Rydberg transition occurs at 7.11 eV and is known as the 2R level. The assignment of this state as optically allowed is certain because of its high intensity in the optical spectra and the near unity quantum defect which identifies the Rydberg orbital as $ns(a_g)$, [49]. The position of the second Rydberg s-type transition is not certain but McDairmid [59] has suggested, after a detailed examination of the optical spectrum, that the transition energy should be about 9.09 eV.

(ii) Rydberg np States

Transitions to the np Rydberg orbitals are optically forbidden and are therefore non-observable in the UV spectrum. For ethylene, the core electrons produce an asymmetric potential which leads to a splitting of the degeneracy of the three p-type and five d-type Rydberg orbitals.

The first experimental evidence for a transition involving a Rydberg p-orbital was discovered by Ross and Lassettre (39) who observed a discrepancy in the intensity distribution of the vibrational levels of the 2R series, compared with the optical spectrum, and the 33 keV energy-loss spectrum of Geiger and Wittmack (50). They attributed this discrepancy to the excitation of a new quadrupole transition at 7.45 eV, underlying the 2R Rydberg levels. Mulliken (51) designated this quadrupole transition at 7.45 eV as $^1(\pi,3p)$. Wilden and Comer (52) were unable to confirm or refute the experimental observations of Ross and Lassettre and it is now generally accepted that the quadrupole excitation at 7.45 eV is spurious.

The magnetic circular dichroism (MCD) experiments of Brith-Linder and Allen (53) indicated a possible $^1(\pi,3p)$ transition at 7.2 eV and Mulliken (54) later assigned this to the $^1(\pi,3p_\sigma)$ transition. However, multi-photon ionisation work by Gedanken et al [55] disputes this assignment. They argue that a more intuitive approach based upon the consideration of term values predicts that the excitations π-3s and π-3p should be separated by 7000-1000 cm^{-1}, whereas the B-LA experiment predicts a separation of less than 1000 cm^{-1}.

The MPI experiments indicate two π-3p transitions occuring at 62905 cm^{-1} (7.80 eV, π-3py) and 66 875 cm^{-1} (8.28 eV, π-3px); where y is the in-plane short axis, and x is the out of plane axis. The presence of a quadrupole state at 7.80 eV with a quantum defect of 0.75 has also been observed in the electron energy loss spectroscopy experiments of both Wilden and Comer (52) and Van Veen (56).

The assignments for these two p-type Rydberg orbitals are also supported by the ab initio CI calculations of both McMurchie and Davidson (57) and Buenker et al (PBP) (48).

There is no concrete experimental evidence for the positions of the π-4p transitions although Wilden and Comer (52) have detected a quadrupole state in their energy loss experiments at the same positions as the 4R' state. The 4R' state has generally been assigned to an nd orbital because of its relatively high intensity in the optical spectrum. The observations of Wilden and Comer however are consistent with a suggestion by Mulliken (51) that the 4p ($3b_{2u}$) Rydberg state could lie at the same energy as the 4R' state.

Wilden and Comer also assign the 4R'' state as electric quadrupole allowed whereas previous assignments based on optical data had assumed that the transition was to a d orbital, because of the small value of the quantum defect (0.25).

(iii) Rydberg nd Transitions

Recent experimental evidence based on the MCD experiments of Snyder et al (58) have shown that both the $3R_{oo}$ and $4R''_{oo}$ Rydberg transitions are composed of two electronic transitions. Since the equilibrium geometries of Rydberg states are expected to be twisted they quote their results for the point group D_2. Their results indicate that the $3R_{oo}$ origin should be assigned to the transitions

$$^1A_1 \longrightarrow {}^1B_2(3d\delta) + {}^1B_3(3d\delta)$$

The $4R_{oo}'''$ transition is assigned to $^1A_1 \longrightarrow 3R_{oo} + \nu_3$, where ν_3 is the totally symmetric H-C-H bending (scissors) fundamental. Under D_2 symmetry, $3d\delta$ decomposes into $b_1 + a$; these correspond respectively to the $1b_{1g}$ and 6_{ag} Rydberg MO's of D_{2h} symmetry.

Table (5) contains Mulliken's assignments [51] of the Rydberg transitions of ethylene, with a few minor adjustments included due to more recent experimental evidence, and table (6) contains the results of the most recent ab initio calculations to date.

Rydberg Triplets

Only four Rydberg triplets states have been observed experimentally (52), and these are tabulated in table (7). Singlet-triplet splittings are generally small, table (7) contains the results of the work by Buenker et al (60), where both singlets and triplets have been calculated for a wide range of states.

Theoretical Method

Multireference CI calculations were performed on several states of ethylene using three geometries. The equilibrium geometry [40] for the ground state was taken to be:-

r_{CC} = 1.339Å, r_{CH} = 1.086Å and <HCH> = 117.6°.

The Rydberg states of ethylene are known to have a twisted equilibrium geometry (D_2) [40] and the geometry used here was taken as:-

r_{CC} = 1.41Å, r_{CH} = 1.08Å, <HCH> = 124.4° and

θ (the dihedral angle) = 37° [61].

The perpendicular geometry (D_{2d}) was also studied using the following geometrical parameters:-

r_{CC} = 1.41Å, r_{CH} = 1.08Å, <HCH> = 124.4°

A relatively small basis set of 39 contracted gaussian functions was used for all three geometries. The basis set consisted of the Dunning[62] (4s2p/2s) double zeta (DZ) contraction of the Huzinaga [63] (9s5p/5s) primitive functions; the hydrogen 5s set was scaled by η^2 = 2.0 as in the work of Whitten [64]. An additional set of diffuse spd functions was added at the centre of charge, with the following exponents:

s,s' = 0.0824, 0.17; p = d = 0.016.

The exponent of the two s functions were obtained by optimising the Rydberg $^1(\pi,3s)$ state at the CI level. This proved to be a time consuming and computationally expensive procedure so the exponents for the p and d diffuse functions were taken from earlier work by Buenker et al [65]. The integral and SCF wavefunctions were obtained with the ATMOL3 suite of programs [66] and the multi-reference CI wavefunctions

were calculated with the MRDCI program [67,68]. Both programs were mounted on a Cray-1s computer at the University of London Computer Centre (ULCC). The configurational subspace spanned all the valence orbitals and their virtual counterparts; only the C 1s core orbitals and their virtual complements were removed. A threshold (T) of 30μH was used in the configuration selection procedure and the MRDCI corrections were added to the CI energies to obtain the CI (T—>0) energies (see Appendix A). The SCF ground state MO's were used as the MO Basis for all of the states studied.

Theoretical Results

Tables (8) - (14) summarise the results obtained for each of the three geometries studied. The MO basis used in each calculation has been the SCF wavefunction for the ground state of the relevant geometry (D_{2h}, D_2, D_{2d}). In general the ground state SCF wavefunction provides a suitable MO basis for truncated CI calculations of different states. It has been found that SCF wavefunctions of excited states can provide a marginally better MO basis for truncated CI wavefunctions but the improvement in the calculated energies is generally small. Determining the best SCF wavefunction to use as the MO basis is time consuming and generally not critical. Therefore the decision to use the ground state SCF MO's is justified by expediency.

Perhaps the major disadvantage of the 39 AO basis used in these calculations is the fact that the $n\,^1B_{3g}$ states cannot be included in the calculations.

To calculate the n^1B_{3g} states would require adding a set of d-functions to each carbon atom. This would then increase the AO basis to 51 orbitals. The main objective of this work was to produce a satisfactory basis set for ethylene which could predict reasonable excitation energies; substituted ethylenes could then be studied with a similar basis set. The addition of d-functions to carbon atoms would drastically increase the computation time required for larger substituted ethylenes and the decision to avoid using d-functions has been based upon this.

A note on the terminology used in this and subsequent chapters is warranted here. Symbolism of the form 5M2R has been used throughout, this implies that a CI calculation using 5 reference (m) configurations and seeking 2 roots (R) has been performed.

1. Planar-Ethylene (D_{2h})

(i) N,T and V states (D_{2h})

The ground state CI energy calculated for planar ethylene is -78.2092 au (table 18). This is rather poor when compared to larger basis sets [48,49] and is attributable to the lack of polarisation functions in the basis set.

The calculated excitation energy for the T state, $^3(\pi,\pi^*)$, is 4.58 eV in good agreement with the experimental value of 4.6 eV. Table 32a indicates the main reference configuration used in this calculation, (M in table 32a denotes a reference configuration) and any secondary

configurations with squared coefficients greater than 0.005 are also included.

The V[#] state, on the other hand, produced a less satisfactory excitation energy of 8.36 eV, see tables 8 and 21a. This was expected since previous work by several authors [46,47,69] indicated the need for a large basis set to adequately describe the V state. The V(1^1B_{1u}) state interacts significantly with the next root of the same symmetry, i.e. the 2^1B_{1u} state. This was particularly noticeable when the V state was calculated in the absence of the second root. This led to the V state having an energy of 0.16 eV higher than that calculated in the presence of the second root.

Buenker [46], using a basis set consisting of 84 orbitals, performed SDCI calculations with the iterative natural orbital procedure (INO) and predicted an excitation energy of 7.96 eV. Palmer [70] using an identical basis set but without the INO procedure, predicted an excitation energy of 8.21 eV. These calculations employed the ground state SCF wavefunction for the MO basis, and while it could be argued that the energy could be improved by using an excited state SCF wavefunction for the MO basis, it appears that the difference of 0.25 eV can be largely attributed to the INO procedure improving the energy of the ground state with respect to that of the V state. Currently the best theoretical calculations on the V stage of ethylene [46,47,69] employ the INO procedure and it seems reasonable to postulate that the present calculations would also improve if the INO procedure had been employed. This however was not done for the sake of expediency; employing the INO procedure

See page IV.29 for further comment on the V state.

to all the calculated states of ethylene would be costly from the computational point of view. The predicted excitation energy of 8.36 eV, does however, compare favourably with earlier theoretical results.

Inspection of the wavefunction reveals that the V state is very diffuse, being largely a linear combination of the π^* orbital and the diffuse 3dxz Rydberg Orbital; a result consistent with earlier calculations.

It is encouraging that the present basis yields a satisfactory excitation energy for the $2\,^1B_{1u}$ ($\pi \longrightarrow \pi^*\text{-}3d\pi$). The calculated value of 9.52 eV being in good agreement with the experimental value of 9.36 eV.

(ii) Rydberg States of Ethylene (D_{2h})

Tables 10,11 and 12 summarise the calculated singlet and triplet excitation energies for the 39 AO basis-set. Table 9 compares the present results with those of Palmer [70] and the experimental excitation energies, and table 8 contains the results of Buenker et al [48] for comparison with the present calculations and those of Palmer.

The present calculations compare very favourably with the results obtained by Buenker et al; while the calculations by Palmer are generally higher by about 0.3 eV on average. Since Palmer has used an identical basis to that of Buenker, the discrepancy can be attributed to the INO procedure employed by Buenker which improves the calculated excitation energies.

The present 39AO basis overestimates the $R^1(\pi,3s)$ state by 0.35 eV, but this is not critical since this does not affect the ordering of the states in this region of the spectrum. The remaining states are in good agreement with the experimental values.

One of the most controversial issues of recent years has been the assignment of the $^1(\pi, 3p\sigma)$ state. Ross and Lassettre [39] claimed that they had observed a quadrupole transition at 7.45 eV and assigned it to a $\pi \longrightarrow 3p$ transition. Later experimental work failed to confirm these observations and it is now believed that the transition at 7.45 eV is spurious.

Brith-Linder and Allen [53] claimed that their magnetic circular dichroism (MCD) experiments indicated a $\pi \longrightarrow 3p\sigma$ transition at 7.2 eV. The multi-photon ionisation (MPI) work of Gedanken et al [55] disputes this assignment. The MPI experiments indicate two $\pi \longrightarrow 3p$ transitions; $\pi \longrightarrow 3p_y$ and $\pi \longrightarrow 3p_x$ at 7.80 and 8.28 eV respectively.

The present calculations are in good agreement with both the MPI experiments and the theoretical calculations of Buenker et al [48]. The $1\,^1B_{2g}$, $^1(\pi,3p_z)$ appears to be accidentally degenerate with the $1\,^1B_{1g}$, $^1(\pi, 3p_y)$ state. Therefore on the basis of the most recent experimental work and the present theoretical calculations it appears that two accidentally degenerate $\pi \longrightarrow 3p$ transitions occur at 7.8 eV and the π-$3p_x$ transition occurs at 8.28 eV.

Mulliken [54] has assigned the peak observed at 8.90 eV to the 1^1Au state. The present calculations are consistent with this assignment but also indicate two other transitions in this region, namely $^1(\pi, 4s)$ and $^1(\pi, 3d_{xy})$. These results are also consistent with Beunker's calculations.

Systematic theoretical studies of the triplet Rydberg states appear to have been neglected. Only Buenker [60] and Nakatsuji [71] appear to have made a significant contribution in this area. Both authors calculate small triplet-singlet splittings for the Rydberg states, the only exception being the splitting of about 0.2 eV for the $\pi \longrightarrow 3s$ transition.

Table (9) contains the results for the triplet Rydberg states. Four states 1^3B_{1g}, 1^3B_{3u}, 1^3Au and 2^3B_{3u} produced triplet excitation energies slightly greater than the corresponding singlets. These anomalous results probably result from using the ground state SCF wavefunction as the MO basis. A lower triplet excitation energy would probably result if the MO basis used in these triplet calculations corresponded to the excited state SCF wavefunction which produced the optimal CI energy for the Rydberg triplets (i.e. the present GS SCF MO basis produces better energies for the singlets).

Nevertheless, these anomalous results are not too disconcerting since the singlet - triplet splittings are very small and the calculated splittings for the remaining states are in good agreement with previous work.

(iii) Excitations from the HOMO σ Orbital ($1b_{3u}$)

The present CI calculations included transitions involving promotion of an electron from the highest occupied sigma orbital ($1b_{3g}$) to a virtual orbital in the main set of reference configurations. However, only in three cases did a transition from the HOMO σ-Orbital appear as one of the lower roots (i.e. low excitation energy) in the CI calculations, see Table 11 and the following:-

2^1Au	$1b_{3g} \longrightarrow 2b_{3u}$	10.66 eV	table 15b
2^1Ag	$1b_{3g} \longrightarrow 2b_{3g}$	11.38 eV	table 19b
2^1B_{2u}	$1b_{3g} \longrightarrow 2b_{1u}$	10.39 eV	table 23b

Beunker [60] using a small basis set of 32 contracted gaussian function, calculated the 2^1B_{1g} ($1b_{3g} \longrightarrow 1b_{2g}(\pi^*)$) state to have a transition energy of 9.89 eV. This state was not detected in the present calculations. However, Palmer [70], using an 84 AO basis set, calculated an excitation energy of 8.93 eV. This transition energy was further reduced to 8.32 eV by employing the INO procedure. It appears then that these results indicate the existence of a new low lying valence shell transition, hitherto undetected by either theoretical or experimental methods.

In order to adequately represent this state a large basis set is required and the INO procedure should be employed. In this respect, the 2^1B_{1g} state is very similar to the V state, i.e. less rigorous theoretical approaches fail to produce a satisfactory excitation energy and the present 39 AO basis is incapable of producing comparable results for this $^1(\sigma,\pi^*)$ state.

2. Twisted Ethylene (D_2)

The Rydberg and ionic states of ethylene have been observed to be twisted by about 30° in their equilibrium geometries [40]. At first sight this seems surprising since twisting reduces the overlap between the pi orbitals; this however is more than compensated by an increase in isovalent hyperconjugation. On the basis of simple qualitative arguments one would expect the equilibrium geometries of the Rydberg and ground state $C_2H_4^+$ ion to be quite similar since the additional electron present in the Rydberg state is in a very diffuse orbital and should therefore contribute little to the overall binding. The vibrational fine structure of the ethylene photo-electron spectrum [72] is very similar to that of the UV spectrum of the first Rydberg transition, confirming the similarities of the two structures.

The T,V and Rydberg states have all been studied with a twisted (D_2) nuclear configuration. The geometric parameters were taken from the recent paper by Foo and Innes [61] in which they determined the equilibrium geometry of the R $^1(\pi, 3s)$ state from the ethylene absorption spectrum (see theoretical procedure).

The main purpose of studying ethylene in the D_2 nuclear configuration was to examine the possible effects of non-vertical adiabatic excitations in the ethylene spectrum. The results are summarised in tables (8), (10) and (13). As one would expect the non vertical transition energies are lower than the corresponding vertical transition energies. For most states lowering (about 0.1—>0.2 eV) of the excitation energy is observed, and therefore non-vertical transitions should not make a significant difference to the interpretation of the spectrum in these regions.

A somewhat larger reduction in the excitation energy is calculated for the T,V,R $^1(\pi, nd\pi)$ states. The lowering of 1 eV observed for the T state is obviously due to the increased stabilisation of the π^* antibonding orbital.

The results for the V, $R^1(\pi, 3p_y)$ and $R^1(\pi, nd\pi)$ states are consistent with Buenker's earlier work [48]. All three states are significantly lowered and tables (40a,b,c) indicate substantial mixing between these states, and therefore non-vertical transitions could be quite important in this region of the spectrum.

Table (10) also contains the calculated non-vertical transition energies for the triplet states. In general the triplet transition energy is lower by about 0.1—>0.2 eV in each case. One state (3^3B_3) however shows a noticeable discrepancy. Here the triplet state is 0.69 eV higher than the singlet. A result which at first sight appears inexplicable and highly improbable. This could possible be due to the inadequacy of the present 39 AO basis. This basis does not contain d-orbitals on the carbon atoms and consequently there are no orbitals of a_u symmetry (for the D_{2h} planar configuration) and therefore it is not possible to calculate any states of B_{3g} symmetry for planar ethylene.

Buenker's results [48] indicated that the transition energy for the 1^1B_{3g}, $^1(\pi, 3d\delta)$ state is 8.92 eV, only 0.06 eV less than the transition energy for the 3^1B_{3u}, $^1(\pi, 4s)$ state. For twisted ethylene (D_2) these two states belong to the same symmetry representation B_3. It is possible that these

two states undergo an avoided crossing when the ethylene molecule is in the twisted configuration. The potential surfaces of the corresponding triplet states need not be similar to the potential surfaces of the singlet states and therefore an avoided crossing involving the triplet states could occur at a different dihedral angle to that of the singlet avoided crossing. If the present geometry is closer to the region corresponding to the triplet avoided crossing, the ommission of transitions involving assymetric combinations of carbon d-orbitals could have a more significant effect on the triplet energy. Therefore one could postulate that the present deficiency in the AO basis is responsible for the anomalous singlet-triplet splitting.

3. Perpendicular Ethylene (D_{2d})

Calculations were also performed on the perpendicular configuration of ethylene. Currently, there is no available data on the equilibrium geometry of the V state, but it has been demonstrated by Raman spectroscopy that the $^1(\pi,\pi^*)$ state prefers a perpendicular nuclear configuration [73]. Buenker [74] however has optimised the geometry of the C-C bond for four states of ethylene in the D_{2d} configuration [^1B_1N r_{CC} = 1.48Å; ^3A_2T r_{CC} = 1.48Å; ^1A_1Z r_{CC} = 1.41Å, $^1B_2$ r_{CC} = 1.43Å]. The present calculations employ an r_{CC} value of 1.41Å (see theoretical methods), which in view of Buenker's results should be adequate for all states.

The results for perpendicular ethylene are tabulated in tables (8) and (14). As one would expect, the Rydberg states all increase sharply in energy as the dihedral angle is increased to 90° and therefore these results are of little practical value.

The N state increases by 2.89 eV (66.65 k cal mol^{-1}). This corresponds to the barrier to rotation about the C=C bond and is in good agreement with the experimental value of 65 k cal mol^{-1} [75].

As expected, both the V and Z states decrease in energy. The calculated excitation energies of 5.85 and 6.06 for the Z and V states respectively are in good agreement with Buenker's values of 6.14(Z) and 6.22(V) [74]. The experimental value for the 0-0 transition in the N-V absorption system is 6.0 eV [76] in good agreement with the present results.

Conclusions

Despite the relatively small size of the present basis it has produced good quantitative results for the Rydberg states. The one major failing has been the inability of the present basis to produce a more acceptable value for the V state (D_{2h}) and the $^1(\sigma,\pi^*)$ state (D_{2h}). Since the main objective of this study has been to produce a small basis set capable of providing a qualitative understanding of the electronic spectra of substituted ethylenes, the present basis has been relatively successful. The inability to produce better results for the V state is not serious since this transition is always very intense in the uv spectrum and is therefore easily identifiable.

Further Comment on the V State

The present calculations predict that the $1\,^1B_{1u}$ state is a mixture of 30% π^* + 60% $3d\pi$ (and vice versa for the 2^1B_{1u} state). Despite the large amount of Rydberg character the 1^1B_{1u} state was correlated with the spectroscopic V state. An excessive amount of Rydberg character was also predicted for the calculated V state of substituted ethylenes and this problem is discussed in greater detail in Chapter 5.

Appendix A - Corrections to Truncated CI calculations

In general it is not possible, for practical reasons, to consider all possible excitations when performing a configuration interaction calculation. Currently, most CI programs require the user to specify a threshold energy (T), the program then discards any configurations whose contribution to the total CI energy is less than the specified threshold energy.

MRDCI(a) operates in this fashion, but also estimates the contribution to the CI energy of the discarded configurations and corrects the CI energy accordingly.

For T = 0, one can consider the total configuration to be divided into three subsets $\{\phi_m\}$, $\{\phi_s\}$ and $\{\phi_r\}$ denoting main, selected and discarded (rejected) configurations respectively. The zero-order wavefunction χ_o and that obtained in the final truncated CI (for a given value of T) can then be defined as

$$\chi_o = \sum_m C_m^o \phi_m \tag{1}$$

and

$$\chi(T) = \sum_m C_m(T)\phi_m + \sum_s C_s(T)\phi_s \tag{2}$$

Similarly, the wavefunction $\chi \equiv \chi(o)$ for the T = 0 CI is represented as

$$\chi = \sum_m C_m(o)\phi_m + \sum_s C_s(o)\phi_s + \sum_r C_r(o)\phi_r \tag{3}$$

By construction the ϕ_r are weakly interacting species (especially when T is small and the set $\{\phi_m\}$ is sufficiently representative), i.e. the mixing coefficients C_m^o of the main configurations are unlikely to be altered by the presence of a given ϕ_r in the secular equation. The coefficient C_r is also expected to be essentially the same in the test calculation (with wavefunction χ_r) as it would be in the T = 0 CI treatment itself; therefore the approximation

$$\chi_r \sim (\chi_o + C_r(o)\phi_r)N \tag{4}$$

should be quite reasonable (χ_r is normalised). The assumption that each ϕ_r is so weakly interacting that it does not alter the relative weighting of the ϕ_m and ϕ_s species relative to their values in $\chi(T)$ yields

$$\chi \sim [\chi(T) + \sum_r C_r(o)\phi_r]N' \tag{5}$$

Using these assumptions, the energy lowering ΔE_r obtained by adding ϕ_r to the original set of main configurations ϕ_m can then be calculated from

$$\begin{aligned}\Delta E_r &= \langle\chi_r|H|\chi_r\rangle - \langle\chi_o|H|\chi_o\rangle \\ &\sim [\langle\chi_o|H|\chi_o\rangle + 2R_e\{C_r(o)\langle\chi_o|H|\phi_r\rangle\} + |C_r(o)|^2\langle\phi_r|H|\phi_r\rangle] \times \\ &\qquad (1 + |C_r(o)|^2)^{-1} - \langle\chi_o|H|\chi_o\rangle \\ &\sim 2R_e\{Cr(o)\langle\chi_o|H|\phi_r\rangle\} + |C_r(o)|^2\{\langle\phi_r|H|\phi_r\rangle - \langle\chi_o|H|\chi_o\rangle\}\end{aligned} \tag{6}$$

Using first order perturbation theory this equation can be simplified further to

$$\Delta E_r \sim C_r(o)\langle\chi_o|H|\phi_r\rangle \tag{6'}$$

In a similar fashion, the total energy $E \equiv E(0)$ of the T = 0 CI is

obtained (using eqn. (5)) as

$$E = \langle\chi|H|\chi\rangle \sim E(T) + \sum_r C_r(o)\langle\chi(T)|H|\phi_r\rangle \qquad (7)$$

Assuming χ_o is a good approximation to $\chi(T)$, the ΔE_r values of eqn. (6) can be substituted for the corresponding terms of the summation in eqn. (7), yielding

$$E \sim E(T) + \sum_r \Delta E_r \qquad (8)$$

This method can be further improved by calculating the corrected CI energies for a range of threshold values and extrapolating to zero to obtain the corrected CI energy for $T \longrightarrow 0$. Therefore, it is possible to predict reliable values for the T = 0 CI energy by choosing a small enough value for T and a sufficiently representative set of main configurations $\{\phi_m\}$.

References

1. R.S. Mulliken and C.C.J. Roothaan, Chem.Rev., 41, 219 (1947).
2. W.S. Gallaway and E.F. Barker, J.Chem.Phys., 10, 88 (1942).
3. H.C. Allen and E.K. Plyler, J.Am.Chem.Soc., 80, 2675 (1959).
4. W.L. Smith and I.M. Mills, J.Chem.Phys., 40, 2095 (1964).
5. R.L. Arnett and B.L. Crawford, J.Chem.Phys., 18, 118 (1950).
6. B.L. Crawford, J.E. Lancaster and R. Inskeep, J.Chem.Phys., 21, 678 (1953).
7. D.A. Dows, J.Chem.Phys., 36, 2833 (1962).
8. M.E. Jacob, J.Chem.Phys., 36, 140 (1962).
9. D.H. Rank, E.R. Schull and D.W.E. Axford, J.Chem.Phys., 18, 116 (1950).
10. B.P. Stoicheff, J.Chem.Phys., 21, 755 (1953).
11. J. Romanko, T. Feldman, E.J. Stansbury and A. McKellary, Can.J.Phys., 32, 735 (1954).
12. T. Feldman, J. Romanko, and H.L. Welsh, Can.J.Phys., 34, 737 (1956).
13. G. Herzberg, "Infra-red and Raman Spectra", D. Van Nostrand Co.Inc., Princeton, N.J., 1945.
14. C. Reid, J.Chem-Phys., 18, 1299 (1950)
15. D.F. Evans, J.Chem.Soc., 1735 (1960).
16. P.G. Wilkinson and R.S. Mulliken, J.Chem.Phys., 23, 1895 (1955).
17. J. Stark and P. Lipp, Z.Physik.Chem., 86, 36 (1913).
18. A. Scheibe and H. Greineisen, Z.Physik.Chem., 25B, 52 (1934).
19. C.P. Snow and C.B. Allsopp, Trans.Faraday Soc., 30, 93 (1934).
20. W.C. Price, Phys.Rev., 47, 444 (1935).
21. M. Zelikoff and K. Watanbe, J.Opt.Soc.Am., 43, 756 (1953).
22. L.C. Jones, Jr., and L.W. Taylor, Anal.Chem., 27, 228(1955).
23. R. McDiarmid and E. Charney, J.Chem.Phys., 47, 1517 (1967).

24. P.G. Wilkinson, Can.J.Phys., 34, 643 (1956).

25. J.M. Schulman, J.W. Moskowitz and C. Hollister, J.Chem.Phys., 46, 5037 (1968).

26. U. Kaldor and I. Shavitt, J.Chem.Phys., 48 (1968).

27. M.B. Robin, H. Basch, N.A. Kuebler, B.E. Kaplan and J. Meinwald, J.Chem.Phys., 48, 5037 (1968).

28. R.S. Mulliken, Phys.Rev. 50, 1017, 1028 (1932).

29. S. Huzinaga, Theor.Chim.Acta., 15, 12 (1969).

30. T.H. Dunning, Jr., W.J. Hunt and W.A. Goddard, Chem.Phys.Letters, 4, 147 (1969).

31. E. Miron, B. Raz and J. Jortner, Chem.Phys.Lett., 6, 563 (1970).

32. M.B. Robin and N.A. Kuebler, J.Mol.Spectrosc., 33, 274 (1970).

33. M. Krauss and S.R. Mielozarek, J.Chem.Phys., 51, 5241 (1969).

34. A.E. Hansen, Theoret.Chim.Acta., 14, 363 (1969).

35. H. Basch and V. McKoy, J.Chem.Phys., 53, 1628 (1970).

36. R.S. Mulliken, Chem.Phys.Lett., 25, 305 (1974).

37. J.A. Ryan and J.L. Whitten, Chem.Phys.Lett., 15, 119 (1972).

38. R.J. Buenker, S.D. Peyerimhoff and H.L. Hsu, Chem.Phys.Lett., 11, 65 (1971).

39. K.J. Ross and E.N. Lassettre, J.Chem.Phys., 44, 4633 (1966).

40. A.J. Merer and R.S. Mulliken, Chem.Rev., 69, 639 (1969).

41. P.G. Wilkinson, Can.J.Phys., 34, 643 (1956).

42. C.K. Ingold and G.W. King, J.Chem.Soc., 2702 (1953).

43. G. Herzberg, Molecular Spectra and Molecular Structure III Electronic Spectra and Electronic Structure of Polyatomic Molecules, p. 128.

44. J.B. Coon, N.W. Naugh and R.D. McKenzie, J.Mol.Spectra, 20, (1966) 107;
V.A. Job, V. Sethuraman and K.K. Innes, J.Mol.Spectry., 30, 365 (1969).

45. R.J. Buenker, S.D. Peyerimhoff, Theoret.Chim.Acta., 27, 243 (1972).

46. R.J. Buenker, S.K. Shiu, S.D. Peyerimhoff, Chem.Phys., 36, 97 (1979).

47. L.E. McMurchie and E.R. Davidson, J.Chem.Phys., 66, 2959 (1977).

48. R.J. Buenker, S.D. Peyerimhoff and C. Petrongolo, J.Chem.Phys., 76, 3655 (1982).

49. Price WC and Tutte WT, Proc.R.Soc., A174, 207-20 (1939).

50. Geiger J. and Wittmack K., Z.Naturf., 208, 628-9 (1965).

51. Mulliken R.S., J.Chem.Phys., 66, 2448 (1977).

52. Wilden D.G. and Comer J., J.Phys.B: Atom Molec.Phys., 13, 1009 (1980).

53. Brith-Linder , and Allen S.D., Chem.Phys.Letts., 47, 32 (1977).

54. Mulliken R.S., J.Chem.Phys., 71, 556 (1979).

55. Gedanken A., Kuebler N.A., Robin M.B., J.Chem.Phys., 76, 46 (1982).

56. Van Veen E.H., Chem.Phys.Lett., 41, 540(1976).

57. McMurchie and Davidson, E.R., J.Chem.Phys., 67, 5613 (1977).

58. Snyder P.A., Schatz P.N., Rowe E.M., Chem.Phys.Letts., 110, 508 (1984).

59. McDairmid, J.Phys.Chem., 84, 64 (1980).

60. Buenker R.J., Peyerimhoff S.D., Kammer W.E., J.Chem.Phys., 55, 814 (1971).

61. Foo P.D. and Innes K.K., J.Chem.Phys., 79, 1197 (1983).

62. Dunning T.H., J.Chem.Phys., 53, 2823 (1970).

63. S. Huzinaga, J.Chem.Phys., 42, 1293 (1965).

64. See Appendix in Peyerimhoff S.D., Buenker R.J. and Allen L.C., J.Chem.Phys., 65, 734 (1966).

65. Buenker R.J., Peyerimhoff S.D., and Fischbach U., Chem.Phys., 5, 265 (1974).

66. V.R. Saunders and M.F. Guest, "Atmol 3" (SERC 1976, RL-76101 and RL-76106).

67. Buenker, R.J. and Peyerimhoff S.D., Theor.Chim.Acta., 35, 33 (1974).

68. Buenker R.J., Peyerimhoff S.D. and Butscher W., Mol.Phys., 35, 771 (1978).

69. Brooks B.R. and Schaefer H.F., J.Chem.Phys., 68, 4839 (1978).

70. Palmer, M.H. to be published.

71. Nakatsuji H., J.Chem.Phys., 80, 3703 (1984).

72. Turner D.W., J.Chem.Soc., 4434 (1964).

73. Zeigler L.D., Hudson B.S., J.Chem.Phys., 79, 1197 (1983).

74. Buenker R.J. and Peyerimhoff S.D., Chem.Phys., 9, 75 (1976).

75. Douglas J.E., Rabinovitch B.S. and Looney F.S., J.Chem.Phys., 23, 315 (1955).
Lifschitz A., Bauer S.H., and Resler E.L., J.Chem.Phys., 38, 2056 (1963).

76. McDiarmid R., J.Chem.Phys., 55, 4669 (1971).

77. Fischer-Hjalmers, I; Kowalewski; Theor.Chim.Acta., 27, 197 (1972).

78. Buenker R.J., Peyerimhoff, S.D. and Shiu S.K., Chem.Phys.Lett., 69, 7 (1980)

Table 1

MO Description for Ethylene

Bonding	I.P. (e.V.)	D_{2h} species	LCAO form for C atoms
		$3b_{1u}$	$2p\sigma-2p\sigma$
CH*		$4a_g$	2s-2s
π^*		$1b_{2g}$	$2p_x-2p_x$
	V,T-N $\pi^* \leftarrow \pi$ R-N 3s←π		
π	10.51	$1b_{3u}$	$2p_x+2p_x$
CH	12.38	$1b_{3g}$	$2p_y-2p_y$
CH	14.47	$3a_g$	$2p\sigma+2p\sigma$
CH	15.63	$1b_{2u}$	$2p_y+2p_y$
CH	18.97	$2b_{1u}$	2s-2s
CC	~23	$2a_g$	2s+2s

Table 2

Orbital Correlations for the States of Ethylene

O_2 $D_{\infty h}$(UM)		C_2H_4 D_{2h}	C_2H_4 D_2	C_2H_4 D_{2d}	O_2 $D_{\infty h}$(UM)	Si Semi-UA
		$(1b_{2g})^0$	$(2b_2)^0$			
$(1\pi_g)^2$		$(1b_{3u})^2$	$(2b_3)^2$	$(2e)^2$	$(1\pi_g)^2$	$(3d\pi)^2$
		$(1b_{3g})^2$	$(1b_3)^2$			
$(1\pi_u)^4$		$(3a_g)^2$	$(3a)^2$	$(1e)^4$	$(1\pi_u)^4$	$(2p\pi)^4$
$(3\sigma_g)^2$		$(1b_{2u})^2$	$(1b_2)^2$	$(3a_1)^2$	$(3\sigma_g)^2$	$(3d\sigma)^2$
$(2\sigma_u)^2$		$(2b_{1u})^2$	$(2b_1)^2$	$(2b_2)^2$	$(2\sigma_u)^2$	$(2p\sigma)^2$
$(2\sigma_g)^2$		$(2a_g)^2$	$(2a)^2$	$(2a_1)^2$	$(2\sigma_g)^2$	$(2s\sigma)^2$

Table 3 - Correlation of the States of Planar and Perpendicular Ethylene with those of the United Molecule, O_2.

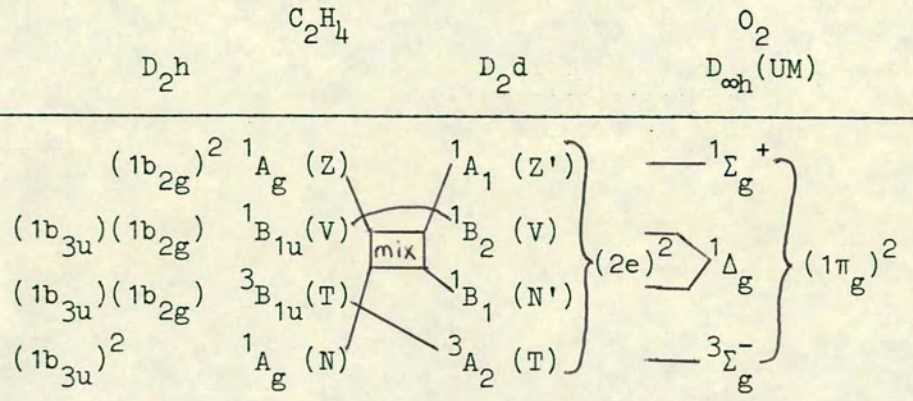

Table 4 - Ground State Vibration Frequencies (cm^{-1}) of C_2H_4 and C_2D_4

			C_2H_4	C_2D_4
a_g	ν_1	C-H stretch	3026.4	2251
	ν_2	C-C stretch	1622.9	1515
	ν_3	<HCH bend	1342.2	981
a_u	ν_4	Torsion	1023	(726)
b_{1u}	ν_5	C-H stretch	2988.7	2201.0
	ν_6	<HCH bend	1443.5	1077.9
b_{2g}	ν_7	CH_2 wagging	943	(780)
b_{2u}	ν_8	C-H stretch	3105.5	2345
	ν_9	CH_2 rocking	826.0	(593)
b_{3g}	ν_{10}	C-H stretch	3102.5	2304
	ν_{11}	CH_2 rocking	(1222)	(1006)
b_{3u}	ν_{12}	CH_2 wagging	949.3	720.0

Table 5 - Summary of literature assignment of the ethylene spectrum

Name	State	Symbol	term value	n*	Poln.	Semi-UAO	Exp Evidence
2R	$^1B_{3u}$	$4a_g$	3.40	2.00	x	3s	Ref.[49]
π^*	$^1B_{1u}$	$1b_{2g}$	2.85	2.18	z	$(3d\pi_x)$	
3R'	$^1B_{1g}$	$2b_{2u}$	2.25	2.46	forbidden[a] (Z)	$3p\pi_y$	MPI [55]
3R''	$^1B_{3u}$	$5a_g$	1.89	2.86	x	$4d\sigma$	
	^1Au	$2b_{3g}$			forbidden[b]	$4d\pi_y$	
	^1Ag	$2b_{3u}$			forbidden[b]	$3p\pi_x$	MPI [55]
3R	$^1B_{2u}$	$1b_{1g}$	1.61	2.91	y	$3d\delta sin$	MCD [58]
	$^1B_{3u}$	$6a_g$			x	$3d\delta cos$	
4R'''	$^1B_{3u}$	$^1A_1 \rightarrow 3R_{oo} + \nu_3$	1.46	3.06	x		MCD [58]
4R'	$^1B_{1u}$	$2b_{2g}$	1.15	3.45	z	$4d\pi_x$	
4R''	$^1B_{3u}$	8ag	1.00	3.70	x	$5d\sigma$	
4R	$^1B_{2u}$	$2b_{2g}$	0.89	3.92		$4d\delta sin$	
	$^1B_{3u}$	9ag				$4d\delta cos$	

[a] For transition to indicated state. But most forbidden transitions are very weakly allowed if the upper state is twisted, as expected.

[b] Transitions to ^1Au and ^1Ag forbidden even if twisted.

Table 6 - Summary of previous theoretical results for ethylene

State	Orbital	McM.D.[a]	F.K.[b]	B.P.[c]
$^1(\pi,4a_g)$	3s	7.26	7.49	7.13
$^1(\pi,2b_{2u})$	$3p_y$	7.93	8.03	7.89
$^1(\pi,1b_{2g})$	π^*	7.96		7.96
$^1(\pi,3b_{1u})$	$3p_z$	8.01	8.19	7.86
$^1(\pi,2b_{3u})$	$3p_x$	8.36	8.42	8.21
$^1(\pi,5a_g)$	$3d_\sigma$	8.80	8.98	8.73
$^1(\pi,2b_{3g})$	$3d_{yz}$	8.99	9.04	8.83
$^1(\pi,6a_g)$	$3d\delta$	8.99	9.03	8.92
$^1(\pi,1b_{1g})$	$3d_{xy}$	9.04	9.04	8.88
$^1(\pi,7a_g)$	4s	9.12	9.06	8.98
$^1(\pi,2b_{2g})$	$3d_{xz}$	9.31	9.43	9.17

[a] McMurchie and Davidson, ref [57]

[b] Fischer-Hjalmers and Kowalewski, ref. [77]

[c] Buenker and Peyerimhoff, ref. [48]

Table 7 - Theoretical results of Buenker et al.

Upper state	Excitation	Polarization	n	CI(PCMO)	Exptl.
^1A_g	...	...	...	0.0	0.0
$^1B_{1u}$	$1b_{1u} \rightarrow 4a_g$	z	3	6.943	7.108
$^1B_{3g}$	$1b_{1u} \rightarrow 2b_{2u}$	yz	3	7.498	
$^1B_{2g}$	$1b_{1u} \rightarrow 3b_{3u}$	xz	3	7.553	
2^1A_g	$1b_{1u} \rightarrow 2b_{1u}$	x^2,y^2,z^2	3	8.035	(8.257)
$^1B_{3u}$	$1b_{1u} \rightarrow 1b_{2g}$	x	3	8.323	(7.66)
2^1B_{1u}	$1b_{1u} \rightarrow 5a_g$	z	3	8.440	8.618
^1A_u	$1b_{1u} \rightarrow 2b_{1g}$	0	3	8.443	
2^1B_{2g}	$1b_{1u} \rightarrow 4b_{3u}$	xz	3	9.329	
2^1B_{3g}	$1b_{1g} \rightarrow 1b_{2g}$	yz	2	9.885	
2^1B_{3u}	$1b_{1u} \rightarrow 2b_{2g}$	x	2	10.730	
2^1A_u	$1b_{1g} \rightarrow 2b_{1u}$	0	3	10.788	
$^1B_{1g}$	$1b_{1g} \rightarrow 4a_g$	xy	3	11.102	
3^1B_{2g}	$3a_g \rightarrow 1b_{2g}$	xz	2	11.341	
3^1B_{3u}	$1b_{1g} \rightarrow 2b_{2u}$	x	3	11.475	
$^1B_{2u}$	$1b_{1g} \rightarrow 3b_{3u}$	y	3	11.799	
3^1B_{3g}	$1b_{1g} \rightarrow 2b_{2g}$	yz	3	11.893	
3^1Au	$1b_{2u} \rightarrow 1b_{2g}$	0	2	12.173	
2^1B_{1g}	$1b_{1g} \rightarrow 5a_g$	xy	3	12.597	
$^3B_{3u}$	$1b_{1u} \rightarrow 1b_{2g}$	x	2	4.255	4.6 (4.4-4.7)
$^3B_{1u}$	$1b_{1u} \rightarrow 4a_g$	z	3	6.795	
$^3B_{3g}$	$1b_{1u} \rightarrow 2b_{2u}$	yz	3	7.469	
$^3B_{2g}$	$1b_{1u} \rightarrow 3b_{3u}$	xz	3	7.493	
^3A_g	$1b_{1u} \rightarrow 2b_{1u}$	x^2,y^2,z^2	3	7.732	

Upper state	Excitation	Polarization	n	CI(PCMO)	Exptl.
2^3B_{1u}	$1b_{1u} \rightarrow 5a_g$	z	3	8.372	
^3A_u	$1b_{1u} \rightarrow 2b_{1g}$	0	3	8.432	
2^3B_{2g}	$1b_{1u} \rightarrow 4b_{3u}$	xz	3	9.294	
2^3B_{3g}	$1b_{1g} \rightarrow 1b_{2g}$	yz	2	9.522	
2^3B_{3u}	$1b_{1u} \rightarrow 2b_{2g}$	x	3	9.530	
2^3Au	$1b_{1g} \rightarrow 2b_{1u}$	0	3	10.770	
3^3B_{2g}	$3a_g \rightarrow 1b_{2g}$	xz	2	10.792	
$^3B_{1g}$	$1b_{1g} \rightarrow 4a_g$	xy	3	10.994	
3^3B_{3u}	$1b_{1g} \rightarrow 2b_{2u}$	x	3	11.308	
$^3B_{2u}$	$1b_{1g} \rightarrow 3b_{3u}$	y	3	11.688	
3^3B_{3g}	$1b_{1g} \rightarrow 2b_{2g}$	yz	3	11.790	
3^3A_u	$1b_{2u} \rightarrow 1b_{2g}$	0	2	12.140	
2^3A_g	$3a_g \rightarrow 4a_g$	x^2,y^2,z^2	3	12.303	
3^3Ag	$1b_{1g} \rightarrow 2b_{1g}$	x^2,y^2,z^2	3	12.463	
2^3B_{1g}	$1b_{1g} \rightarrow 5a_g$	xy	3	12.577	

Table 8 Excitation Energies for Planar Ethylene and Twisted Ethylene

		excitation energy / eV				excitation energy / eV			
transition	D_{2h} Symmetry State	Buenker Ref.[48]	Palmer Ref.[70]	39 basis	D_2 Symmetry State	39 basis	D_{2d} Symmetry (C_{2v})	39 basis	MHP [Ref.[70]
$^3(\pi,\pi^*)$	1^3B_{1u}	4.35	-	4.58	1^3B_1	3.58	-	-	-
$^1(\pi,3s)$	1^1B_{3u}	7.13	7.54	7.46	1^1B_3	7.29	1^1B_1 1^1B_2	8.51	8.03
$^1(\pi,3p_z)$	1^1B_{2g}	7.86	8.13	7.86	1^1B_2	7.73	3^1A_1	9.01	9.53
$^1(\pi,3p_y)$	1^1B_{1g}	7.89	8.17	7.86	1^1B_1	7.28	2^1A_2	8.90	9.63
$^1(\pi,\pi^*)$	1^1B_{1u}	7.96	8.21	8.36	2^1B_1	7.51	$Z1^1A_1$	5.85	5.49
$^1(\pi,3p_x)$	1^1Ag	8.21	8.52	8.18	1^1A_1	7.99	2^1B_1 1^1B_2	9.14	9.44
$^1(\pi,3d\sigma)$	2^1B_{3u}	8.73	9.23	8.77	2^1B_3	8.63	3^1B_1 1^1B_2	9.95	9.96
$^1(\pi,3d_{yz})$	1^1Au	8.83	9.19	8.86	2^1A_1	8.76	-	-	
$^1(\pi,3d_{xy})$	1^1B_{2u}	8.88	9.25	8.89	2^1B_2	8.75	4^1B_1 1^1B_2	10.07	
$^1(\pi,4s)$	3^1B_{3u}	8.98	9.38	8.86	3^1B_3	8.78	-	-	
$2^1(\pi,\pi^*\text{-}nd\pi)$	2^1B_{1u}	9.17	9.53	9.52	3^1B_1	8.95	-	-	
							V 2^1A_1	6.06	5.63
							N 1^1A_2	2.89	2.96

Table 9 Excitation Energies for Planar Ethylene

State	Transition	excitation energy / eV 39 basis	MHP	experimental
1^3B_{3u}	$\pi\rightarrow 3s$	7.24	7.42	6.98[a]
1^1B_{3u}		7.46	7.54	7.11[b]
1^3B_{2g}	$\pi\rightarrow 3p_z$	7.83	8.06	7.78[a]
1^1B_{2g}		7.86	8.13	7.83[c]
1^3B_{1g}	$\pi\rightarrow 3p_y$	7.87	8.16	7.78[a]
1^1B_{1g}		7.86	8.17	7.83[c]
1^3B_{1u}	$\pi\rightarrow\pi^*$	4.58	4.61	4.6[d]
1^1B_{1u}		8.36	8.21	7.65[d]
1^3Ag	$\pi\rightarrow 3p_x$	8.14	8.38	8.15[a]
1^1Ag		8.18	8.52	8.26[b]
2^3B_{3u}	$\pi\rightarrow 3d\sigma$	8.79	9.36	8.57[a]
2^1B_{3u}		8.77	9.23	8.62[b]
1^3Au	$\pi\rightarrow 3d_{yz}$	8.93	9.39	
1^1Au		8.86	9.19	8.90
1^3B_{2u}	$\pi\rightarrow 3d_{xy}$	8.91	9.38	
1^1B_{2u}		8.89	9.25	
$^3B_{3u}$	$\pi\rightarrow 4s$	8.87	9.39	
2^1B_{3u}		8.86	9.38	
2^1B_{1u}	$\pi\rightarrow\pi^*-nd\pi$	9.01	9.41	
		9.52	9.53	9.36[b]

[a] ref. 52

[b] refs. 40 & 51.

[c] ref. 56

[d] ref. 78

Table 10 Excitation Energies for Twisted Ethylenes (D_2)

State	transition	excitation energy / eV
1^3B_3	$\pi\rightarrow 3s$	7.10
1^1B_3		7.29
1^3B_2	$\pi\rightarrow {}^3p_z$	7.54
1^1B_2		7.73
1^3B_1	$\pi\rightarrow\pi^*$	3.58
1^1B_1	$\pi\rightarrow 3p_y$	7.28
2^3B_1	$\pi\rightarrow 3p_y$	7.51
2^1B_1	$\pi\rightarrow\pi^*$	7.51
1^3A_1	$\pi-3p_x$	7.81
1^1A_1		7.99
2^3B_3	$\pi\rightarrow 3d\sigma$	8.51
2^1B_3		8.63
2^3A_1	$\pi\rightarrow 3d_{yz}$	8.59
2^1A_1		8.76
2^3B_2	$\pi\rightarrow 3d_{xy}$	8.63
2^1B_2		8.75
3^3B_3	$\pi\rightarrow 4s$	9.47
3^1B_3		8.78
3^3B_1	$\pi\rightarrow\pi^*-nd\pi$	8.71
3^1B_1		8.95

Table 11 Ethylene D_{2h} singlets

State	no. of main configurations	(Coefficient)^2	Correction/a.u.	CI energy/ a.u.	excitation energy/eV	table no.
$1\,^1A_u$	6M2R	.9300	-.01179	-77.8835	8.86	15a
$2\,^1A_u$	6M2R	.8863	-.02475	-77.8175	10.66	15b
$1\,^1A_u$	3M2R	.9132	-.01629	-77.8838	8.85	16a
$2\,^1A_u$	3M2R	.9037	-.01864	-77.7270	12.12	16b
$1\,^1A_u$	5M2R	.9289	-.01195	-77.8831	8.87	17a
$2\,^1A_u$	5M2R	.8913	-.02131	-77.7254	13.16	17b
$X\,^1A_g$	6M2R	.9334	-.01104	-78.2092	-	18a
$1\,^1A_g$	6M2R	.9204	-.01393	-77.9085	8.18	18b
$1\,^1A_g$	5M2R	.9213	-.01384	-77.9086	8.18	19a
$2\,^1A_g$	5M2R	.8871	-.0246	-77.7910	11.38	19b
$1\,^1B_{1u}$	5M2R	.9198	-.0143	-77.9024	8.35	20a
$2\,^1B_{1u}$	5M2R	.9114	-.0173	-77.8567	9.59	20b
$1\,^1B_{1u}$	6M2R	.9202	-.0142	-77.9010	8.36	21a
$2\,^1B_{1u}$	6M2R	.9121	-.0173	-77.8592	9.52	21b
$1\,^1B_{2u}$	4M1R	.9302	-.0116	-77.8809	8.89	22
$1\,^1B_{2u}$	3M2R	.9199	-.0178	-77.8809	8.89	23a
$2\,^1B_{2u}$	3M2R	.8815	-.0262	-77.8273	10.39	23b
$1\,^1B_{3u}$	9M3R	.92320	-.0134	-77.9325	7.53	24a
$2\,^1B_{3u}$	9M3R	.9179	-.0143	-77.8859	8.80	24b
$3\,^1B_{3u}$	9M3R	.9133	-.0157	-77.8834	8.87	24c

....Cont.

Table 11 (Cont'd..)

State	No. of main configurations	(Coefficient)^2	Correction/a.u.	CI energy/ a.u.	excitation energy/eV	table no.
$1\,^1B_{3u}$	6M4R	.9175	-.0149	-77.9351	7.46	25a
$2\,^1B_{3u}$	6M4R	.9127	-.0159	-77.8869	8.77	25b
$3\,^1B_{3u}$	6M4R	.9081	-.0173	-77.8835	8.86	25c
$4\,^1B_{3u}$	6M4R	.9061	-.0178	-77.8411	10.01	25d
$1\,^1B_{1g}$	5M2R	.9222	-.1036	-77.9204	7.86	26a
$2\,^1B_{1g}$	5M2R	.9047	-.0178	-77.8021	11.08	26b
$1\,^1B_{1g}$	5M2R	.9265	-.0125	-77.9214	7.83	27a
$2\,^1B_{1g}$	5M2R	.9050	-.0179	-77.8019	11.08	27b
$1\,^1B_{2g}$	6M2R	.9253	-.0128	-77.9204	7.86	28a
$2\,^1B_{2g}$	6M2R	.8902	-.0215	-77.7856	11.52	28b
$1\,^1B_{2g}$	5M1R	.9281	-.0122	-77.9195	7.88	29

Table 12 Ethylene D_{2h} Triplets

State	No. of main configurations	Σ(Coefficient)	Correction/ a.u.	CI Energy/ a.u.	Excitation Energy/eV	Table No.
1^3Au	6M2R	.9342	-.0110	-.77.8813	8.93	30a
2^3Au	6M2R	.8868	-.0250	-.77.8208	10.57	30b
1^3Ag	4M1R	.9301	-.0117	-.77.9100	8.14	31
1^3B_{1u}	4M2R	.9942	-.0086	-78.0409	4.58	32a
2^3B_{1u}	4M2R	.9164	-.0155	-77.8783	9.01	32b
1^3B_{2u}	5M1R	.9355	-.0107	-77.8814	8.91	33
1^3B_{2u}	3M2R	.9228	-.0137	-77.8798	8.96	34a
2^3B_{2u}	3M2R	.8769	-.0273	-77.8305	10.30	34b
1^3B_{3u}	6M4R	.9215	-.0146	-77.9431	7.24	35a
2^3B_{3u}	6M4R	.9140	-.0156	-77.8861	8.79	35b
3^3B_{3u}	6M4R	.9072	-.0174	-77.8833	8.87	35c
4^3B_{3u}	6M4R	.9127	-.0166	-77.8523	9.71	35d
1^3B_{1g}	5M2R	.9307	-.0117	-77.9199	7.87	36a
2^3B_{1g}	5M2R	.9130	-.0156	-77.8030	11.05	36b
1^3B_{2g}	5M2R	.9297	-.0120	-77.9215	7.83	37a
2^3B_{2g}	5M2R	.9040	-.0185	-77.7942	11.29	37b

Table 13 Ethylene D_2 Excitation Energies

State	No. of main Configurations	Σ(Coefficient)^2	Correction/a.u.	CI Energy/ a.u.	Excitation Energy/eV	Table No.
$1\,^1A_1$	3M3R	.9061	-.0178	-77.9156	7.99	38a
$2\,^1A_1$	3M3R	.9099	-.0171	-77.8873	8.76	38b
$3\,^1A_1$	3M3R	.8177	-.0364	-77.7564	12.32	38c
$1\,^1B_3$	4M4R	.9110	-.0171	-77.9413	7.29	39a
$2\,^1B_3$	4M4R	.9068	-.0178	-77.8919	8.63	39b
$3\,^1B_3$	4M4R	.9086	-.0173	-77.8866	8.78	39c
$4\,^1B_3$	4M4R	.9028	-.0189	-77.8480	9.82	39d
$1\,^1B_1$	5M3R	.9002	-.0202	-77.9416	7.28	40a
$2\,^1B_1$	5M3R	.9140	-.0173	-77.9333	7.51	40b
$3\,^1B_1$	5M3R	.9104	-.0177	-77.8802	8.95	40c
$1\,^1B_2$	3M3R	.9084	-.0177	-77.9251	7.73	41a
$2\,^1B_2$	3M3R	.9110	-.0168	-77.8878	8.75	41b
$3\,^1B_2$	3M3R	.8833	-.0232	-77.7972	11.212	41c
$1\,^3A_1$	3M3R	.9149	-.0166	-77.9224	7.81	42a
$2\,^3A_1$	3M3R	.9144	-.0167	-77.8936	8.59	42b
$3\,^3A_1$	3M3R	.8918	-.0215	-77.7479	12.55	42c
$1\,^3B_3$	4M4R	.9181	-.0159	-77.9481	7.10	43a
$2\,^3B_3$	4M4R	.9094	-.0177	-77.8966	8.51	43b
$3\,^3B_3$	4M4R	.9093	-.0177	-77.8613	9.47	43c
$4\,^3B_3$	4M4R	.9028	-.0189	-77.8480	9.83	43d

Cont'd...

Table 13 (Cont'd)

State	No. of main Configurations	$\Sigma(\text{Coefficient})^2$	Correction/a.u.	CI Energy/ a.u.	Excitation Energy/eV	Table No.
$1\,^3B_1$	6M4R	.9406	-.0098	-78.0776	3.58	44a
$2\,^3B_1$	6M4R	.9157	-.0167	-77.9333	7.51	44b
$3\,^3B_1$	6M4R	.9152	-.0165	-77.8892	8.71	44c
$4\,^3B_1$	6M4R	.8384	-.0355	-77.8677	9.29	44d
$1\,^3B_2$	3M3R	.9126	-.0172	-77.9322	7.54	45a
$2\,^3B_2$	3M3R	.9148	-.0164	-77.8921	8.63	45b
$3\,^3B_2$	3M3R	.8983	-.0206	-77.8152	10.72	45c

Table 14 Ethylene D_{2d} Excitation Energies

State	No. of main Configurations	$\Sigma(\text{Coefficient})^2$	Correction/a.u.	CI Energy/a.u.	Excitation Energy/eV	Table No.
$1\,^1A_1$	8M4R	.8939	-.0236	-77.9940	5.85	46a
$2\,^1A_1$	8M4R	.9003	-.0211	-77.9862	6.06	46b
$3\,^1A_1$	8M4R	.9072	-.0183	-77.8782	9.01	46c
$4\,^1A_1$	8M4R	.9077	-.0182	-77.8761	9.06	46d
$1\,^1B_1$	10M4R	.9122	-.0168	-77.8972	8.49	47a
$2\,^1B_1$	10M4R	.9091	-.0175	-77.8742	9.11	47b
$3\,^1B_1$	10M4R	.9093	-.0171	-77.8434	9.95	47c
$4\,^1B_1$	10M4R	.9157	-.0157	-77.8391	10.06	47d
$1\,^1B_2$	10M4R	.9122	-.0167	-77.8959	8.52	48a
$2\,^1B_2$	10M4R	.9091	-.0174	-77.8734	9.14	48b
$3\,^1B_2$	10M4R	.9092	-.0171	-77.8431	9.96	48c
$4\,^1B_2$	10M4R	.9157	-.0157	-77.8391	10.07	48d
$1\,^1A_2$	7M3R	.9307	-.0114	-78.1031	2.89	49a
$2\,^1A_2$	7M3R	.9121	-.0173	-77.8821	8.90	49b
$3\,^1A_2$	7M3R	.9154	-.0165	-77.8787	8.99	49c

Tables 15-37 refer to planar ethylene (D_{2h})

Tables 15a and b n ^1Au, 6M2R

Table 15 a $1\,^1Au$ $^1(\pi, 3dyz)$

(Coefficient)^2	$2a_g$	$2b_{1u}$	$1b_{2u}$	$3a_g$	$1b_{3g}$	$1b_{3u}$	$2b_{3u}$	$2b_{3g}$	$3b_{2u}$	$3b_{3g}$	$3b_{3u}$
.9089M	2	2	2	2	2	1	–	1	–	–	–
.0059M	2	2	2	2	2	–	–	1	–	–	1
.0046M	2	2	2	2	2	1	–	–	–	1	–
.0000M	2	2	2	2	1	2	1	–	–	–	–
.0057M	2	2	1	2	2	1	–	1	1	–	–
.0052M	2	2	2	2	1	1	–	1	–	1	–

Table 15b $2\,^1Au$

(Coefficient)^2	$2a_g$	$2b_{1u}$	$1b_{2u}$	$3a_g$	$1b_{3g}$	$1b_{3u}$	$2b_{3u}$	$2b_{3g}$	$2b_{2g}$	$3b_{2u}$	$3b_{3g}$	$3b_{3u}$
.0000M	2	2	2	2	2	1	–	1	–	–	–	–
.0000M	2	2	2	2	2	–	–	1	–	–	–	1
.0000M	2	2	2	2	2	1	–	–	–	–	1	–
.8863M	2	2	2	2	1	2	1	–	–	–	–	–
.0102	2	2	2	2	1	–	1	–	2	–	–	–
.0000M	2	2	1	2	2	1	–	1	–	1	–	–
.0000M	2	2	2	2	1	1	–	1	–	–	1	–
.0112	2	2	1	2	2	1	1	–	1	–	–	–
.0095	2	2	2	2	1	1	1	–	–	–	1	–

Tables 16a and b n ^{1}Au 3M2R

Table 16a 1 ^{1}Au $^1(\pi, 3dyz)$

(Coefficient)^2	$2a_g$	$2b_{1u}$	$1b_{2u}$	$3a_g$	$1b_{3g}$	$1b_{3u}$	$2b_{3g}$	$2b_{2g}$	$2b_{2u}$	$3b_{2g}$	$3g_{3u}$
.8946M	2	2	2	2	2	1	1	–	–	–	–
.0056	2	2	2	2	2	1	–	–	–	–	1
.0181M	2	2	2	2	2	1	–	–	–	1	–
.0005M	2	2	2	2	2	–	–	1	1	–	–
.0053	2	2	1	2	2	1	1	–	1	–	–

Table 16b 2 ^{1}Au

(Coefficient)^2	$2a_g$	$2b_{1u}$	$1b_{2u}$	$3a_g$	$1b_{3g}$	$1b_{3u}$	$2b_{3s}$	$2b_{2g}$	$3b_{2u}$	$3b_{3g}$	$4b_{3g}$
.0185M	2	2	2	2	2	1	1	–	–	–	–
.8676M	2	2	2	2	2	1	–	–	–	1	–
.0073	2	2	2	2	2	1	–	–	–	–	1
.0175M	2	2	2	2	2	–	–	1	1	–	–

Tables 17a and b n ^{1}Au 5M2R

Table 17a 1 $^1(\pi, 3dyz)$

(Coefficient)^2	$2a_g$	$2b_{1u}$	$1b_{2u}$	$3a_g$	$1b_{3g}$	$1b_{3u}$	$2b_{3g}$	$2b_{2g}$	$2b_{2u}$	$3b_{3g}$	$3b_{3u}$	$4b_{3g}$
.8942M	2	2	2	2	2	1	1	–	–	–	–	–
.0058M	2	2	2	2	2	–	1	–	–	–	1	–
.0183M	2	2	2	2	2	1	–	–	–	1	–	–
.0055M	2	2	1	2	2	1	1	–	1	–	–	–
.0051M	2	2	2	2	1	1	1	–	–	1	–	–

Table 17b $2\,^1Au$

(Coefficient)^2	$2a_g$	$2b_{1u}$	$1b_{2u}$	$3a_g$	$1b_{3g}$	$1b_{3u}$	$2b_{3g}$	$2b_{2g}$	$3b_{2u}$	$3b_{3g}$	$3b_{3u}$	$4b_{3g}$
.0186M	2	2	2	2	2	1	1	–	–	–	–	–
.0003M	2	2	2	2	2	–	1	–	–	–	1	–
.8718M	2	2	2	2	2	1	–	–	–	1	–	–
.0073	2	2	2	2	2	1	–	–	–	–	–	1
.0140	2	2	2	2	2	–	–	1	1	–	–	–
.0002M	2	2	1	2	2	1	1	–	1	–	–	–
.0004M	2	2	2	2	1	1	1	–	–	1	–	–

Tables 18a and b n ^1Ag 6M2R

Table 18a X'Ag

(Coefficient)^2	$2a_g$	$2b_{1u}$	$1b_{2u}$	$3a_g$	$1b_{3g}$	$1b_{3u}$	$2b_{3u}$	$2b_{2g}$	$3b_{2u}$	$3b_{3u}$	$3b_{2g}$
.9148M	2	2	2	2	2	2	–	–	–	–	–
.0134M	2	2	2	2	2	–	–	2	–	–	–
.0000M	2	2	2	2	2	1	1	–	–	–	–
.0000M	2	2	2	2	2	–	1	–	–	1	–
.0050M	2	2	2	2	2	–	–	1	–	–	1
.0001M	2	2	1	2	2	1	1	–	1	–	–

Table 18b $1\,^1Ag$ $^1(\pi, 3px)$

$(\text{Coefficient})^2$	$2a_g$	$2b_{1u}$	$1b_{2u}$	$3a_g$	$1b_{3g}$	$1b_{3u}$	$2b_{3u}$	$2b_{2g}$	$3b_{2u}$	$3b_{3u}$	$3b_{2g}$
.0001M	2	2	2	2	2	2	–	–	–	–	–
.0010M	2	2	2	2	2	–	–	2	–	–	–
.9072M	2	2	2	2	2	1	1	–	–	–	–
.0063M	2	2	2	2	2	–	1	–	–	1	–
.0011M	2	2	2	2	2	–	–	1	–	–	1
.0048M	2	2	1	2	2	1	1	–	1	–	–

Tables 19a and b $n\,^1Ag$ 5M2R

Table 19a $1\,^1Ag$ $^1(\pi, 3px)$

$(\text{Coefficient})^2$	$2a_g$	$2b_{1u}$	$1b_{2u}$	$3a_g$	$1b_{3g}$	$1b_{3u}$	$2b_{3u}$	$2b_{3g}$	$2b_{2g}$	$3b_{2u}$	$3b_{3u}$	$3b_{2g}$
.9077M	2	2	2	2	2	1	1	–	–	–	–	–
.0062M	2	2	2	2	2	–	1	–	–	–	1	–
.0023M	2	2	2	2	2	1	–	–	–	–	1	–
.0002M	2	2	2	2	1	2	–	1	–	–	–	–
.0048M	2	2	1	2	2	1	1	–	–	1	–	–

Table 19b 2 ^1A_g

(Coefficient)^2	$2a_g$	$2b_{1u}$	$1b_{2u}$	$3a_g$	$1b_{3g}$	$1b_{3u}$	$2b_{3u}$	$2b_{3g}$	$2b_{2g}$	$3b_{2u}$	$3b_{3u}$	$3b_{2g}$
.0003M	2	2	2	2	2	1	1	–	–	–	–	–
.0000M	2	2	2	2	2	–	1	–	–	–	1	–
.0003M	2	2	2	2	2	1	–	–	–	–	1	–
.8865M	2	2	2	2	1	2	–	1	–	–	–	–
.01014	2	2	1	2	2	1	1	–	–	1	–	–
.0000M	2	2	1	2	2	1	1	–	–	1	–	–
.0087	2	2	2	2	1	1	–	1	–	–	1	–
.0057	2	2	2	2	1	–	–	1	1	–	–	1
.0113	2	2	1	2	2	1	–	1	1	–	–	–

Tables 20a and b n $^1B_{1u}$ 5M2R

Table 20a 1 $^1B_{1u}$ $^1(\pi,\pi^*)$

(Coefficient)^2	$2a_g$	$2b_{1u}$	$1b_{2u}$	$3a_g$	$1b_{3g}$	$1b_{3u}$	$1b_{2g}$	$2b_{2g}$	$3b_{2u}$	$3b_{3g}$	$3b_{3u}$
.64711M	2	2	2	2	2	1	1	–	–	–	–
.0035M	2	2	2	2	2	–	1	–	–	–	1
.2632M	2	2	2	2	2	1	–	1	–	–	–
.0033M	2	2	1	2	2	1	1	–	1	–	–
.0026M	2	2	2	2	1	1	1	–	–	1	–

Table 20b 2 $^1B_{1u}$ (π,π^*-3dxz)

(Coefficient)^2	$2a_g$	$2b_{1u}$	$1b_{2u}$	$3a_g$	$1b_{3g}$	$1b_{3u}$	$1b_{2g}$	$2b_{2g}$	$3b_{2u}$	$3b_{3g}$	$3b_{3u}$
.2654M	2	2	2	2	2	1	1	-	-	-	-
.0029M	2	2	2	2	2	-	1	-	-	-	1
.6389M	2	2	2	2	2	1	-	1	-	-	-
.0021M	2	2	1	2	2	1	1	-	1	-	-
.0022M	2	2	2	2	1	1	1	-	-	1	-

Tables 21a and b n $^1B_{1u}$ 6M2R

Table 21a 1 $^1B_{1u}$ $^1(\pi,\pi^*)$

(Coefficient)^2	$2a_g$	$2b_{1u}$	$1b_{2u}$	$3a_g$	$1b_{3g}$	$1b_{3u}$	$2b_{2u}$	$1b_{2g}$	$2b_{2g}$	$3b_{2u}$	$3b_{3g}$	$3b_{3u}$
.6503M	2	2	2	2	2	1	-	1	-	-	-	-
.0035M	2	2	2	2	2	-	-	1	-	-	-	1
.2599M	2	2	2	2	2	1	-	-	1	-	-	-
.0005M	2	2	2	2	1	2	1	-	-	-	-	-
.0037M	2	2	1	2	2	1	-	1	-	1	-	-
.0027M	2	2	2	2	1	1	-	1	-	-	1	-

Table 21b 2 $^1B_{1u}$ $^1(\pi,\pi^*$-3dxz)

(Coefficient)^2	$2a_g$	$2b_{1u}$	$1b_{2u}$	$3a_g$	$1b_{3g}$	$1b_{3u}$	$2b_{2u}$	$1b_{2g}$	$2b_{2g}$	$3b_{2u}$	$3b_{3g}$	$3b_{3u}$
.2621M	2	2	2	2	2	1	-	1	-	-	-	-
.0028M	2	2	2	2	2	-	-	1	-	-	-	1
.6418M	2	2	2	2	2	1	-	-	1	-	-	-
.0010M	2	2	2	2	1	2	1	-	-	-	-	-
.0021M	2	2	1	2	2	1	-	1	-	1	-	-
.0022M	2	2	2	2	1	1	-	1	-	-	1	-

Table 22 $1\,^1B_{2u}$ $^1(\pi, 3dxy)$

(Coefficient)^2	$2a_g$	$2b_{1u}$	$1b_{2u}$	$3a_g$	$1b_{3g}$	$1b_{3u}$	$1b_{1g}$	$3b_{2u}$	$3b_{3g}$	$3b_{3a}$
.91363657M	2	2	2	2	2	1	1	–	–	–
.00624900M	2	2	2	2	2		1	–	–	1
.00538394M	2	2	1	2	2	1	1	1	–	–
.00488828M	2	2	2	2	1	1	1	–	1	–

Tables 23a and b n $^1B_{2u}$ 2M2R

Table 23a $1\,^1B_{2u}$ $^1(\pi, 3dxz)$

(Coefficient)^2	$2a_g$	$2b_{1u}$	$1b_{2u}$	$3a_g$	$1b_{3g}$	$1b_{3u}$	$3b_{1u}$	$1b_{1g}$	$2b_{2g}$	$4b_{1u}$	$3b_{3u}$	$3b_{2g}$	$3b_{2u}$
.9136M	2	2	2	2	2	1	–	1	–	–	–	–	–
.0063M	2	2	2	2	2	–	–	1	–	–	1	–	–
.0000M	2	2	2	2	1	2	1	–	–	–	–	–	–
.0052	2	2	1	2	2	1	–	1	–	–	–	–	1

Table 23b $2\,^1B_{2u}$

(Coefficient)^2	$2a_g$	$2b_{1u}$	$1b_{2u}$	$3a_g$	$1b_{3g}$	$1b_{3u}$	$3b_{1u}$	$1b_{1g}$	$2b_{2g}$	$4b_{1u}$	$3b_{3u}$	$3b_{2g}$	$3b_{2u}$
.0000M	2	2	2	2	2	1	–	1	–	–	–	–	–
.0000M	2	2	2	2	2	–	–	1	–	–	1	–	–
.8815M	2	2	2	2	1	2	1	–	–	–	–	–	–
.0073	2	2	2	2	1	2	–	–	–	1	–	–	–
.0099	2	2	2	2	1	–	1	–	2	–	–	–	–
.0107	2	2	1	2	2	1	1	–	1	–	–	–	–
.0084	2	2	2	2	1	1	1	–	–	–	1	–	–
.0056	2	2	2	2	1	–	1	–	1	–	–	1	–

Tables 24a,b,c n $^1B_{3u}$ 9M3R

Table 24a 1 $^1B_{3u}$ $^1(\pi, 3s)$

(Coefficient)^2	$2a_g$	$2b_{1u}$	$1b_{2u}$	$3a_g$	$1b_{3g}$	$1b_{3u}$	$4a_g$	$5a_g$	$6a_g$	$7a_g$	$3b_{2u}$	$3b_{3g}$	$3b_{3u}$
.8697M	2	2	2	2	2	1	1	–	–	–	–	–	–
.0023M	2	2	2	2	2	1	–	1	–	–	–	–	–
.0000M	2	2	2	2	2	1	–	–	1	–	–	–	–
.0405M	2	2	2	2	2	1	–	–	–	1	–	–	–
.0056M	2	2	2	2	2	–	1	–	–	–	–	–	1
.0000M	2	2	2	2	2	–	–	1	–	–	–	–	1
.0000M	2	2	2	2	2	–	–	–	1	–	–	–	1
.0050M	2	2	1	2	2	1	1	–	–	–	1	–	–
.0000M	2	2	1	2	2	1	–	1	–	–	1	–	–

Table 24b 2 $^1B_{3u}$ $^1(\pi, 3d\sigma)$

(Coefficient)^2	$2a_g$	$2b_{1u}$	$1b_{2u}$	$3a_g$	$1b_{3g}$	$1b_{3u}$	$4a_g$	$5a_g$	$6a_g$	$7a_g$	$3b_{2u}$	$3b_{3g}$	$3b_{3u}$
.0035M	2	2	2	2	2	1	1	–	–	–	–	–	–
.8988M	2	2	2	2	2	1	–	1	–	–	–	–	–
.0016M	2	2	2	2	2	1	–	–	1	–	–	–	–
.0028M	2	2	2	2	2	1	–	–	–	1	–	–	–
.0000M	2	2	2	2	2	–	1	–	–	–	–	–	1
.0058M	2	2	2	2	2	–	–	1	–	–	–	–	1
.0000M	2	2	2	2	2	–	–	–	1	–	–	–	1
.0000M	2	2	1	2	2	1	1	–	–	–	1	–	–
.0054M	2	2	1	2	2	1	–	1	–	–	1	–	–

Table 24c 3 $^1B_{3u}$ $^1(\pi, 4s)$

(Coefficient)^2	$2a_g$	$2b_{1u}$	$1b_{2u}$	$3a_g$	$1b_{3g}$	$1b_{3u}$	$4a_g$	$5a_g$	$6a_g$	$7a_g$	$3b_{2u}$	$3b_{3g}$	$3b_{3u}$
.0000M	2	2	2	2	2	1	1	–	–	–	–	–	–
.0014M	2	2	2	2	2	1	–	1	–	–	–	–	–
.9056M	2	2	2	2	2	1	–	–	1	–	–	–	–
.0000M	2	2	2	2	2	1	–	–	–	1	–	–	–
.0000M	2	2	2	2	2	–	1	–	–	–	–	–	1
.0000M	2	2	2	2	2	–	–	1	–	–	–	–	1
.0062M	2	2	2	2	2	–	–	–	1	–	–	–	1
.0000M	2	2	1	2	2	1	1	–	–	–	1	–	–
.0000M	2	2	1	2	2	1	–	1	–	–	1	–	–

Tables 25a-d n $^1B_{3u}$ 6M4R

Table 25a 1 $^1B_{3u}$ $^1(\pi, 3s)$

(Coefficient)^2	$2a_g$	$2b_{1u}$	$1b_{2u}$	$3a_g$	$1b_{3g}$	$1b_{3u}$	$4a_g$	$5a_g$	$6a_g$	$7a_g$	$3b_{2u}$	$3b_{3u}$
.7886M	2	2	2	2	2	1	1	–	–	–	–	–
.0046M	2	2	2	2	2	1	–	1	–	–	–	–
.0000M	2	2	2	2	2	1	–	–	1	–	–	–
.1190M	2	2	2	2	2	1	–	–	–	1	–	–
.0052M	2	2	2	2	2	–	1	–	–	–	–	1
.0000M	2	2	2	2	2	–	–	1	–	–	–	1

Table 25b $2\ ^1B_{3u}$ $^1(\pi, 3d\sigma)$

(Coefficient)^2	$2a_g$	$2b_{1u}$	$1b_{2u}$	$3a_g$	$1b_{3g}$	$1b_{3u}$	$4a_g$	$5a_g$	$6a_g$	$7a_g$	$3b_{2u}$	$3b_{3u}$
.0125M	2	2	2	2	2	1	1	–	–	–	–	–
.8816M	2	2	2	2	2	1	–	1	–	–	–	–
.0019M	2	2	2	2	2	1	–	–	1	–	–	–
.0109M	2	2	2	2	2	1	–	–	–	1	–	–
.0001M	2	2	2	2	2	–	1	–	–	–	–	1
.0057M	2	2	2	2	2	–	–	1	–	–	–	1
.0052	2	2	1	2	2	1	–	1	–	–	1	–

Table 25c $3\ ^1B_{3u}$ $^1(\pi, 4s)$

(Coefficient)^2	$2a_g$	$2b_{1u}$	$1b_{2u}$	$3a_g$	$1b_{3g}$	$1b_{3u}$	$4a_g$	$5a_g$	$6a_g$	$7a_g$	$3b_{2u}$	$3b_{3u}$
.0000M	2	2	2	2	2	1	1	–	–	–	–	–
.0016M	2	2	2	2	2	1	–	1	–	–	–	–
.9064M	2	2	2	2	2	1	–	–	1	–	–	–
.0000M	2	2	2	2	2	1	–	–	–	1	–	–
.0000M	2	2	2	2	2	–	1	–	–	–	–	1
.0000M	2	2	2	2	2	–	–	1	–	–	–	1
.0062	2	2	2	2	2	–	–	–	1	–	–	1
.0051	2	2	1	2	2	1	–	–	1	–	1	–

Table 25d $4\,^1B_{3u}$

(Coefficient)^2	$2a_g$	$2b_{1u}$	$1b_{2u}$	$3a_g$	$1b_{3g}$	$1b_{3u}$	$4a_g$	$5a_g$	$6a_g$	$7a_g$	$3b_{2u}$	$3b_{3u}$
.1134M	2	2	2	2	2	1	1	–	–	–	–	–
.0201M	2	2	2	2	2	1	–	1	–	–	–	–
.0000M	2	2	2	2	2	1	–	–	1	–	–	–
.7736M	2	2	2	2	2	1	–	–	–	1	–	–
.0008M	2	2	2	2	2	–	1	–	–	–	–	1
.0002M	2	2	2	2	2	–	–	1	–	–	–	1

Tables 26a and b n $^1B_{1g}$ 5M2R

Table 26a 1 $^1B_{1g}$ $^1(\pi, 3py)$

(Coefficient)^2	$2a_g$	$2b_{1u}$	$1b_{2u}$	$3a_g$	$1b_{3g}$	$1b_{3u}$	$2b_{2u}$	$1b_{2g}$	$3b_{2u}$	$3b_{3u}$	$5b_{2u}$
.8670M	2	2	2	2	2	1	1	–	–	–	–
.0053M	2	2	2	2	2	–	1	–	–	1	–
.0448M	2	2	2	2	2	1	–	–	1	–	–
.0000M	2	2	2	2	1	2	–	1	–	–	–
.0050M	2	2	1	2	2	1	1	–	1	–	–

Table 26b 2 $^1B_{1g}$

(Coefficient)^2	$2a_g$	$2b_{1u}$	$1b_{2u}$	$3a_g$	$1b_{3g}$	$1b_{3u}$	$2b_{2u}$	$1b_{2g}$	$3b_{2u}$	$3b_{3u}$	$5b_{2u}$
.0449M	2	2	2	2	2	1	1	–	–	–	–
.0001M	2	2	2	2	2	–	1	–	–	1	–
.8583M	2	2	2	2	2	1	–	–	1	–	–
.0082	2	2	2	2	2	1	–	–	–	–	1
.0002M	2	2	2	2	1	2	–	1	–	–	–
.0008M	2	2	1	2	2	1	1	–	1	–	–

Tables 27a and b n $^1B_{1g}$ 5M2R

Table 27a 1 $^1B_{1g}$ $^1(\pi, 3p_y)$

(Coefficient)^2	$2a_g$	$2b_{1u}$	$1b_{2u}$	$3a_g$	$1b_{3g}$	$1b_{3u}$	$2b_{2u}$	$1b_{2g}$	$3b_{2u}$	$3b_{3g}$	$3b_{3u}$	$5b_{2u}$
.8670M	2	2	2	2	2	1	1	–	–	–	–	–
.0053M	2	2	2	2	2	–	1	–	–	–	1	–
.0449M	2	2	2	2	2	1	–	–	1	–	–	–
.0050M	2	2	1	2	2	1	1	–	1	–	–	–
.0049M	2	2	2	2	1	1	1	–	–	1	–	–

Table 27b 2 $^1B_{1g}$

(Coefficient)^2	$2a_g$	$2b_{1u}$	$1b_{2u}$	$3a_g$	$1b_{3g}$	$1b_{3u}$	$2b_{2u}$	$1b_{2g}$	$3b_{2u}$	$3b_{3u}$	$5b_{2u}$
.0449M	2	2	2	2	2	1	1	–	–	–	–
.0006M	2	2	2	2	2	–	1	–	–	1	–
.8583M	2	2	2	2	2	1	–	–	1	–	–
.0082	2	2	2	2	2	1	–	–	–	–	1
.0008M	2	2	1	2	2	1	1	–	1	–	–
.0005M	2	2	2	2	1	1	1	–	1	–	–

Tables 28a and b n $^1B_{2g}$ 6M2R

Table 28a 1 $^1B_{2g}$ $^1(\pi, 3p_z)$

(Coefficient)^2	$2a_g$	$2b_{1u}$	$1b_{2u}$	$3a_g$	$1b_{3g}$	$1b_{3u}$	$3b_{1u}$	$1b_{1g}$	$2b_{2g}$	$7a_g$	$3b_{2u}$	$4b_{1u}$	$3b_{2g}$	$3b_{3u}$
.8646M	2	2	2	2	2	1	1	–	–	–	–	–	–	–
.0052M	2	2	2	2	2	–	1	–	–	–	–	–	–	1
.0456M	2	2	2	2	2	1	–	–	–	–	–	1	–	–
.0000M	2	2	2	2	1	2	–	1	–	–	–	–	–	–
.0054M	2	2	1	2	2	1	1	–	–	–	1	–	–	–
.0045M	2	2	2	2	1	1	1	–	–	–	–	–	1	–

Table 28b 2 $^1B_{2g}$

(Coefficient)^2	$2a_g$	$2b_{1u}$	$1b_{2u}$	$3a_g$	$1b_{3g}$	$1b_{3u}$	$3b_{1u}$	$1b_{1g}$	$2b_{2g}$	$7a_g$	$3b_{2u}$	$4b_{1u}$	$3b_{3g}$	$3b_{3}$
.0467M	2	2	2	2	2	1	1	–	–	–	–	–	–	–
.0006M	2	2	2	2	2	–	1	–	–	–	–	–	–	1
.8420M	2	2	2	2	2	1	–	–	–	–	–	1	–	–
.0083	2	2	2	2	2	–	–	–	1	1	–	–	–	–
.0000M	2	2	2	2	1	2	–	1	–	–	–	–	–	–
.0003M	2	2	1	2	2	1	1	–	–	–	1	–	–	–
.0005M	2	2	2	2	1	1	1	–	–	–	–	–	1	–

Table 29 1 $^1B_{2g}$ 5M1R

Coefficient	$2a_g$	$2b_{1u}$	$1b_{2u}$	$3a_g$	$1b_{3g}$	$1b_{3u}$	$3b_{1u}$	$3b_{2u}$	$4b_{1u}$	$3b_{3g}$	$3b_{3u}$
.9000M	2	2	2	2	2	1	1	–	–	–	–
.0055M	2	2	2	2	2	–	1	–	–	–	1
.0122M	2	2	2	2	2	1	–	–	1	–	–
.0056M	2	2	1	2	2	1	1	1	–	–	–
.0048M	2	2	2	2	1	1	1	–	–	1	–

Tables 30a and b n ^{3}Au 6M2R

Table 30a 1 ^3A_u $^3(\pi, 3d_{yz})$

(Coefficient)^2	$2a_g$	$2b_{1u}$	$1b_{2u}$	$3a_g$	$1b_{3g}$	$1b_{3u}$	$2b_{3u}$	$2b_{3g}$	$2b_{2g}$	$3b_{2u}$	$3b_{3g}$	$3b_{3u}$	$3b_{2g}$
.9105M	2	2	2	2	2	1	–	1	–	–	–	–	–
.0062M	2	2	2	2	2	–	–	1	–	–	–	1	–
.0054M	2	2	2	2	2	1	–	–	–	–	1	–	–
.0000M	2	2	2	2	1	2	1	–	–	–	–	–	–
.0061M	2	2	1	2	2	1	–	1	–	1	–	–	–
.0060M	2	2	2	2	1	1	–	1	–	–	1	–	–

Table 30b 2 ^3A_u

(Coefficient)^2	$2a_g$	$2b_{1u}$	$1b_{2u}$	$3a_g$	$1b_{3g}$	$1b_{3u}$	$2b_{3u}$	$2b_{3g}$	$2b_{2g}$	$3b_{2u}$	$3b_{3g}$	$3b_{3u}$	$3b_{2g}$
.0000M	2	2	2	2	2	1	–	1	–	–	–	–	–
.0000M	2	2	2	2	2	–	–	1	–	–	–	1	–
.0000M	2	2	2	2	2	1	–	–	–	–	1	–	–
.8868M	2	2	2	2	1	2	1	–	–	–	–	–	–
.0104	2	2	2	2	1	–	1	–	2	–	–	–	–
.0000M	2	2	1	2	2	1	–	1	–	1	–	–	–
.0000M	2	2	2	2	1	1	–	1	–	–	–	1	–
.0113	2	2	1	2	2	1	1	–	1	–	–	–	–
.0099	2	2	1	2	2	1	1	–	–	–	–	1	–
.0058	2	2	2	2	1	–	1	–	1	–	–	–	1

Table 31 $1\ ^3A_g$ $^3(\pi, 3pz)$

$(Coefficient)^2$	$2a_g$	$2b_{1u}$	$1b_{2u}$	$3a_g$	$1b_{3g}$	$1b_{3u}$	$2b_{3u}$	$3b_{2u}$	$3b_{3u}$
.9045M	2	2	2	2	2	1	1	-	-
.0060M	2	2	2	2	2	-	1	-	1
.0144M	2	2	2	2	2	1	-	-	1
.0050M	2	2	1	2	2	1	1	1	-

Tables 32a and b $n\ ^3B_{1u}$ 4M2R

Table 32a $1\ ^3B_{1u}$ $^3(\pi,\pi^*)$

$(Coefficient)^2$	$2a_g$	$2b_{1u}$	$1b_{2u}$	$3a_g$	$1b_{3g}$	$1b_{3u}$	$1b_{2g}$	$2b_{2g}$	$3b_{2u}$	$3b_{3g}$	$3b_{3u}$	$3b_{2g}$
.0853M	2	2	2	2	2	1	1	-	-	-	-	-
.8290M	2	2	2	2	2	1	-	1	-	-	-	-
.0277M	2	2	2	2	2	1	-	-	-	-	-	1
.00216M	2	2	2	2	2	-	-	1	-	-	1	-

Table 32b $2\ ^3B_{1u}$ $^3(\pi, 3dxz)$

	$2a_g$	$2b_{1u}$	$1b_{2u}$	$3a_g$	$1b_{3g}$	$1b_{3u}$	$1b_{2s}$	$2b_{2g}$	$3b_{2u}$	$3b_{3g}$	$3b_{3u}$	$3b_{2g}$
.8310M	2	2	2	2	2	1	1	-	-	-	-	-
.0056	2	2	2	2	2	-	1	-	-	-	1	-
.0799M	2	2	2	2	2	1	-	1	-	-	-	-
.0048M	2	2	2	2	2	1	-	-	-	-	-	1
.0006M	2	2	2	2	2	-	-	1	-	-	1	-
.0053	2	2	1	2	2	1	1	-	1	-	-	-
.0050	2	2	2	2	1	1	1	-	-	1	-	-

Table 33 $1\,^3B_{2u}$ $^1(\pi, 3d_{xy})$

(Coefficient)^2	$2a_g$	$2b_{1u}$	$1b_{2u}$	$3a_g$	$1b_{3g}$	$1b_{3u}$	$2b_{3u}$	$1b_{2g}$	$3b_{2u}$	$3b_{3g}$	$3b_{2u}$
.9163M	2	2	2	2	2	1	–	1	–	–	–
.0016M	2	2	2	2	2	–	1	1	–	–	–
.0065M	2	2	2	2	2	–	–	1	–	–	1
.0055M	2	2	1	2	2	1	–	1	1	–	–
.0056M	2	2	2	2	1	1	–	1	–	1	–

Tables 34 a and b n $^3B_{2u}$ 3M2R

Table 34a $1\,^3B_{2u}$ $^1(\pi, 3d_{xy})$

(Coefficient)^2	$2a_g$	$2b_{1u}$	$1b_{2u}$	$3a_g$	$1b_{3g}$	$1b_{3u}$	$3b_{1u}$	$1b_{1g}$	$2b_{2g}$	$3b_{2u}$	$4b_{1u}$	$3b_{3g}$	$3b_{3u}$	$3b_2$
.91635M	2	2	2	2	2	1	–	1	–	–	–	–	–	–
.0064M	2	2	2	2	2	–	–	1	–	–	–	–	1	–
.0000M	2	2	2	2	1	2	1	–	–	–	–	–	–	–
.0054	2	2	1	2	2	1	–	1	–	1	–	–	–	–
.0050	2	2	2	2	1	1	–	1	–	–	–	1	–	–

Table 34b $2\,^3B_{2u}$

(Coefficient)^2	$2a_g$	$2b_{1u}$	$1b_{2u}$	$3a_g$	$1b_{3g}$	$1b_{3u}$	$3b_{1u}$	$1b_{1g}$	$2b_{2g}$	$3b_{2u}$	$4b_{1u}$	$3b_{3g}$	$3b_{3u}$	$3b_{2g}$
.0000M	2	2	2	2	2	1	–	1	–	–	–	–	–	–
.0000M	2	2	2	2	2	–	–	1	–	–	–	–	1	–
.8769M	2	2	2	2	1	2	1	–	–	–	–	–	–	–
.0125	2	2	2	2	1	2	–	–	–	–	1	–	–	–
.0100	2	2	2	2	1	–	1	–	2	–	–	–	–	–
.0107	2	2	1	2	2	1	1	–	1	–	–	–	–	–
.0086	2	2	2	2	1	1	1	–	–	–	–	–	1	–
.0057	2	2	2	2	1	–	1	1	–	–	–	–	–	1

)

Tables 35a-d $n\ ^3B_{3u}\ 6M4R$

Table 35a $1\ ^3B_{3u}\ ^3(\pi, 3s)$

$(\text{Coefficient})^2$	$2a_g$	$2b_{1u}$	$1b_{2u}$	$3a_g$	$1b_{3g}$	$1b_{3u}$	$4a_g$	$5a_g$	$6a_g$	$7a_g$	$3b_{2u}$	$3b_{3u}$
.7399M	2	2	2	2	2	1	1	–	–	–	–	–
.0056M	2	2	2	2	2	1	–	1	–	–	–	–
.0007M	2	2	2	2	2	1	–	–	1	–	–	–
.1705M	2	2	2	2	2	1	–	–	–	1	–	–
.0049M	2	2	2	2	2	–	1	–	–	–	–	1
.0000M	2	2	2	2	2	–	–	1	–	–	–	1

Table 35b $2\ ^3B_{3u}\ ^3(\pi, 3d\sigma)$

$(\text{Coefficient})^2$	$2a_g$	$2b_{1u}$	$1b_{2u}$	$3a_g$	$1b_{3g}$	$1b_{3u}$	$4a_g$	$5a_g$	$6a_g$	$7a_g$	$3b_{2u}$	$3b_{3u}$
.0185M	2	2	2	2	2	1	1	–	–	–	–	–
.8643M	2	2	2	2	2	1	–	1	–	–	–	–
.0114M	2	2	2	2	2	1	–	–	1	–	–	–
.0139M	2	2	2	2	2	1	–	–	–	1	–	–
.0000M	2	2	2	2	2	–	1	–	–	–	–	1
.0057M	2	2	2	2	2	–	–	1	–	–	–	1
.0052	2	2	1	2	2	1	–	1	–	–	1	–

Table 35c $3\ {}^3B_{3u}$ $^3(\pi, 4s)$

$(\text{Coefficient})^2$	$2a_g$	$2b_{1u}$	$1b_{2u}$	$3a_g$	$1b_{3g}$	$1b_{3u}$	$4a_g$	$5a_g$	$6a_g$	$7a_g$	$3b_{2u}$	$3b_{3u}$
.0030M	2	2	2	2	2	1	1	–	–	–	–	–
.0093M	2	2	2	2	2	1	–	1	–	–	–	–
.8932M	2	2	2	2	2	1	–	–	1	–	–	–
.0016M	2	2	2	2	2	1	–	–	–	1	–	–
.0000M	2	2	2	2	2	–	1	–	–	–	–	1
.0001M	2	2	2	2	2	–	–	1	–	–	–	1
.0060	2	2	2	2	2	–	–	–	1	–	–	1

Table 35d $4\ {}^3B_{3u}$

$(\text{Coefficient})^2$	$2a_g$	$2b_{1u}$	$1b_{2u}$	$3a_g$	$1b_{3g}$	$1b_{3u}$	$4a_g$	$5a_g$	$6a_g$	$7a_g$	$3b_{2u}$	$3b_{3u}$
.1542M	2	2	2	2	2	1	1	–	–	–	–	–
.0306M	2	2	2	2	2	1	–	1	–	–	–	–
.0016M	2	2	2	2	2	1	–	–	1	–	–	–
.7247M	2	2	2	2	2	1	–	–	–	1	–	–
.0014M	2	2	2	2	2	–	1	–	–	–	–	1
.0002M	2	2	2	2	2	–	–	1	–	–	–	1

Tables 36a and b n $^3B_{1g}$ 5M2R

Table 36a 1 $^3B_{1g}$ $^3(\pi, 3py)$

(Coefficient)^2	$2a_g$	$2b_{1u}$	$1b_{2u}$	$3a_g$	$1b_{3g}$	$1b_{3u}$	$2b_{2u}$	$3b_{2u}$	$3b_{3g}$	$3b_{3u}$	$5b_{2u}$
.8616M	2	2	2	2	2	1	1	–	–	–	–
.0056M	2	2	2	2	2	–	1	–	–	1	–
.0532M	2	2	2	2	2	1	–	1	–	–	–
.0051M	2	2	1	2	2	1	1	1	–	–	–
.0052M	2	2	2	2	1	1	1	–	1	–	–

Table 36b 2 $^3B_{1g}$

(Coefficient)^2	$2a_g$	$2b_{1u}$	$1b_{2u}$	$3a_g$	$1b_{3g}$	$1b_{3u}$	$2b_{2u}$	$3b_{2u}$	$3b_{3g}$	$3b_{3u}$	$5b_{2u}$
.0527M	2	2	2	2	2	1	1	–	–	–	–
.0006M	2	2	2	2	2	–	1	–	–	1	–
.8580M	2	2	2	2	2	1	–	1	–	–	–
.0011M	2	2	1	2	2	1	1	1	–	–	–
.0006M	2	2	2	2	1	1	1	–	1	–	–
.0093	2	2	2	2	2	1	–	–	–	–	1

Tables 37a and b n $^3B_{2g}$ 5M2R

Table 37a 1 $^3B_{2g}$ $^3(\pi, 3pz)$

(Coefficient)^2	$2a_g$	$2b_{1u}$	$1b_{2u}$	$3a_g$	$1b_{3g}$	$1b_{3u}$	$3b_{1u}$	$3b_{2u}$	$4b_{1u}$	$3b_{3g}$	$3b_{3u}$
.8477M	2	2	2	2	2	1	1	–	–	–	–
.0055M	2	2	2	2	2	–	1	–	–	–	1
.0658M	2	2	2	2	2	1	–	–	1	–	–
.9956M	2	2	1	2	2	1	1	1	–	–	–
.0052M	2	2	2	2	1	1	1	–	–	1	–

Table 37b $2\ ^3B_{2g}$

(Coefficient)^2	$2a_g$	$2b_{1u}$	$1b_{2u}$	$3a_g$	$1b_{3g}$	$1b_{3u}$	$3b_{1u}$	$3b_{3u}$	$4b_{1u}$	$3b_{3g}$	$3b_{3u}$
.0665M	2	2	2	2	2	1	1	-	-	-	-
.0007M	2	2	2	2	2	-	1	-	-	-	1
.8355M	2	2	2	2	2	1	-	-	1	-	-
.0005M	2	2	1	2	2	1	1	1	-	-	-
.0008M	2	2	2	2	1	1	1	-	-	1	-

Tables 38a-c n $^1A_1$ 3M3R; Tables 38-45 refer to twisted ethylene (D_2)

Table 38a $1\ ^1A_1$ $^1(\pi, 3px)$

(Coefficient)^2	2a	$2b_1$	$1b_2$	3a	$1b_3$	$2b_3$	$3b_3$	$3b_2$	$4b_3$	$4b_2$	$5b_2$	$5b_3$	$6b_3$
.8976M	2	2	2	2	2	1	1	-	-	-	-	-	-
.0070	2	2	2	2	2	-	1	-	-	-	-	-	1
.0004M	2	2	2	2	2	1	-	-	1	-	-	-	-
.0087M	2	2	2	2	2	1	-	-	-	-	-	1	-

Table 38b, $2\ ^1A_1$ $^1(\pi, 3d_{yz})$

(Coefficient)^2	2a	$2b_1$	$1b_2$	3a	$1b_3$	$2b_3$	$3b_3$	$3b_2$	$4b_3$	$4b_2$	$5b_2$	$5b_3$	$6b_3$
.0001M	2	2	2	2	2	1	1	-	-	-	-	-	-
.8979M	2	2	2	2	2	1	-	-	1	-	-	-	-
.0119M	2	2	2	2	2	1	-	-	-	-	-	1	-
.0067	2	2	2	2	2	-	-	-	1	-	-	-	1

Table 38c $3\ ^1A_1$

(Coefficient)^2	2a	2b$_1$	1b$_2$	3a	1b$_3$	2b$_3$	3b$_3$	3b$_2$	4b$_3$	4b$_2$	5b$_2$	5b$_3$	6b$_3$
.0599	2	2	2	2	2	-	-	-	-	2	-	-	-
.0056M	2	2	2	2	2	1	1	-	-	-	-	-	-
.0129M	2	2	2	2	2	1	-	-	1	-	-	-	-
.7991M	2	2	2	2	2	1	-	-	-	-	-	1	-
.0148	2	2	2	2	2	-	-	1	-	1	-	-	-
.0087	2	2	2	2	2	-	-	-	-	1	1	-	-
.0072	2	2	1	2	2	2	-	-	-	1	-	-	-

Tables 39a-d n $^1B_3$ 4M4R

Table 39a $1\ ^1B_3$ $^1(\pi,3s)$

(Coefficient)^2	2a	2b$_1$	1b$_2$	3a	1b$_3$	2b$_3$	4a	5a	6a	7a	6b$_3$
.7862M	2	2	2	2	2	1	1	-	-	-	-
.0050M	2	2	2	2	2	1	-	1	-	-	-
.0001M	2	2	2	2	2	1	-	-	1	-	-
.1197M	2	2	2	2	2	1	-	-	-	1	-
.0060	2	2	2	2	2	-	1	-	-	-	1

Table 39b $2\ ^1B_3$

(Coefficient)^2	2a	2b$_1$	1b$_2$	3a	1b$_3$	2b$_3$	4a	5a	6a	7a	6b$_3$
.0146M	2	2	2	2	2	1	1	-	-	-	-
.8699M	2	2	2	2	2	1	-	1	-	-	-
.0089M	2	2	2	2	2	1	-	-	1	-	-
.0134M	2	2	2	2	2	1	-	-	-	1	-
.0066	2	2	2	2	2	-	-	1	-	-	1

Table 39c $3\,^1B_3$

(Coefficient)^2	2a	$2b_1$	$1b_2$	3a	$1b_3$	$2b_3$	4a	5a	6a	7a	$6b_3$
.0000M	2	2	2	2	2	1	1	–	–	–	–
.0101M	2	2	2	2	2	1	–	1	–	–	–
.8984M	2	2	2	2	2	1	–	–	1	–	–
.0000M	2	2	2	2	2	1	–	–	–	1	–
.0072	2	2	2	2	2	–	–	–	1	–	1

Table 39d $4\,^1B_3$

(Coefficient)^2	2a	$2b_1$	$1b_2$	3a	$1b_3$	$2b_3$	4a	5a	6a	7a	$6b_3$
.1108M	2	2	2	2	2	1	1	–	–	–	–
.0238M	2	2	2	2	2	1	–	1	–	–	–
.0002M	2	2	2	2	2	1	–	–	1	–	–
.7678M	2	2	2	2	2	1	–	–	–	1	–
.0053	2	2	2	2	2	–	–	–	–	1	1

Tables 40a-c n $^1B_1$ 5MBR

Table 40a 1 $^1B_1$ $^1(\pi, 3p_y)$

(Coefficient)^2	2a	2b$_1$	1b$_2$	3a	1b$_3$	2b$_3$	2b$_2$	3b$_2$	4b$_2$	5b$_2$	6b$_3$	7b$_2$
.1383M	2	2	2	2	2	1	1	–	–	–	–	–
.2438M	2	2	2	2	2	1	–	1	–	–	–	–
.5173M	2	2	2	2	2	1	–	–	1	–	–	–
.0000M	2	2	2	2	2	1	–	–	–	1	–	–
.0008M	2	2	2	2	2	1	–	–	–	–	–	1
.0115M	2	2	2	2	1	2	–	–	1	–	–	–

Table 40b 2 $^1B_1$ $^1(\pi,\pi^*)$

(Coefficient)^2	2a	2b$_1$	1b$_2$	3a	1b$_3$	2b$_3$	2b$_2$	3b$_2$	4b$_2$	5b$_2$	6b$_3$	7b$_2$
.7620M	2	2	2	2	2	1	1	–	–	–	–	–
.0061	2	2	2	2	2	–	1	–	–	–	1	–
.0668M	2	2	2	2	2	1	–	1	–	–	–	–
.0727M	2	2	2	2	2	1	–	–	1	–	–	–
.0124M	2	2	2	2	2	1	–	–	–	1	–	–
.0002M	2	2	2	2	2	1	–	–	–	–	–	1
.0000M	2	2	2	2	1	2	–	–	1	–	–	–

Table 40c 3 $^1B_1$ $^1(\pi, 3d_{xz})$

(Coefficient)^2	2a	2b$_1$	1b$_2$	3a	1b$_3$	2b$_3$	2b$_2$	3b$_2$	4b$_2$	5b$_2$	6b$_3$	7b$_2$
.0032M	2	2	2	2	2	1	1	–	–	–	–	–
.6035M	2	2	2	2	2	1	–	1	–	–	–	–
.3012M	2	2	2	2	2	1	–	–	1	–	–	–
.0000M	2	2	2	2	2	1	–	–	–	1	–	–
.0026M	2	2	2	2	2	1	–	–	–	–	–	1
.0000M	2	2	2	2	1	2	–	–	1	–	–	–
.0069	2	2	2	2	2	–	–	1	–	–	1	–

Tables 41a-c n $^1B_2$ 3M3R

Table 41a 1 $^1B_2$ $^1(\pi, 3p_z)$

(Coefficient)^2	2a	2b$_1$	1b$_2$	3a	1b$_3$	2b$_3$	3b$_1$	4b$_1$	4b$_2$	7a	5b$_1$	6b$_3$
.8670M	2	2	2	2	2	1	1	-	-	-	-	-
.0062M	2	2	2	2	2	-	1	-	-	-	-	1
.0001M	2	2	2	2	2	1	-	1	-	-	-	-
.0412M	2	2	2	2	2	1	-	-	-	-	1	-

Table 41b 2 $^1B_2$ $^1(\pi, 3d_{yz})$

(Coefficient)^2	2a	2b$_1$	1b$_2$	3a	1b$_3$	2b$_3$	3b$_1$	4b$_1$	4b$_2$	7a	5b$_1$	6b$_3$
.0008M	2	2	2	2	2	1	1	-	-	-	-	-
.9044M	2	2	2	2	2	1	-	1	-	-	-	-
.0059M	2	2	2	2	2	1	-	-	-	-	1	-
.0071	2	2	2	2	2	-	-	1	-	-	-	1

Table 41c 3 $^1B_2$

(Coefficient)^2	2a	2b$_1$	1b$_2$	3a	1b$_3$	2b$_3$	3b$_1$	4b$_1$	4b$_2$	7a	5b$_1$	6b$_3$
.0412M	2	2	2	2	2	1	1	-	-	-	-	-
.0068M	2	2	2	2	2	1	-	1	-	-	-	-
.8353M	2	2	2	2	2	1	-	-	-	-	1	-
.0101	2	2	2	2	2	-	-	-	1	1	-	-

Tables 42a-c n $^3A_1$ 3M3R

Table 42a $1\,^3A_1$

(Coefficient)^2	2a	$2b_1$	$1b_2$	3a	$1b_3$	$2b_3$	$3b_3$	$4b_3$	$4b_2$	$5b_2$	$5b_3$	$6b_3$	$7b_3$
.9020M	2	2	2	2	2	1	1	–	–	–	–	–	–
.0070	2	2	2	2	2	–	1	–	–	–	–	1	–
.0043M	2	2	2	2	2	1	–	1	–	–	–	–	–
.0074M	2	2	2	2	2	1	–	–	–	–	1	–	–

Table 42b $2\,^3A_1$

(Coefficient)^2	2a	$2b_1$	$1b_2$	3a	$1b_3$	$2b_3$	$3b_3$	$4b_3$	$4b_2$	$5b_2$	$5b_3$	$6b_3$	$7b_3$
.0034M	2	2	2	2	2	1	1	–	–	–	–	–	–
.8953M	2	2	2	2	2	1	–	1	–	–	–	–	–
.0157M	2	2	2	2	2	1	–	–	–	–	1	–	–
.0069	2	2	2	2	2	1	–	–	–	–	–	1	–

Table 42c $3\,^3A_1$

(Coefficient)^2	2a	$2b_1$	$1b_2$	3a	$1b_3$	$2b_3$	$3b_3$	$4b_3$	$4b_2$	$5b_2$	$5b_3$	$6b_3$	$7b_3$
.0089M	2	2	2	2	2	1	1	–	–	–	–	–	–
.0147M	2	2	2	2	2	1	–	1	–	–	–	–	–
.8682M	2	2	2	2	2	1	–	–	–	–	1	–	–
.0055	2	2	2	2	2	1	–	–	–	–	–	–	1
.0104	2	2	2	2	2	–	–	–	1	1	–	–	–

Tables 43a-d n $^3B_3$ 4M4R

Table 43a 1 $^3B_3$

(Coefficient)^2	2a	2b$_1$	1b$_2$	3a	1b$_3$	2b$_3$	4a	5a	6a	7a	6b$_3$
.7389M	2	2	2	2	2	1	1	–	–	–	–
.0076M	2	2	2	2	2	1	–	1	–	–	–
.0008M	2	2	2	2	2	1	–	–	1	–	–
.1708M	2	2	2	2	2	1	–	–	–	1	–
.0055	2	2	2	2	2	–	1	–	–	–	1

Table 43b 2 $^3B_3$

(Coefficient)^2	2a	2b$_1$	1b$_2$	3a	1b$_3$	2b$_3$	4a	5a	6a	7a	6b$_3$
.0231M	2	2	2	2	2	1	1	–	–	–	–
.8705M	2	2	2	2	2	1	–	1	–	–	–
.0027M	2	2	2	2	2	1	–	–	1	–	–
.0129M	2	2	2	2	2	1	–	–	–	1	–
.0068	2	2	2	2	2	–	–	1	–	–	1

Table 43c 3 $^3B_3$

(Coefficient)^2	2a	2b$_1$	1b$_2$	3a	1b$_3$	2b$_3$	4a	5a	6a	7a	6b$_3$
.0013M	2	2	2	2	2	1	1	–	–	–	–
.0024M	2	2	2	2	2	1	–	1	–	–	–
.9049M	2	2	2	2	2	1	–	–	1	–	–
.0006M	2	2	2	2	2	1	–	–	–	1	–
.0072	2	2	2	2	2	–	–	–	1	–	1

Table 43d 4 $^3B_3$

(Coefficient)^2	2a	2b$_1$	1b$_2$	3a	1b$_3$	2b$_3$	4a	5a	6a	7a	6b$_3$
.1109M	2	2	2	2	2	1	1	-	-	-	-
.0238M	2	2	2	2	2	1	-	1	-	-	-
.0002M	2	2	2	2	2	1	-	-	1	-	-
.7678M	2	2	2	2	2	1	-	-	-	1	-
.0053	2	2	2	2	2	-	-	-	-	1	1

Tables 44a-d n $^3B_1$ 6M4R

Table 44a 1 $^3B_1$

(Coefficient)^2	2a	2b$_1$	1b$_2$	3a	1b$_3$	2b$_3$	2b$_2$	3b$_2$	4b$_2$	5b$_2$	6b$_3$	7b$_2$
.0087M	2	2	2	2	2	1	1	-	-	-	-	-
.1231M	2	2	2	2	2	1	-	1	-	-	-	-
.7854M	2	2	2	2	2	1	-	-	1	-	-	-
.0003M	2	2	2	2	2	1	-	-	-	1	-	-
.0225M	2	2	2	2	2	1	-	-	-	-	-	1
.0006M	2	2	2	2	1	2	-	-	1	-	-	-

Table 44b 2 $^3B_1$

(Coefficient)^2	2a	2b$_1$	1b$_2$	3a	1b$_3$	2b$_3$	2b$_2$	3b$_2$	4b$_2$	5b$_2$	6b$_3$	7b$_2$
.8907M	2	2	2	2	2	1	1	-	-	-	-	-
.0067	2	2	2	2	2	-	1	-	-	-	1	-
.0070M	2	2	2	2	2	1	-	1	-	-	-	-
.0043M	2	2	2	2	2	1	-	-	1	-	-	-
.0130M	2	2	2	2	2	1	-	-	-	1	-	-
.0003M	2	2	2	2	2	1	-	-	-	-	-	1
.0004M	2	2	2	2	1	2	-	-	1	-	-	-

Table 44c $3\ ^3B_1$

(Coefficient)^2	2a	$2b_2$	$1b_2$	3a	$1b_3$	$2b_3$	$2b_2$	$3b_2$	$4b_2$	$5b_2$	$6b_3$	$7b_2$
.0030M	2	2	2	2	2	1	1	-	-	-	-	-
.7865M	2	2	2	2	2	1	-	1	-	-	-	-
.1211M	2	2	2	2	2	1	-	-	1	-	-	-
.0002M	2	2	2	2	2	1	-	-	-	1	-	-
.0041M	2	2	2	2	2	1	-	-	-	-	-	1
.0003M	2	2	2	2	1	2	-	-	1	-	-	-

Table 44d $4\ ^3B_1$

(Coefficient)^2	2a	$2b_1$	$1b_2$	3a	$1b_3$	$2b_3$	$2b_2$	$3b_2$	$4b_2$	$5b_2$	$6b_3$	$7b_2$
.0007M	2	2	2	2	2	1	1	-	-	-	-	-
.0003M	2	2	2	2	2	1	-	1	-	-	-	-
.0002M	2	2	2	2	2	1	-	-	1	-	-	-
.0002M	2	2	2	2	2	1	-	-	-	1	-	-
.0002M	2	2	2	2	2	1	-	-	-	-	-	1
.0102	2	2	1	2	2	1	-	-	2	-	-	-
.0584	2	2	2	2	1	2	-	1	-	-	-	-
.8354M	2	2	2	2	1	2	-	-	1	-	-	-
.0144	2	2	2	2	1	2	-	-	-	-	-	1

Tables 45a-c n $^3B_2$ 3M3R

Table 45a 1 $^3B_2$

(Coefficient)^2	2a	2b$_1$	1b$_2$	3a	1b$_3$	2b$_3$	3b$_1$	4b$_1$	4b$_2$	7a	5b$_1$	6b$_3$
.8473M	2	2	2	2	2	1	1	–	–	–	–	–
.0063	2	2	2	2	2	–	1	–	–	–	–	1
.0006M	2	2	2	2	2	1	–	1	–	–	–	–
.0647M	2	2	2	2	2	1	–	–	–	–	1	–

Table 45b 2 $^3B_2$

(Coefficient)^2	2a	2b$_1$	1b$_2$	3a	1b$_3$	2b$_3$	3b$_1$	4b$_1$	4b$_2$	7a	5b$_1$	6b$_3$
.0024M	2	2	2	2	2	1	1	–	–	–	–	–
.9036M	2	2	2	2	2	1	–	1	–	–	–	–
.0088M	2	2	2	2	2	1	–	–	–	–	1	–
.0073	2	2	2	2	2	–	–	1	–	–	–	1

Table 45c 3 $^3B_2$

(Coefficient)^2	2a	2b$_1$	1b$_2$	3a	1b$_3$	2b$_3$	3b$_1$	4b$_1$	4b$_2$	7a	5b$_1$	6b$_3$
.0634M	2	2	2	2	2	1	1	–	–	–	–	–
.0109M	2	2	2	2	2	1	–	1	–	–	–	–
.8239M	2	2	2	2	2	1	–	–	–	–	1	–
.0051	2	2	2	2	2	–	–	–	1	1	–	–

Tables 46-49 refer to perpendicular ethylene (D_{2d})

Tables 46a-d n $^1A_1$ 8M4R

Table 46a 1 $^1A_1$

(Coefficient)^2	$3a_1$	$4a_1$	$1b_1$	$1b_2$	$5a_1$	$2b_1$	$2b_2$	$3b_1$	$3b_2$	$5b_1$	$5b_2$	$6b_1$	$6b_2$
.4098M	2	2	2	2	2	2	-	-	-	-	-	-	-
.4098M	2	2	2	2	2	-	2	-	-	-	-	-	-
.0338M	2	2	2	1	2	2	1	-	-	-	-	-	-
.0032M	2	2	2	2	2	-	1	-	1	-	-	-	-
.0081	2	2	2	2	2	-	1	-	-	-	-	-	1
.0338M	2	2	1	2	2	1	2	-	-	-	-	-	-
.0032M	2	2	2	2	2	1	-	1	-	-	-	-	-
.0081	2	2	2	2	2	1	-	-	-	-	-	1	-
.0001M	2	2	2	1	2	1	1	1	-	-	-	-	-
.0001M	2	2	1	2	2	1	1	-	1	-	-	-	-

Table 46b 2 $^1A_1$

(Coefficient)^2	$3a_1$	$4a_1$	$1b_1$	$1b_2$	$5a_1$	$2b_1$	$2b_2$	$3b_1$	$2b_2$	$5b_1$	$5b_2$	$6b_1$	$6b_2$
.4117M	2	2	2	2	2	2	-	-	-	-	-	-	-
.4117M	2	2	2	2	2	-	2	-	-	-	-	-	-
.0341M	2	2	2	1	2	2	1	-	-	-	-	-	-
.0042M	2	2	2	2	2	-	1	-	1	-	-	-	-
.0086	2	2	2	2	2	-	1	-	-	-	-	-	1
.0341M	2	2	1	2	2	1	2	-	-	-	-	-	-
.0042M	2	2	2	2	2	1	-	1	-	-	-	-	-
.0086	2	2	2	2	2	1	-	-	-	-	-	1	-
.0001M	2	2	2	1	2	1	1	1	-	-	-	-	-
.0001M	2	2	1	2	2	1	1	-	1	-	-	-	-

Tables 47a-d n $^1B_1$ 10M4R

Table 47a 1 $^1B_1$ $^1(\pi,-3s)$

(Coefficient)^2	$3a_1$	$4a_1$	$1b_1$	$1b_2$	$5a_1$	$2b_1$	$2b_2$	$6a_1$	$7a_1$	$8a_1$	$1a_2$	$9a_1$	$10a_1$	$5b_1$	$5b_2$
.6713M	2	2	2	2	2	1	-	1	-	-	-	-	-	-	-
.1810M	2	2	2	2	2	1	-	-	1	-	-	-	-	-	-
.0010M	2	2	2	2	2	1	-	-	-	1	-	-	-	-	-
.0001M	2	2	2	2	2	1	-	-	-	-	-	1	-	-	-
.0372M	2	2	2	2	2	1	-	-	-	-	-	-	1	-	-
.0000M	2	2	2	2	2	-	1	-	-	-	1	-	-	-	-
.0184M	2	2	2	1	2	1	1	1	-	-	-	-	-	-	-
.0000M	2	2	1	2	2	1	1	-	-	-	1	-	-	-	-
.0030M	2	2	2	1	2	1	1	-	1	-	-	-	-	-	-
.0000M	2	2	2	1	2	1	1	-	-	1	-	-	-	-	-

Table 47b 2 $^1B_1$ $^1(\pi, 3p_x)$

(Coefficient)^2	$3a_1$	$4a_1$	$1b_1$	$1b_2$	$5a_1$	$2b_1$	$2b_2$	$6a_1$	$7a_1$	$8a_1$	$1a_2$	$9a_1$	$10a_1$	$5b_1$	$5b_2$
.1795M	2	2	2	2	2	1	-	1	-	-	-	-	-	-	-
.6906M	2	2	2	2	2	1	-	-	1	-	-	-	-	-	-
.0000M	2	2	2	2	2	1	-	-	-	1	-	-	-	-	-
.0016M	2	2	2	2	2	1	-	-	-	-	-	1	-	-	-
.0017M	2	2	2	2	2	1	-	-	-	-	-	-	1	-	-
.0001M	2	2	2	2	2	-	1	-	-	-	1	-	-	-	-
.0096M	2	2	2	1	2	1	1	1	-	-	-	-	-	-	-
.0000M	2	2	1	2	2	1	1	-	-	-	1	-	-	-	-
.0261M	2	2	2	1	2	1	1	-	1	-	-	-	-	-	-
.0000M	2	2	2	1	2	1	1	-	-	1	-	-	-	-	-

Table 47c $3\ ^1B_1$ $^1(\pi, 3d_{x^2-y^2})$

(Coefficient)^2	$3a_1$	$4a_1$	$1b_1$	$1b_2$	$5a_1$	$2b_1$	$2b_2$	$6a_1$	$7a_1$	$8a_1$	$1a_2$	$9a_1$	$10a_1$	$5b_1$	$5b_2$
.0005M	2	2	2	2	2	1	–	1	–	–	–	–	–	–	–
.0002M	2	2	2	2	2	1	–	–	1	–	–	–	–	–	–
.8805M	2	2	2	2	2	1	–	–	–	1	–	–	–	–	–
.0000M	2	2	2	2	2	1	–	–	–	–	–	1	–	–	–
.0001M	2	2	2	2	2	1	–	–	–	–	–	–	1	–	–
.0000M	2	2	2	2	2	–	1	–	–	–	1	–	–	–	–
.0062M	2	2	1	2	2	1	–	–	–	1	–	–	–	1	–
.0000M	2	2	1	2	2	1	1	–	–	–	1	–	–	–	–
.0000M	2	2	2	1	2	1	1	–	1	–	–	–	–	–	–
.0280M	2	2	2	1	2	1	1	–	–	1	–	–	–	–	–

Table 47d $4\ ^1B_1$ $^1(\pi, 3dxy)$

(Coefficient)^2	$3a_1$	$4a_1$	$1b_1$	$1b_2$	$5a_1$	$2b_1$	$2b_2$	$6a_1$	$7a_1$	$8a_1$	$1a_2$	$9a_1$	$10a_1$	$5b_1$	$5b_2$
.0001M	2	2	2	2	2	1	–	1	–	–	–	–	–	–	–
.0000M	2	2	2	2	2	1	–	–	1	–	–	–	–	–	–
.0000M	2	2	2	2	2	1	–	–	–	1	–	–	–	–	–
.0000M	2	2	2	2	2	1	–	–	–	–	–	1	–	–	–
.0000M	2	2	2	2	2	1	–	–	–	–	–	–	1	–	–
.8873M	2	2	2	2	2	–	1	–	–	–	1	–	–	–	–
.0000M	2	2	2	1	2	1	1	1	–	–	–	–	–	–	–
.0283M	2	2	1	2	2	1	1	–	–	–	1	–	–	–	–
.0000M	2	2	2	1	2	1	1	–	1	–	–	–	–	–	–
.0000M	2	2	2	1	2	1	1	–	–	1	–	–	–	–	–
.0064	2	2	2	1	2	1	1	–	–	1	–	–	–	–	–

Tables 48a-d n $^1B_2$ 10M4R

Table 48a 1 $^1B_2$ $^1(\pi, 3\tilde{s})$

(Coefficient)^2	$3a_1$	$4a_1$	$1b_1$	$1b_2$	$5a_1$	$2b_1$	$2b_2$	$6a_1$	$7a_1$	$8a_1$	$1a_2$	$9a_1$	$10a_1$	$5b_1$	$5b_2$
.6699M	2	2	2	2	2	–	1	1	–	–	–	–	–	–	–
.1824M	2	2	2	2	2	–	1	–	1	–	–	–	–	–	–
.0010M	2	2	2	2	2	–	1	–	–	1	–	–	–	–	–
.0001M	2	2	2	2	2	–	1	–	–	–	–	1	–	–	–
.0371M	2	3	2	2	2	–	1	–	–	–	–	–	1	–	–
.0000M	2	2	2	2	2	1	–	–	–	–	1	–	–	–	–
.0184M	2	2	1	2	2	1	1	1	–	–	–	–	–	–	–
.0051	2	2	2	1	2	–	1	1	–	–	–	–	–	–	1
.0031M	2	2	1	2	2	1	1	–	1	–	–	–	–	–	–
.0000M	2	2	1	2	2	1	1	–	–	1	–	–	–	–	–
.0000M	2	2	2	1	2	1	1	–	–	–	1	–	–	–	–

Table 48b 2 $^1B_2$ $^1(\pi, 3p_z)$

(Coefficient)^2	$3a_1$	$4a_1$	$1b_1$	$1b_2$	$5a_1$	$2b_1$	$2b_2$	$6a_1$	$7a_1$	$8a_1$	$1a_2$	$9a_1$	$10a_1$	$5b_1$	$5b_2$
.1808M	2	2	2	2	2	–	1	1	–	–	–	–	–	–	–
.6889M	2	2	2	2	2	–	1	–	1	–	–	–	–	–	–
.0000M	2	2	2	2	2	–	1	–	–	1	–	–	–	–	–
.0016M	2	2	2	2	2	–	1	–	–	–	–	1	–	–	–
.0017M	2	2	2	2	2	–	1	–	–	–	–	–	1	–	–
.0001M	2	2	2	2	2	1	–	–	–	–	1	–	–	–	–
.0097M	2	2	1	2	2	1	1	1	–	–	–	–	–	–	–
.0263M	2	2	1	2	2	1	1	–	1	–	–	–	–	–	–
.0000M	2	2	1	2	2	1	1	–	–	1	–	–	–	–	–
.0000M	2	2	2	1	2	1	1	–	–	–	1	–	–	–	–

Table 48c 3 $^1B_2$

(Coefficient)^2	$3a_1$	$4a_1$	$1b_1$	$1b_2$	$5a_1$	$2b_1$	$2b_2$	$6a_1$	$7a_1$	$8a_1$	$1a_2$	$9a_1$	$10a_1$	$5b_1$	$5b_2$
.0006M	2	2	2	2	2	–	1	1	–	–	–	–	–	–	–
.0003M	2	2	2	2	2	–	1	–	1	–	–	–	–	–	–
.8803M	2	2	2	2	2	–	1	–	–	1	–	–	–	–	–
.0000M	2	2	2	2	2	–	1	–	–	–	–	1	–	–	–
.0000M	2	2	2	2	2	–	1	–	–	–	–	–	1	–	–
.0000M	2	2	2	2	2	1	–	–	–	–	1	–	–	–	–
.0000M	2	2	1	2	2	1	1	1	–	–	–	–	–	–	–
.0000M	2	2	1	2	2	1	1	–	1	–	–	–	–	–	–
.0280	2	2	1	2	2	1	1	–	–	1	–	–	–	–	–
.0062	2	2	2	1	2	1	1	–	–	–	1	–	–	–	–
.0000M	2	2	2	1	2	1	1	–	–	–	1	–	–	–	–

Table 48d 4 $^1B_2$

(Coefficient)^2	$3a_1$	$4a_1$	$1b_1$	$1b_2$	$5a_1$	$2b_1$	$2b_2$	$6a_1$	$7a_1$	$8a_1$	$1a_2$	$9a_1$	$10a_1$	$5b_1$	$5b_2$
.0001M	2	2	2	2	2	–	1	1	–	–	–	–	–	–	–
.0000M	2	2	2	2	2	–	1	–	1	–	–	–	–	–	–
.0000M	2	2	2	2	2	–	1	–	–	1	–	–	–	–	–
.0000M	2	2	2	2	2	–	1	–	–	–	–	1	–	–	–
.0000M	2	2	2	2	2	–	1	–	–	–	–	–	1	–	–
.8873M	2	2	2	2	2	1	–	–	–	–	1	–	–	–	–
.0000M	2	2	1	2	2	1	1	1	–	–	–	–	–	–	–
.0000M	2	2	1	2	2	1	1	–	1	–	–	–	–	–	–
.0000M	2	2	1	2	2	1	1	–	–	1	–	–	–	–	–
.0283M	2	2	2	1	2	1	1	–	–	–	1	–	–	–	–
.0064	2	2	1	2	2	1	–	–	–	–	1	–	–	1	–

Tables 49 a-c n $^1A_2$ 7M3R

Table 49a 1 $^1A_2$

(Coefficient)^2	$3a_1$	$4a_1$	$1b_1$	$1b_2$	$5a_1$	$2b_1$	$2b_2$	$3b_1$	$3b_2$	$4b_1$	$4b_2$
.4306M	2	2	2	2	2	1	1	–	–	–	–
.0000M	2	2	2	2	2	–	1	1	–	–	–
.0000M	2	2	2	2	2	–	1	–	–	1	–
.0000M	2	2	2	2	2	1	–	–	1	–	–
.0000M	2	2	2	2	2	1	–	–	–	–	1
.0000M	2	2	1	2	2	1	1	1	–	–	–
.0000M	2	2	2	1	2	1	1	–	1	–	1

Table 49b 2 $^1A_2$

(Coefficient)^2	$3a_1$	$4a_1$	$1b_1$	$1b_2$	$5a_1$	$2b_1$	$2b_2$	$3b_1$	$3b_2$	$4b_1$	$4b_2$
.0000M	2	2	2	2	2	1	1	–	–	–	–
.4416M	2	2	2	2	2	–	1	1	–	–	–
.0015M	2	2	2	2	2	–	1	–	–	1	–
.4372M	2	2	2	2	2	1	–	–	1	–	–
.0014M	2	2	2	2	2	1	–	–	–	–	1
.0153M	2	2	1	2	2	1	1	1	–	–	–
.0151M	2	2	2	1	2	1	1	–	1	–	–

Table 49c $3\ ^1A_2$

(Coefficient)^2	$3a_1$	$4a_1$	$1b_1$	$1b_2$	$5a_1$	$2b_1$	$2b_2$	$3b_1$	$3b_2$	$4b_1$	$4b_2$
.0000M	2	2	2	2	2	1	1	–	–	–	–
.4425M	2	2	2	2	2	–	1	1	–	–	–
.0015M	2	2	2	2	2	–	1	–	–	1	–
.4424M	2	2	2	2	2	1	–	–	1	–	–
.0015M	2	2	2	2	2	1	–	–	–	–	1
.0137M	2	2	1	2	2	1	1	1	–	–	–
.0137M	2	2	2	1	2	1	1	–	1	–	–

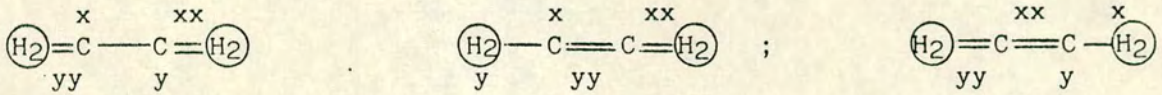

($^3A_2$, $^1B_1$; $^1B_2$, $^1A_1$ states)

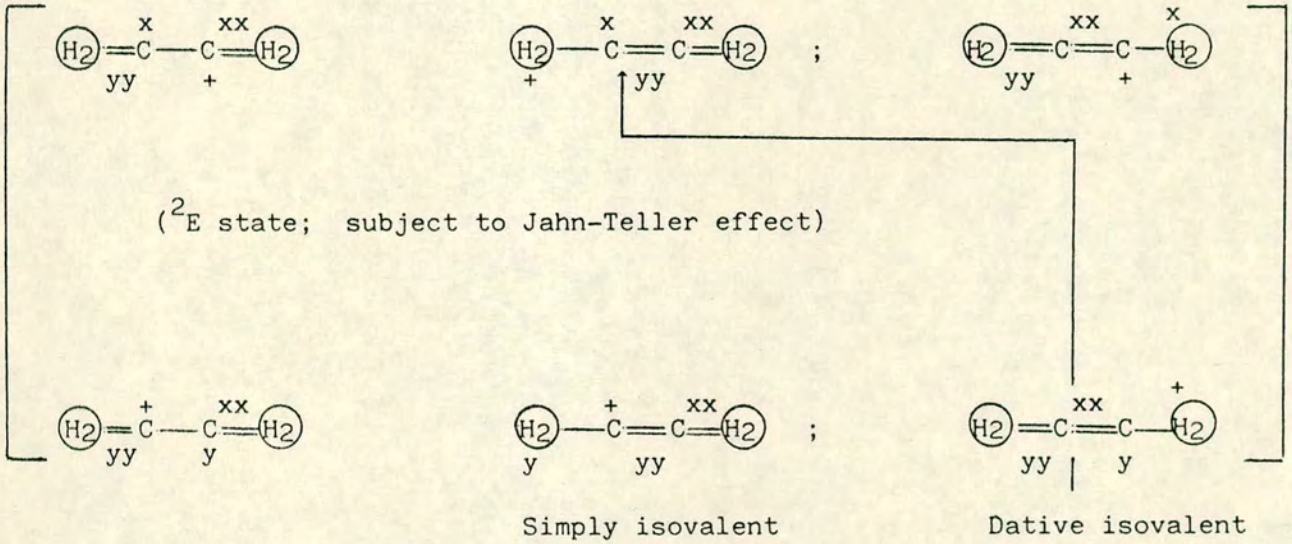

Figure 1. Isovalent (first order) hyperconjugation in perpendicular C_2H_4 and $C_2H_4^+$

CHAPTER V

A THEORETICAL STUDY OF THE ELECTRONIC SPECTRA OF SOME SUBSTITUTED ETHYLENES USING AB INITIO CI CALCULATIONS

Introduction

While substituted ethylenes have been studied extensively by spectroscopists, theoreticians have tended to ignore these larger olefins in favour of the smaller more symmetrical ethylene molecule. The few theoretical studies which have been performed involve less rigorous semi-empirical methods which have proven to be less than satisfactory.

The most intense feature of the electronic spectra of alkylated ethylenes is the N-V transition. The position of the N-V maximum moves slightly to the red with increasing numbers of alkyl groups; thus the N-V maximum at 7.66 eV for ethylene is lowered to 6.57 eV for tetramethylethylene [1,2].

Identification of the Rydberg states of substituted ethylenes has proven difficult, however the first (low energy) Rydberg states have been identified. Successive methylation reduces the first ionisation potential (see Table 1) at almost exactly the same rate as the R-N systems are shifted to the red; this is hardly surprising in view of the ionic nature of the Rydberg states. This almost linear dependence of the positions of the first bands of the R-N systems on the number of alkyl substituents was first noted by Carr and Stucklen [3]. This observation coupled with the accepted interpretation of the ethylene spectrum led them to propose a Rydberg assignment for those bands in the spectra of substituted ethylenes which could be correlated with the $^1(\pi,3s)$ state of ethylene. Further experimental evidence for this assignment was provided by Robin et al [4] who demonstrated that the vibrational fine structure of the R-N systems of alkylated ethylenes disappear in the presence of high pressures of N_2.

Successive methylation also results in a slight lowering of the singlet-triplet, T-N transition. The low energy electron impact energy-loss spectra of ethylene and its six methylated derivatives [2] indicate a shift from 4.32 eV for ethylene to 4.10 eV for tetramethyl ethylene; each additional methyl substituent lowering the transition energy by about 0.06 eV.

Table 1 summarises the effects of methylation on the T, R and V states of ethylene [5]. The effects of methylation on the T, R and V states can be explained in terms of valence bond theory, in which the T state is covalent and the V and R states are ionic. Hyperconjugation stabilises the V and R states but has a significantly lesser effect on the covalent T state.

Theoretical results for four substituted ethylenes are presented here: propene, 2 methyl propene, cis but-2-ene and trans but-2-ene. The basis sets used consisted of a double zeta atomic basis supplemented with a set of diffuse orbitals (s,s',p,d) at the mid point of the c=c double bond. The atomic basis and the exponents of the diffuse orbitals were identical to those used for ethylene, see Chapter 4.

Ideally one should optimise the exponents of the diffuse orbitals for each substituted ethylene; this however is computationally expensive and was not purused for practical reasons. Nevertheless, the present basis sets should enable a qualitative assignment of the spectra to be undertaken, but it should be noted that the present bases will not provide a satisfactory description for the $^1(\pi,\pi^*)$ or $^1(\sigma,\pi^*)$ states. In the case of the V state this is not serious since this

state is readily recognised by its high intensity in the electronic spectra. However it is not possible to locate the $^1(\sigma,\pi^*)$ state with the present basis sets.

\Theoretical Procedure

Ab initio truncated CI calculations (using a threshold energy of T=30 μHartrees) were performed with the MRDCI program mounted on a Cray-1s computer at ULCC (University of London Computer Centre). The carbon 1s core electrons were frozen in each case allowing only excitations involving the valence electrons. The configurational subspace was further reduced by removing the highest unoccupied orbitals from the CI calculations. In the case of propene the 12 highest unoccupied σ orbitals were removed, and in the three isomeric butenes studied, the 15 highest unoccupied σ orbitals were removed.

The low energy electron scattering spectra of ethylene, propene, cis but-2-ene, trans but-2-ene and 2 methyl propene have been supplied by Dr. Isobel Walker (Stirling University) and are indicated in Figures 1 to 5. Electron scattering spectroscopy, in which excited molecular states are produced by impact with low energy electrons, when combined with UV spectroscopy, provides a useful method of investigating electronic spectra. The selection rules applicable to UV spectroscopy do not hold for electron scattering experiments, and generally one can observe optically forbidden transitions as well as spin forbidden ones. The relative intensities of forbidden transitions are a function of the energy of the scattering electrons. Figures (1) to (5) contain spectra at different threshold energies (E_r). The optical maxima are also indicated.

Propene (Cs)

The microwave structure of propene [6] has been used in the following calculations:

$r(C=C) = 1.336 \pm .004 \text{Å}$

$r(C-C) = 1.501 \pm .004 \text{Å}$

$\angle CCC = 124.3° \pm 0.3°$

The ground state SCF wavefunction was used as the MO basis for the CI calculations. As discussed previously in Chapter 4 the ground state MO's do not necessarily provide the optimal MO basis but the results for ethylene demonstrate that the effects are almost negligible (from the point of view of optimum accuracy).

The electron energy loss spectrum of propene is indicated in Figure (2) and Table (2) outlines several previous spectroscopic assignments of the propene spectrum. The theoretical results are summarised in Table (3) and Tables (4-10).

The present calculations predict that the $^1(\pi,3s)$ Rydberg state occurs at 6.69 eV (see Tables 3, 4, 7a) and therefore one can assign the peak at 6.55 eV to the 3s Rydberg state.

The calculations on ethylene indicated that the $^1(\pi,3p_y)$ and $^1(\pi,3p_z)$ states are accidentally degenerate. The addition of a methyl group removes this degeneracy. The lower symmetry of propene allows substantial mixing of the Rydberg $3p_y$ and $3p_z$ orbitals resulting in two $3p\sigma$ orbitals

which are linear combinations of the original $3p_y$ and $3p_z$ orbitals. The main difference in these two orbitals is the orientation of the nodal plane. The $(3p_y-3p_z)$ combination has a nodal plane perpendicular to the long axis of the molecule and has been denoted $3p\perp$; the $(3p_y+3p_z)$ combination has a nodal plane parallel to the long axis, and is denoted $3p||$. The calculations indicate that a new accidental degeneracy is introduced; the $^1(\pi,3\pi_x)$ and the $^1(\pi,3p||)$ states becoming accidentally degenerate.

The $^1(\pi,3p\pi_x)$ state in ethylene has a term value of about 2.2 eV and therefore one would expect the A' state resulting from $\pi\rightarrow 3p\pi_x$ transition in propene to have a similar value. The peak at 7.59 eV in Figure (2) has a term value of 2.1 eV. The calculations predict a value of 7.43 eV for the $\pi\rightarrow 3p\pi_x$ transition, see Tables (3, 4, 6a) and therefore one can be reasonably certain that the peak at 7.59 eV corresponds to the $\pi\rightarrow 3p_x$ transition.

The cross section for electron impact excitation at 7.08 eV has an energy dependence which differs from that of either the R or V state indicating that it arises from a separate transition. The state at 7.08 eV has a term value of about 2.6 eV and Robin [14] has suggested that the $\pi\rightarrow 3p$ Rydberg states in olefins should have term values between 2.3 and 2.7 eV. The present calculations predict the $^1(\pi,3p\perp)$ transition to occur at 7.18 eV (see Tables 3, 4, 7b) confirming that the peak at 7.08 eV corresponds to a Rydberg $^1(\pi,3p\sigma)$ state.

The results for ethylene clearly indicated that the present basis set is incapable of adequately describing the V state, and as expected, the V state for propene is poorly represented. The present calculations predict that the $2^1A'$ state is largely Rydberg in character ($3d_{xz}-3d_{xy}$, + a little π^*), while the $4^1A'$ state is a largely valence state (π^* + a little $3d_{xz}-3d_{xy}$). These results suggest that the $4^1A'$ state should be correlated with the spectroscopic V state at 7.23 eV. This implies that the present calculations are in error by 1.91 eV. Furthermore if one accepts this assignment, how does one interpret the results for the $2^1A'$ state? The $2^1A'$ state has a calculated transition energy of 8.05 eV and on the basis of energy would appear to be a better candidate for the V state, but unfortunately it is largely Rydberg in character.

Buenker et al [24] using a small basis set of 32 contracted Gaussian functions experienced a similar problem with their results for ethylene. They calculated the transition energies of the 1^1B_{3u} and 2^1B_{3u} states to be 8.32 eV and 10.73 eV respectively. The 1^1B_{3u} state was largely Rydberg in character while the 2^1B_{3u} state was mostly valence. Since one generally associates the V state with the $\pi\rightarrow\pi^*$ transition, their results appeared to be in error by about 3 eV. Buenker et al argue that by improving the basis set the 1^1B_{3u} state would become more valence like. This argument is also supported by the more recent calculations in the literature (see Chapter 4). Therefore the V state for ethylene and substituted ethylenes is very basis set dependent.

Buenker et al also suggest that the valence/Rydberg character of the V state is a function of the dihedral angle (H-C=C-H). Therefore the 1^1B_{3u} state of planar ethylene could possess a significant amount

of Rydberg character, but as the dihedral angle increases it becomes more valence like. They also suggest that the intensity maximum at 7.66 eV in the ethylene spectrum corresponds to a non-vertical transition ($\pi \rightarrow \pi^*$). Using these arguments they conclude that the 1^1B_{3u} state, in spite of its diffuse nature can be correlated with the spectroscopic V state. Furthermore, the discrepancy of 0.66 eV between the calculated excitation energy for the 1^1B_{3u} state and the spectroscopic V state is possibly due to the experimental intensity maximum corresponding to a non-vertical transition.

Further theoretical work by Buenker et al (see Chapter 4) supported their earlier hypotheses and on the basis of these arguments the $2^1A'$ state of propene has been correlated with the spectroscopic V state.

One further problem of the theoretical description of the propene V state warrants discussion. The most recent calculations on ethylene (see Chapter 4) indicated that the percentage Rydberg character of the V state varied markedly with the basis set. The low symmetry of propene (C_s) provides a mechanism whereby the π^* orbital can interact with both the $3d_{xy}$ and $3d_{xz}$ Rydberg orbitals. Therefore it is possible that not only is the V state basis set dependent but the corresponding Rydberg states are also basis set dependent. Thus if one were to use a larger basis set would the π^* orbital be contaminated by components of diffuse Rydberg orbitals, and if not, how would this affect the Rydberg orbitals themselves and the calculated transition energies for the Rydberg states?

The $4\,^1A'$ state is largely valence and one now has the additional problem of correlating it with an experimental state. Table 2 indicates

that there is considerable experimental evidence for a $\pi \rightarrow 3d$ transition at 8.80 eV. The theoretical results indicate that the only state calculated to lie near this region is the $4\,^1A'$ state. Therefore the peak at 8.80 eV has tentatively been assigned $\pi \rightarrow 3d\pi$ (in spite of the fact that $4\,^1A'$ is largely valence).

The spectrum in Figure (2) also contains peaks at ca 8.0, 8.2, 8.3 and 8.45 eV, consistent with the results quoted by Kupperman et al [1]. The present calculations predict several states to lie within the region between 8.0 and 8.3 eV. The $4\,^1A'$ $^1(\pi, 3d_{xy} + 3d_{xz})$, $4\,^1A''$ $^1(\pi, 3d\sigma)$, $5\,^1A''$ $^1(\pi, 3d_{yz})$ and $6A''$ $^1(\pi, 4_s)$ are all predicted to occur within this region, see Tables (3, 4). One could therefore tentatively assign these 4 states to the 4 experimental peaks observed in this region. But it should be emphasised that the present calculations are probably not accurate enough to predict the correct ordering, and in view of the low symmetry of propene there is the additional possibility that the results are strongly basis set dependent.

Finally the correlations between the calculated electronic states of propene and ethylene are illustrated in Figure (6).

Triplet States

The calculated values for the propene triplet states are summarised in Tables (3) and (4). The calculated transition energy for the T state (4.44 eV) is in good agreement with the experimental value of 4.28 eV [2]. The singlet-triplet splittings (with the exception of the T and V states) are predicted to be small. Some triplet states are predicted to have slightly greater transition energies than the

corresponding singlets. This could be attributed to the SCF ground state MO basis providing better energies for the singlet state with respect to the triplet states. Two states however (1A'' and 2A'') are predicted to have triplet transition energies which are significantly greater than the corresponding singlets. It is not obvious why this should be but two possibilities are:

(i) the present basis set, being rather small, is not sufficient to correctly predict singlet-triplet splittings.

(ii) the absence of d orbitals on the carbon atoms (discussed previously in Chapter 4) results in a situation where the absence of these orbitals has a greater effect on the triplets with respect to the singlets.

One other interesting result is that the $5\,^3A''$ and $6\,^3A''$ states interact strongly while the corresponding singlets do not.

2 Methyl Propene (C_{2v}, I.P.=9.4 eV).

The microwave structure reported by Scharpen and Laurie [15] was used in the present study. The ground state SCF wavefunction was used as the MO basis and the theoretical results are summarised in Tables (11-22).

The electron scattering spectra is illustrated in Figure (3). The positions of maximum absorption in the UV are indicated and the $R(B_2)$ state at 6.17 eV and the V state are labelled [3, 16]. The present calculations predict that the $^1(\pi,3_s)$ state occurs at 6.61 eV, and

therefore one can assign the Rydberg transition at 6.17 eV to the $^1(\pi,3_s)$ state, see Tables (11, 12, 16a).

The $\pi\rightarrow 3p_y$ transition is optically forbidden and has previously been assigned to a weak band at 6.94 eV in the optical spectrum [17]. This assignment is also consistent with the term value of 2.5 eV associated with this peak. The present calculations tend to dispute this assignment. The $^1(\pi,3p_y)$ transition energy is predicted to be 7.42 eV while the calculated transition energies for the $^1(\pi,3p_x)$ and $^1(\pi,3p_z)$ states are 7.18 eV and 7.35 eV respectively, see Tables (11, 12, 15a, 14a, 16b).

The $\pi\rightarrow 3p$ transitions are forbidden for centrosymmetric olefins and are not expected to be much stronger in non-centrosymmetric ones. Therefore the weak band observed in the optical spectrum at 6.94 eV could be due to the $^1(\pi,3p_x)$ state, since this transition is also expected to be weak.

In view of the fact that the present diffuse functions have not been optimised for 2 methyl propene, the accuracy of the present calculations may be somewhat doubtful. Therefore the present calculations may not be reliable enough to predict the correct ordering of the $\pi\rightarrow 3p$ transitions, but indicate that all three transitions occur in the region 7→7.4 eV. The spectrum in Figure (3) shows peaks at ca 6.95 eV, 7.10 eV and 7.25 eV; these peaks appear to be the best candidates for the $\pi\rightarrow 3p$ transitions.

The electron impact-spectroscopy experiments of Kupperman et al [1, 2] indicate that there are peaks at 7.78, 7.96, 8.17 and 8.37 eV. The

present calculations predict 4 states to have comparable transition energies in this region: $3\,^1B_1\ ^1(\pi,3d\sigma)$; $2\,^1A_2\ ^1(\pi,3d_{yz})$; $4\,^1B_1\ ^1(\pi,4s)$; $1\,^1B_2\ ^1(\pi,3d_{xy})$, see tables (11) and (12).

The $2\,^1A_1$ state has a calculated transition energy of 8.08 eV, (Tables (11, 12, 14b)) and is largely Rydberg ($3d_{xz}$) in character. It is also contaminated by a small amount of the π^* orbital and has been correlated with the spectroscopic V state (6.58 eV). The theoretical results overestimate the transition energy by 1.5 eV and predict excessive Rydberg character. As in the case of propene this appears to be due largely to deficiencies in the present basis set.

The $3\,^1A_1$ state, on the other hand, is largely valence (π^*) in character and has a calculated transition energy of 9.19 eV. Despite the valence nature of this state it has been correlated with the spectroscopic $^1(\pi,3d\pi)$ state in order to be consistent with propene.

Triplet States

The results for the triplet states are summarised in Tables (11) and (12). The calculated excitation energy for the $^3(\pi,\pi^*)$ state (4.75 eV) is disappointing. Not only is it poor when compared to the experimental value of 4.22 eV [2], it is also significantly higher than the ethylene T state (see Chapter 4) and propene.

In general the singlet-triplet splittings are predicted to be quite small. In some cases the singlet-triplet splitting is predicted to have the wrong sign and this is probably due to the ground state SCF MO basis providing a better basis for the singlets with respect to the corresponding triplets.

Intravalence Transitions

Excepting the $3\,^1A_1$ state, the present calculations predict several intravalence transitions to occur in the region of 9 eV. These are generally of the type $\sigma \rightarrow \pi^*/\sigma^*$ and $\pi \rightarrow \sigma^*$ and will not be discussed further.

Cis But-2-ene (C_{2v}, I.P.=9.13 eV)

The geometry of cis but-2-ene was based on that of propene, the angle of the additional methyl group with respect to the C=C axis was assumed to be the same, as in propene and the C-C (methyl) bond length was also assumed to be unchanged. The geometric parameters are summarised below.

$r(C=C) = 1.336\,\text{Å}$

$r(C-C) = 1.501\,\text{Å}$

$\angle CCC = 124.3°$

The conformer used in the study is indicated below

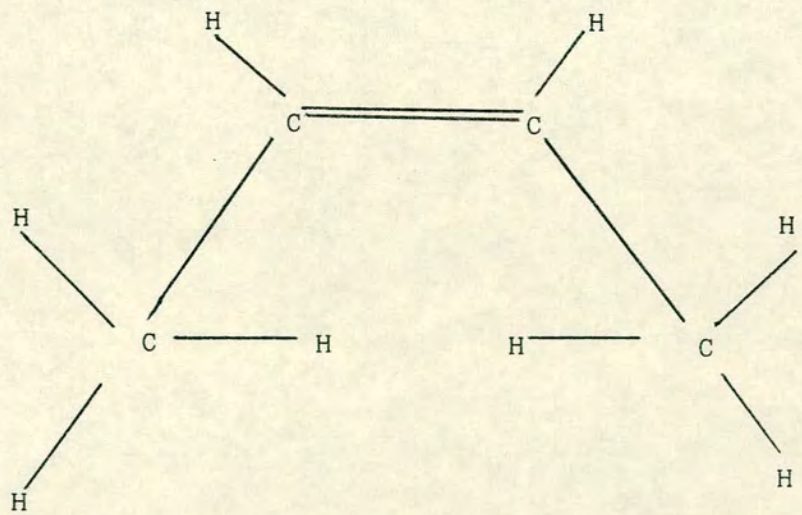

The ground state SCF wavefunction was used as the MO basis for the CI calculations. Table (23) contains a brief summary of previous assignments for the electronic spectrum of cis but-2-ene. The electron energy loss spectrum is indicated in Figure (4). The first Rydberg (B_1) state has an excitation energy of 5.98 eV. Other members of this Rydberg series ($\pi \rightarrow ns$) have been positioned at 7.56 eV (n=4) and 8.25 eV (n=5) and these are marked 4R and 5R on Figure (4) [23]. E_{max} for the $V(B_2)$ state is 7.12 eV. Positions of other optical maxima are indicated on the spectra [20-22].

The $^1(\pi,3s)$ state is calculated to have an excitation energy of 6.57 eV, see Tables (24, 25, 29a), in rather poor agreement with the experimental value (5.98 eV), this however does not affect the qualitative interpretation of the spectrum in this region. The optical spectrum shows absorption peaks at 6.16 eV, 6.34 eV and 6.44 eV. The present calculations predict no transitions other than $\pi \rightarrow 3s$ in this region and therefore it seems likely that these additional peaks are part of the Rydberg transition and should therefore be interpreted as vibrational fine structure.

The $1\,^1B_2$ state is largely Rydberg in character ($3d_{xy}$ + a little π^*) and from the point of view of energy is the best candidate for correlation with the spectroscopic V state. The calculated transition energy of 7.85 eV is in rather poor agreement with the experimental value (7.12 eV), but this is consistent with previous results.

The $2\,^1B_2$ state has a calculated transition energy of 8.93 eV and is predicted to be a mostly valence state (π^*). It has been correlated with the spectroscopic $^1(\pi,3d_{xy})$ state; although the spectroscopic

$^1(\pi,3d_{xy})$ state has not yet been identified experimentally. The present theoretical procedure appears to predict the orbital character of the $1\,^1B_2$ and $2\,^1B_2$ states incorrectly and this again has been attributed to deficiencies in the present basis set.

The $\pi\rightarrow 3p$ transitions produce states of symmetry A_2 ($\pi\rightarrow 3p_z$, optically forbidden), B_2 ($\pi\rightarrow 3p_y$, electric dipole allowed) and A_1 ($\pi\rightarrow 3p_x$, electric dipole allowed). The present calculations predict the Rydberg $^1(\pi,3p_x)$, $^1(\pi,3p_y)$ and $^1(\pi,3p_z)$ to have transition energies of 6.96, 7.11 and 7.14 eV respectively. These values appear to be a little too high since one would expect the Rydberg 3p states to have term values of about 2.5 eV. In any case the diffuse V band centred at 7.10 eV probably obscures these transitions.

The $^1(\pi,4s)$ transition is predicted to occur at 7.87 eV, Tables (24, 25, 29d), and agrees well with previous experimental assignments. The calculations also predict several Rydberg transitions involving d orbitals to occur in this region: $3\,^1B_1$, $^1(\pi 3d)$; $2\,^1A_2$, $^1(\pi,3d_{yz})$; $3\,^1A_1$, $^1(\pi,3d_{xz})$, see Tables (24, 25).

Triplet States

The $^3(\pi,\pi^*)$ state is predicted to have an excitation energy of 4.46 eV, Tables (24, 25, 34a, 35), in reasonably good agreement with the experimental value of 4.21 eV [2]. The Rydberg singlet-triplet splittings are predicted to be small, Table 25, and, somewhat surprisingly, in view of previous results are all predicted to have the correct sign.

Intravalence Transitions

The remaining states in Table 24 are all due to intravalence excitations involving $\sigma \rightarrow \pi^*/\sigma^*$ and $\pi \rightarrow \sigma^*$ and will not be discussed further.

Trans But-2-ene (C_{2h}, I.P.=9.13 eV)

The geometry for trans but-2-ene has been based on the microwave structure of propene [6]. The geometric parameters for the additional methyl group being taken from propene itself. The conformer used corresponded to that which possessed the highest symmetry (C_{2h}) and is indicated below.

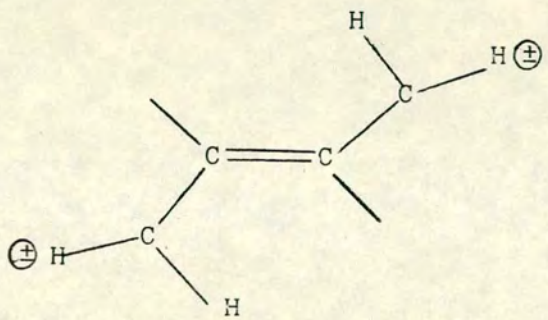

The ground state SCF wavefunction was used as the MO basis for the CI calculations. The present theoretical results are summarised in Tables (37-47) and Table (36) outlines several previous spectroscopic assignments.

The electron energy loss spectrum of trans but-2-ene is indicated in Figure (5); previous optical assignments are also indicated [20-23]. The spectroscopic $^1(\pi,3s)$ state has an excitation energy of 6.12 eV. The present calculations predict an excitation energy of 6.39 eV, Tables (37, 38, 41a), in relatively good agreement with experiment.

The present calculations indicate that substantial mixing occurs between the Rydberg $3p_x$ and $3p_y$ orbitals, resulting in two $3p_\sigma$ orbitals which are linear combinations of the original $3p_x$ and $3p_y$ orbitals. The main difference between these orbitals is the orientation of the nodal plane. The $(3p_x-3p_y)$ combination has a nodal plane parallel to the long axis of the molecule and the $(3p_x+3p_y)$ combination has a nodal plane perpendicular to the long axis; they have been donated $3p||$ and $3p\perp$ respectively.

Transitions of the type $\pi\rightarrow 3p$ are dipole forbidden for centrosymmetric olefins. The present calculations predict that the excitation energies for the $^1(\pi,3p_z)$, $^1(\pi,3p||)$ and $^1(\pi,3p\perp)$ are 6.98, 6.75 and 6.95 eV respectively, Tables (37, 38, 42a, 42b, 40a). One generally expects the $\pi\rightarrow 3p$ transitions to have term values of about 2.5 eV, and therefore it appears that the present calculations may possibly overestimate the excitation energies, a feature which has been observed with the other substituted olefins studied. However, the spectroscopic V state has a maximum at 7.08 eV and the experimental results (Figure (5)) indicate that E_{max} has a dependency on E_r. This suggests that one $\pi\rightarrow 3p$ transition could possibly occur in the region of 7.0 to 7.1 eV. Both the $^1(\pi,3p_z)$ and $^1(\pi,3p\perp)$ states are possible candidates.

The $1\,^1Bu$ state has a calculated transition energy of 7.64 eV and is predicted to be largely Rydberg $(3d_{xz}+3d_{yz})$ in nature. On the basis of arguments discussed previously this state has been correlated with the spectroscopic V state (7.08 eV). As expected the present calculations significantly overestimate the excitation energy.

The $3\,^1Bu$ state is predicted to be largely valence in character

(π^* + a little $3d_{xz}+3d_{yz}$) and has been correlated with the spectroscopic $^1(\pi,3d)$ state. These assignments are not consistent with the predicted orbital character of the 1^1Bu and 3^1Bu states but are more consistent with the accepted interpretation of the spectrum.

The symmetry of trans but-2-ene (C_{2h}) provides a mechanism (as in the case of propene) whereby the π^* orbital can interact with both the Rydberg $3d_{xz}$ and $3d_{yz}$ orbitals, therefore it is possible that the results for all three ^1Bu states are strongly basis set dependent.

The present calculations predict several Rydberg states ($\pi \rightarrow 3d$) to have excitation energies around 7.5 eV, Tables (37, 38, 41b, 41c, 43b). These results are in good agreement with the experimental data, see Figure (5). The $\pi \rightarrow 4s$ transition (4R in Figure (5)) has been located at 7.80 eV. The present calculations predict an excitation energy of 7.94 eV for this state, Tables (37, 38, 41d), in good agreement with experiment, but it should also be noted that the wavefunction indicates that the Rydberg $3d_{xy}$, 3d and 4s orbitals interact strongly with one another.

Triplet States

The $^3(\pi,\pi^*)$ state is predicted to have an excitation energy of 4.47 eV in reasonably good agreement with the experimental value of 4.24 [2]. The singlet-triplet splittings for the Rydberg states are calculated to be small, and in only one case (2Au) is the sign incorrectly predicted.

Intravalence Transitions

Table (37) contains several states whose excitation energies are greater than 9 eV. These states involve intravalence transitions of the type $\sigma \rightarrow \sigma^*$, $\sigma \rightarrow \pi^*$ and $\pi \rightarrow \sigma^*$ and will not be discussed further.

Conclusions

The results for the Rydberg $\pi \rightarrow 3p$ and $\pi \rightarrow 3d$ transitions have generally been quite good; the difference between theory and experiment being ca 0.2 eV. The results for the $^1(\pi,3s)$ state have been somewhat erratic. Cis but-2-ene and 2 methyl propene have a rather large discrepancy between the calculated and experimental values, while propene and trans but-2-ene produced more acceptable results. Fortunately this has not affected the interpretation of the spectra in these regions.

The V state has been poorly represented in each case. The V state (or that state which was chosen to correlate with the spectroscopic V state) was always predicted to be largely Rydberg 3d in character. This appears to be due to the limited size of the basis set used, since larger basis set calculations on ethylene overcome this problem. The spectroscopic $^1(\pi,3d\pi)$ state was always predicted to be largely valence in character and this again appears to be due to the basis set.

As discussed previously, the symmetry of propene (C_s) and trans but-2-ene (C_{2h}) provides a mechanism whereby the "V" state could possibly affect the calculated energies of the Rydberg $^1(\pi,3d)$ states, and therefore the present basis set should be expanded to overcome this potential problem. The exponents of the Rydberg orbitals were not optimised for any of the substituted ethylenes studied. Optimisation of the basis set is computationally expensive but would nevertheless improve the present results.

Figure (6) correlates the calculated transition energies for the present series of olefins with ethylene. The trends are fairly clear cut. In each case methylation reduces the transition energies of the Rydberg states, although there are one or two anomalous results (e.g. propene $^1(\pi,3s)$ state is lower than that of 2 methyl propene) which could be attributed to the inadequacies of the present basis sets.

Considering the limitations of the present theoretical procedure, the results have generally been satisfactory, although larger basis sets are clearly necessary.

References

1. Kuppermann, A., Flicker, W.M., Mosher, O.A., Chemical Reviews, 1979, Vol. 79, p. 77.
2. Flicker, W.M., Mosher, O.A., Kuppermann, A., Chem.Phys.Lett., 56, 36 (1975).
3. Carr, E.P., and Stücklen, H., J.Chem.Phys., 4, 751 (1936).
4. Robin, M.B., Basch, H., Kuebler, N.A., Kaplan, B.E., Meinwald, J., J.Chem.Phys., 48, 5037 (1968).
5. Merer, A.J., Mulliken, R.S., Chemical Reviews, 69, 639 (1969)
6. Lide, D.R. and Christensen, D., J.Chem.Phys., 35, 1374, (1961).
7. Buenker, R.J., Peyerimhoff, S.D. and Butscher, W., Mol.Phys., 35, 771 (1978).
8. Dance, D.F. and Walker, I.C., Proc.R.Soc. Lond. A., 334, 259-277 (1973).
9. Bowman, C.R. and Miller, W.D., J.Chem.Phys., 42, 681 (1965).
10. Watson, F.H. and McGlynn, S.P., Theoret.Chim.Acta., 21, 309 (1971).
11. Samson, J.A.R., Marmo, F.F. and Watanabe, K., J.Chem.Phys., 36, 783 (1962).
12. Bralsford, R., Harries, P.V. and Price, W.C., Proc.R.Soc. Lond. A, 258, 459 (1960).
13. Overson, A.A., Russell, B.R. and Jones, P.R., Chem.Phys.Lett., 17, 98 (1972).
14. Robin, M.B., "Higher Excited States of Polyatomic Molecules", Vol. II, 1975 (Academic Press, N.Y.).
15. Scharpen, L.H. and Laurie, V.W., J.Chem.Phys., 39, 1733 (1963).

16. Gary, J.T. and Pickett, L.W., J.Chem.Phys., 22, 599 (1954).

17. McDiarmid, R., J.Chem.Phys., 55, 2426 (1971).

18. Brongersma, H.H., Hart, J.A. and Oosterhoff, L.J., 1967 Nobel Symposium 5, Fast Reactions and Primary Processes in Reaction Kinetics (Ed. S. Claesson), p. 211.

19. Brongersma, H.H., 1968, Ph.D. Dissertation, University of Leiden.

20. Von Trepka, L., and Nevert, H., Z.Naturfosch, 18a, 1295 (1963).

21. Sanche, L., and Schulz, G.J., J.Chem.Phys., 58, 479, (1973).

22. Verhaart, G.J. and Brongersma, H.H., Chem.Phys., 52, 431 (1980).

23. McDiarmid, R., J.Chem.Phys., 50, 2328, (1969).

24. Buenker, R.J., Peyerimhoff, S.D. and Kammer, W.E., J.Phys.Chem., 55, 814 (1971).

Table 1 Observed Vertical Frequencies and Term Values for the V-N and R-N Systems of C_2H_4 and its Methyl Substituted Derivatives (in eV)

No. of Methyl Groups	I.P. of π MO	Observed System Maxima		Orbital term Values	
		V-N	R-N	$1b_{2g}(\pi^*)$	4ag(35)
0	10.51	7.58	7.15	2.93	3.36
1	9.73	7.15	6.72	2.58	3.01
2(1,1)	9.23	6.68	6.19	2.55	3.04
2(1,2-cis)	9.13	7.10	6.03	2.03	3.10
2(1,2-trans)	9.13	6.97	6.09	2.16	3.04
3	8.68	6.75	5.74	1.93	2.94
4	8.30	6.61	5.40	1.69	2.90

Table 2 Spectroscopic Assignments of Propene

Excitation process	Excited state	Ref. [8]	Ref. [9]	UV
$\pi\rightarrow\pi^*$	T	4.35	4.4	4.2 [10]
$\pi\rightarrow$ 3s	T_R(?)	5.8-6.4	-	-
$\pi\rightarrow$ 3s	R	6.7	-	6.72[11]
$\pi\rightarrow\pi^*$	V	7.1	-	7.15[11]
$\pi\rightarrow$ nd	R'	8.9	8.8	8.8 [11]
ionization	-	-	-	9.73[12]

Table 3 CI Results for Propene

State	No. of main Configurations	Σcoeff^2	Correction lau	CI/au	Excitation Energy/eV	Table no.
GS	3M1R	.9476	-.0079	-117.2098	_	5
$1^1A'$	4M4R	.9177	-.0146	-116.9376	7.41	6a
$2^1A'$	4M4R	.9201	-.0140	-116.9138	8.05	6b
$3^1A'$	4M4R	.9226	-.0135	-116.9060	8.27	6c
$4^1A'$	4M4R	.9112	-.0162	-116.8738	9.14	6d
$1^1A''$	8M6R	.9241	-.0139	-116.9641	6.69	7a
$2^1A''$	8M6R	.9182	-.0147	-116.9460	7.18	7b
$3^1A''$	8M6R	.9125	-.0157	-116.9375	7.41	7c
$4^1A''$	8M6R	.9200	-.0146	-116.9150	8.02	7d
$5^1A''$	8M6R	.9205	-.0139	-116.9095	8.17	7e
$6^1A''$	8M*R	.9222	-.0136	-116.9046	8.30	7f
$1^3A'$	5M2R	.9602	-.0059	-117.0434	4.53	8a
$2^3A'$	5M2R	.9247	-.0132	-116.9358	7.46	8b
$1^3A'$	4M4R	.9175	-.0139	-117.0467	4.44	9a
$2^3A'$	4M4R	.9233	-.0134	-116.9361	7.45	9b
$3^3A'$	4M4R	.9267	-.0130	-116.9091	8.18	9c
$4^3A'$	4M4R	.9267	-.0128	-116.9033	8.34	9d
$1^3A''$	8M6R	.9295	-.0122	-116.9560	6.91	10a
$2^3A''$	8M6R	.9211	-.0138	-116.9422	7.28	10b
$3^3A''$	8M6R	.9139	-.0154	-116.9368	7.43	10c
$4^3A''$	8M6R	.9239	-.0136	-116.9103	8.15	10d
$5^3A''$	8M6R	.9253	-.0134	-116.9137	8.05	10e
$6^3A''$	8M6R	.9182	-.0148	-116.9129	8.08	10f

Table 4 Calculated Transition Energies of Propene

State	Transition	Excitation Energy/eV	
		Singlet	Triplet
1A"	$\pi \rightarrow 3s$	6.69	6.91
2A"	$\pi \rightarrow 3p_{\perp}$	7.18	7.28
3A"	$\pi \rightarrow 3p_{\parallel}$	7.41	7.43
1A'	$\pi \rightarrow 3p\pi_x$	7.41	7.45
2A'	$\pi \rightarrow \pi^*$	8.05	4.44
4A"	$\pi \rightarrow 3d\sigma$	8.02	8.15
5A"	$\pi \rightarrow 3d_{yz}$	8.17	8.05 *
6A"	$\pi \rightarrow 4s$	8.30	8.08 *
3A'	$\pi \rightarrow (3\ d_{xy}+d_{xz})$	8.27	8.34
4A'	$\pi \rightarrow 3d\pi$	9.14	8.18

* These two states interact significantly

Table 5 Propene Ground State X A'

$(\text{coefficient})^2$	4a'	5a'	6a'	7a'	8a'	9a'	10a'	1a''	2a''	6a''	10a''
.92638 M	2	2	2	2	2	2	2	2	2	-	-
.0160 M	2	2	2	2	2	2	2	2	-	2	-
.0052 M	2	2	2	2	2	2	2	2	-	1	1

Table 6a Propene $1\,^1A'$ $^1(\pi, 3p_x)$

$(\text{coefficient})^2$	4a'	5a'	6a'	7a'	8a'	9a'	10a'	1a''	2a''	3a''	4a''	5a''	6a''
.8969 M	2	2	2	2	2	2	2	2	1	1	-	-	-
.0034 M	2	2	2	2	2	2	2	2	1	-	1	-	-
.0083 M	2	2	2	2	2	2	2	2	1	-	-	1	-
.0165 M	2	2	2	2	2	2	2	2	1	-	-	-	1

Table 6b Propene $2\,^1A'$ $^1(\pi, 3d\pi)$

$(\text{coefficient})^2$	4a'	5a'	6a'	7a'	8a'	9a'	10a'	1a''	2a''	3a''	4a''	5a''	6a''
.0070 M	2	2	2	2	2	2	2	2	1	1	-	-	-
.7909 M	2	2	2	2	2	2	2	2	1	-	1	-	-
.0486 M	2	2	2	2	2	2	2	2	1	-	-	1	-
.0736 M	2	2	2	2	2	2	2	2	1	-	-	-	1

Table 6c Propene $3^1A'$ $^1(\pi, 3d_{xy} + 3d_{xz})$

(coefficient)^2	4a'	5a'	6a'	7a'	8a'	9a'	10a'	1a''	2a''	3a''	4a''	5a''	6a''
.0016 M	2	2	2	2	2	2	2	2	1	1	-	-	-
.0580 M	2	2	2	2	2	2	2	2	1	-	1	-	-
.8621 M	2	2	2	2	2	2	2	2	1	-	-	1	-
.0010 M	2	2	2	2	2	2	2	2	1	-	-	-	1

Table 6d Propene $4^1A'$ $^1(\pi,\pi^*)$

(coefficient)^2	4a'	5a'	6a'	7a'	8a'	9a'	10a'	1a''	2a''	3a''	4a''	5a''	6a''
.0127 M	2	2	2	2	2	2	2	2	1	1	-	-	-
.0707 M	2	2	2	2	2	2	2	2	1	-	1	-	-
.0090 M	2	2	2	2	2	2	2	2	1	-	-	1	-
.8188 M	2	2	2	2	2	2	2	2	1	-	-	-	1

Tables 7a - f n^1A'' States

Table 7a Propene $1^1A''$ $^1(\pi, 3s)$

(coefficient)^2	4a'-8a'	9a'	10a'	1a"	2a"	11a'	12a'	13a'	14a'	15a'	16a'	17a'	19a'
.8633M	10	2	2	2	1	1	-	-	-	-	-	-	-
.0303M	10	2	2	2	1	-	1	-	-	-	-	-	-
.0006M	10	2	2	2	1	-	-	1	-	-	-	-	-
.0000M	10	2	2	2	1	-	-	-	1	-	-	-	-
.0000M	10	2	2	2	1	-	-	-	-	1	-	-	-
.0002M	10	2	2	2	1	-	-	-	-	-	-	1	-
.0013M	10	2	2	2	1	-	-	-	-	-	-	-	1
.0283M	10	2	2	2	1	-	-	-	-	-	1	-	-

Table 7b Propene $2^1A''$ $^1(\pi, 3p_\perp)$

(coefficient)^2	4a'-8a'	9a'	10a'	1a"	2a"	11a'	12a'	13a'	14a'	15a'	16a'	17a'	19a'
.0320M	10	2	2	2	1	1	-	-	-	-	-	-	-
.8757M	10	2	2	2	1	-	1	-	-	-	-	-	-
.0025M	10	2	2	2	1	-	-	1	-	-	-	-	-
.0003M	10	2	2	2	1	-	-	-	1	-	-	-	-
.0003M	10	2	2	2	1	-	-	-	-	1	-	-	-
.0001M	10	2	2	2	1	-	-	-	-	-	1	-	-
.0003M	10	2	2	2	1	-	-	-	-	-	-	1	-
.0070M	10	2	2	2	1	-	-	-	-	-	-	-	1

Table 7c Propene $3^1A''$ $^1(\pi, 3p_\parallel)$

(coefficient)^2	4a'-8a'	9a'	10a'	1a"	2a"	11a'	12a'	13a'	14a'	15a'	16a'	17a'	19a'
.0003M	10	2	2	2	1	1	-	-	-	-	-	-	-
.0025M	10	2	2	2	1	-	1	-	-	-	-	-	-
.9079M	10	2	2	2	1	-	-	1	-	-	-	-	-
.0004M	10	2	2	2	1	-	-	-	1	-	-	-	-
.0000M	10	2	2	2	1	-	-	-	-	1	-	-	-
.0001M	10	2	2	2	1	-	-	-	-	-	1	-	-
.0000M	10	2	2	2	1	-	-	-	-	-	-	1	-
.0013M	10	2	2	2	1	-	-	-	-	-	-	-	1

Table 7d Propene $4^1A''$ $^1(\pi, 3d\sigma)$

(coefficient)^2	4a'-8a'	9a'	10a'	1a"	2a"	11a'	12a'	13a'	14a'	15a'	16a'	17a'	19a'
.0000M	10	2	2	2	1	1	-	-	-	-	-	-	-
.0004M	10	2	2	2	1	-	1	-	-	-	-	-	-
.0000M	10	2	2	2	1	-	-	1	-	-	-	-	-
.0000M	10	2	2	2	1	-	-	-	1	-	-	-	-
.9184M	10	2	2	2	1	-	-	-	-	1	-	-	-
.0010M	10	2	2	2	1	-	-	-	-	-	1	-	-
.0001M	10	2	2	2	1	-	-	-	-	-	-	1	-
.0001M	10	2	2	2	1	-	-	-	-	-	-	-	1

Table 7e Propene $5^1A''$ $^1(\pi, 3d_{yz})$

(coefficient)^2	4a'-8a'	9a'	10a'	1a"	2a"	11a'	12a'	13a'	14a'	15a'	16a'	17a'	19a'
.0000M	10	2	2	2	1	1	-	-	-	-	-	-	-
.0002M	10	2	2	2	1	-	1	-	-	-	-	-	-
.0005M	10	2	2	2	1	-	-	1	-	-	-	-	-
.9149M	10	2	2	2	1	-	-	-	1	-	-	-	-
.0000M	10	2	2	2	1	-	-	-	-	1	-	-	-
.0025M	10	2	2	2	1	-	-	-	-	-	1	-	-
.0000M	10	2	2	2	1	-	-	-	-	-	-	1	-
.0023M	10	2	2	2	1	-	-	-	-	-	-	-	1

Table 7f Propene $6^1A''$ $^1(\pi, 4s)$

(coefficient)^2	4a'-8a'	9a'	10a'	1a"	2a"	11a'	12a'	13a'	14a'	15a'	16a'	17a'	19a'
.0003M	10	2	2	2	1	1	-	-	-	-	-	-	-
.0001M	10	2	2	2	1	-	1	-	-	-	-	-	-
.0002M	10	2	2	2	1	-	-	1	-	-	-	-	-
.0024M	10	2	2	2	1	-	-	-	1	-	-	-	-
.0010M	10	2	2	2	1	-	-	-	-	1	-	-	-
.9162M	10	2	2	2	1	-	-	-	-	-	1	-	-
.0009M	10	2	2	2	1	-	-	-	-	-	-	1	-
.0012M	10	2	2	2	1	-	-	-	-	-	-	-	1

Tables 8 a,b n $^3A'$ States

Table 8a Propene $1^3A'$ $^3(\pi,\pi^*)$

(coefficient)^2	4a'	5a'	6a'	7a'	8a'	9a'	10a'	1a"	2a"	3a"	4a"	6a"	9a"	10a"
.0198M	2	2	2	2	2	2	2	2	1	1	-	-	-	-
.0167M	2	2	2	2	2	2	2	2	1	-	1	-	-	-
.8763M	2	2	2	2	2	2	2	2	1	-	-	1	-	-
.0333M	2	2	2	2	2	2	2	2	1	-	-	-	-	1
.0141M	2	2	2	2	2	2	2	1	2	-	-	-	1	-

Table 8b Propene $2^3A'$ $^3(\pi, 3p_x)$

(coefficient)^2	4a'	5a'	6a'	7a'	8a'	9a'	10a'	1a"	2a"	3a"	4a"	6a"	9a"	10a"
.9054M	2	2	2	2	2	2	2	2	1	1	-	-	-	-
.0006M	2	2	2	2	2	2	2	2	1	-	1	-	-	-
.0179M	2	2	2	2	2	2	2	2	1	-	-	1	-	-
.0006M	2	2	2	2	2	2	2	2	1	-	-	-	-	1
.0002M	2	2	2	2	2	2	2	1	2	-	-	-	1	-

Tables 9a - d n $^3A'$

Table 9a Propene $1^3A'$ $^3(\pi,\pi^*)$

(coefficient)^2	4a'	5a'	6a'	7a'	8a'	9a'	10a'	1a"	2a"	3a"	4a"	5a"	6a"	9a"	10a"
.0185M	2	2	2	2	2	2	2	2	1	1	-	-	-	-	-
.0297M	2	2	2	2	2	2	2	2	1	-	1	-	-	-	-
.0023M	2	2	2	2	2	2	2	2	1	-	-	1	-	-	-
.8671M	2	2	2	2	2	2	2	2	1	-	-	-	1	-	-
.0309M	2	2	2	2	2	2	2	2	1	-	-	-	-	-	1
.0114M	2	2	2	2	2	2	2	1	2	-	-	-	1	-	-

Table 9b . Propene $2^3A'$ $^3(\pi, 3p_x)$

(coefficient)^2	4a'	5a'	6a'	7a'	8a'	9a'	10a'	1a"	2a"	3a"	4a"	5a"	6a"	9a"	10a"
.9037M	2	2	2	2	2	2	2	2	1	1	-	-	-	-	-
.0036M	2	2	2	2	2	2	2	2	1	-	1	-	-	-	-
.0013M	2	2	2	2	2	2	2	2	1	-	-	1	-	-	-
.0148M	2	2	2	2	2	2	2	2	1	-	-	-	1	-	-

Table 9c Propene . $3^3A'$

(coefficient)^2	4a'	5a'	6a'	7a'	8a'	9a'	10a'	1a"	2a"	3a"	4a"	5a"	6a"	9a"	10a"
.0010M	2	2	2	2	2	2	2	2	1	-	-	-	-	-	-
.8707M	2	2	2	2	2	2	2	2	1	-	1	-	-	-	-
.0289M	2	2	2	2	2	2	2	2	1	-	-	1	-	-	-
.02616M	2	2	2	2	2	2	2	2	1	-	-	-	1	-	-

Table 9d Propene . $4^3A'$

(coefficient)^2	4a'	5a'	6a'	7a'	8a'	9a'	10a'	1a"	2a"	3a"	4a"	5a"	6a"	9a"	10a"
.0014M	2	2	2	2	2	2	2	2	1	1	-	-	-	-	-
.0217M	2	2	2	2	2	2	2	2	1	-	1	-	-	-	-
.8927M	2	2	2	2	2	2	2	2	1	-	-	1	-	-	-
.0060M	2	2	2	2	2	2	2	2	1	-	-	-	1	-	-
.0050	2	2	2	2	2	2	2	2	1	-	-	-	-	1	-

Tables 10a - f n^3A''

Table 10a . Propene, $1\,^3A''\ ^1(\pi, 3s)$

$(\text{coefficient})^2$	4a'-8a'	9a'	10a'	1a"	2a"	11a'	12a'	13a'	14a'	15a'	16a'	17a'	19a'
.8592M	10	2	2	2	1	1	-	-	-	-	-	-	-
.0248M	10	2	2	2	1	-	1	-	-	-	-	-	-
.0000M	10	2	2	2	1	-	-	1	-	-	-	-	-
.0001M	10	2	2	2	1	-	-	-	1	-	-	-	-
.0000M	10	2	2	2	1	-	-	-	-	1	-	-	-
.0005M	10	2	2	2	1	-	-	-	-	-	1	-	-
.0436M	10	2	2	2	1	-	-	-	-	-	-	1	-
.0012M	10	2	2	2	1	-	-	-	-	-	-	-	1

Table 10b Propene $2\,^3A''\ ^3(\pi, 3p)$

$(\text{coefficient})^2$	4a'-8a'	9a'	10a'	1a"	2a"	11a'	12a'	13a'	14a'	15a'	14a'	17a'	19a'
.0255M	10	2	2	2	1	1	-	-	-	-	-	-	-
.8788M	10	2	2	2	1	-	1	-	-	-	-	-	-
.0058M	10	2	2	2	1	-	-	1	-	-	-	-	-
.0003M	10	2	2	2	1	-	-	-	1	-	-	-	-
.0002M	10	2	2	2	1	-	-	-	-	1	-	-	-
.0002M	10	2	2	2	1	-	-	-	-	-	1	-	-
.0004M	10	2	2	2	1	-	-	-	-	-	-	1	-
.0099M	10	2	2	2	1	-	-	-	-	-	-	-	1

Table 10c Propene. $3^3A''$ $^3(\pi, 3p)$

$(\text{coefficient})^2$	4a'-8a'	9a'	10a'	1a"	2a"	11a'	12a'	13a'	14a'	15a'	16a'	17a'	19a'
.0001M	10	2	2	2	1	1	-	-	-	-	-	-	-
.0058M	10	2	2	2	1	-	1	-	-	-	-	-	-
.9054M	10	2	2	2	1	-	-	1	-	-	-	-	-
.0004M	10	2	2	2	1	-	-	-	1	-	-	-	-
.0001M	10	2	2	2	1	-	-	-	-	1	-	-	-
.0001M	10	2	2	2	1	-	-	-	-	-	1	-	-
.0000M	10	2	2	2	1	-	-	-	-	-	-	1	-
.0018M	10	2	2	2	1	-	-	-	-	-	-	-	-

Table 10d Propene $4^3A''$ $^3(\pi, 3d\sigma)$

$(\text{coefficient})^2$	4a'-8a'	9a'	10a'	1a"	2a"	11a'	12a'	13a'	14a'	15a'	16a'	17a'	19a'
.0000M	10	2	2	2	1	1	-	-	-	-	-	-	-
.0002M	10	2	2	2	1	-	1	-	-	-	-	-	-
.0000M	10	2	2	2	1	-	-	1	-	-	-	-	-
.0000M	10	2	2	2	1	-	-	-	1	-	-	-	-
.9206M	10	2	2	2	1	-	-	-	-	1	-	-	-
.0026M	10	2	2	2	1	-	-	-	-	-	1	-	-
.0003M	10	2	2	2	1	-	-	-	-	-	-	1	-
.0000M	10	2	2	2	1	-	-	-	-	-	-	-	1

Table 10e Propene $5^3A''$ $^3(\pi, 3dyz)$

$(coefficient)^2$	4a'-8a'	9a'	10a'	1a"	2a"	11a'	12a'	13a'	14a'	15a'	16a'	17a'	19a'
.0009M	10	2	2	2	1	1	-	-	-	-	-	-	-
.0000M	10	2	2	2	1	-	1	-	-	-	-	-	-
.0006M	10	2	2	2	1	-	-	1	-	-	-	-	-
.4329M	10	2	2	2	1	-	-	-	1	-	-	-	-
.0013M	10	2	2	2	1	-	-	-	-	1	-	-	-
.4814M	10	2	2	2	1	-	-	-	-	-	1	-	-
.0021M	10	2	2	2	1	-	-	-	-	-	-	1	-
.0065M	10	2	2	2	1	-	-	-	-	-	-	-	1

Table 10f Propene $6^3A''$ $^3(\pi, 4s)$

$(coefficient)^2$	4a'-8a'	9a'	10a'	1a"	2a"	11a'	12a'	13a'	14a'	15a'	16a'	17a'	19a'
.0003M	10	2	2	2	1	1	-	-	-	-	-	-	-
.0003M	10	2	2	2	1	-	1	-	-	-	-	-	-
.0008M	10	2	2	2	1	-	-	1	-	-	-	-	-
.4896M	10	2	2	2	1	-	-	-	1	-	-	-	-
.0015M	10	2	2	2	1	-	-	-	-	1	-	-	-
.4247M	10	2	2	2	1	-	-	-	-	-	1	-	-
.0009M	10	2	2	2	1	-	-	-	-	-	-	1	-
.0000M	10	2	2	2	1	-	-	-	-	-	-	-	1

Table 11 2 Methyl Propene - Calculated Transition Energies

State	No. of main Configurations	$\Sigma coeff^2$	Correction /au	CI/a.u.	Excitation Energy/eV	Table no.
GS	2M1R	.9358	-.0128	-156.2814	-	13
1^1A_1	5M3R	.9130	-.0189	-156.0173	7.18	14a
2^1A_1	5M3R	.9120	-.0191	-155.9843	8.08	14b
3^1A_1	5M3R	.9044	-.0213	-155.9435	9.19	14c
1^1A_2	5M3R	.9125	-.0189	-156.0085	7.42	15a
2^1A_2	5M3R	.9152	-.0183	-155.9858	8.04	15b
3^1A_2	5M3R	.8767	-.0304	-155.9237	9.73	15c
1^1B_1	7M5R	.9161	-.0180	-156.0283	6.88	16a
2^1B_1	7M5R	.9068	-.0204	-156.0112	7.35	16b
3^1B_1	7M5R	.9121	-.0192	-155.9887	7.96	16c
4^1B_1	7M5R	.9131	-.0188	-155.9851	8.06	16d
5^1B_1	7M5R	.9098	-.0196	-155.9303	9.55	16e
1^1B_2	4M2R	.9172	-.0177	-155.9826	8.13	17a
2^1B_2	4M2R	.8788	-.0300	-155.9333	9.47	17b
1^3A_1	5M3R	.9033	-.0204	-156.1067	4.75	18a
2^3A_1	5M3R	.9147	-.0184	-156.0099	7.39	18b
3^3A_1	5M3R	.9163	-.0179	-155.9822	8.14	18c
1^3A_1	6M1R	.9561	-.0086	-156.1073	4.74	19
1^3A_2	5M3R	.9151	-.0184	-156.0084	7.43	20a
2^3A_2	5M3R	.9182	-.0181	-155.9915	7.89	20b
3^3A_2	5M3R	.8619	-.0343	-155.9305	9.55	20c
1^3B_1	7M5R	.9203	-.0176	-156.0384	6.61	21a
2^3B_1	7M5R	.9083	-.0198	-156.0078	7.44	21b
3^3B_1	7M5R	.9110	-.0201	-155.9976	7.72	21c
4^3B_1	7M5R	.9163	-.0189	-155.9946	7.80	21d
5^3B_1	7M5R	.9140	-.0189	-155.9403	9.28	21e
1^3B_2	4M2R	.9209	-.0169	-155.9821	8.14	22a
2^3B_2	4M2R	.8759	-.0312	-155.9390	9.31	22b

Table 12 2 Methyl Propene - Calculated Transition Energies

State	Transition	Singlet	Triplet
1^1B_1	$\pi \rightarrow 3s$	6.88	6.61
1^1A_1	$\pi \rightarrow 3p_x$	7.18	4.75(T)
2^1B_1	$\pi \rightarrow 3p_z$	7.35	7.44
1^1A_2	$\pi \rightarrow 3p_y$	7.42	7.43
3^1B_1	$\pi \rightarrow d\sigma$	7.96#	7.72#
2^1A_2	$\pi \rightarrow 3d_{yz}$	8.04	7.89
4^1B_1	$\pi \rightarrow 4s$	8.06#	7.80#
2^1A_1	$\pi \rightarrow \pi^*$	8.08	7.39
1^1B_2	$\pi \rightarrow 3dxy$	8.13	8.14
3^1A_1	$\pi \rightarrow 3dxz$	9.19	8.14

- these states interact significantly

Table 13 2 Methyl Propene Ground State (1^1A_1)

$(\text{coefficient})^2$	$4a_1$-$8a_1$	$1b_1$	$2b_1$	$2b_2$-$5b_2$	$1a_2$	$5b_1$	$9b_1$
.9198M	10	2	2	8	2	-	-
.0125M	10	2	-	8	2	2	-
.0035M	10	2	-	8	2	1	1

Tables 14 a-c n^1A_1 States

Table 14a 2-methyl propene 1^1A_1 $^1(\pi, 3p_x)$

(coefficient)^2	$4a_1$-$7a_1$	$8a_1$	$2b_2$-$4b_2$	$5b_2$	$1a_2$	$1b_1$	$2b_1$	$3b_1$	$4b_1$	$5b_1$	$9a_1$	$6b_2$
.8860M	8	2	6	2	2	2	1	1	-	-	-	-
.0000M	8	2	6	2	2	2	1	-	1	-	-	-
.0269M	8	2	6	2	2	2	1	-	-	1	-	-
.0000M	8	1	6	2	2	2	2	-	-	-	1	-
.0000M	8	2	6	1	2	2	2	-	-	-	-	1

Table 14b 2-methyl propene 2^1A_1 $^1(\pi, 3d\pi)$

(coefficient)^2	$4a_1$-$7a_1$	$8a_1$	$2b_2$-$4b_2$	$5b_2$	$1a_2$	$1b_1$	$2b_1$	$3b_1$	$4b_1$	$5b_1$	$9a_1$	$6b_2$
.0000M	8	2	6	2	2	2	1	1	-	-	-	-
.9056M	8	2	6	2	2	2	1	-	1	-	-	-
.0061M	8	2	6	2	2	2	1	-	-	1	-	-
.0000M	8	1	6	2	2	2	2	-	-	-	1	-
.0000M	8	2	6	1	2	2	2	-	-	-	-	1

Table 14c 2-methyl propene 3^1A_1 $^1(\pi, \pi^*)$

(coefficient)^2	$4a_1$-$7a_1$	$8a_1$	$2b_2$-$4b_2$	$5b_2$	$1a_2$	$1b_1$	$2b_1$	$3b_1$	$4b_1$	$5b_1$	$9a_1$	$6b_2$
.0279M	8	2	6	2	2	2	1	1	-	-	-	-
.0070M	8	2	6	2	2	2	1	-	1	-	-	-
.8696M	8	2	6	2	2	2	1	-	-	1	-	-
.0000M	8	1	6	2	2	2	2	-	-	-	1	-
.0000M	8	2	6	1	2	2	2	-	-	-	-	1

Tables 15a-c n^1A_2 States

Tables 15a 2-methyl propene 1^1A_2 $^1(\pi, 3py)$

(coefficient)^2	$4a_1$-$7a_1$	$8a_1$	$2b_2$-$4b_2$	$5b_2$	$1a_2$	$1b_1$	$2b_1$	$6b_2$	$7b_2$	$8b_2$	$3b_1$	$2a_2$
.9117M	8	2	6	2	2	2	1	1	-	-	-	-
.0000M	8	2	6	2	2	2	1	-	1	-	-	-
.0008M	8	2	6	2	2	2	1	-	-	1	-	-
.0000M	8	1	6	2	2	2	2	-	-	-	-	1
.0000M	8	2	6	1	2	2	2	-	-	-	1	-

Table 15b 2 methyl propene 2^1A_2 $^1(\pi, 3dyz)$

(coefficient)^2	$4a_1$-$7a_1$	$8a_1$	$2b_2$-$4b_2$	$5b_2$	$1a_2$	$1b_1$	$2b_1$	$6b_2$	$7b_2$	$8b_2$	$3b_1$	$2a_2$
.0000M	8	2	6	2	2	2	1	1	-	-	-	-
.9081M	8	2	6	2	2	2	1	-	1	-	-	-
.0070M	8	2	6	2	2	2	1	-	-	1	-	-
.0000M	8	1	6	2	2	2	2	-	-	-	-	1
.0000M	8	2	6	1	2	2	2	-	-	-	1	-

Table 15c 2 methyl propene 3^1A_2

(coefficient)^2	$4a_1$-$7a_1$	$8a_1$	$2b_2$-$4b_2$	$5b_2$	$1a_2$	$1b_1$	$2b_1$	$6b_2$	$7b_2$	$8b_2$	$3b_1$	$2a_2$
.0000M	8	2	6	2	2	2	1	1	-	-	-	-
.0001M	8	2	6	2	2	2	1	-	1	-	-	-
.0000M	8	2	6	2	2	2	1	-	-	1	-	-
.0000M	8	1	6	2	2	2	2	-	-	-	-	1
.8765M	8	2	6	1	2	2	2	-	-	-	1	-

Tables 16a-e n $^1B_1$ States

Table 16a 2 methyl propene 1^1B_1 $^1(\pi, 3s)$

(coefficient)^2	$4a_1$-$7a_1$	$8a_1$	$2b_2$-$4b_2$	$5b_2$	$1a_2$	$1b_1$	$2b_1$	$9a_1$	$10a_1$	$11a_1$	$12a_1$	$13a_1$	$3b_1$	$2a_2$
.8418M	8	2	6	2	2	2	1	1	-	-	-	-	-	-
.0021M	8	2	6	2	2	2	1	-	1	-	-	-	-	-
.0027M	8	2	6	2	2	2	1	-	-	1	-	-	-	-
.0000M	8	2	6	2	2	2	1	-	-	-	1	-	-	-
.0694M	8	2	6	2	2	2	1	-	-	-	-	1	-	-
.0001M	8	1	6	2	2	2	2	-	-	-	-	-	1	-
.0000M	8	2	6	1	2	2	2	-	-	-	-	-	-	1

Table 16b 2 methyl propene 2^1B_1 $^1(\pi, 3pz)$

(coefficient)^2	$4a_1$-$7a_1$	$8a_1$	$2b_2$-$4b_2$	$5b_2$	$1a_2$	$1b_1$	$2b_1$	$9a_1$	$10a_1$	$11a_1$	$12a_1$	$13a_1$	$3b_1$	$3a_2$
.0035M	8	2	6	2	2	2	1	1	-	-	-	-	-	-
.9020M	8	2	6	2	2	2	1	-	1	-	-	-	-	-
.0003M	8	2	6	2	2	2	1	-	-	1	-	-	-	-
.0002M	8	2	6	2	2	2	1	-	-	-	1	-	-	-
.0008M	8	2	6	2	2	2	1	-	-	-	-	1	-	-
.0000M	8	1	6	2	2	2	2	-	-	-	-	-	1	-
.0000M	8	2	6	1	2	2	2	-	-	-	-	-	-	1

Table 16c 2 methyl propene 3^1B_1 $^1(\pi, d\sigma)$

(coefficient)^2	$4a_1$-$7a_1$	$8a_1$	$2b_2$-$4b_2$	$5b_2$	$1a_2$	$1b_1$	$2b_1$	$9a_1$	$10a_1$	$11a_1$	$12a_1$	$13a_1$	$3b_1$	$3a_2$
.0033M	8	2	6	2	2	2	1	1	-	-	-	-	-	-
.0000M	8	2	6	2	2	2	1	-	1	-	-	-	-	-
.3495M	8	2	6	2	2	2	1	-	-	1	-	-	-	-
.5538M	8	2	6	2	2	2	1	-	-	-	1	-	-	-
.0054M	8	2	6	2	2	2	1	-	-	-	-	1	-	-
.0000M	8	1	6	2	2	2	2	-	-	-	-	-	1	-
.0000M	8	2	6	1	2	2	2	-	-	-	-	-	-	1

Table 16d 2 methyl propene 4^1B_1 $^1(\pi, 4s)$

(coefficient)^2	$4a_1$-$7a_1$	$8a_1$	$2b_2$-$4b_2$	$5b_2$	$1a_2$	$1b_1$	$2b_1$	$9a_1$	$10a_1$	$11a_1$	$12a_1$	$13a_1$	$3b_1$	$3a_2$
.0020M	8	2	6	2	2	2	1	1	-	-	-	-	-	-
.0008M	8	2	6	2	2	2	1	-	1	-	-	-	-	-
.5562M	8	2	6	2	2	2	1	-	-	1	-	-	-	-
.3535M	8	2	6	2	2	2	1	-	-	-	1	-	-	-
.0007M	8	2	6	2	2	2	1	-	-	-	-	1	-	-
.0000M	8	1	6	2	2	2	2	-	-	-	-	-	1	-
.0000M	8	2	6	1	2	2	2	-	-	-	-	-	-	1

Table 16e 2 methyl propene 5^1B_1

(coefficient)^2	$4a_1$-$7a_1$	$8a_1$	$2b_2$-$4b_2$	$5b_2$	$1a_2$	$1b_1$	$2b_2$	$9a_1$	$10a_1$	$11a_1$	$12a_1$	$13a_1$	$3b_1$	$3a_2$
.06555M	8	2	6	2	2	2	1	1	-	-	-	-	-	-
.0017M	8	2	6	2	2	2	1	-	1	-	-	-	-	-
.0076M	8	2	6	2	2	2	1	-	-	1	-	-	-	-
.0020M	8	2	6	2	2	2	1	-	-	-	1	-	-	-
.8329M	8	2	6	2	2	2	1	-	-	-	-	1	-	-
.0000M	8	1	6	2	2	2	2	-	-	-	-	-	1	-
.0000M	8	2	6	1	2	2	2	-	-	-	-	-	-	1

Tables 17 a,b n^1B_2 States

Table 17a 2 methyl propene 1^1B_2 $^1(\pi, 3dxy)$

(coefficient)^2	$4a_1$-$7a_1$	$8a_1$	$2b_2$-$4b_2$	$5b_2$	$1a_2$	$1b_1$	$2b_1$	$2a_2$	$3a_2$	$6b_2$	$9a_1$
.9170M	8	2	6	2	2	2	1	1	-	-	-
.0001M	8	2	6	2	2	2	1	-	1	-	-
.0000M	8	1	6	2	2	2	2	-	-	1	-
.0000M	8	2	6	1	2	2	2	-	-	-	1

Table 17b 2 methyl propene 2^1B_2

(coefficient)^2	$4a_1$-$7a_1$	$8a_1$	$2b_2$-$4b_2$	$5b_2$	$1a_2$	$1b_1$	$2b_1$	$2a_2$	$3a_2$	$6b_2$	$9a_1$
.0000M	8	2	6	2	2	2	1	1	-	-	-
.0000M	8	2	6	2	2	2	1	-	1	-	-
.0000M	8	1	6	2	2	2	2	-	-	1	-
.8788M	8	2	6	1	2	2	2	-	-	-	1

Tables 18 a-c n^3A_1

Table 18a 2 methyl propene 1^3A_1 $^3(\pi, \pi^*)$

$(\text{coefficient})^2$	$4a_1$-$7a_1$	$8a_1$	$2b_2$-$4b_2$	$5b_2$	$1a_2$	$1b_1$	$2b_1$	$3b_1$	$4b_1$	$5b_1$	$9a_1$	$6b_2$
.0834M	8	2	6	2	2	2	1	1	-	-	-	-
.0021M	8	2	6	2	2	2	1	-	1	-	-	-
.8179M	8	2	6	2	2	2	1	-	-	1	-	-
.0000M	8	1	6	2	2	2	2	-	-	-	1	-
.0000M	8	2	6	1	2	2	2	-	-	-	-	1

Table 18b 2 methyl propene 2^3A_1 $^3(\pi, 3px)$

$(\text{coefficient})^2$	$4a_1$-$7a_1$	$8a_1$	$2b_2$-$4b_2$	$5b_2$	$1a_2$	$1b_1$	$2b_1$	$3b_1$	$4b_1$	$5b_1$	$9a_1$	$6b_2$
.8356M	8	2	6	2	2	2	1	1	-	-	-	-
.0018M	8	2	6	2	2	2	1	-	1	-	-	-
.0773M	8	2	6	2	2	2	1	-	-	1	-	-
.0000M	8	1	6	2	2	2	2	-	-	-	1	-
.0000M	8	2	6	1	2	2	2	-	-	-	-	1

Table 18c 2 methyl propene 3^3A_1 $^3(\pi, 3d\pi)$

$(\text{coefficient})^2$	$4a_1$-$7a_1$	$8a_1$	$2b_2$-$4b_2$	$5b_2$	$1a_2$	$1b_1$	$2b_1$	$3b_1$	$4b_1$	$5b_1$	$9a_1$	$6b_2$
.0009M	8	2	6	2	2	2	1	1	-	-	-	-
.9118M	8	2	6	2	2	2	1	-	1	-	-	-
.0036M	8	2	6	2	2	2	1	-	-	1	-	-
.0000M	8	1	6	2	2	2	2	-	-	-	1	-
.0000M	8	2	6	1	2	2	2	-	-	-	-	1

Table 19 2 methyl propene 1^3A_1 $^3(\pi, \pi^*)$

(coefficient)^2	$4a_1$-$8a_1$	$2b_2$-$5b_2$	$1a_2$	$1b_1$	$2b_1$	$3b_1$	$4b_1$	$5b_1$	$6b_1$	$9b_1$
.0323M	10	8	2	2	1	1	-	-	-	-
.0009M	10	8	2	2	1	-	1	-	-	-
.8646M	10	8	2	2	1	-	-	1	-	-
.0154M	10	8	2	2	1	-	-	-	1	-
.0273M	10	8	2	2	1	-	-	-	-	1
.0157M	10	8	2	1	2	-	-	1	-	-

Tables 20 a-c n^3A_2 States

Table 20a 2 methyl propene 1^3A_2 $^3(\pi, 3p_y)$

(coefficient)^2	$4a_1$-$7a_1$	$8a_1$	$2b_2$-$4b_2$	$5b_2$	$1a_2$	$1b_1$	$2b_1$	$6b_2$	$7b_2$	$8b_2$	$3b_1$	$2a_2$
.9140M	8	2	6	2	2	2	1	1	-	-	-	-
.0001M	8	2	6	2	2	2	1	-	1	-	-	-
.0010M	8	2	6	2	2	2	1	-	-	1	-	-
.0000M	8	1	6	2	2	2	2	-	-	-	-	1
.0000M	8	2	6	1	2	2	2	-	-	-	1	-

Table 20b 2 methyl propene 2^3A_2 $^3(\pi, 3d_{yz})$

(coefficient)^2	$4a_1$-$7a_1$	$8a_1$	$2b_2$-$4b_2$	$5b_2$	$1a_2$	$1b_1$	$2b_1$	$6b_2$	$7b_2$	$8b_2$	$3b_1$	$2a_2$
.0001M	8	2	6	2	2	2	1	1	-	-	-	-
.9082M	8	2	6	2	2	2	1	-	1	-	-	-
.0098M	8	2	6	2	2	2	1	-	-	1	-	-
.0000M	8	1	6	2	2	2	2	-	-	-	-	1
.0000M	8	2	6	1	2	2	2	-	-	-	1	-

Table 20c 2 methyl propene 3^3A_2

$(\text{coefficient})^2$	$4a_1$-$7a_1$	$8a_1$	$2b_2$-$4b_2$	$5b_2$	$1a_2$	$1b_1$	$2b_1$	$6b_2$	$7b_2$	$8b_2$	$3b_1$	$2a_2$
.0000M	8	2	6	2	2	2	1	1	-	-	-	-
.0000M	8	2	6	2	2	2	1	-	1	-	-	-
.0000M	8	2	6	2	2	2	1	-	-	1	-	-
.0000M	8	1	6	2	2	2	2	-	-	-	-	1
.8618M	8	2	6	1	2	2	2	-	-	-	1	-

Tables 21 a-c n^1B_1 States

Tables 21a 2 methyl propene 1^3B_1 $^3(\pi, 3s)$

$(\text{coefficient})^2$	$4a_1$-$7a_1$	$8a_1$	$2b_2$-$4b_2$	$5b_2$	$1a_2$	$1b_1$	$2b_1$	$9a_1$	$10a_1$	$11a_1$	$12a_1$	$13a_1$	$3b_1$	$3a_2$
.8283M	8	2	6	2	2	2	1	1	-	-	-	-	-	-
.0013M	8	2	6	2	2	2	1	-	1	-	-	-	-	-
.0045M	8	2	6	2	2	2	1	-	-	1	-	-	-	-
.0001M	8	2	6	2	2	2	1	-	-	-	1	-	-	-
.0861M	8	2	6	2	2	2	1	-	-	-	-	1	-	-
.0001M	8	1	6	2	2	2	2	-	-	-	-	-	1	-
.0000M	8	2	6	1	2	2	2	-	-	-	-	-	-	1

Table 21b 2 methyl propene 2^3B_1 $^3(\pi, 3p_z)$

$(\text{coefficient})^2$	$4a_1$-$7a_1$	$8a_1$	$2b_2$-$4b_2$	$5b_2$	$1a_2$	$1b_1$	$2b_1$	$9a_1$	$10a_1$	$11a_1$	$12a_1$	$13a_1$	$3b_1$	$3b_2$
.0024M	8	2	6	2	2	2	1	1	-	-	-	-	-	-
.9046M	8	2	6	2	2	2	1	-	1	-	-	-	-	-
.0003M	8	2	6	2	2	2	1	-	-	1	-	-	-	-
.0002M	8	2	6	2	2	2	1	-	-	-	1	-	-	-
.0008M	8	2	6	2	2	2	1	-	-	-	-	1	-	-
.0000M	8	1	6	2	2	2	2	-	-	-	-	-	1	-
.0000M	8	2	6	1	2	2	2	-	-	-	-	-	-	1

Table 21c 2 methyl propene 3^3B_1 $^3(\pi, 3d\sigma+4s)$

(coefficient)^2	$4a_1$-$7a_1$	$8a_1$	$2b_2$-$4b_2$	$5b_2$	$1a_2$	$1b_1$	$2b_1$	$9a_1$	$10a_1$	$11a_1$	$12a_1$	$13a_1$	$3b_1$	$3b_2$
.0071M	8	2	6	2	2	2	1	1	-	-	-	-	-	-
.0001M	8	2	6	2	2	2	1	-	1	-	-	-	-	-
.4591M	8	2	6	2	2	2	1	-	-	1	-	-	-	-
.4359M	8	2	6	2	2	2	1	-	-	-	1	-	-	-
.0088M	8	2	6	2	2	2	1	-	-	-	-	1	-	-
.0000M	8	1	6	2	2	2	2	-	-	-	-	-	1	-
.0000M	8	2	6	1	2	2	2	-	-	-	-	-	-	1

Table 21d 2 methyl propene 4^3B_1 $^3(\pi, 3d\sigma+4s)$

(coefficient)^2	$4a_1$-$7a_1$	$8a_1$	$2b_2$-$4b_2$	$5b_2$	$1a_2$	$1b_1$	$2b_1$	$9a_1$	$10a_1$	$11a_1$	$12a_1$	$13a_1$	$3b_1$	$3b_2$
.0023M	8	2	6	2	2	2	1	1	-	-	-	-	-	-
.0007M	8	2	6	2	2	2	1	-	1	-	-	-	-	-
.4279M	8	2	6	2	2	2	1	-	-	1	-	-	-	-
.4849M	8	2	6	2	2	2	1	-	-	-	1	-	-	-
.0005M	8	2	6	2	2	2	1	-	-	-	-	1	-	-
.0000M	8	1	6	2	2	2	2	-	-	-	-	-	1	-
.0000M	8	2	6	1	2	2	2	-	-	-	-	-	-	1

Table 21e 2 methyl propene 5^3B_1

(coefficient)^2	$4a_1$-$7a_1$	$8a_1$	$2b_2$-$4b_2$	$5b_2$	$1a_2$	$1b_1$	$2b_1$	$9a_1$	$10a_1$	$11a_1$	$12a_1$	$13a_1$	$3b_1$	$3b_2$
.0795M	8	2	6	2	2	2	1	1	-	-	-	-	-	-
.0014M	8	2	6	2	2	2	1	-	1	-	-	-	-	-
.0127M	8	2	6	2	2	2	1	-	-	1	-	-	-	-
.0031M	8	2	6	2	2	2	1	-	-	-	1	-	-	-
.8173M	8	2	6	2	2	2	1	-	-	-	-	1	-	-
.0000M	8	1	6	2	2	2	2	-	-	-	-	-	1	-
.0000M	8	2	6	1	2	2	2	-	-	-	-	-	-	1

Table 22 a,b n^3B_2 States

Table 22a 2 methyl propene 1^3B_2 $^3(\pi, 3dxy)$

(coefficient)^2	$4a_1$-$7a_1$	$8a_1$	$2b_2$-$4b_2$	$5b_2$	$1a_2$	$1b_1$	$2b_1$	$2a_2$	$3a_2$	$6b_2$	$9a_1$
.9207M	8	2	6	2	2	2	1	1	-	-	-
.0001M	8	2	6	2	2	2	1	-	1	-	-
.0000M	8	1	6	2	2	2	2	-	-	1	-
.0000M	8	2	6	1	2	2	2	-	-	-	1

Table 22b 2 methyl propene 2^3B_2

(coefficient)^2	$4a_1$-$7a_1$	$8a_1$	$2b_2$-$4b_2$	$5b_2$	$1a_2$	$1b_1$	$2b_1$	$2a_2$	$3a_2$	$6b_2$	$9a_1$
.0000M	8	2	6	2	2	2	1	1	-	-	-
.0000M	8	2	6	2	2	2	1	-	1	-	-
.0000M	8	1	6	2	2	2	2	-	-	1	-
.8759M	8	2	6	1	2	2	2	-	-	-	1

Table 23 Cis But-2-ene Previous Spectroscopic Assisgnments

Excitation Process	Excited State	Ref.[8]	Ref.[18]	UV
$\pi \rightarrow \pi^*$	T	4.3	4.3	-
$\pi \rightarrow 3s$	T_R	-	-	5.0 [10]
$\pi \rightarrow 3s$	R	6.1	6.1	6.03[16]
$\pi \rightarrow \pi^*$	V	7.0	7.2	7.10[16]
ionisation				9.13[12]

Table 24 Cis But-2-ene

State	No. of main Configurations	Σ coeff^2	Correction (a.u.)	CI/a.u.	Excitation Energy/eV	Table No.
G.S.	3M1R	.9362	-.0124	-156.2726	-	26
1^1A_1	3M3R	.9176	-.0177	-156.0112	7.11	27a
2^1A_1	3M3R	.9196	-.0172	-155.9827	7.89	27b
3^1A_1	3M3R	.9074	-.0207	-155.8700	10.95	27c
1^1A_2	3M3R	.9132	-.0188	-156.0101	7.14	28a
2^1A_2	3M3R	.9137	-.0187	-155.9850	7.82	28b
3^1A_2	3M3R	.8967	-.0283	-155.8470	11.58	28c
1^1B_1	5M5R	.9190	-.0174	-156.0310	6.57	29a
2^1B_1	5M5R	.9070	-.0203	-156.0154	6.96	29b
3^1B_1	5M5R	.9128	-.0188	-155.9871	7.77	29c
4^1B_1	5M5R	.9173	-.0177	-155.9834	7.87	29d
5^1B_1	5M5R	.9137	-.0187	-155.9253	9.49	29e
1^1B_2	2M2R	.9158	-.0181	-155.9839	7.85	30a
2^1B_2	2M2R	.9078	-.0204	-155.9444	8.93	30b
1^3A_1	3M3R	.9222	-.0170	-156.0167	6.96	31a
2^3A_1	3M3R	.9243	-.0166	-155.9879	7.75	31b
3^3A_1	3M3R	.8973	-.0230	-155.8881	10.46	31c
1^3A_2	3M3R	.9165	-.0187	-156.0168	6.96	32a
2^3A_2	3M3R	.9160	-.0186	-155.9909	7.66	32b
3^3A_2	3M3R	.8729	-.0289	-155.8610	11.20	32c
1^3B_1	5M5R	.9238	-.0167	-156.0382	6.38	33a
2^3B_1	5M5R	.9090	-.0204	-156.0220	6.82	33b
3^3B_1	5M5R	.9137	-.0191	-155.9943	7.57	33c
4^3B_1	5M5R	.9217	-.0174	-155.9908	7.67	33d
5^3B_1	5M5R	.9169	-.0182	-155.9364	9.15	33e
1^3B_2	3M2R	.9100	-.0194	-156.1088	4.46	34a
2^3B_2	3M2R	.9248	-.0167	-155.9913	7.65	34b
1^3B_2	4M1R	.9558	-.0086	-156.1043	4.58	35

Cis-but-2-ene

Table 25

State	Transition	Singlet	Triplet
$1B_1$	$\pi \rightarrow 3s$	6.57	6.38
$2B_1$	$\pi \rightarrow 3p_z$	6.96	6.82
$1A_1$	$\pi \rightarrow 3p_x$	7.11	6.96
$1A_2$	$\pi \rightarrow 3p_y$	7.14	6.96
$3B_1$	$\pi \rightarrow 3d\sigma$	7.77	7.57
$2A_2$	$\pi \rightarrow 3d_{yz}$	7.82	7.66
$1B_2$	$\pi \rightarrow \pi^*$	7.85	4.46
$4B_1$	$\pi \rightarrow 4s$	7.87	7.67
2^1A_1	$\pi \rightarrow 3dxz$	7.89	7.75
$2B_2$	$\pi \rightarrow nd\pi$	8.93	7.65

Table 26 Cis But-2-ene Ground State X^1A_1

$(\text{coefficient})^2$	$3a_1$-$7a_1$	$1a_2$	$1b_1$	$3b_2$-$6b_2$	$2b_1$	$3a_2$	$6a_2$
.9174M	10	2	2	8	2	-	-
.0146M	10	2	2	8	-	2	-
.0042M	10	2	2	8	-	1	1
.0021	10	2	1	8	1	2	-

Tables 27 a-c n^1A_1 States

Table 27a Cis But-2-ene 1^1A_1 $^1(\pi, 3p_x)$

(coefficient)^2	$3a_1$-$7a_1$	$1a_2$	$1b_1$	$3b_2$-$6b_2$	$2b_1$	$3b_1$	$4b_1$	$5b_1$	$3a_2$
.9084M	10	2	2	8	1	1	-	-	-
.0065M	10	2	2	8	1	-	1	-	-
.0026M	10	2	2	8	1	-	-	1	-

Table 27b Cis But-2-ene 2^1A_1 $^1(\pi, 3dxz)$

(coefficient)^2	$3a_1$-$7a_1$	$1a_2$	ab_1	$3b_2$-$6b_2$	$2b_1$	$3b_1$	$4b_1$	$5b_1$	$3a_2$
.0063M	10	2	2	8	1	1	-	-	-
.9107M	10	2	2	8	1	-	1	-	-
.0026M	10	2	2	8	1	-	-	1	-

Table 27c Cis But-2-ene 3^1A_1

(coefficient)^2	$3a_1$-$7a_1$	$1a_2$	$1b_1$	$3b_2$-$6b_2$	$2b_1$	$3b_1$	$4b_1$	$5b_1$	$3a_2$
.0030M	10	2	2	8	1	1	-	-	-
.0021M	10	2	2	8	1	-	1	-	-
.9024M	10	2	2	8	1	-	-	1	-
.0066	10	1	2	8	1	-	-	1	1

Tables 28 a-c n^1A_2 States

Table 28a Cis But-2-ene 1^1A_2 $^1(\pi, 3p_y)$

$(coefficient)^2$	$3a_1$-$7a_1$	$1a_2$	$1b_1$	$3b_2$-$6b_2$	$2b_1$	$7b_2$	$8b_2$	$9b_2$	$3a_2$	$12a_1$
.8919M	10	2	2	8	1	1	-	-	-	-
.0095M	10	2	2	8	1	-	1	-	-	-
.0117M	10	2	2	8	1	-	-	1	-	-

Table 28b Cis But-2-ene 2^1A_2 $^1(\pi, 3dyz)$

$(coefficient)^2$	$3a_1$-$7a_1$	$1a_2$	$1b_1$	$3b_2$-$6b_2$	$2b_1$	$7b_2$	$8b_2$	$9b_2$	$3a_2$	$12a_1$
.0114M	10	2	2	8	1	1	-	-	-	-
.8961M	10	2	2	8	1	-	1	-	-	-
.0062M	10	2	2	8	1	-	-	1	-	-
.0051	10	1	2	8	1	-	1	-	1	

Table 28c Cis But-2-ene 3^1A_2

$(coefficient)^2$	$3a_1$-$7a_1$	$1a_2$	$1b_1$	$3b_2$-$6b_2$	$2b_1$	$7b_2$	$8b_2$	$9b_2$	$3a_2$	$12a_1$
.0108M	10	2	2	8	1	1	-	-	-	-
.0085M	10	2	2	8	1	-	1	-	-	-
.8774M	10	2	2	8	1	-	-	1	-	-
.0061	10	2	2	8	-	-	-	-	1	1
.0076	10	1	2	8	1	-	-	1	1	-

Tables a-e n^1B_1 States

Table 29a Cis But-2-ene 1^1B_1 $^1(\pi, 3s)$

(coefficient)^2	$3a_1$-$7a_1$	$1a_2$	$1b_1$	$3b_2$-$5b_2$	$6b_2$	$2b_1$	$8a_1$	$9a_1$	$10a_1$	$11a_1$	$12a_1$	$13a_1$	$14a_1$
.8384M	10	2	2	6	2	1	1	-	-	-	-	-	-
.0081M	10	2	2	6	2	1	-	1	-	-	-	-	-
.0018M	10	2	2	6	2	1	-	-	1	-	-	-	-
.0025M	10	2	2	6	2	1	-	-	-	1	-	-	-
.0682M	10	2	2	6	2	1	-	-	-	-	1	-	-

Table 29b Cis But-2-ene 2^1B_1 $^1(\pi, 3p_z)$

(coefficient)^2	$3a_1$-$7a_1$	$1a_2$	$1b_1$	$3b_2$-$5b_2$	$6b_2$	$2b_1$	$8a_1$	$9a_1$	$10a_1$	$11a_1$	$12a_1$	$13a_1$	$14a_1$
.0081M	10	2	2	6	2	1	1	-	-	-	-	-	-
.8975M	10	2	2	6	2	1	-	1	-	-	-	-	-
.0000M	10	2	2	6	2	1	-	-	1	-	-	-	-
.0009M	10	2	2	6	2	1	-	-	-	1	-	-	-
.0005M	10	2	2	6	2	1	-	-	-	-	1	-	-
.0071M	10	2	2	6	2	1	-	-	-	-	-	1	-

Table 29c Cis But-2-ene 3^1B_1 $^1(\pi, 3d\sigma)$

(coefficient)^2	$3a_1$-$7a_1$	$1a_2$	$1b_1$	$3b_2$-$5b_2$	$6b_2$	$2b_1$	$8a_1$	$9a_1$	$10a_1$	$11a_1$	$12a_1$	$13a_1$	$14a_1$
.0040M	10	2	2	6	2	1	1	-	-	-	-	-	-
.0001M	10	2	2	6	2	1	-	1	-	-	-	-	-
.8938M	10	2	2	6	2	1	-	-	1	-	-	-	-
.0111M	10	2	2	6	2	1	-	-	-	1	-	-	-
.0038M	10	2	2	6	2	1	-	-	-	-	1	-	-
.0051	10	2	2	6	2	1	-	-	-	-	-	-	1

Table 29d Cis But-2-ene 4^1B_1 $^1(\pi, 4s)$

(coefficient)^2	$3a_1$-$7a_1$	$1a_2$	$1b_1$	$3b_2$-$5b_2$	$6b_2$	$2b_1$	$8a_1$	$9a_1$	$10a_1$	$11a_1$	$12a_1$	$13a_1$	$14a_1$
.0034M	10	2	2	6	2	1	1	-	-	-	-	-	-
.0011M	10	2	2	6	2	1	-	1	-	-	-	-	-
.0089M	10	2	2	6	2	1	-	-	1	-	-	-	-
.9013M	10	2	2	6	2	1	-	-	-	1	-	-	-
.0026M	10	2	2	6	2	1	-	-	-	-	1	-	-

Table 29e Cis But-2-ene 5^1B_1

(coefficient)^2	$3a_1$-$7a_1$	$1a_2$	$1b_1$	$3b_2$-$5b_2$	$6b_2$	$2b_1$	$8a_1$	$9a_1$	$10a_1$	$11a_1$	$12a_1$	$13a_1$	$14a_1$
.0660M	10	2	2	6	2	1	1	-	-	-	-	-	-
.0000M	10	2	2	6	2	1	-	1	-	-	-	-	-
.0048M	10	2	2	6	2	1	-	-	1	-	-	-	-
.0051M	10	2	2	6	2	1	-	-	-	1	-	-	-
.8378M	10	2	2	6	2	1	-	-	-	-	1	-	-

Tables 30 a,b n^1B_2 States

Table 30a Cis But-2-ene 1^1B_2 $^1(\pi, 3d\pi)$

$(coefficient)^2$	$3a_1$-$7a_1$	$1a_2$	$1b_1$	$3b_2$-$6b_2$	$2b_1$	$2a_2$	$3a_2$
.9147M	10	2	2	8	1	1	-
.0011M	10	2	2	8	1	-	1

Table 30b Cis But-2-ene 2^1B_2 $^1(\pi, \pi^*)$

$(coefficient)^2$	$3a_1$-$7a_1$	$1a_2$	$1b_1$	$3b_2$-$6b_2$	$2b_1$	$2a_2$	$3a_2$
.0011M	10	2	2	8	1	1	-
.9066M	10	2	2	8	1	-	1

Tables 31 a-c n^3A_1 States

Table 31a Cis But-2-ene 1^3A_1 $^3(\pi, 3p_x)$

$(coefficient)^2$	$3a_1$-$7a_1$	$1a_2$	$1b_1$	$3b_2$-$6b_2$	$2b_1$	$3b_1$	$4b_1$	$5b_1$	$3a_2$	$4a_2$
.9161M	10	2	2	8	1	1	-	-	-	-
.0039M	10	2	2	8	1	-	1	-	-	-
.0024M	10	2	2	8	1	-	-	1	-	-

Table 31b Cis But-2-ene 2^3A_1 $^3(\pi, 3dxz)$

$(coefficient)^2$	$3a_1$-$7a_1$	$1a_2$	$1b_1$	$3b_2$-$6b_2$	$2b_1$	$3b_1$	$4b_1$	$5b_1$	$3a_2$	$4a_2$
.0035M	10	2	2	8	1	1	-	-	-	-
.9183M	10	2	2	8	1	-	1	-	-	-
.0025M	10	2	2	8	1	-	-	1	-	-

Table 31c Cis But-2-ene 3^3A_1

$(coefficient)^2$	$3a_1$-$7a_1$	$1a_2$	$1b_1$	$3a_1$-$6b_2$	$2b_1$	$3b_1$	$4b_1$	$5b_1$	$3a_2$	$4a_2$
.0029M	10	2	2	8	1	1	-	-	-	-
.0020M	10	2	2	8	1	-	1	-	-	-
.8925M	10	2	2	8	1	-	-	1	-	-
.0062	10	1	2	8	2	-	-	-	1	-
.0099	10	1	2	8	2	-	-	-	-	1
.0054	10	1	2	8	1	-	-	1	1	-

Tables 32 a-c n^3A_2 States

Table 32a Cis But-2-ene 1^3A_2 $^3(\pi, 3p_y)$

$(coefficient)^2$	$3a_1$-$7a_1$	$1a_2$	$1b_1$	$3b_2$-$6b_2$	$2b_1$	$7b_2$	$8b_2$	$9b_2$	$10b_2$	$3a_2$	$12a_1$
.8946M	10	2	2	8	1	1	-	-	-	-	-
.0091M	10	2	2	8	1	-	1	-	-	-	-
.0128M	10	2	2	8	1	-	-	1	-	-	-

Table 32b Cis But-2-ene 2^3A_2 $^3(\pi, 3d_{yz})$

(coefficient)^2	$3a_1$-$7a_1$	$1a_2$	$1b_1$	$3b_2$-$6b_2$	$2b_1$	$7b_2$	$8b_2$	$9b_2$	$10b_2$	$3a_2$	$12a_1$
.0110M	10	2	2	8	1	1	-	-	-	-	-
.8971M	10	2	2	8	1	-	1	-	-	-	-
.0079M	10	2	2	8	1	-	-	1	-	-	-
.0066	10	2	2	8	1	-	-	-	1	-	-
.0052	10	1	2	8	1	-	1	-	-	1	-

Table 32c Cis But-2-ene 3^3A_2

(coefficient)^2	$3a_1$-$7a_1$	$1a_2$	$1b_1$	$3b_2$-$6b_2$	$2b_1$	$7b_2$	$8b_2$	$9b_2$	$10b_2$	$3a_2$	$12a_1$
.0114M	10	2	2	8	1	1	-	-	-	-	-
.0113M	10	2	2	8	1	-	1	-	-	-	-
.8502M	10	2	2	8	1	-	-	1	-	-	-
.0062	10	2	1	8	2	-	-	1	-	-	-
.0115	10	1	2	8	2	-	-	-	-	-	1
.0061	10	1	2	8	1	-	-	1	-	1	-

Tables 33a-e n^3B_1 States

Table 33a Cis But-2-ene 1^3B_1 $^3(\pi, 3s)$

(coefficient)^2	$3a_1$-$7a_1$	$1a_2$	$1b_1$	$3b_2$-$5b_2$	$6b_2$	$2b_1$	$8a_1$	$9a_1$	$10a_1$	$11a_1$	$12a_1$	$13a_1$	$14a_1$
.8223M	10	2	2	6	2	1	1	-	-	-	-	-	-
.0115M	10	2	2	6	2	1	-	1	-	-	-	-	-
.0032M	10	2	2	6	2	1	-	-	1	-	-	-	-
.0026M	10	2	2	6	2	1	-	-	-	1	-	-	-
.0840M	10	2	2	6	2	1	-	-	-	-	1	-	-

Table 33b Cis But-2-ene 2^3B_1 $^3(\pi, 3p_z)$

(coefficient)^2	$3a_1$-$7a_1$	$1a_2$	$1b_1$	$3b_2$-$5b_2$	$6b_2$	$2b_1$	$8a_1$	$9a_1$	$10a_1$	$11a_1$	$12a_1$	$13a_1$	$14a_1$
.0116M	10	2	2	6	2	1	1	-	-	-	-	-	-
.8962M	10	2	2	6	2	1	-	1	-	-	-	-	-
.0000M	10	2	2	6	2	1	-	-	1	-	-	-	-
.0005M	10	2	2	6	2	1	-	-	-	1	-	-	-
.0008M	10	2	2	6	2	1	-	-	-	-	1	-	-
.0084	10	2	2	6	2	1	-	-	-	-	-	1	-
.0052	10	2	2	6	2	1	-	-	-	-	-	-	1

Table 33c Cis But-2-ene 3^3B_1 $^3(\pi, 3d\sigma)$

(coefficient)^2	$3a_1$-$7a_1$	$1a_2$	$1b_1$	$3b_2$-$5b_2$	$6b_2$	$2b_1$	$8a_1$	$9a_1$	$10a_1$	$11a_1$	$12a_1$	$13a_1$	$14a_1$
.0078M	10	2	2	6	2	1	1	-	-	-	-	-	-
.0002M	10	2	2	6	2	1	-	1	-	-	-	-	-
.8864M	10	2	2	6	2	1	-	-	1	-	-	-	-
.0121M	10	2	2	6	2	1	-	-	-	1	-	-	-
.0073M	10	2	2	6	2	1	-	-	-	-	1	-	-
.0080M	10	2	2	6	2	1	-	-	-	-	-	-	1

Table 33d Cis But-2-ene 4^3B_1 $^3(\pi, 4s)$

(coefficient)^2	$3a_1$-$7a_1$	$1a_2$	$1b_1$	$3b_2$-$5b_2$	$6b_2$	$2b_1$	$8a_1$	$9a_1$	$10a_1$	$11a_1$	$12a_1$	$13a_1$	$14a_1$
.0034M	10	2	2	6	2	1	1	-	-	-	-	-	-
.0007M	10	2	2	6	2	1	-	1	-	-	-	-	-
.0164M	10	2	2	6	2	1	-	-	1	-	-	-	-
.8987M	10	2	2	6	2	1	-	-	-	1	-	-	-
.0025	10	2	2	6	2	1	-	-	-	-	1	-	-

Table 33e Cis But-2-ene 5^3B_1

(coefficient)^2	$3a_1$-$7a_1$	$1a_2$	$1b_1$	$3b_2$-$5b_2$	$6b_2$	$2b_1$	$8a_1$	$9a_1$	$10a_1$	$11a_1$	$12a_1$	$13a_1$	$14a_1$
.0791M	10	2	2	6	2	1	1	-	-	-	-	-	-
.0001M	10	2	2	6	2	1	-	1	-	-	-	-	-
.0106M	10	2	2	6	2	1	-	-	1	-	-	-	-
.0060M	10	2	2	6	2	1	-	-	-	1	-	-	-
.8211M	10	2	2	6	2	1	-	-	-	-	1	-	-

Tables 34 a,b n^3B_2 States

Table 34a Cis But-2-ene 1^3B_2 $^3(\pi, \pi^*)$

(coefficient)^2	$3a_1$-$7a_1$	$1a_2$	$1b_1$	$3b_2$-$6b_2$	$2b_1$	$2a_2$	$3a_2$	$4a_2$	$5a_2$	$6a_2$
.0011M	10	2	2	8	1	1	-	-	-	-
.9037M	10	2	2	8	1	-	1	-	-	-
.0053M	10	2	2	8	1	-	-	1	-	-
.0047	10	2	2	8	1	-	-	-	1	-
.0267	10	2	2	8	1	-	-	-	-	1
.0177	10	2	1	8	2	-	-	1	-	-

Table 34b Cis But-2-ene 2^3B_2 $^3(\pi, 3d\pi)$

(coefficient)^2	$3a_1$-$7a_1$	$1a_2$	$1b_1$	$3b_2$-$6b_2$	$2b_1$	$2a_2$	$3a_2$	$4a_2$	$5a_2$	$6a_2$
.9194M	10	2	2	8	1	1	-	-	-	-
.0012M	10	2	2	8	1	-	1	-	-	-
.0042M	10	2	2	8	1	-	-	1	-	-

Table 35 Cis But-2-ene 1^3B_2 $^3(\pi,\pi^*)$

(coefficient)^2	$3a_1$-$7a_1$	$1a_2$	$1b_1$	$3b_2$-$6b_2$	$2b_1$	$3a_2$	$4a_2$	$6a_2$
.9012M	10	2	2	8	1	1	-	-
.0209M	10	2	1	8	2	1	-	-
.0055M	10	2	2	8	1	-	1	-
.0281M	10	2	2	8	1	-	-	1

Table 36 Previous Spectroscopic Assignments for Trans But-2-ene

Excitation Process	Excited State	Ref. [8]	Ref. [19]	U.V.
$\pi\rightarrow\pi^*$	T	4.4	4.3	4.1 [10]
$\pi\rightarrow 3s$	T_R	-	-	5.0 [10]
$\pi\rightarrow 3s$	R	6.0	-	6.09[16]
$\pi\rightarrow\pi^*$	V	7.1	6.8	6.97[16]
ionisation	-	-	-	9.13[12]

Table 37 Trans But-2-ene

State	No. of Main Configurations	$\Sigma coeff^2$	Correction (a.u.)	CI/a.u.	Excitation energy/eV	Table No.
GS	3M1R	.9359	-.0127	-156.2825	-	39
1^1Ag	4M3R	.9163	-.0187	-156.0261	6.98	40a
2^1Ag	4M3R	.8800	-.0802	-155.9352	9.45	40b
3^1Ag	4M3R	.8925	-.0256	-155.8540	11.66	40c
1^1Au	5M5R	.9161	-.0191	-156.0478	6.39	41a
2^1Au	5M5R	.9107	-.0204	-156.0077	7.48	41b
3^1Au	5M5R	.9138	-.0198	-156.0045	7.56	41c
4^1Au	5M5R	.9147	-.0186	-155.9908	7.94	41d
5^1Au	5M5R	.9127	-.0198	-155.9369	9.41	41e
1^1Bg	5M3R	.9100	-.0203	-156.0343	6.75	42a
2^1Bg	5M3R	.9084	-.0209	-156.0269	6.95	42b
3^1Bg	5M3R	.9026	-.0222	-155.9016	10.36	42c
1^1Bu	4M3R	.9124	-.0194	-156.00	7.64	43a
2^1Bu	4M3R	.9142	-.0191	-155.9964	7.79	43b
3^1Bu	4M3R	.8825	-.0297	-155.9303	9.58	43c
1^3Ag	4M3R	.9235	-.0174	-156.0328	6.79	44a
2^3Ag	4M3R	.8788	-.0299	-155.9321	9.54	44b
3^3Ag	4M3R	.8424	-.0391	-155.8926	10.61	44c
1^3Au	5M5R	.9227	-.0176	-156.0491	6.35	45a
2^3Au	5M5R	.9134	-.0197	-156.0074	7.49	45b
3^3Au	5M5R	.9162	-.0193	-156.0048	7.56	45c
4^3Au	5M5R	.9186	-.0186	-156.0009	7.66	45d
5^3Au	5M5R	.9166	-.0190	-155.9468	9.13	45e
1^3Bg	5M3R	.9129	-.0201	-156.0406	6.58	46a
2^3Bg	5M3R	.9117	-.0207	-156.0332	6.78	46b
3^3Bg	5M3R	.9024	-.0221	-155.9017	10.36	46c
1^3Bu	5M3R	.9111	-.0194	-156.1184	4.47	47a
2^3Bu	5M3R	.9160	-.0192	-156.0055	7.54	47b
3^3Bu	5M3R	.9200	-.0184	-156.0027	7.61	47c

Table 38 Trans But-2-ene

State	Transition	Excitation Energy/eV Singlet	Triplet
1Au	$\pi \rightarrow 3s$	6.39	6.35
2Ag	$\pi \rightarrow 3p_z$	6.98	6.79
1Bg	$\pi \rightarrow 3p\|\|$	6.75	6.58
2Bg	$\pi \rightarrow 3p\perp$	6.95	6.78
2Au	$\pi \rightarrow 3dxy$ #	7.48	7.49
3Au	$\pi \rightarrow 3d\sigma$ #	7.56	7.56
1Bu	$\pi \rightarrow \pi^*$	7.64	4.47
2Bu	$\pi \rightarrow 3dxz+3dyz$	7.79	7.54
4Au	$\pi \rightarrow 4s$ #	7.94	7.66
3Bu	$\pi \rightarrow 3d\pi$	9.58	7.61

- These states are mixed

Table 39 Trans But-2-ene GS (X^1Ag)

(coefficient)^2	3ag-7ag	1au	2au	3bu-6bu	1bg	4bg	7bg
.9183M	10	2	2	8	2	-	-
.0135M	10	2	-	8	2	2	-
.0041M	10	2	-	8	2	1	1

Tables 40 a-c n^1Ag States

Table 40a Trans But-2-ene 1^1Ag $^1(\pi, 3p_z)$

$(coefficient)^2$	3ag-6ag	7ag	1au	3bu-6bu	1bg	2au	3au	4au	5au	8ag	12ag	4bg	5bg
.9117M	8	2	2	8	2	1	1	-	-	-	-	-	-
.0023M	8	2	2	8	2	1	-	1	-	-	-	-	-
.0022M	8	2	2	8	2	1	-	-	1	-	-	-	-
.0001M	8	1	2	8	2	2	-	-	-	1	-	-	-

Table 40b Trans But-2-ene 2^1Ag

$(coefficient)^2$	3ag-6ag	7ag	1au	3bu-6bu	1bg	2au	3au	4au	5au	8ag	12ag	4bg	5bg
.0001M	8	2	2	8	2	1	1	-	-	-	-	-	-
.0006M	8	2	2	8	2	1	-	1	-	-	-	-	-
.0001M	8	2	2	8	2	1	-	-	1	-	-	-	-
.8792M	8	1	2	8	2	2	-	-	-	1	-	-	-
.0076	8	1	2	8	2	2	-	-	-	-	1	-	-
.0106	8	1	2	8	2	-	-	-	-	1	-	2	-
.0059													

Table 40c Trans But-2-ene 3^1Ag

$(coefficient)^2$	3ag-6ag	7ag	1au	3bu-6bu	1bg	2au	3au	4au	5au	8ag	12ag	4bg	5bg
.0023M	8	2	2	8	2	1	1	-	-	-	-	-	-
.8896M	8	2	2	8	2	1	-	1	-	-	-	-	-
.0000M	8	2	2	8	2	1	-	-	1	-	-	-	-
.0006M	8	1	2	8	2	2	-	-	-	1	-	-	-
.0071	8	2	2	8	2	-	-	-	-	-	-	1	1
.0067	8	2	2	8	1	1	-	1	-	-	-	1	-

Table 41 a-e n^1Au

Table 41a Trans But-2-ene 1^1Au $^1(\pi, 3s)$

$(coefficient)^2$	3ag-7ag	1au	3bu-6bu	1bg	2au	8ag	9ag	10ag	11ag	12ag	13ag
.8566M	10	2	8	2	1	1	-	-	-	-	-
.0007M	10	2	8	2	1	-	1	-	-	-	-
.0038M	10	2	8	2	1	-	-	1	-	-	-
.0003M	10	2	8	2	1	-	-	-	1	-	-
.0546M	10	2	8	2	1	-	-	-	-	1	-

Table 41b Trans But-2-ene 2^1Au $^1(\pi, 3dxy)$

$(coefficient)^2$	3ag-7ag	1au	3bu-6bu	1bg	2au	8ag	9ag	10ag	11ag	12ag	13ag
.0017M	10	2	8	2	1	1	-	-	-	-	-
.9025M	10	2	8	2	1	-	1	-	-	-	-
.0009M	10	2	8	2	1	-	-	1	-	-	-
.0034M	10	2	8	2	1	-	-	-	1	-	-
.0022M	10	2	8	2	1	-	-	-	-	1	-
.0066	10	2	8	2	1	-	-	-	-	-	1

Table 41c Trans But-2-ene 3^1Au $^1(\pi, 3d\sigma)$

$(coefficient)^2$	3ag-7ag	1au	3bu-6bu	1bg	2au	8ag	9ag	10ag	11ag	12ag	13ag
.0073M	10	2	8	2	1	1	-	-	-	-	-
.0021M	10	2	8	2	1	-	1	-	-	-	-
.8797M	10	2	8	2	1	-	-	1	-	-	-
.0161M	10	2	8	2	1	-	-	-	1	-	-
.0086M	10	2	8	2	1	-	-	-	-	1	-

Table 41d Trans But-2-ene 4^1Au $^1(\pi, 4s)$

(coefficient)^2	3ag-7ag	1au	3bu-6bu	1bg	2au	8ag	9ag	10ag	11ag	12ag	13ag
.0002M	10	2	8	2	1	1	-	-	-	-	-
.0028M	10	2	8	2	1	-	1	-	-	-	-
.0187M	10	2	8	2	1	-	-	1	-	-	-
.8922M	10	2	8	2	1	-	-	-	1	-	-
.0086M	10	2	8	2	1	-	-	-	-	1	-

Table 41e Trans But-2-ene 5^1Au

(coefficient)^2	3ag-7ag	1au	3bu-6bu	1bg	2au	8ag	9ag	10ag	11ag	12ag	13ag
.0499M	10	2	8	2	1	1	-	-	-	-	-
.0023M	10	2	8	2	1	-	1	-	-	-	-
.0019M	10	2	8	2	1	-	-	1	-	-	-
.0027M	10	2	8	2	1	-	-	-	1	-	-
.8459M	10	2	8	2	1	-	-	-	-	1	-

Tables 42a-c n^1Bg

Table 42a Trans But-2-ene 1^1Bg $^1(\pi, 3p||)$

$(\text{coefficient})^2$	3ag-6ag	7ag	3bu-5bu	6bu	1au	1bg	2au	7bu	8bu	9bu	10bu	2bg	3au
.8950M	8	2	6	2	2	2	1	1	-	-	-	-	-
.0002M	8	2	6	2	2	2	1	-	1	-	-	-	-
.0148M	8	2	6	2	2	2	1	-	-	1	-	-	-
.0053	8	2	6	2	2	2	1	-	-	-	1	-	-
.0000M	8	1	6	2	2	2	2	-	-	-	-	1	-
.0000M	8	2	6	1	2	2	2	-	-	-	-	-	1

Table 42b Trans But-2-ene 2^1Bg $^1(\pi, 3p\perp)$

$(\text{coefficient})^2$	3ag-6ag	7ag	3bu-5bu	6bu	1au	1bg	2au	7bu	8bu	9bu	10bu	2bg	3au
.0007M	8	2	6	2	2	2	1	1	-	-	-	-	-
.8943M	8	2	6	2	2	2	1	-	1	-	-	-	-
.0134M	8	2	6	2	2	2	1	-	-	1	-	-	-
.0055	8	2	6	2	2	2	1	-	-	-	1	-	-
.0000M	8	1	6	2	2	2	2	-	-	-	-	1	-
.0000M	8	2	6	1	2	2	2	-	-	-	-	-	1

Table 42c Trans But-2-ene 3^1Bg

$(\text{coefficient})^2$	3ag-6ag	7ag	3bu-5bu	6bu	1au	1bg	2au	7bu	8bu	9bu	10bu	2bg	3au
.0156M	8	2	6	2	2	2	1	1	-	-	-	-	-
.0126M	8	2	6	2	2	2	1	-	1	-	-	-	-
.8744M	8	2	6	2	2	2	1	-	-	1	-	-	-
.0061	8	2	6	2	2	2	1	-	-	-	1	-	-
.0000M	8	1	6	2	2	2	2	-	-	-	-	1	-
.0000M	8	2	6	1	2	2	2	-	-	-	-	-	1

Tables 43 a-c n^1Bu

Table 43a Trans But-2-ene 1^1Bu $^1(\pi, 3d\pi)$

$(coefficient)^2$	3ag-6ag	7ag	3bu-5bu	6bu	lau	1bg	2au	2bg	3bg	7bu	4bg	8ag
.9093M	8	2	6	2	2	2	1	1	-	-	-	-
.0032M	8	2	6	2	2	2	1	-	1	-	-	-
.0000M	8	1	6	2	2	2	2	-	-	1	-	-
.0000M	8	2	6	1	2	2	2	-	-	-	-	1

Table 43b Trans But-2-ene 2^1Bu $^1(\pi, 3dxz+3dyz)$

$(coefficient)^2$	3ag-6ag	7ag	3bu-5bu	6bu	lau	1bg	2au	2bg	3bg	7bu	4bg	8ag
.0029M	8	2	6	2	2	2	1	1	-	-	-	-
.9113M	8	2	6	2	2	2	1	-	1	-	-	-
.0000M	8	1	6	2	2	2	2	-	-	1	-	-
.0000M	8	2	6	1	2	2	2	-	-	-	-	1

Table 43c Trans But-2-ene 3^1Bu $^1(\pi,\pi^*)$

$(coefficient)^2$	3ag-6ag	7ag	3bu-5bu	6bu	lau	1bg	2au	2bg	3bg	7bu	4bg	8ag
.0000M	8	2	6	2	2	2	1	1	-	-	-	-
.0000M	8	2	6	2	2	2	1	-	1	-	-	-
.8824M	8	1	6	2	2	2	2	-	-	1	-	-
.0001M	8	2	6	1	2	2	2	-	-	-	-	1
.0195	8	1	6	2	2	2	-	-	-	1	2	-

Tables 44a-c n^3Ag States

Table 44a Trans But-2-ene 1^3Ag $^3(\pi, 3p_z)$

$(coefficient)^2$	3ag-6ag	7ag	3bu-6bu	1au	1bg	2au	3au	4au	5au	8ag	12ag	4bg	5bg
.9175M	8	2	8	2	2	1	1	-	-	-	-	-	-
.0019M	8	2	8	2	2	1	-	1	-	-	-	-	-
.0041M	8	2	8	2	2	1	-	-	1	-	-	-	-
.0000M	8	1	8	2	2	2	-	-	-	1	-	-	-

Table 44b Trans But-2-ene 2^3Ag

$(coefficient)^2$	3ag-6ag	7ag	3bu-6bu	1au	1bg	2au	3au	4au	5au	8ag	12ag	4bg	5bg
.0000M	8	2	8	2	2	1	1	-	-	-	-	-	-
.0001M	8	2	8	2	2	1	-	1	-	-	-	-	-
.0000M	8	2	8	2	2	1	-	-	1	-	-	-	-
.8787M	8	1	8	2	2	2	-	-	-	1	-	-	-
.0113	8	1	8	2	2	2	-	-	-	-	1	-	-
.0113	8	1	8	2	2	-	-	-	-	1	-	2	-

Table 44c Trans But-2-ene 3^3Ag

$(coefficient)^2$	3ag-6ag	7ag	3bu-6bu	1au	1bg	2au	3au	4au	5au	8ag	12ag	4bg	5bg
.0022M	8	2	6	2	2	1	1	-	-	-	-	-	-
.8395M	8	2	6	2	2	1	-	1	-	-	-	-	-
.0004M	8	2	6	2	2	1	-	-	1	-	-	-	-
.0003M	8	1	8	2	2	2	-	-	-	1	-	-	-
.0214	8	2	8	2	1	2	-	-	-	-	-	-	1

Tables 45a-e n^3Au States

Table 45a Trans But-2-ene 1^3Au $^3(\pi, 3s)$

$(coefficient)^2$	3ag-7ag	lau	3bu-6bu	lbg	2au	8ag	9ag	10ag	llag	12ag	13ag	14ag
.8449M	10	2	8	2	1	1	-	-	-	-	-	-
.0017M	10	2	8	2	1	-	1	-	-	-	-	-
.0061M	10	2	8	2	1	-	-	1	-	-	-	-
.0006M	10	2	8	2	1	-	-	-	1	-	-	-
.0694M	10	2	8	2	1	-	-	-	-	1	-	-

Table 45b Trans But-2-ene 2^3Au $^3(\pi, 3dxy)$

$(coefficient)^2$	3ag-7ag	lau	3bu-6bu	$1b_{1g}$	2au	8ag	9ag	10ag	llag	12ag	13ag	14ag
.0057M	10	2	8	2	1	1	-	-	-	-	-	-
.8709M	10	2	8	2	1	-	1	-	-	-	-	-
.0107M	10	2	8	2	1	-	-	1	-	-	-	-
.0205M	10	2	8	2	1	-	-	-	1	-	-	-
.0057M	10	2	8	2	1	-	-	-	-	1	-	-
.0101	10	2	8	2	1	-	-	-	-	-	1	-

Table 45c Trans But-2-ene 3^3Au $^3(\pi, 3d\sigma)$

$(coefficient)^2$	3ag-7ag	lau	3bu-6bu	$1b_{1g}$	2au	8ag	9ag	10ag	llag	12ag	13ag	14ag
.0107M	10	2	8	2	1	1	-	-	-	-	-	-
.0238M	10	2	8	2	1	-	1	-	-	-	-	-
.7774M	10	2	8	2	1	-	-	1	-	-	-	-
.0943M	10	2	8	2	1	-	-	-	1	-	-	-
.0101M	10	2	8	2	1	-	-	-	-	1	-	-
.0060	10	2	8	2	1	-	-	-	-	-	-	1

Table 45d Trans But-2-ene $4\,^3Au$ $^3(\pi, 4s)$

(coefficient)^2	3ag-7ag	1au	3bu-6bu	$1b_{1g}$	2au	8ag	9ag	10ag	11ag	12ag	13ag	14ag
.0000M	10	2	8	2	1	1	-	-	-	-	-	-
.0094M	10	2	8	2	1	-	1	-	-	-	-	-
.1090M	10	2	8	2	1	-	-	1	-	-	-	-
.8000M	10	2	8	2	1	-	-	-	1	-	-	-
.0002M	10	2	8	2	1	-	-	-	-	1	-	-

Table 45e Trans But-2-ene $5\,^3Au$

(coefficient)^2	3ag-7ag	1au	3bu-6bu	$1b_{1g}$	2au	8ag	9ag	10ag	11ag	12ag	13ag	14ag
.0604M	10	2	8	2	1	1	-	-	-	-	-	-
.0052M	10	2	8	2	1	-	1	-	-	-	-	-
.0158M	10	2	8	2	1	-	-	1	-	-	-	-
.0046M	10	2	8	2	1	-	-	-	1	-	-	-
.8306M	10	2	8	2	1	-	-	-	-	1		

Tables 46 a-c n^3Bg States

Table 46a Trans But-2-ene 1^3Bg $^3(\pi, 3p||)$

$(coefficient)^2$	3ag-6ag	7ag	3bu-5bu	6bu	lau	lbg	2au	7bu	8bu	9bu	10bu	2bg	3au	12bu
.8981M	8	2	6	2	2	2	1	1	-	-	-	-	-	-
.0004M	8	2	6	2	2	2	1	-	1	-	-	-	-	-
.0144M	8	2	6	2	2	2	1	-	-	1	-	-	-	-
.0073	8	2	6	2	2	2	1	-	-	-	1	-	-	-
.0000M	8	1	6	2	2	2	2	-	-	-	-	1	-	-
.0000M	8	2	6	1	2	2	2	-	-	-	-	-	1	-

Table 46b Trans But-2-ene 2^3Bg $^3(\pi, 3p\underline{|})$

$(coefficient)^2$	3ag-6ag	7ag	3bu-5bu	6bu	lau	lbg	2au	7bu	8bu	9bu	10bu	2bg	3au	12bu
.0001M	8	2	6	2	2	2	1	1	-	-	-	-	-	-
.8973M	8	2	6	2	2	2	1	-	1	-	-	-	-	-
.0142M	8	2	6	2	2	2	1	-	-	1	-	-	-	-
.0067	8	2	6	2	2	2	1	-	-	-	1	-	-	-
.0000M	8	1	6	2	2	2	2	-	-	-	-	1	-	-
.0000M	8	2	6	1	2	2	2	-	-	-	-	-	1	-

Table 46c Trans But-2-ene 3^3Bg

$(coefficient)^2$	3ag-6ag	7ag	3bu-5bu	6bu	lau	lbg	2au	7bu	8bu	9bu	10bu	2bg	3au	12bu
.0168M	8	2	6	2	2	2	1	1	-	-	-	-	-	-
.0117M	8	2	6	2	2	2	1	-	1	-	-	-	-	-
.8739M	8	2	6	2	2	2	1	-	-	1	-	-	-	-
.0098	8	2	6	2	2	2	1	-	-	-	1	-	-	-
.0052	8	2	6	2	2	2	1	-	-	-	-	-	-	1
.0000M	8	1	6	2	2	2	2	-	-	-	-	1	-	-
.0000M	8	2	6	1	2	2	2	-	-	-	-	-	1	-

Tables 47 a-c n^3Bu States

Table 47a Trans But-2-ene 1^3Bu $^3(\pi, \pi^*)$

$(coefficient)^2$	3ag-6ag	7ag	3bu-5bu	6bu	lau	1bg	2au	2bg	3bg	4bg	5bg	6bg	7bu	8ag
.0308M	8	2	6	2	2	2	1	1	-	-	-	-	-	-
.0067M	8	2	6	2	2	2	1	-	1	-	-	-	-	-
,8734M	8	2	6	2	2	2	1	-	-	1	-	-	-	-
.0263	8	2	6	2	2	2	1	-	-	-	-	1	-	-
.0000M	8	1	6	2	2	2	2	-	-	-	-	-	1	-
.0174	8	2	6	2	1	2	2	-	-	1	-	-	-	-
.0000M	8	2	6	1	2	2	2	-	-	-	-	-	-	1

Table 47b Trans But-2-ene $^1(\pi, 3dxz+3dyz)$ 2^3Bu

$(coefficient)^2$	3ag-6ag	7ag	3bu-5bu	6bu	lau	1bg	2au	2bg	3bg	4bg	5bg	6bg	7bu	8ag
.7129M	8	2	6	2	2	2	1	1	-	-	-	-	-	-
.1895M	8	2	6	2	2	2	1	-	1	-	-	-	-	-
.0134M	8	2	6	2	2	2	1	-	-	1	-	-	-	-
.0066	8	2	6	2	2	2	1	-	-	-	1	-	-	-
.0000M	8	1	6	2	2	2	2	-	-	-	-	-	1	-
.0000M	8	2	6	1	2	2	2	-	-	-	-	-	-	1

Table 47c Trans But-2-ene 3^3Bu

$(coefficient)^2$	3ag-6ag	7ag	3bu-5bu	6bu	lau	1bg	2au	2bg	3bg	4bg	5bg	6bg	7bu	8ag
.1752M	8	2	6	2	2	2	1	1	-	-	-	-	-	-
.7229M	8	2	6	2	2	2	1	-	1	-	-	-	-	-
.0220M	8	2	6	2	2	2	1	-	-	1	-	-	-	-
.0000M	8	1	6	2	2	2	2	-	-	-	-	-	1	-
.0000M	8	2	6	1	2	2	2	-	-	-	-	-	-	1

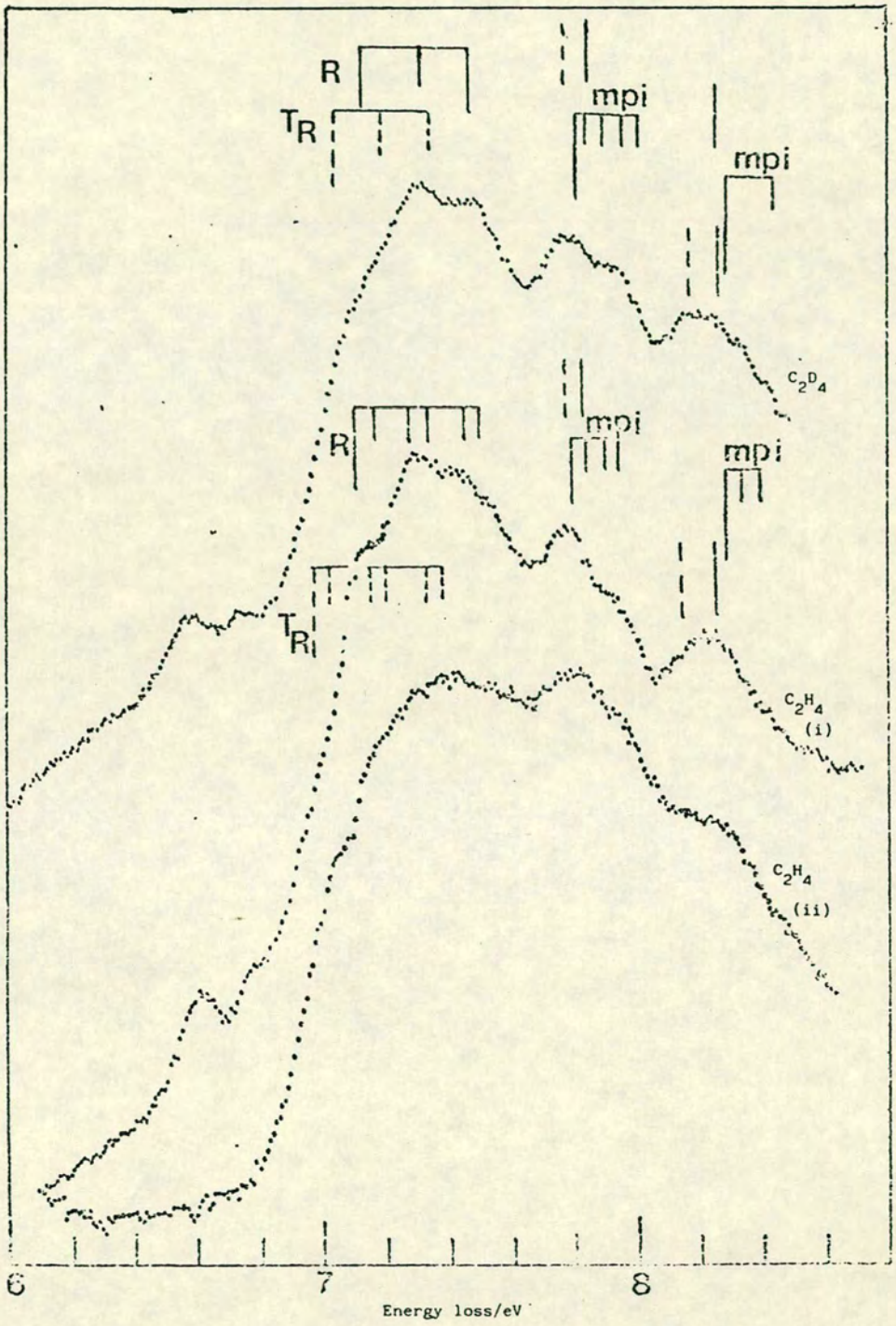

Figure 1 - Ethylene

(i) Scattered-electron spectrum recorded in the d.c. mode at W and hence E~0.02eV (ii) Scattered-electron spectrum recorded in the a.c. mode for $E_r \sim 0.8$eV.

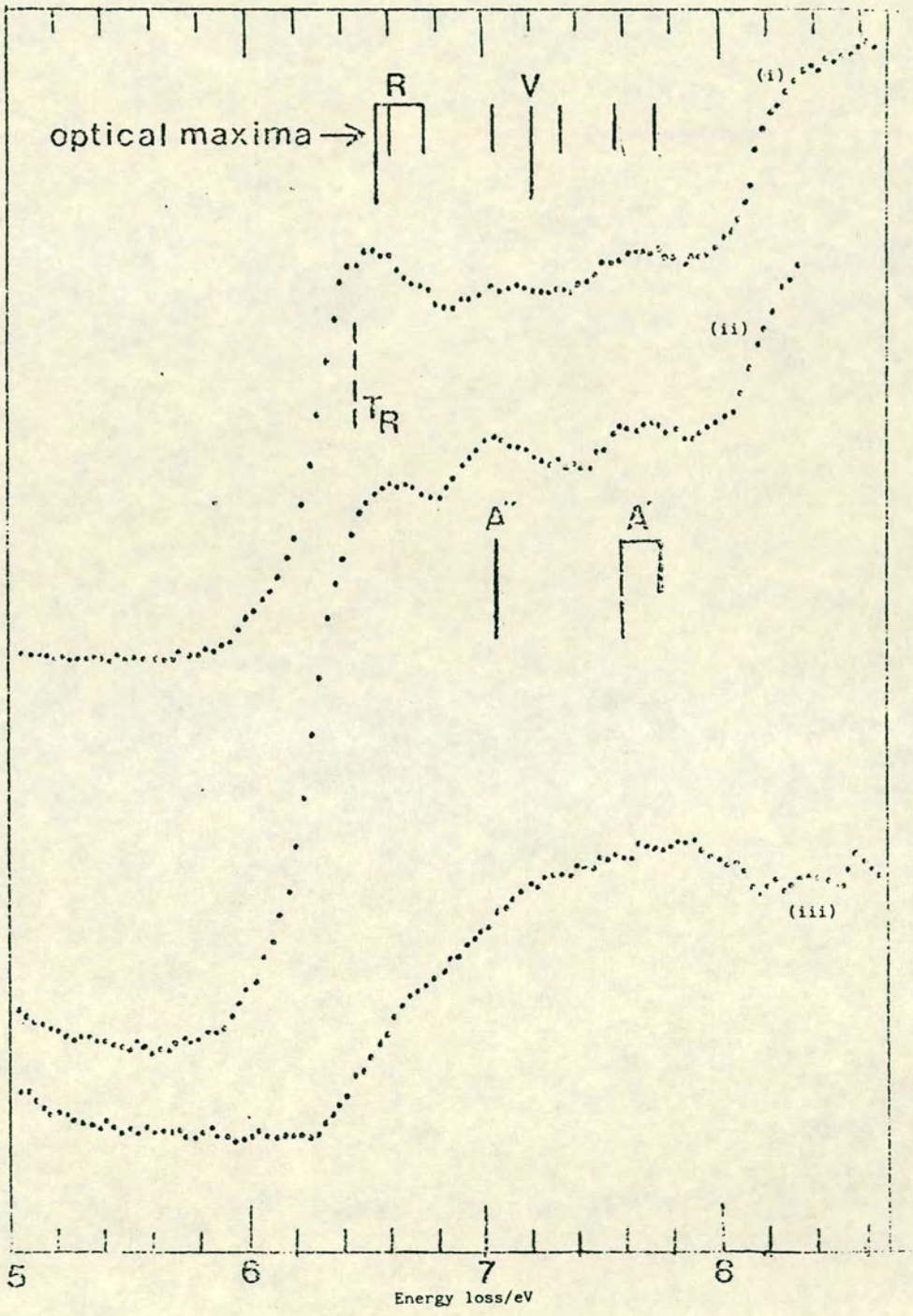

Figure 2 - Propene

(i) E_r ≈0.1eV and (ii) E_r ≈0.2eV are d.c. spectra. (iii) E_r ≈1.3eV is an a.c. spectrum. The y-axis scale is not constant between spectra.

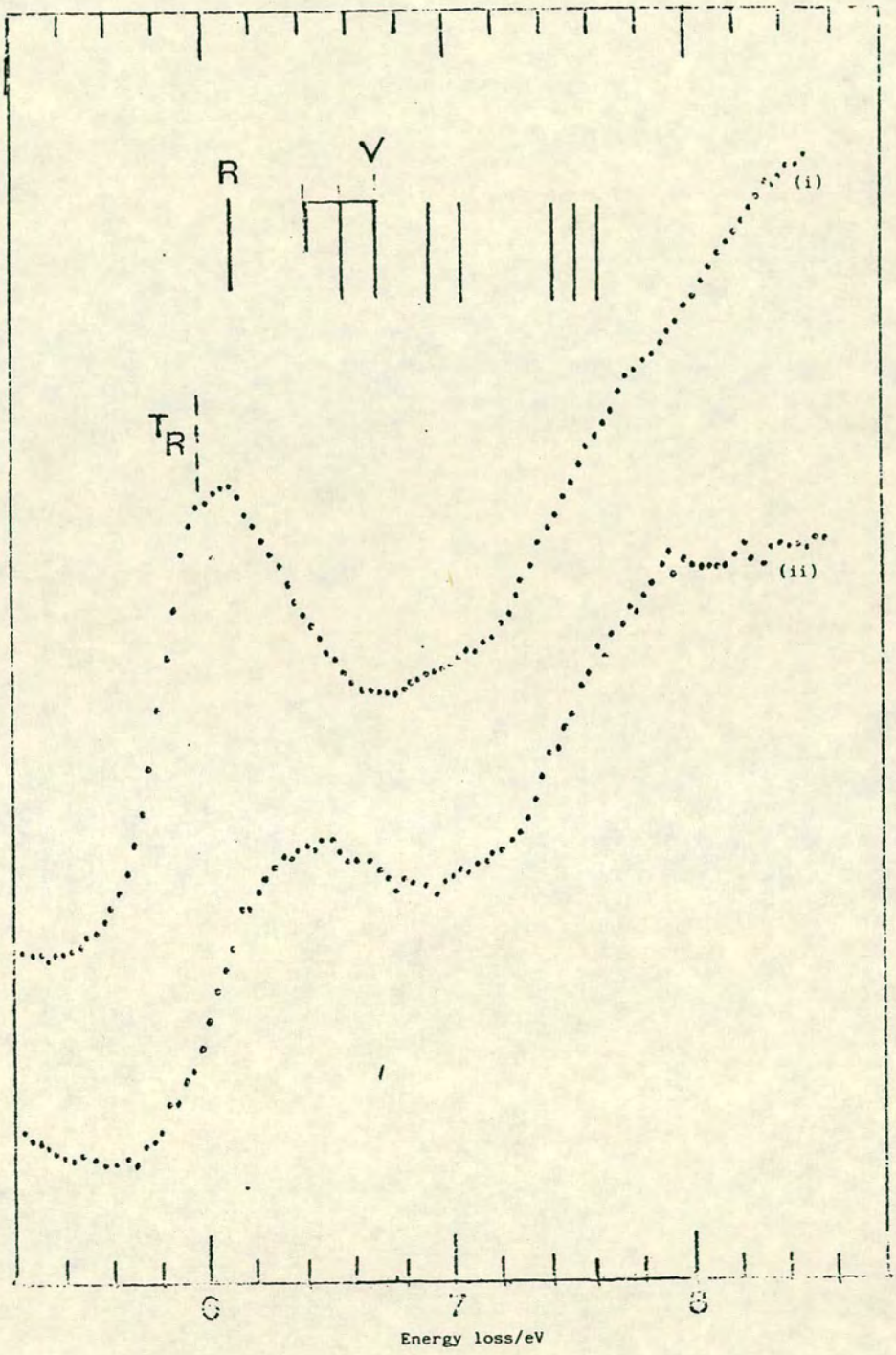

Figure 3 - 2 Methyl Propene

(i) E_r ≈0.1eV (d.c.) (ii) E_r ≈1eV (a.c.)
The y-axis scale is not constant between spectra.

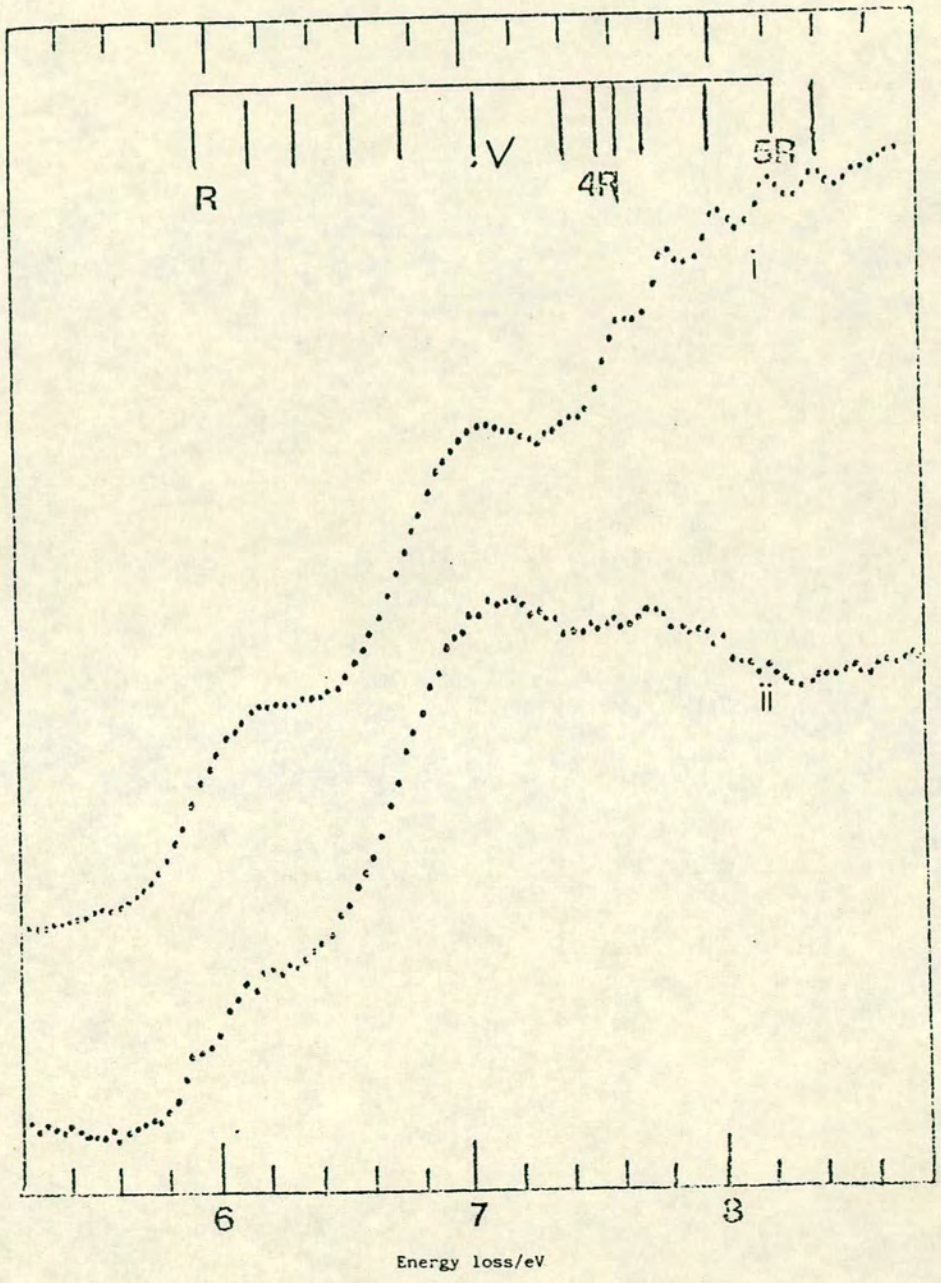

Figure 4 - Cis But-2-ene

(i) $E_r \approx 0.2$eV (d.c.) (ii) $E_r \approx 1$eV (a.c.)
The y-axis scale is not constant between spectra.

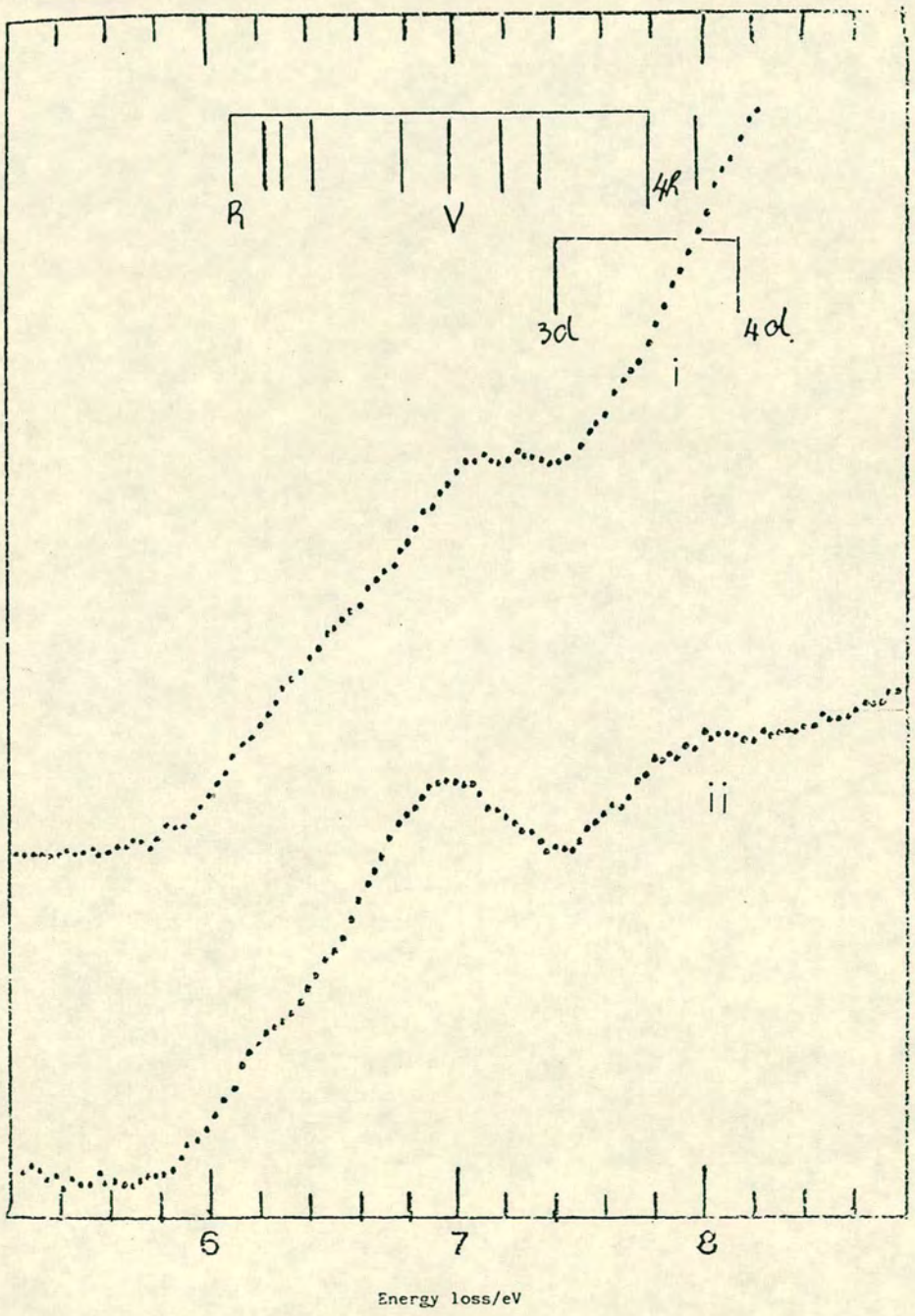

Figure 5 - Trans But-2-ene

(i) $E_r \simeq 0.1$eV (d.c.) (ii) $E_r \simeq 1$ eV (a.c.)
The y-axis scale is not constant between spectra.

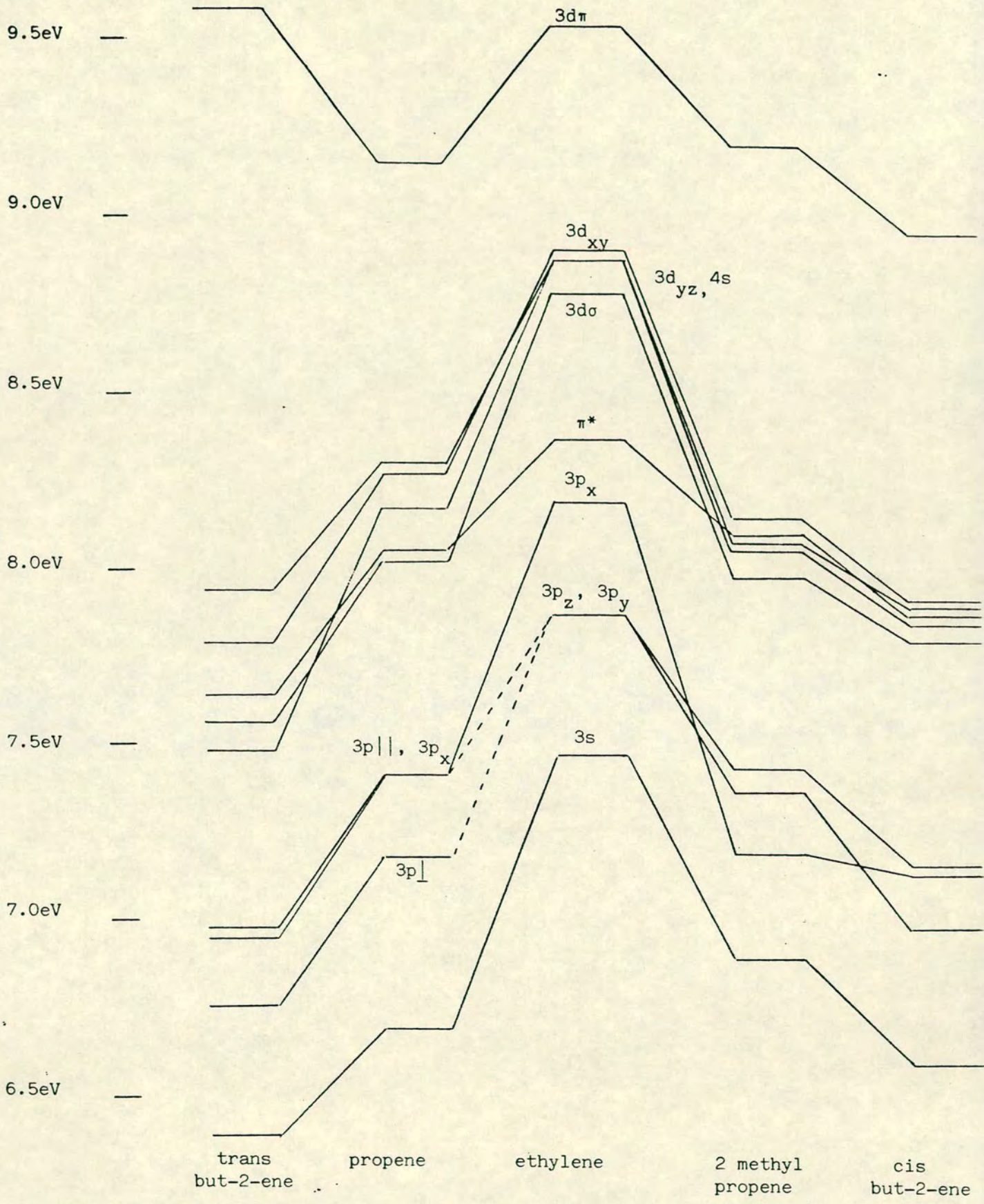

Figure (6). Correlation diagram for computed singlet excitation energies in the mono-olifins studies.

CHAPTER VI

A theoretical Study of the Photo-Electron Spectra of the Azoles Using Ab Inition CI Calculations

Introduction

Five-membered aromatic heterocyclic compounds have been the subject of several theoretical investigations. These compounds are of considerable significance in very diverse experimental chemical areas. They comprise the fundamental constituents of many explosive compounds, and more important, they form the building blocks of many natural biological molecules and pharmacological agents. By themselves they also form several classes of very important medicinal chemicals acting as anti-helmintics, anti-histamine compounds, anti-bacterial and anti-fungal agents.

The objective of the work in this chapter was to obtain a more detailed interpretation of the photoelectron spectra of these molecules using ab initio CI calculations. The photoelectron spectra were provided by Drs. M.H. Palmer and I. Simpson (Edinburgh University) and Appendix A contains a brief outline of photo-electron spectroscopy.

The basis set for the SCF calculations consisted of the Dunning (4s2p/2s) double zeta (DZ) contraction [1] of the Huzinaga [2] (9s5p/5s) primitive functions; the hydrogen 5s set was scaled by $\eta^2 = 2.0$ as in the work of Whitten [3]. The SCF wavefunctions were obtained with the ATMOL3 suite of programs [4]. The ground state SCF wavefunction was used as the MO basis in each case, and the multi-reference CI calculations were performed using the MRDCI program [5,6]. All calculations were performed on the Cray-1s computer at the University of London Computer Centre (ULCC).

Most of the previous theoretical work on azoles has relied upon ΔSCF calculations and Koopmans' Theorem to assign the PE spectra. Apart from the inherent inaccuracy of these methods, it is not possible to determine the ionisation potentials for 'shake-up' states. A 'shake-up' state is one in which ionisation is accompanied by promotion of a second electron to an orbital of higher energy. Configuration interaction enables one to investigate 'shake-up' states and also provides more reliable results for single ionisations.

Successive aza substitution of the pyrrole system results in the following trends:

(i) Replacement of ≥CH by ≥N: results in transformation of a σ-CH bonding orbital to one of lone pair character, which has a lower binding energy. When more than one nitrogen is present in a symmetric molecule the lone pairs can exist as linear combinations; symmetric (LP_N^+) and anti-symmetric (LP_N^-). In general the symmetric combination is more stable than the antisymmetric one. For assymmetric molecules the LP_N exist as semi-localised lone pairs and cannot be easily interpreted as combinations, especially for the tetrazoles.

(ii) The valence orbital energies fall into two distinct groupings for the azoles. The first band lies in the 8-10 eV region for pyrrole, moves to successively higher binding energy upon successive aza substitution, and lies at 11-15.5 eV in tetrazole. It contains two levels for pyrrole and (2 + n) levels in the other azoles, where n is the number of imino nitrogens. The second region (at 14-16 eV) in pyrrole again

moves to higher binding energy on successive nitrogen substitution and contains 6-n levels, where n is the number of imino nitrogens.

The cross-section of LP_N and orbitals with 's' character increases with He(II) radiation, and therefore the He(I) and He(II) spectra provide an experimental method of verifying some of the theoretical assignments reported here. The spectra of substituted azoles have also been used to determine the dominant gas phase tautomer in those cases where tautomerism might complicate the spectra. This to, provides an experimental means of verifying the theoretical conclusions.

Pyrrole

The microwave geometry of pyrrole [7] has been used in the present calculations. The numbering system and geometry are indicated below.

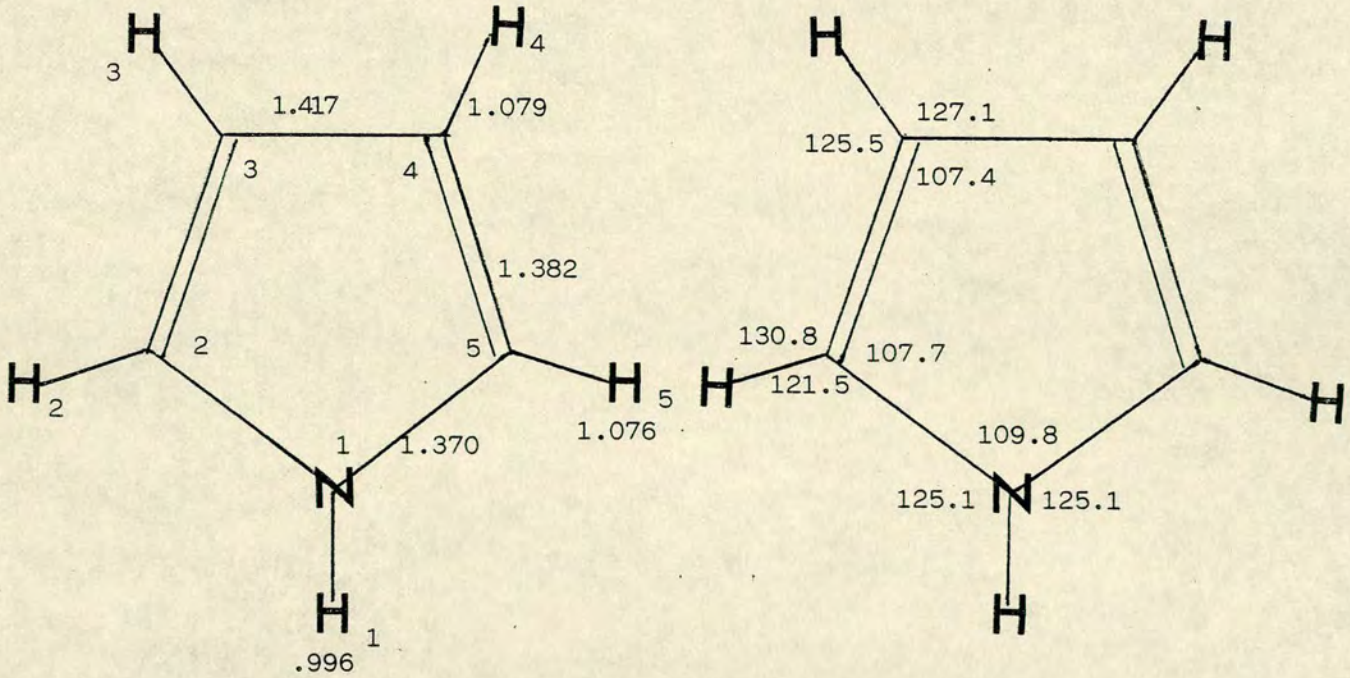

The core electrons were frozen allowing only excitations involving the valence electrons. The configurational subspace was further reduced by excluding the 12 highest unoccupied σ orbitals ($7a_1$, $5b_2$) from the calculations.

There have been several theoretical investigations of the PES of pyrrole and these are summarised in Table 1. The most sophisticated calculations are those of Von Niessen et al [13] who have employed the 'Many Body Approach' which corrects for electron correlation and reorganisation. Their results are summarised in Table 2.

As Table 1 indicates, the various theoretical interpretations (based largely on Koopmans' Theorem) do not completely agree with one another, and the results of Von Niessen (Table 2) indicate no shake up states. The present set of calculations appear to be the most comprehensive to date and predict the existence of several, hitherto unassigned, shake up states.

The present SCF wavefunction has a calculated ground state energy of -208.7408 au. Table 3 contains the calculated eigenvalues for the nine highest occupied SCF MO's and a brief description of each orbital. The three lowest unoccupied orbitals are: $3b_1$ (0.1703 au), $10a_1$ (0.1709 au), $2a_2$ (0.2256 au).

Three reference configurations have been used to calculate the ground state CI energy (3M1R) and a calculated GS energy of -209.0476 au was obtained (Table 6).

The complete results are summarised in Tables 4-10(d). In general the number of reference configurations and roots calculated for each symmetry were systematically increased until self-consistency with respect to further expansion of the set of reference configurations was achieved. Table 5 summarises all of the calculations performed. Inspection of Table 5 indicates that the final set of calculations for each symmetry are self-consistent and one would not expect further CI to improve these results significantly.

Table 4 indicates the existence of several shake up states: 2^2B_1, 2^2A_2, 3^2B_1, 3^2A_2, 4^2B_1, 4^2A_2, 3^2B_2 and 4^2A_1. These shake up states all involve excitations of the $\sigma/\pi \rightarrow \pi^*$ type where the π^* orbitals involved are $2a_2$ and $3b_1$. Ignoring shake up states temporarily, the present calculations predict the following order for the IP's:

$$1a_2 < 2b_1 < 9a_1 < 6b_2 < 5b_2 < 8a_1 < 7a_1 < 4b_2.$$

If one now compares this order with the previous results based on Koopmans' Theorem, Table 1, the most noticeable feature is the absence of ionisation from the $1b_1$ orbital. The present calculations predict ionisation from the $1b_1$ orbital to be accompanied by a significant amount of shake up. This observation is supported by the CI calculations of Tanaka et al [15]; their results also indicating that the 2^2B_1 state involves a considerable amount of shake up. They have calculated the ionisation potentials of the 1^2A_2, 1^2B_1 and 2^2B_1 states to be 8.10, 8.94 and 13.33 eV respectively. The present calculations predict the following

ionisation potentials: 1^2A_2 7.94 eV, 1^2B_1 8.87 eV, 2^2B_1 12.28 eV. Hence the present results disagree markedly with Taneka et al on the IP of the 2^2B_1 state. It should be noted that their calculations were somewhat more restrictive. Correlation was restricted to the π electrons and they did not calculate any higher roots of B_1 symmetry. The present calculations indicate that the 3^2B_1 and 4^2B_1 states also exhibit a significant amount of shake up and can therefore interact with the 2^2B_1 state. Therefore the discrepancy of 1 eV can be attributed largely to the interaction between the 2^2B_1, 3^2B_1 and 4^2B_1 states.

Palmer et al [14] have positioned the vertical ionisation potentials at 8.23, 9.22, 12.85, 13.65, 14.3, 14.7 and 17.5 eV, fig.(1). The assignment of the first two peaks at 8.23 and 9.22 eV as 1^2A_2 and 1^2B_1 respectively is consistent with earlier theoretical work based on Koopmans' theorem, Table 1.

The theoretical results suggest that the band centred at 12.85 eV results from two ionisations; ionisation from the $9a_1$ and $2b_1$ orbitals. Inspection of the PE spectrum indicates a sharp peak at about 12.5 eV which may be the result of an adiabatic (0-0) ionisation of a π-type orbital, consistent with the present results. The band centred at 13.65 eV can be associated with the 1^2B_2 state, while the band at 14.3 eV can be associated with the 2^2B_2 and 2^2A_1 states. The peak at 14.7 eV is less intense than the neighbouring bands and the calculations indicate three shake up states (2^2A_2, 3^2B_1 and 3^2A_2) in this region; the lesser intensity of this peak is also

consistent with the present assignment of shake up states. The band at 17.5 eV can be correlated with the 3^2A_1 and 3^2B_2 states.

The theoretical results are summarised in Table 4 and Table 11 summarises the present spectral assignment.

Imidazole

The microwave structure of Christen et al [16] has been used in the present study. The numbering system and geometry used are indicated below.

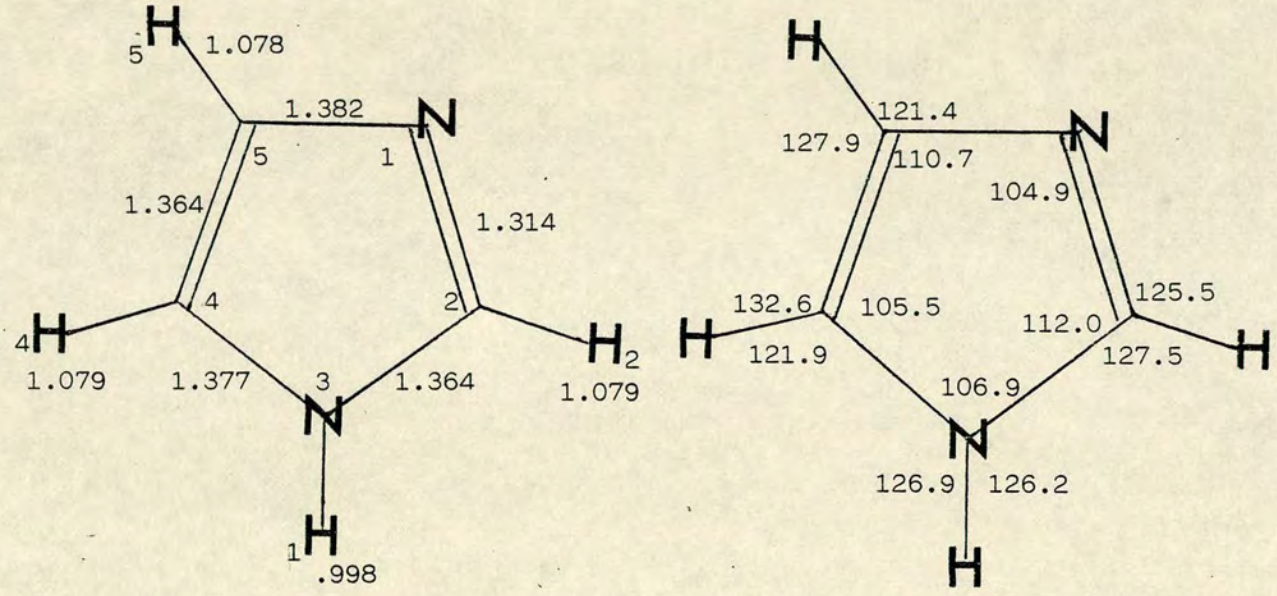

The core electrons were frozen allowing only excitations involving the valence electrons. The configurational subspace was further reduced by excluding the 14 highest unoccupied orbitals.

The photoelectron spectrum of imidazole has been reported by Palmer et al [14] and is indicated in figure 2. They have determined the values of the vertical ionisation potentials

to be 8.78, 10.3, 10.7, 14.0, 14.7, 15.3 and 15.7 eV.

There have been several theoretical studies of imidazole and these are summarised in Table 12. The calculations based on Koopmans' theorem are not entirely satisfactory for the interpretation of the PE spectrum and the more sophisticated SCF X_α calculations, while providing better calculated I.P.'s, do not predict any shake up states.

The present calculations are the first full valence shell CI calculations for imidazole. The SCF wavefunction yields a ground state energy of -224.72763698 a.u. Table 13 contains the eigenvalues of the nine highest occupied orbitals and a brief description of each orbital. The four lowest unoccupied orbitals are 4a'' (4.30 eV), 16a' (4.34 eV), 5a'' (5.76 eV) and 17a' (6.16 ev).

Three reference configurations have been used to calculate the ground state CI energy (3M1R) and a calculated energy of -225.0574 a.u. was obtained (Table 16). Table 14 summarises all the calculations performed. The number of reference configurations and roots calculated were increased until self-consistency was achieved. Inspection of Table 14 reveals that self-consistency was only achieved for the 9M6R (A'') set. These calculations were computationally expensive and further work was not done because it was felt that the present set of results would be sufficient to interpret the PE spectrum.

Table 15 summarises the calculated vertical IP's Several, hitherto unassigned, shake up states are predicted. The strongest transitions in the PE spectrum correspond to those states arising from ionisation only. Therefore if one temporarily ignores shake up states, the most intense peaks are predicted to occur at 8.67 eV ($1^2A''$), 9.21 eV ($1^2A'$), 9.89 eV ($2^2A''$), 14.04 eV ($3^2A'$), 15.06 eV ($4^2A'$), 15.13 eV ($5^2A'$).

The vibrational fine structure of the first peak at 8.78 eV suggests that it results from ionisation from a π-orbital. This assignment is in agreement with the present calculations; the $1^2A''$ state has a calculated I.P. of 8.67 eV. The intensity of the second band is roughly twice that of the first, indicating the existence of two states in this region. Furthermore, the intensity of the second peak relative to the first increases with He(II) radiation, suggesting that one state corresponds to ionisation from a lone pair.

The $2^2A''$ state has a calculated I.P. of 9.89 eV and can therefore be assigned to the second band. The $1^2A'$ state has a calculated I.P. of 9.21 eV (8M6R) and is relatively stable with respect to changes in the reference configurations. Since this state corresponds to ionisation from the nitrogen lone pair it to must be assigned to the second band. This however implies that the present calculations are in error by about 1 eV for this state.

There are two possible reasons for this. Firstly, the chosen set of reference configurations did not explicitly include $\sigma \rightarrow \sigma^*$

correlation. Secondly, and much more likely, is the need for polarization functions in the SCF wavefunction. An error of 1 eV is rather large and need not necessarily be due entirely to the lack of σ/σ^* correlation. Since the $1^2A'$ state involves ionisation from the highly localised nitrogen lone pair, it is necessary to adequately describe the spatial distribution of the lone pair for both the neutral molecule and the ion. If the present SCF wavefunction is inadequate in this respect no amount of additional CI can correct this deficiency.

The remaining states arising from ionisation only [$3^2A'$, $4^2A'$, $5^2A'$] are in good agreement with the experimentally determined IP's [14] of 14.0, 14.7 and 15.3 (Table 15). Several shake up states are also predicted by the present calculations and these are: $3^2A''$, $2^2A''$, $4^2A''$, $5^2A''$, $6^2A''$ and $6^2A'$. All of the shake-up states occur in the region between about 13.2 eV and 16.5 eV. Two shake up states ($2^2A'$, $3^2A''$) are predicted to lie very close together (Table 15) and the PE spectrum indicates a pronounced shoulder at about 13.7 eV. In the light of the present calculations, this relatively intense shoulder probably arises from the combined intensities of these two shake up states.

Finally, Table 19 summarises the present assignment of the imidazole PE spectrum.

Pyrazole

The microwave structure of Nygaard et al [7] has been used in the present study. The numbering system and geometry used are indicated below.

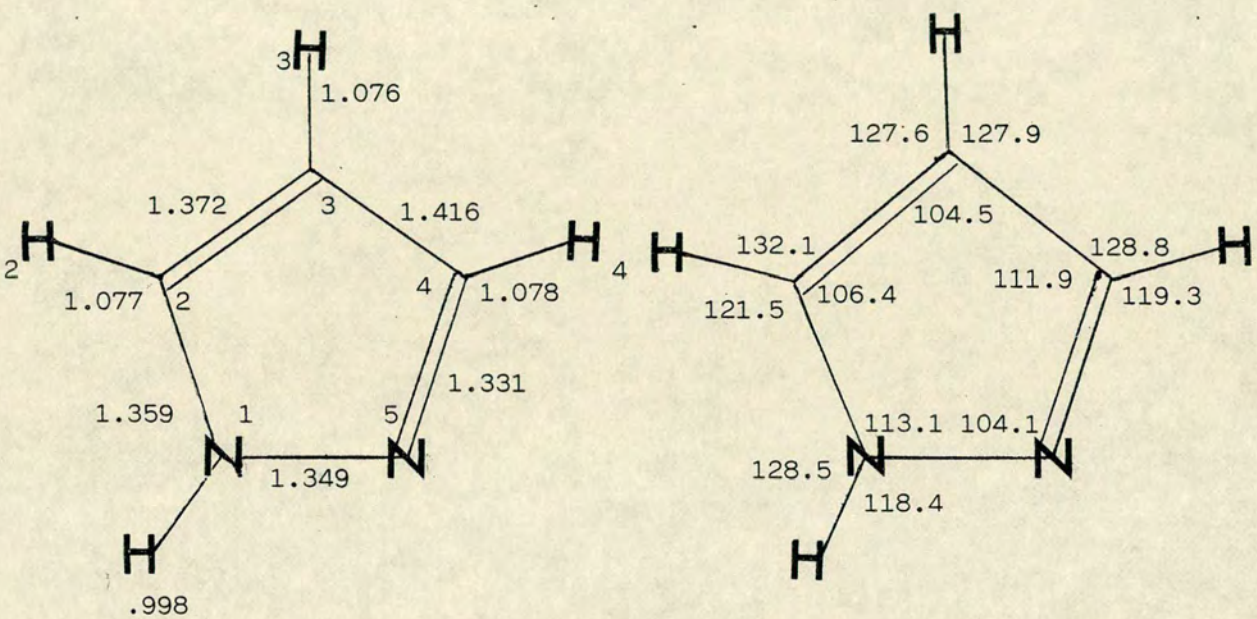

The core electrons were frozen allowing only excitations involving the valence electrons. The configurational subspace was further reduced by excluding the 14 highest unoccupied σ-orbitals. The SCF wavefunction was used as the MO basis (E_{SCF} = -224.710568 a.u.) and Table 20 contains a brief description of the 9 highest occupied SCF MO's.

Several theoretical studies using Koopmans' theorem have been employed to interpret the PE spectrum of pyrazole and these are summarised in Table 21. Koopmans' theorem has generally proved inadequate and satisfactory results have only been achieved for the first two I.P.'s. No CI studies have as yet been reported in the literature.

The calculations are summarised in Tables 22 and 23. The ground state CI energy was calculated to be -225.0469 a.u. (3M1R, Table 24). The number of reference configurations and roots calculated for each symmetry was increased until self-consistency was achieved. Inspection of Table 22 reveals that only one state, $5^2A''$ (10M5R), has probably not achieved self-consistency. The density is 0.75 and the correction term is significantly larger than the other states.

The PE spectrum of pyrazole is indicated in Figure 3 and Palmer et al [14] have determined the vertical ionisation potentials to be 9.15, 9.88, 10.7, 13.6, 14.7, 15.1 and 17.5 eV. The calculations generally fit in well with the PE spectrum. The first peak at 9.15 eV has been assigned to the $1^2A''$ state. The second peak at 9.88 eV correlates best with the calculated I.P. for the $2^2A''$ state.

The third band is centred at 10.7 eV. The present calculations predict ionisation from the LP_N orbital to occur at 10.06 eV. This state is best correlated with the band at 10.7 eV. The theoretical calculations under-estimate the ionisation potential

by 0.5-0.7 eV depending on the reference set chosen. As was previously experienced with imidazole the error probably arises from the absence of polarization functions in the SCF wave-function.

Three other states are predicted to arise from ionisation only: $2^2A'$ 13.94 eV, $3^2A'$ 14.94 eV and $4^2A'$ 15.53 eV. These states would be expected to be more intense than any shake up states and the calculated IP's closely match the observed vertical IP's at 13.6, 14.7 and 15.1 eV. The remaining states exhibit a significant amount of shake up and explain the broad diffuse nature of the spectrum in the region between 13.5 and 16 eV. Table 27 summarises the present theoretical assignment of the PE spectrum of pyrazole.

1,2,4-Triazole

1,2,4-Triazole has been largely neglected by theoretical chemists; only Palmer et al [14,21] have attempted to assign the PE spectrum using ab initio SCF calculations and Koopmans' theorem. Palmer [21] has compared the PE spectrum of 1,2,4-triazole with the spectra of the 1- and 4-methylated compounds and concluded that the 1H-tautomer is dominant in the gas phase, a result supported by his ab initio calculations. Palmer's results were based upon his theoretically determined geometries for the 1H- and 4H-tautomers. The geometries being determined in both cases by gradient optimisation with the program HONDO, using a minimal basis set.

CI calculations have been performed on both tautomers. The core electrons were frozen in each case allowing only excitations involving the valence electrons. The configurational subspace was further reduced by removing the 12 highest unoccupied σ-orbitals.

In the absence of experimental data the computed geometry of Palmer et al has been used for the 4H-tautomer. This yielded a ground state CI energy of -241.09500130 a.u. (5M1R). Initially, the estimated microwave structure reported by Bolton et al [22] was used for the 1H-tautomer, but the ground state CI energy was calculated to be higher than the 4H-tautomer, E_{CI} = -241.04619 a.u. (2M1R). This disagrees with the experimental observations and theoretical results of Palmer, and has been attributed to inaccuracies of the reported microwave structure which was based on several approximated parameters. This problem was overcome by using Palmer's computed geometry for the 1H-tautomer which yielded a ground state CI energy of -241.09716 a.u. (5M1R, Table 31), in agreement with the earlier work of Palmer. Therefore the present CI calculations predict the 1H-tautomer to be more stable by 5.67 kJ mol^{-1}.

The geometries and labelling systems used are indicated below:

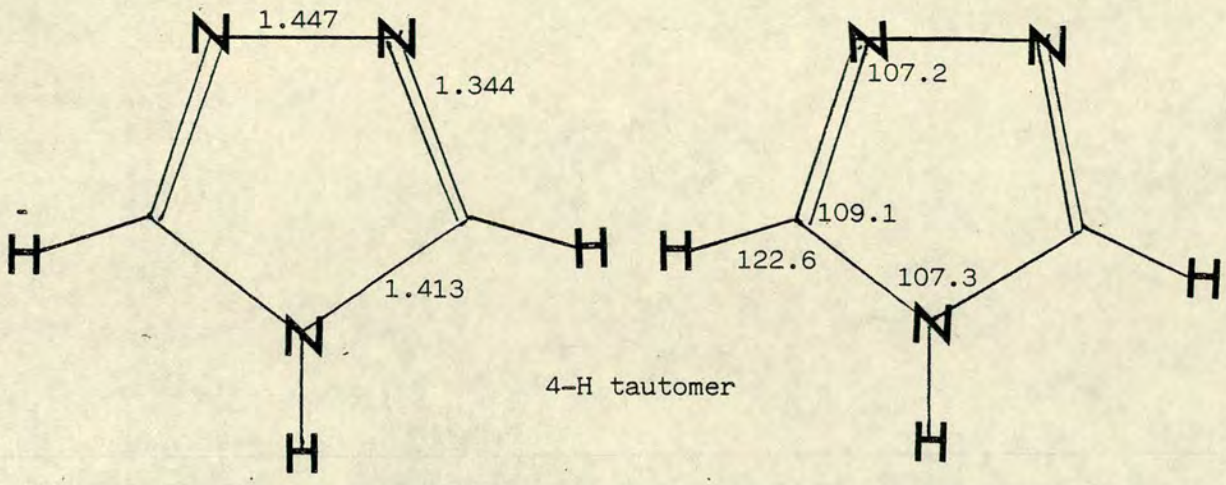

4-H tautomer

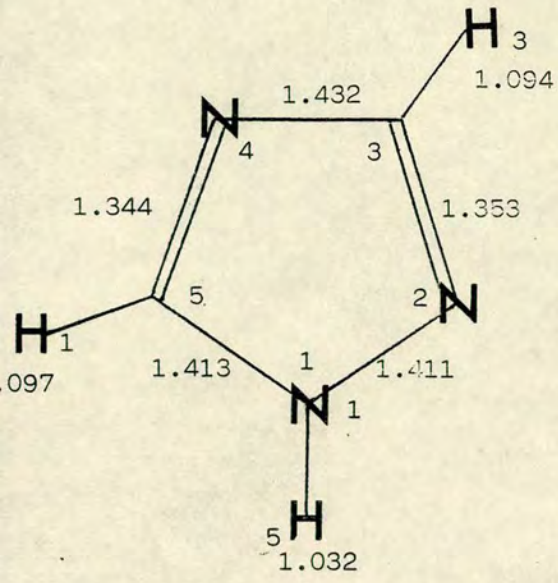

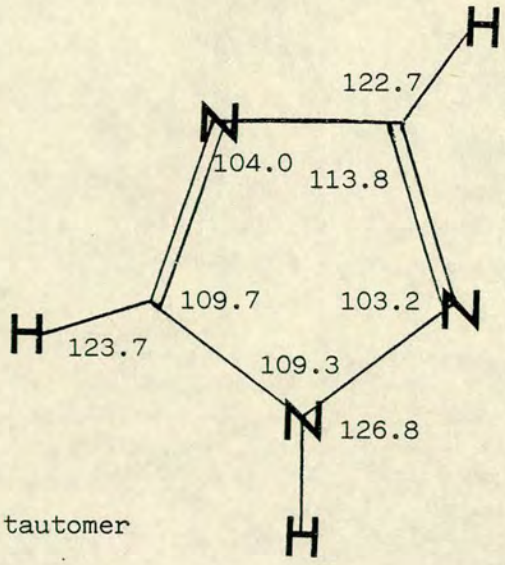

1-H tautomer

Table 28 contains a brief description of the 9 highest occupied SCF MO's for the 1H-tautomer. The 4 lowest unoccupied SCF MO's are: 4a'' (3.16 eV), 16a' (4.28 eV), 5a'' (4.82), 17a' (5.61 eV).

The present theoretical interpretation has been based upon the assumption that only the 1H-tautomer contributes to the PE spectrum. The number of reference configurations and roots calculated were gradually increased while attempting to achieve self-consistency for as many roots as possible. The results are summarised in Tables 29 and 30.

The PE spectrum of 1,2,4-triazole is indicated in Figure 4. Palmer et al [14] have determined the experimental vertical ionisation potentials to be 10.0, 10.56, 11.1, 12.15, 14.6, 15.1, 16.0 and 18.2 eV. The first peak at 10.0 eV is due to ionisation from the 3a'' (π) orbital; the calculated IP for the $1^2A''$ state being 10.16 eV.

The assignment of the second band at 10.56 eV is not so trivial. Introduction of an additional imino nitrogen results in the two

nitrogen lone pairs forming linear combinations. If one visualises the 1,2,4-triazole 1H-tautomer as having pseudo C_{2v} symmetry, then the linear combinations can be described as a symmetric combination ($LP_{N2} + LP_{N4}$) and an assymetric combination ($LP_{N2} - LP_{N4}$); these have been denoted LP_{N+} and LP_{N-} respectively. The present calculations predict ionisation from the LP_{N-} orbital to occur at 10.22 eV, while ionisation from the 2a'' (π) orbital is predicted to occur at 10.42 eV.

The theoretical results suggest that there are two possible assignments for the second band. Previous experience with pyrazole and imidazole indicated that the present theoretical approach can seriously underestimate ionisation from lone pairs. This observation suggests that the second band should be assigned to the 2A'' state, while the third band at 11.1 eV is due to ionisation from the LP_{N-} orbital. The fourth band centred at 12.15 eV must be due to ionisation from the LP_{N+} orbital. The only state calculated to lie near this region is the $2^2A'$ state which has a calculated ionisation potential which varies according to the reference configurations chosen (11.44-11.79 eV). Again ionisation from a lone pair has been seriously underestimated and this result provides further support for the assignment of the third band as ionisation from the LP_{N-} orbital.

Only one other state involving solely ionisation is predicted by the present calculations. Ionisation from the 13a' orbital has a calculated value of 14.97 eV and has been assigned to the peak at 15.1 eV in the PE spectrum. The remaining states are all

predicted to exhibit a significant amount of shake up and the results are summarised in Table 30. The present theoretical interpretation of the PE spectrum is summarised in Table 34.

1,2,3 Triazole

1,2,3-Triazole has been largely neglected by theoreticians, only Palmer et al [14,21] have studied the triazoles by ab initio SCF methods. In the absence of experimentally determined structures, the theoretical structures of Palmer et al [21] have been used. Palmer determined the structures of both the 1H (C_s) and 2H (C_{2v}) tautomers by optimising the geometry of each at the SCF level using the program HONDO and a minimal basis set. The labelling system and geometries used are indicated below:

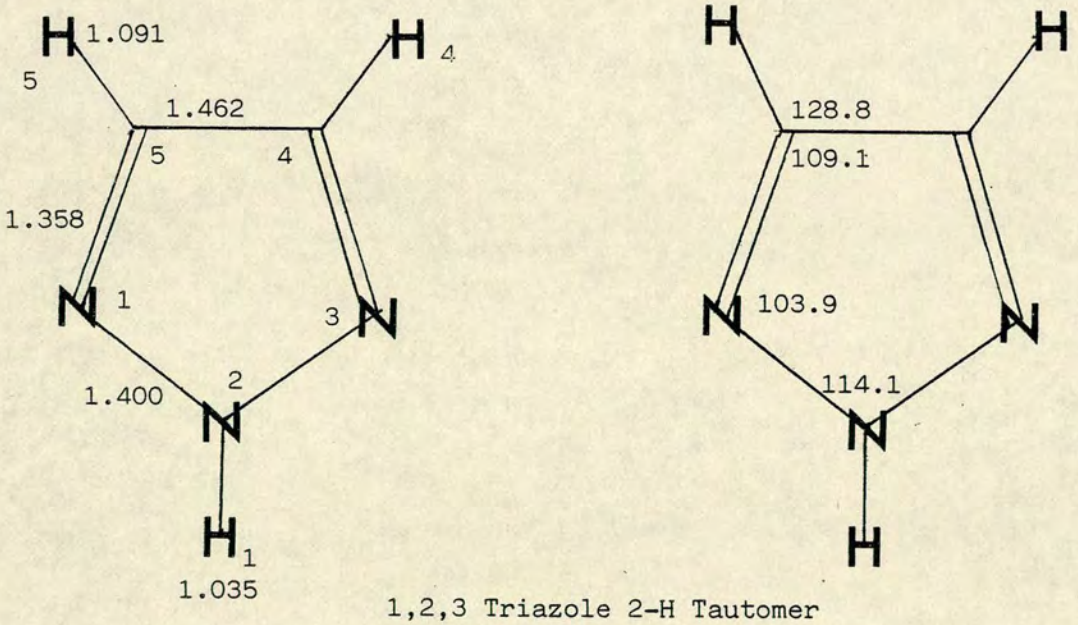

1,2,3 Triazole 2-H Tautomer

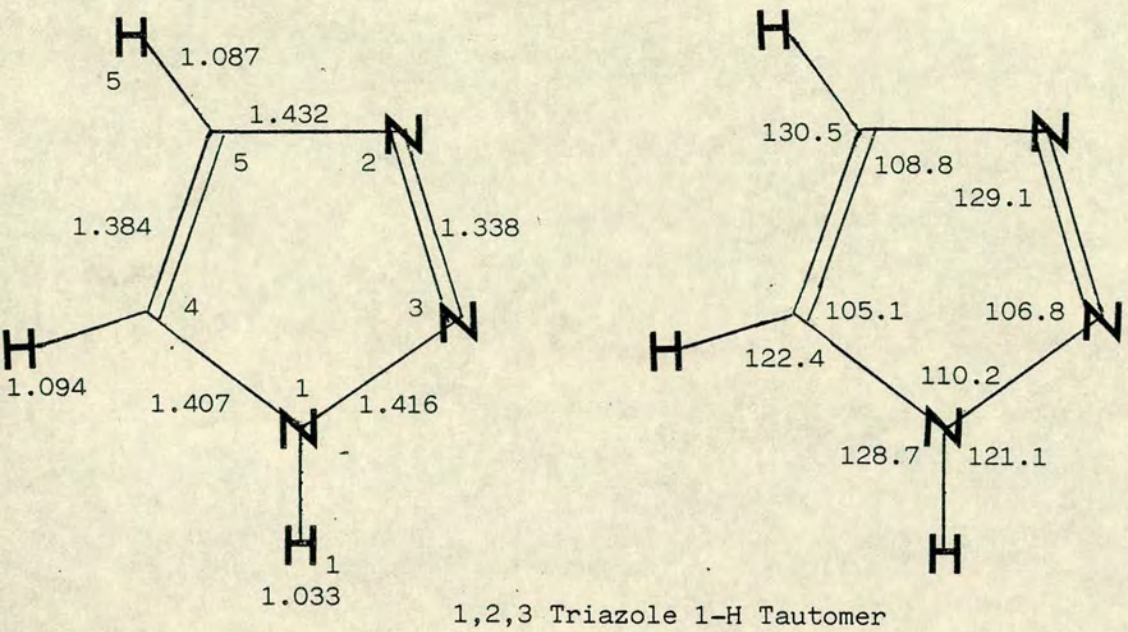

1,2,3 Triazole 1-H Tautomer

Palmer [21] using a double zeta (DZ) basis set (identical to the basis set used here) calculated the relative stabilities of each tautomer (1H-1,2,3-triazole -240.6571 a.u., 2H-1,2,3-triazole -240.6631 a.u.) and found the 2H tautomer to be more stable by 15.76 kJ mol^{-1}. Palmer has also assigned the PE spectrum of 1,2,3-triazole using Koopmans' theorem, and assuming only the 2H tautomer contributes to the spectrum.

The present calculations represent the first truncated CI study of 1,2,3-triazole and provide a more complete interpretation of the PE spectrum. The SCF wavefunctions for both the 1H and 2H tautomers are identical to those of Palmer et al [21]. Table (39) contains a brief description of the 9 highest unoccupied SCF MO's for the 2H tautomer. The 4 lowest unoccupied MO's are: $3b_1$ (2.76 eV),

$10a_1$ (4.56 eV), $2a_2$ (4.85 eV), $11a_1$ (5.89 eV).

CI calculations have been carried out for both tautomers. In each case the core electrons were frozen and the configurational subspace was further reduced by removing the 12 highest unoccupied σ orbitals ($7a_1$, $5b_2$ in the case of the 2H form).

The CI calculations reinforce the conclusion of Palmer et al that the 2H tautomer is more stable than the 1H form. The calculated CI energies (1M1R) for the 1H and 2H tautomers are -241.0525 a.u. and -241.077 a.u. respectively, indicating that the 2H form is significantly more stable (by 64 kJ mol^{-1}). It is therefore unlikely that the 1-H tautomer contributes to the PE spectrum. This conclusion is supported by the PE spectra for the 1- and 2-methylated compounds, Figures 6 and 7. A comparison of these spectra with the parent compound, Figure 5, indicates that the 2-methyl-1,2,3-triazole spectrum best resembles that of 1,2,3-triazole; and therefore the 2H tautomer is dominant in the gas phase.

Tables 35 and 36 summarise the results for the 1H tautomer. In view of the significantly greater stability of the 2H form, most of the computational effort was concentrated on this tautomer. Tables 40 and 41 summarise the results.

A more accurate calculation of the CI ground state for the 2H tautomer has been carried out. An 8M3R calculation has been performed for the ground state and the two lowest excited singlet states of A_1 symmetry. The ground state has a computed energy of -241.0876 a.u.,

table 42. The two excited states have transition energies of 5.49 eV ($2b_1 \rightarrow 3b_1$) and 8.32 eV ($1a_2 \rightarrow 2a_2$).

The PE spectrum of 1,2,3-triazole is indicated in Figure 5. Palmer et al [14] have determined the vertical ionisation potentials to be 10.06, 10.9, 12.1, 15.0, 15.6 and 17.6 eV. The lowest ionised state 1^2B_1 has a calculated I.P. of 9.90 eV and is relatively stable with respect to expansion of the set of reference configurations, table 40. This state corresponds to ionisation from a weakly bonding π orbital and is in good agreement with the experimental value of 10.06 eV.

Inspection of the PE spectrum, Figure 5, reveals that the second peak (at 10.9 eV) is roughly twice the intensity of the first and third peaks. Furthermore, the relative intensity of the second peak increases when He(II) is used as the radiation source. Therefore the second peak is the result of two ionisations and one state involves ionisation from a nitrogen lone pair. The present calculations indicate that two states are predicted to occur in this region; the 1^2A_2 state (10.55 eV) corresponding to ionisation from a 'π' orbital and the 1^2B_2 state (10.60 eV) corresponding to ionisation from the LP_N- orbital. Both of these states are relatively unaffected by alterations to the set of reference configurations, Table 40.

The third peak at 12.05 eV is due to ionisation from the LP_N+ orbital. The 1^2A_1 state varies significantly with respect to changes in the set of reference configurations, Table 40, but since this is the

only state calculated to lie in this region this is the only assignment possible.

Only two other states are predicted to result from ionisation only. The 3^2B_2 state has a calculated I.P. of 15.38 eV and the 3^2A_1 state has an I.P. of 15.60 eV. The remaining states are all predicted to exhibit a significant amount of shake up and this therefore explains the diffuse nature in these regions of the spectrum. Inspection of Table 40 reveals that self consistency has been achieved for most of these states and therefore further CI should not significantly alter the present results.

The present assignment of the PE spectrum is summarised in Table 47.

Tetrazole

Tetrazole can exist in two tautomeric forms. Both the 1H and 2H tautomers have been studied by Palmer et al [21]. A comparison of the PE spectrum of tetrazole with the spectra of the 1- and 2-methyl compounds suggests that tetrazole exists in the 2H form in the gas phase [21]. This observation has not been supported by the ab initio SCF calculations of Palmer [21]. Palmer has determined the geometries of both the 1H and 2H tautomers by gradient optimisation using the program HONDO with minimal basis sets. Double zeta calculations using these equilibrium geometries predict the 1H tautomer to be slightly more stable (by 0.79 kJ mol^{-1}). The CI calculations of Mazurek and Osman [23] predict the 2H tautomer to be more stable by 1.1 kcal/mol in agreement with the present theoretical results.

The computed geometries of Palmer et al [21] have been used in the present study. The geometries and labelling systems are indicated below.

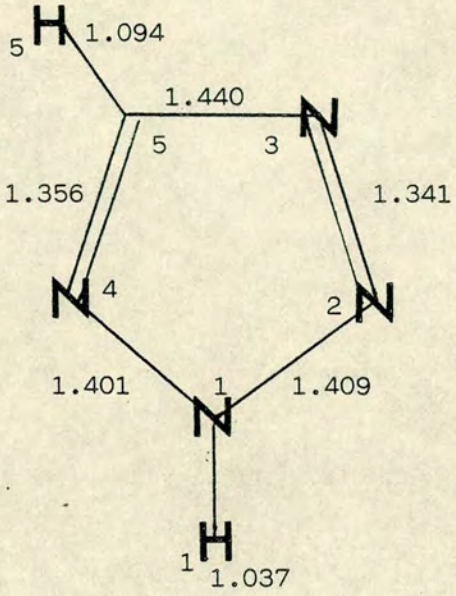

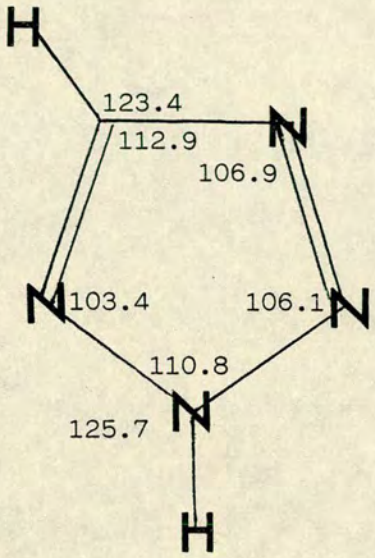

2-H Tautomer

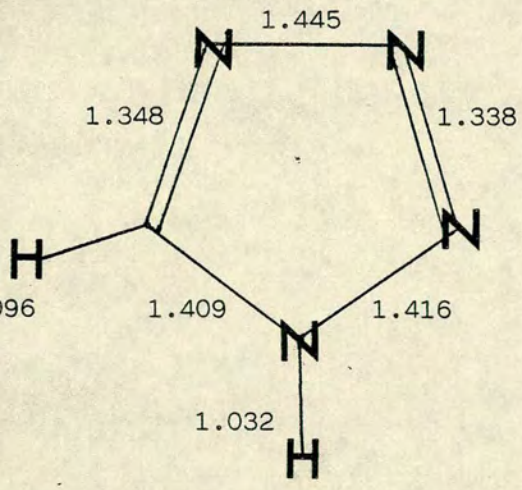

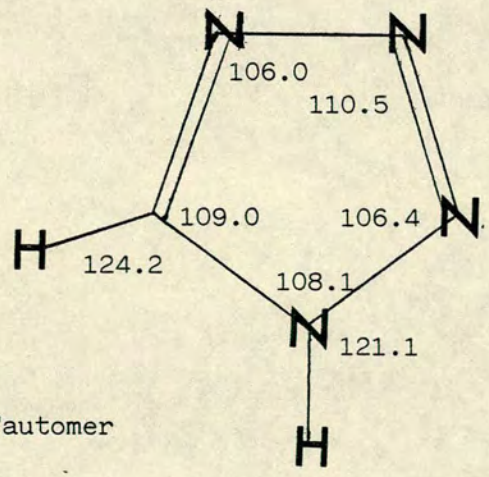

1-H Tautomer

Table 48 contains a brief description of the 9 highest occupied SCF MO's for the 2H tautomer. The four lowest unoccupied SCF MO's are: 4a" (1.99 eV), 5a" (3.97 eV), 16a' (4.07 eV) and 17a' (5.79 eV).

CI calculations have been performed on each tautomer. The core electrons were frozen and the 12 highest unoccupied orbitals were removed. The 2H tautomer is predicted to be significantly more stable than the 1H form. The ground state CI energy (1M1R) of the 1H tautomer is -257.0191 a.u. while the CI energy (1M1R) of the 2H tautomer is -257.0567 a.u.; a difference of 98.7 kJ mol^{-1}. This result is supported by the PE spectra of the 1- and 2-methylated compounds, Figures 9 and 10 respectively. The PE spectrum of 2-methyl tetrazole closely resembles that of tetrazole suggesting that the 2H tautomer is dominant in the gas phase.

The first three IP's of each symmetry for the 1H tautomer have been calculated and are summarised in Table 49. Due to the large difference between the ground state CI energies of the 1H and 2H tautomers it has been assumed that only the 2H tautomer contributes to the PE spectrum. The PE spectrum of tetrazole is illustrated in figure 8. Palmer et al [14] have determined the experimental ionisation potentials to be 11.3, 12.1, 13.63, 16.1 and 18.5 eV. The results for the 2H tautomer are summarised in Tables 50 and 51. It was difficult to achieve self consistency for most of the calculated IP's.

Inspection of Table 50 indicates that several states vary significantly with respect to the set of reference configurations and the number of roots calculated.

The first two peaks in the PE spectrum are of almost equal intensity; the present calculations suggest four states occur in this region and therefore each peak can be associated with two ionised states. The first peak centred at 11.3 eV is due to the $1^2A'$ and $1^2A''$ states. Ionisation from the 3a'' orbital has a calculated I.P. of 11.03 eV and is relatively stable with respect to the set of reference configurations chosen. The $1^2A'$ state (ionisation from $LP_{2N4-N2-N3}$) is also relatively insensitive to the chosen reference configurations and has a calculated IP of 11.15 eV.

The present calculations suggest that the second peak is due to the $2^2A'$ and $2^2A''$ states. The $2^2A'$ states varies considerably with respect to the chosen reference configurations (11.58-11.90 eV). The $2^2A''$ state also varies (by 0.2 eV) depending on the set of reference configurations (11.39-11.59 eV). The ionisation potentials are also significantly underestimated by the present theoretical treatment.

The third peak (centred at 13.63 eV) is due to ionisation from the 13a' orbital. This state also varies significantly with respect to the chosen set of reference configurations (12.96-13.32 eV). The remaining states are predicted to involve a significant amount of shake up. The shake up states are all associated with either the fourth or fifth peaks in the spectrum. Both peaks are broad and diffuse. They are also of less intensity than the first three peaks, and this is consistent with the present assignment of shake up states.

The present theoretical assignment is summarised in Table 55.

Conclusions

The present theoretical approach has generally provided acceptable results. The most noticeable inadequacy of the present theoretical procedure is the inability to predict acceptable results for ionisation from lone pairs. It appears that the present basis sets should be supplemented by polarisation functions in an attempt to overcome this problem. The basis sets might be further improved by the addition of diffuse Rydberg orbitals at the centre of mass; since this may well have a significant effect on the 'shake up' states.

References

1. Dunning, T.H., J.Chem.Phys., 53, 2823 (1970).
2. Huzinaga, S., J.Chem.Phys., 42, 1293 (1965).
3. See Appendix in Peyerimhoff, S.D., Buenker, R.J. and Allen, L.C., J.Chem.Phys., 65, 734 (1966).
4. Saunders, V.R. and Guest, M.F., "Atmol3" (SERC 1976, RL-76101 and RL-76106).
5. Buenker, R.J. and Peyerimhoff, S.O., Theor.Chim.Acta., 35, 33 (1974).
6. Buenker, R.J., Peyerimhoff, S.O. and Butscher, W., Mol.Phys., 35, 771 (1978).
7. Nygaard, L., Christen, D., Tormud Nielsen, J., Jonas Pedersen, E., Snerling, O., Vestergaard, E. and de Sorensen, G., J.Mol.Struc., 22, 401 (1974).
8. Genson, D.W. and Christoffersen, R.E., J.Am.Chem.Soc., 94, 6904 (1972).
9. Mely, B. and Pullman, A., Theor.Chim.Acta., 13, 278 (1969).
10. Clementi, E., Clementi, H. and Davis, D.R., J.Chem.Phys., 46, 4725 (1967).
11. Palmer, M.H., Gaskell, A.J. and Barber, M.S., Theor.Chim.Acta., 23, 52 (1971).
12. Preston, H. and Kaufman, J., Int.J.Quantum.Chem.Symp., 7, 207 (1973).
13. Von Niessen W., Cederbaum, L.S. and Diercksen, G.H.F., J.Am.Chem.Soc., 98, 2066 (1976).
14. Cradock, S., Findlay, R.H. and Palmer, M.H., Tetrahedron, 29, 2173 (1973).

15. Tanaka, K., Nomura, T., Takeshi, N., Tatewaki, H., Takada, T., Kashiwagi, H., Sasaki, F. and Ohno, K., J.Chem.Phys., 67, 5738 (1979).

16. Christen, D., Griffiths, J.H., Sheridan, J., Z.Naturforsch, 37a, 1378 (1982).

17. Case, D.A., Cook, M., Karplus, M., J.Chem.Phys., 73, 3294 (1980).

18. Tae-Kyu Ha, J.Mol.Struc., 51, 87 (1979).

19. Simpson, I., Ph.D. Thesis, Edinburgh University (1980).

20. Berthier, G., Praud, L., Serre, J., The Jerusalem Symp. on Quantum Chemistry and Biochemistry, Vol. 2 (1969), p. 40.

21. Palmer, M.H., Simpson, I. and Wheeler, R.J., Z.Naturforsch., 36a, 1246 (1981).

22. Bolton, K., Brown, R.D., Burden, F.R. and Mishra, A., J.Mol.Struct., 27, 261 (1975).

23. Mazurek, A.P. and Osman, P., J.Phys.Chem., 89, 460 (1985).

Appendix A

Photoelectron Spectroscopy

Photoelectron spectroscopy involves the application of the photoelectric effect to the study of the electronic structure of molecules. Ejection of an electron is possible whenever the ionisation potential (E_I) is less than or equal to the photon energy ($h\nu$). Conservation of energy between the ion and the ejected electron requires that

$$h\nu = E_K + E_I \qquad (1)$$

where E_I is the ionisation energy and E_K is the kinetic energy of the ejected electron. If one now rearranges equation (1)

$$E_K = h\nu - E_I \qquad (2)$$

it is obvious that by using monoenergetic radiation one can determine the ionisation potential by measuring the kinetic energy of the ejected electron. Thus, photoelectron spectroscopy involves the measurement of the kinetic energies (E_K) of photoelectrons ejected by monoenergetic radiation in order to determine the ionisation potentials (E_I), intensities, and angular distributions of these electrons.

The ionisation energy, E_I, can be written as

$$E_I = E_j + E^+_{vib} + E^+_{rot} \qquad (3)$$

where E_j is the adiabatic ionisation energy for ejection of an electron from level j and E^+_{vib} and E^+_{rot} are the vibrational and rotational energies of the positive ion. Vibrational structure is

often within the resolution of most photoelectron spectrometers but rotational fine structure is rarely observed.

(i) Direct Photoionisation

Direct photoionisation is the process by which an electron is ejected from a molecule M(X; v'') in its electronic ground state (X), and vibrational level v'', thereby producing a molecular ion $M^+(x, v')$ in any one of its electronic states x and vibrational levels v' such that

$$M(X;\ v'') + h\nu \rightarrow M^+(x;\ v') \qquad (4)$$

The probability of such a transition is determined by the square of the transition moment integral

$$M = \langle \Psi'' \mid \Sigma p \mid \Psi' \rangle \qquad (5)$$

where p is the dipole moment operator and the sum extends over all electrons i and nuclei j. The dipole length matrix element of equation (5) can be expressed either as a dipole velocity integral

$$M_v = \frac{h^2}{mE} \langle \Psi'' \mid \Sigma \nabla \mid \Psi' \rangle \qquad (6)$$

or as a dipole acceleration integral

$$M_a = \frac{h^2}{mE^2} \langle \Psi'' \mid \Sigma \nabla V \mid \Psi' \rangle \qquad (7)$$

where ∇ is the gradient operator and $\nabla V = Z/r^2$.

Using the Born-Oppenheimer approximation, the wavefunction can be separated into the product of electronic and nuclear functions

$$\Psi(r;\ R) = \Psi_e(r;\ R)\Psi_n(R) \qquad (8)$$

If one neglects the interactions between vibrational and rotational motion, the nuclear wavefunction $\Psi(R)$ can be expressed as a product of vibrational Ψ_v and rotational Ψ_τ wavefunctions

$$\Psi_n(R) = (\frac{1}{R})\,\Psi_v(R)\Psi_\tau(R) \qquad (9)$$

The dipole operator can also be separated into electronic and nuclear dependent parts.

$$\sum_{i,j} p = \sum_i p_e + \sum_j P_n \qquad (10)$$

Substituting these results into equation (5) yields

$$M = \iint \Psi_e^{*''}(r;R)(\frac{1}{R})\Psi_v^{*''}(R)\Psi_\tau^{*''}(R) \mid \sum_i p_e + \sum_j p_n \mid \Psi_e'(r;R) \times (\frac{1}{R})\Psi_v'(R)\Psi_\tau'(R)dr\,dR \qquad (11)$$

The above integral can be separated according to the electronic and nuclear operators

$$M = \int (\frac{1}{R})\Psi_v^{*''}(R)\Psi_\tau^{*''}(R)\left(\frac{1}{R}\right)\Psi_v'(R)\Psi_\tau'(R)dR \int \Psi_e^{*''}(r;R) \mid \sum_i p_e \mid \Psi_e'(r;R)dr$$
$$+ \int (\frac{1}{R})\Psi_v^{*''}(R)\Psi_v^{*''}(R) \mid \sum_j p_n \mid (\frac{1}{R})\Psi_v'(R)\Psi_\tau'(R)dR \int \Psi_e^{*''}(r;R)\Psi_e'(r;R)dr \qquad (12)$$

The second term in equation (12) vanishes because electron eigenfunctions belonging to different electronic states are orthogonal. Equation 12 can be further simplified by integration over rotational coordinates

$$M = \int \Psi^{*''}(R)\Psi_\tau'(R)\sin\theta\cos\phi\,d\theta\,d\phi \int \Psi_v^{*''}(R)\Psi_v'(R)dR$$
$$\times \int \Psi_e^{*''}(r;R) \mid \sum_i p_e \mid \Psi_e'(r;R)dr \qquad (13)$$

The first integral in equation 13 is a constant for any given combination of rotational levels J'', J' and the second and third integrals are, to a good approximation, independent of J, and therefore equation 13 can be simplified to

$$M = \int \Psi_v^{*''}(R)\Psi_v'(R)dR \int \Psi_e^{*''}(r;R) \mid \sum_i p_e \mid \Psi_e'(r;R)dr \qquad (14)$$

The second integral in equation 14

$$M_e(r;R) = \int \Psi_e^{*''}(r;R) \mid \sum_i p_e \mid \Psi_e'(r;R)dr \qquad (15)$$

is the electric dipole moment for a given nuclear configuration (R); in most cases it varies only slightly with (R).

One can express equation 15 as a Taylor series expansion about the R value corresponding to the maximum in the product $\Psi_v^{*''}\ \Psi_v'$ (usually the equilibrium ground state configuration R_o) as

$$M_e(r;R) = M_e(r;R_o) + \left[\frac{\partial M_e(r;R)}{\partial R}\right]_{R_o}(R-R_o) + \ldots\ldots \qquad (16)$$

In general electronic transition moments are usually calculated using only the first term and therefore

$$M_e(r;R_o) = \int \Psi_e^{*''}(r;R_o) \mid \sum_i p_e \mid \Psi_e'(r;R_o)dr \qquad (17)$$

assuming that the variation of M_e with R is negligible.

(ii) 'Shake Up' States

A 'shake-up' state is one in which ionisation is accompanied by simultaneous excitation of another electron into an unoccupied orbital. Equation 17 has been derived on the assumption that photoionisation is a single step one-electron process in which the interaction between a neutral molecule and a photon can be described by a one electron operator. In order to describe two electron processes (such as shake-up states) one need only replace the single determinant wavefunction with the more correct CI expansion of the wavefunction.

The wavefunction Ψ_j of the jth electronic state can be expressed as a configuration interaction expansion over all electronic configurations Φ_i belonging to the same spin and symmetry species.

$$\Psi_j = \sum_{i=1}^{\infty} C_{ij} \Phi_i \qquad (18)$$

Substituting this into equation 17 yields

$$M_e = \langle \Psi'' \mid p \mid \sum_{i=1}^{\infty} C_{ij}\Phi_i \rangle = \sum_{i=1}^{\infty} C_{ij} \langle \Psi'' \mid p \mid \Phi_i \rangle \qquad (19)$$

Transitions to the state described by Ψ_j are allowed if any of the components in the summation of equation 19 are non zero. The intensities of such transitions are determined by the square of equation 19, i.e. the square of the configuration interaction coefficients and the transition moment integral, $\sum_k \mid C_{kj} \langle \Psi'' \mid p \mid \Phi_k \rangle \mid^2$, for the allowed configurations Φ_K in the expansion over the i configurations.

(iii) Adiabatic and Vertical Ionisation Energies

Several different ionisation energies can be measured, depending on the degree of vibrational excitation of the ions. The two most commonly reported ionisation energies are:

1. The adiabatic ionisation energy E_{Ia} which corresponds to the following transition

$$M(X, v'' = 0) + h\nu \rightarrow M^{+}(x, v' = 0) + e^{-} \qquad (20)$$

This is the minimum energy required to eject an electron from a molecule in its ground vibrational state and transform it into a positive ion in the lowest vibrational level of an electronic state x of the ion.

2. The vertical ionisation energy E_{Iv} which corresponds to the transition

$$M(X, v'' = 0) + h\nu \rightarrow M^{+}(x, v' = n) + e^{-} \qquad (21)$$

where n is the value of the vibrational quantum number v' which corresponds to the vibrational level whose wavefunction gives the largest overlap with the v'' = 0 wavefunction. This is the most probable transition and usually corresponds to the vertical transitions where the internuclear separations of the ionic state are similar to those of the ground state.

Table 1 - Different Theoretical Assignments of the PES Spectrum of Pyrrole

Genson et al [8]	$1a_2(\pi)$	$2b_1(\pi)$	$9a_1$	$1b_1(\pi)$	$6b_2$	$5b_2$	$8a_1$	$7a_1$	$4b_2$	$6a_1$
Pullman et al [9]	$1a_2(\pi)$	$2b_1(\pi)$	$9a_1$	$6b_2$	$1b_1(\pi)$	$5b_2$	$8a_1$	$7a_1$	$4b_2$	$6a_1$
Clementi et al [10] and Palmer et al [11]	$1a_2(\pi)$	$2b_1(\pi)$	$9a_1$	$6b_2$	$5b_2$	$1b_1(\pi)$	$8a_1$	$7a_1$	$4b_2$	$6a_1$
Preston et al [12]	$1a_2(\pi)$	$2b_1(\pi)$	$9a_1$	$6b_2$	$1b_1(\pi)$	$5b_2$	$8a_1$	$7a_1$	$4b_2$	$6a_1$
Von Niessen et al [13]	$1a_2(\pi)$	$2b_1(\pi)$	$9a_1$	$6b_2$	$1b_1(\pi)$	$5b_2$	$8a_1$	$7a_1$	$4b_2$	$6a_1$

Table 2 Theoretical Results of Van Niessen et al [13]

I.P.(exptl)	Theoretical [13]	MO
8.21	8.17	$1a_2(\pi)$
9.20	8.92	$2b_1(\pi)$
12.60	12.98	$9a_1$
∿13.0	13.39	$6b_2$
∿13.7	13.70	$1b_1(\pi)$
∿14.3	14.37	$5b_2$
∿14.8	14.86	$8a_1$
∿17.5	18.17	$7a_1$
∿18.1	18.96	$4b_2$
∿18.8	19.64	$6a_1$

Table 3 Eigenvalues for SCF MO's

Eigenvalue/a.u.	Symmetry	Centres/bond orbitals
-.8004	$6a_1$	C5N1H1C2 - C3H3C4H4
-.7708	b_2	N1 + C2C3H3 - C5C4H4
-.7415	$7a_1$	N1C2H2C3C4C5H5
-.5989	$8a_1$	N1H1 - C2C3H3C4H4C5H5
-.5856	$5b_2$	N1C2H2C5H5
-.5739	$1b_1$	N1C2C3C4C5
-.5485	$6b_2$	C2N1C5 - C3C4
-.5316	$9a_1$	C2H2C5H5 - C3H3C4H4
-.3519	$2b_1$	N1 - C3 - C4
-.3018	$1a_2$	C2C3 - C4C5

Table 4 Calculated Ionisation Potentials for Pyrroles

State	I.P./e.V.	Excitation Process	Table No.
1^2A_2	7.96	$-1a_2$	8a
1^2B_1	8.87	$-2b_1$	9a
2^2B_1	12.28	$-1b_1+[-1a_2+(1a_2\rightarrow 3b_1)]$	9b
1^2A_1	12.76	$-9a_1$	7a
1^2B_2	13.40	$-6b_2$	10a
2^2B_2	14.40	$-5b_2$	10b
2^2A_1	14.50	$-8a_1$	7b
2^2A_2	14.51	$-1a_2+(2b_1\rightarrow 3b_1)$	8b
3^2B_1	14.67	$-1a_2+(1a_2\rightarrow 3b_1)$	9c
3^2A_2	15.18	$[-1a_2+(1a_2\rightarrow 2a_2)]$ + $[-1a_2+(2b_1\rightarrow 3b_1)]$	8c
4^2B_1	16.59	$[-2b_1+(2b_1\rightarrow 3b_1)]$ + $[-2b_1+(1a_2\rightarrow 2a_2)]$	9d
4^2A_2	16.99	$[-1a_2+(1a_2\rightarrow 2a_2)]$ + $[-1a_2+(2b_1\rightarrow 3b_1)]$	8d
3^2A_1	17.11	$-7a_1$	7c
3^2B_2	17.65	$-9a_1+(1a_2\rightarrow 3b_1)$	10c
4^2B_2	18.03	$-4b_2$	10d
4^2A_1	18.30	$-1a_2+(6b_2\rightarrow 3b_1)$	7d

Table 5 Pyrrole - Summary of Calculations

State	No. of main Configurations	Σcoefficient^2	Correction/a.u	CI energy/ a.u.	I.P./eV
GS	3M1R	.9073	-.0246	-209.0476	-
1^2A_1	3M3R	.8612	-.0446	-208.5756	12.84
2^2A_1	3M3R	.8639	-.0438	-208.5079	14.69
3^2A_1	3M3R	.8275	-.0577	-208.3915	17.85
1^2A_1	6M4R	.8651	-.0426	-208.5794	12.74
2^2A_1	6M4R	.8633	-.0439	-208.5131	14.54
3^2A_1	6M4R	.8666	-.0427	-208.4170	17.16
4^2A_1	6M4R	.8068	-.0679	-208.3944	17.78
1^2A_1	9M4R	.8657	-.0422	-208.5788	12.76
2^2A_1	9M4R	.8635	-.0440	-208.5147	14.50
3^2A_1	9M4R	.8692	-.0419	-208.4187	17.11
4^2A_1	9M4R	.8512	-.0470	-208.3752	18.30
1^2A_2	2M2R	.8832	-.0330	-208.7553	7.95
2^2A_2	2M2R	.6981	-.0993	-208.5056	14.75
1^2A_2	7M4R	.8957	-.0286	-208.7559	7.94
2^2A_2	7M4R	.8283	-.0516	-208.5110	14.60
3^2A_2	7M4R	.8593	-.0410	-208.4912	15.14
4^2A_2	7M4R	.8397	-.0527	-208.4225	17.01
1^2A_2	9M4R	.9033	-.0262	-208.7550	7.96
2^2A_2	9M4R	.8630	-.0409	-208.5142	14.51
3^3A_2	9M4R	.8730	-.0372	-208.4897	15.18
4^2A_2	9M4R	.8640	-.0435	-208.4233	16.99
1^2B_1	2M2R	.8702	-.0381	-208.7205	8.90
2^2B_1	2M2R	.7410	-.0865	-208.5874	12.52
1^2B_1	5M4R	.8765	-.0358	-208.7229	8.84
2^2B_1	5M4R	.8478	-.0465	-208.5914	12.41
3^2B_1	5M4R	.8269	-.0543	-208.5190	14.38
4^2B_1	5M4R	.7701	-.0752	-208.4595	16.00

Cont'd....

Table 5 (cont'd)

State	No. of main Configurations	coefficient^2	Correction/a.u.	CI energy/ a.u.	I.P./eV
1^2B_1	11M4R	.8994	-.0274	-208.7216	8.87
2^2B_1	11M4R	.8762	-.0369	-208.5962	12.28
3^2B_1	11M4R	.8737	-.0376	-208.5086	14.67
4^2B_1	11M4R	.8356	-.0506	-208.4378	16.59
1^2B_2	2M2R	.8655	-.0427	-208.5526	13.47
2^2B_2	2M2R	.8644	-.0431	-208.5164	14.45
1^2B_2	5M4R	.8683	-.0412	-208.5570	13.35
2^2B_2	5M4R	.8648	-.0426	-208.5185	14.40
3^2B_2	5M4R	.8102	-.0681	-208.4145	17.23
4^2B_2	5M4R	.7094	-.1009	-208.3870	17.97
1^2B_2	8M4R	.8704	-.0403	-208.5552	13.40
2^2B_2	8M4R	.8648	-.0425	-208.5182	14.41
3^2B_2	8M4R	.8470	-.0500	-208.3988	17.65
4^2B_2	8M4R	.8457	-.0508	-208.3850	18.03

Table 6 Pyrrole - Ground State $X\ ^1A_1$

Coefficient^2	$4a_1$-$9a_1$	$1b_1$	$2b_1$	$3b_1$	$3b_2$-$5b_2$	$6b_2$	$1a_2$	$2a_2$
.8959M	12	2	2	-	6	2	2	-
.0056M	12	2	2	2	6	2	-	-
.0058M	12	2	1	1	6	-	1	1

Table 7a Pyrrole 1^2A_1

Coefficient^2	$4a_1$-$6a_1$	$7a_1$	$8a_1$	$9a_1$	$1b_1$	$2b_1$	$3b_1$	$5b_1$	$3b_2$	$4b_2$	$5b_2$	$6b_2$	$1a_2$	$2a_2$
.8574M	6	2	2	1	2	2	-	-	2	2	2	2	2	-
.0002M	6	1	2	2	2	2	-	-	2	2	2	2	2	-
.0001M	6	2	1	2	2	2	-	-	2	2	2	2	2	-
.0027M	6	2	2	1	2	2	-	-	2	2	2	2	1	1
.0003M	6	2	1	2	2	1	1	-	2	2	2	2	2	-
.0024M	6	2	2	2	2	2	1	-	2	2	1	2	1	-
.0023M	6	2	2	2	2	2	1	-	2	2	2	1	1	-
.0002M	6	2	2	2	2	2	-	1	2	2	2	1	1	-
.0000M	6	2	2	2	2	1	2	-	2	2	2	1	1	-

Table 7b Pyrrole 2^2A_1

Coefficient^2	$4a_1$-$6a_1$	$7a_1$	$8a_1$	$9a_1$	$1b_1$	$2b_1$	$3b_1$	$5b_1$	$3b_2$	$4b_2$	$5b_2$	$6b_2$	$1a_2$	$2a_2$
.0002M	6	2	2	1	2	2	-	-	2	2	2	2	2	-
.0000M	6	1	2	2	2	2	-	-	2	2	2	2	2	-
.8574M	6	2	1	2	2	2	-	-	2	2	2	2	2	-
.0019M	6	2	2	1	2	2	-	-	2	2	2	2	1	1
.0006M	6	2	1	2	2	1	1	-	2	2	2	2	2	-
.0000M	6	2	2	2	2	2	1	-	2	2	1	2	1	-
.0034M	6	2	2	2	2	2	1	-	2	2	2	1	1	-
.0000M	6	2	2	2	2	2	-	1	2	2	2	1	1	-
.0000M	6	2	2	2	2	1	2	-	2	2	2	1	1	-

Table 7c Pyrrole 3^2A_1

Coefficient^2	$4a_1$-$6a_1$	$7a_1$	$8a_1$	$9a_1$	$1b_1$	$2b_1$	$3b_1$	$5b_1$	$3b_2$	$4b_2$	$5b_2$	$6b_2$	$1a_2$	$2a_2$
.0002M	6	2	2	1	2	2	-	-	2	2	2	2	2	-
.7897M	6	1	2	2	2	2	-	-	2	2	2	2	2	-
.0000M	6	2	1	2	2	2	-	-	2	2	2	2	2	-
.0172M	6	2	2	1	2	2	-	-	2	2	2	2	1	1
.0026M	6	2	1	2	2	1	1	-	2	2	2	2	2	-
.0544M	6	2	2	2	2	2	1	-	2	2	1	2	1	-
.0048M	6	2	2	2	2	2	1	-	2	2	2	1	1	-
.0002M	6	2	2	2	2	2	-	1	2	2	2	1	1	-
.0001M	6	2	2	2	2	1	2	-	2	2	2	1	1	-

Table 7d Pyrrole 4^2A_1

Coefficient^2	$4a_1$-$6a_1$	$7a_1$	$8a_1$	$9a_1$	$1b_1$	$2b_1$	$3b_1$	$5b_1$	$3b_2$	$4b_2$	$5b_2$	$6b_2$	$1a_2$	$2a_2$
.0001M	6	2	2	1	2	2	-	-	2	2	2	2	2	-
.0036M	6	1	2	2	2	2	-	-	2	2	2	2	2	-
.0000M	6	2	1	2	2	2	-	-	2	2	2	2	2	-
.0030M	6	2	2	1	2	2	-	-	2	2	2	2	1	1
.0110M	6	2	1	2	2	1	1	-	2	2	2	2	2	-
.0005M	6	2	2	2	2	2	1	-	2	2	1	2	1	-
.7945M	6	2	2	2	2	2	1	-	2	2	2	1	1	-
.0246M	6	2	2	2	2	2	-	1	2	2	2	1	1	-
.0140M	6	2	2	2	2	1	2	-	2	2	2	1	1	-

Table 8a Pyrrole 1^2A_2

Coefficient^2	$4a_1$-$9a_1$	$1b_1$	$2b_1$	$3b_1$	$4b_1$	$5b_1$	$6b_1$	$3b_2$-$6b_2$	$1a_2$	$2a_2$	$4a_2$
.8732M	12	2	2	-	-	-	-	8	1	-	-
.0053M	12	2	2	-	-	-	-	8	-	1	-
.0009M	12	2	2	-	-	-	-	8	-	-	1
.0059M	12	2	-	-	-	-	-	8	2	1	-
.0088M	12	1	2	1	-	-	-	8	1	-	-
.0028M	12	2	1	1	-	-	-	8	1	-	-
.0029M	12	2	1	-	-	1	-	8	1	-	-
.0006M	12	1	1	2	-	-	-	8	1	-	-
.0028M	12	2	1	1	-	-	-	8	-	1	-

Table 8b Pyrrole 2^2A_2

Coefficient^2	$4a_1$-$9a_1$	$1b_1$	$2b_1$	$3b_1$	$4b_1$	$5b_1$	$6b_1$	$3b_2$-$6b_2$	$1a_2$	$2a_2$	$4a_2$
.0140M	12	2	2	-	-	-	-	8	1	-	-
.1476M	12	2	2	-	-	-	-	8	-	1	-
.0078M	12	2	2	-	-	-	-	8	-	-	1
.0237M	12	2	-	-	-	-	-	8	2	1	-
.0246M	12	1	2	1	-	-	-	8	1	-	-
.5992M	12	2	1	1	-	-	-	8	1	-	-
.0163M	12	2	1	-	-	1	-	8	1	-	-
.0121M	12	1	1	2	-	-	-	8	1	-	-
.0176M	12	2	1	1	-	-	-	8	-	1	-
.0083	12	2	-	2	-	-	-	8	1	-	-
.0085	12	1	1	-	-	-	-	8	2	1	-

Table 8c Pyrrole 3^2A_2

Coefficient^2	$4a_1$-$9a_1$	$1b_1$	$2b_1$	$3b_1$	$4b_1$	$5b_1$	$6b_1$	$3b_2$-$6b_2$	$1a_2$	$2a_2$	$4a_2$
.0006M	12	2	2	-	-	-	-	8	1	-	-
.3278M	12	2	2	-	-	-	-	8	-	1	-
.0188M	12	2	2	-	-	-	-	8	-	-	1
.0083M	12	2	-	-	-	-	-	8	2	1	-
.0099M	12	1	2	1	-	-	-	8	1	-	-
.4718M	12	2	1	1	-	-	-	8	1	-	-
.0096M	12	2	1	-	-	1	-	8	1	-	-
.0090M	12	1	1	2	-	-	-	8	1	-	-
.0173M	12	2	1	1	-	-	-	8	-	1	-
.0075	12	-	2	-	-	-	-	8	2	1	-
.0082	12	1	1	-	-	-	-	8	2	1	-

Table 8d Pyrrole 4^2A_2

Coefficient^2	$4a_1$-$9a_1$	$1b_1$	$2b_1$	$3b_1$	$4b_1$	$5b_1$	$6b_1$	$3b_2$-$6b_2$	$1a_2$	$2a_2$	$4a_2$
.0024M	12	2	2	-	-	-	-	8	1	-	-
.3079M	12	2	2	-	-	-	-	8	-	1	-
.0079M	12	2	2	-	-	-	-	8	-	-	1
.0274M	12	2	-	-	-	-	-	8	2	1	-
.0221M	12	1	2	1	-	-	-	8	1	-	-
.4786M	12	2	1	1	-	-	-	8	1	-	-
.0008M	12	2	1	-	-	1	-	8	1	-	-
.0153M	12	1	1	2	-	-	-	8	1	-	-
.0015	12	2	1	1	-	-	-	8	-	1	-
.0098	12	2	-	2	-	-	-	8	1	-	-

Table 9a Pyrrole 1^2B_1

Coefficient[2]	$4a_1$-$9a_1$	$1b_1$	$2b_1$	$3b_1$	$5b_1$	$3b_2$-$6b_2$	$1a_2$	$2a_2$	$4a_2$
.8591M	12	2	1	-	-	8	2	-	-
.0010M	12	1	2	-	-	8	2	-	-
.0006M	12	2	-	1	-	8	2	-	-
.0064M	12	2	1	2	-	8	-	-	-
.0037M	12	2	1	-	-	8	-	2	-
.0009M	12	-	2	1	-	8	2	-	-
.0001M	12	2	2	1	-	8	-	-	-
.0000M	12	2	2	-	1	8	-	-	-
.0103M	12	1	1	1	-	8	2	-	-
.0156M	12	2	1	-	-	8	1	1	-
.0018M	12	1	2	-	-	8	1	1	-

Table 9b Pyrrole 2^2B_1

Coefficient[2]	$4a_1$-$9a_1$	$1b_1$	$2b_1$	$3b_1$	$5b_1$	$3b_2$-$6b_2$	$1a_2$	$2a_2$	$4a_2$
.0007M	12	2	1	-	-	8	2	-	-
.5102M	12	1	2	-	-	8	2	-	-
.0713M	12	2	-	1	-	8	2	-	-
.0037M	12	2	1	2	-	8	-	-	-
.0025M	12	2	1	-	-	8	-	2	-
.0009M	12	-	2	1	-	8	2	-	-
.2546M	12	2	2	1	-	8	-	-	-
.0092M	12	2	2	-	1	8	-	-	-
.0019M	12	1	1	1	-	8	2	-	-
.0106M	12	2	1	-	-	8	1	1	-
.0105M	12	1	2	-	-	8	1	1	-

Table 9c Pyrrole 3^2B_1

Coefficient^2	$4a_1$-$9a_1$	$1b_1$	$2b_1$	$3b_1$	$5b_1$	$3b_2$-$6b_2$	$1a_2$	$2a_2$	$4a_2$
.0022M	12	2	1	-	-	8	2	-	-
.1662M	12	1	2	-	-	8	2	-	-
.0228M	12	2	-	1	-	8	2	-	-
.0016M	12	2	1	2	-	8	-	-	-
.0001M	12	3	1	-	-	8	-	2	-
.0082M	12	-	2	1	-	8	2	-	-
.5060M	12	2	2	1	-	8	-	-	-
.0137M	12	2	2	-	1	8	-	-	-
.0179M	12	1	1	1	-	8	2	-	-
.1276M	12	2	1	-	-	8	1	1	-
.0075M	12	1	2	-	-	8	1	1	-
.0096	12	2	1	-	-	8	1	-	1

Table 9d Pyrrole 4^2B_1

Coefficient^2	$4a_1$-$9a_1$	$1b_1$	$2b_1$	$3b_1$	$5b_1$	$3b_2$-$6b_2$	$1a_2$	$2a_2$	$4a_2$
.0001M	12	2	1	-	-	8	2	-	-
.0212M	12	1	2	-	-	8	2	-	-
.3217M	12	2	-	1	-	8	2	-	-
.0275M	12	2	1	2	-	8	-	-	-
.0138M	12	2	1	-	-	8	-	2	-
.0178M	12	-	2	1	-	8	2	-	-
.0019M	12	2	2	1	-	8	-	-	-
.0001M	12	2	2	-	1	8	-	-	-
.0124M	12	1	1	1	-	8	2	-	-
.4164M	12	2	1	-	-	8	1	1	-
.0027M	12	1	2	-	-	8	1	1	-
.0160	12	2	1	-	-	8	1	-	1
.0139	12	2	-	1	-	8	1	1	-

Table 10a Pyrrole 1^2B_2

Coefficient^2	$4a_1$-$8a_1$	$9a_1$	$1b_1$	$2b_1$	$3b_1$	$3b_2$	$4b_2$	$5b_2$	$6b_2$	$1a_2$	$2a_2$	$5b_1$
.8546M	10	2	2	2	-	2	2	2	1	2	-	-
.0003M	10	2	2	2	-	2	1	2	2	2	-	-
.0048M	10	2	2	2	-	2	2	1	2	2	-	-
.0054M	10	2	-	1	1	2	2	2	1	2	-	-
.0013M	10	2	2	2	-	2	2	2	1	1	1	-
.0037M	10	1	2	2	1	2	2	2	2	1	-	-
.0003M	10	1	2	2	-	2	2	2	2	1	-	1
.0001M	10	1	2	1	2	2	2	2	2	1	-	-

Table 10b Pyrrole 2^2B_2

Coefficient^2	$4a_1$-$8a_1$	$9a_1$	$1b_1$	$2b_1$	$3b_1$	$3b_2$	$4b_2$	$5b_2$	$6b_2$	$1a_2$	$2a_2$	$5b_1$
.0056M	10	2	2	2	-	2	2	2	1	2	-	-
.0000M	10	2	2	2	-	2	1	2	2	2	-	-
.8532M	10	2	2	2	-	2	2	1	2	2	-	-
.0001M	10	2	-	1	1	2	2	2	1	2	-	-
.0002M	10	2	2	2	-	2	2	2	1	1	1	-
.0054M	10	1	2	2	1	2	2	2	2	1	-	-
.0002M	10	1	2	2	-	2	2	2	2	1	-	1
.0000M	10	1	2	1	2	2	2	2	2	1	-	-

Table 10c Pyrrole 3^2B_2

Coefficient^2	$4a_1$-$8a_1$	$9a_1$	$1b_1$	$2b_1$	$3b_1$	$3b_2$	$4b_2$	$5b_2$	$6b_2$	$1a_2$	$2a_2$	$5b_1$
.0000M	10	2	2	2	-	2	2	2	1	2	-	-
.0379M	10	2	2	2	-	2	1	2	2	2	-	-
.0001M	10	2	2	2	-	2	2	1	2	2	-	-
.0008M	10	2	-	1	1	2	2	2	1	2	-	-
.0004M	10	2	2	2	-	2	2	2	1	1	1	-
.7660M	10	1	2	2	1	2	2	2	2	1	-	-
.0254M	10	1	2	2	-	2	2	2	2	1	-	1
.0163M	10	1	2	1	2	2	2	2	2	1	-	-
.0101	10	1	2	1	-	2	2	2	2	1	-	-

Table 10d Pyrrole 4^2B_2

Coefficient^2	$4a_1$-$8a_1$	$9a_1$	$1b_1$	$2b_1$	$3b_1$	$3b_2$	$4b_2$	$5b_2$	$6b_2$	$1a_2$	$2a_2$	$5b_1$
.0007M	10	2	2	2	-	2	2	2	1	2	-	-
.7350M	10	2	2	2	-	2	1	2	2	2	-	-
.0005M	10	2	2	2	-	2	2	1	2	2	-	-
.0076M	10	2	-	1	1	2	2	2	1	2	-	-
.0150M	10	2	2	2	-	2	2	2	1	1	1	-
.0738M	10	1	2	2	1	2	2	2	2	1	-	-
.0020M	10	1	2	2	-	2	2	2	2	1	-	1
.0012M	10	1	2	1	2	2	2	2	2	1	-	-

Table 11 Theoretical Assignment of the PES of Pyrrole

Vertical I.P./eV	State	Table No.
8.23	1^2A_2	8a
9.22	1^2B_1	9a
12.85	2^2B_1	9b
	1^2A_1	7a
13.65	1^2B_2	10a
14.3	2^2B_2	10b
14.7	2^2A_1	7b
	2^2A_2	8b
	3^2B_1	9c
	3^2A_2	8c
17.5	4^2B_1	9d
	4^2A_2	8d
	3^2A_1	7c
	3^2B_2	10c

Table 12 Previous Theoretical Studies of Imidazole

Symmetry	SCF X_α [17]	Koopmans' [18]	Koopmans' [19]	Koopmans' [20]
10'	18.99	21.95	21.99	23.71
11a'	18.08	21.02	20.94	21.84
12a'	15.67	16.76	16.78	18.59
13a'	15.40	16.67	16.65	17.60
14a'	15.10	15.76	15.72	17.33
15a'	11.90	11.77	11.76	12.83
1a"	12.90	16.55	16.59	18.57
2a"	10.05	11.09	11.07	12.71
3a"	8.38	9.19	9.02	11.17

Table 13 SCF Eigenvalues for Imidazole

Eigenvalue/eV	Symmetry	Centres/Bond Orbitals
22.01	10a'	N3C2N1H/C5H5C4H4
20.93	11a'	C2H2N3C4 - N1H1C5H5
16.87	12a'	N1C5H5C4N3C2
16.62	1a"	N1C2N3C4C5
16.57	13a'	C2H2N1C5H5
15.69	14a'	C2H2 - N3C4H4
11.75	15a'	N3LP
11.06	2a"	N1C2 - N3C4
9.13	3a"	N3C2N1 - C4C5

Table 14 CI Results for Imidazole

No. of reference Configurations	State	Σcoefficient^2	Correction/ a.u.	CI Energy/a.u.	I.P./eV
3M1R	X^1A^1	.9103	-.0260	-225.0574	-
6M4R	$1^2A'$	.8560	-.0507	-224.7134	9.36
6M4R	$2^2A'$	.8663	-.0459	-224.5402	14.07
6M4R	$3^2A'$	.8679	-.0449	-224.5059	15.00
6M4R	$4^2A'$	.8644	-.0461	-224.4960	15.28
8M5R	$1^2A'$	.8839	-.0383	-224.7155	9.30
8M5R	$2^2A'$	.8126	-.0727	-224.5594	13.55
8M5R	$3^2A'$	.8652	-.0464	-224.5421	14.02
8M5R	$4^2A'$	.8688	-.0441	-224.5010	15.14
8M5R†	$5^2A'$	Root 4 repeated			
9M5R	$1^2A'$	.8843	-.0381	-224.7154	9.31
9M5R	$2^2A'$	.8657	-.0464	-224.5431	13.99
9M5R	$3^2A'$	.8308	-.0603	-224.5261	14.46
9M5R†	$4^2A'$	Root 3 repeated			
9M5R	$5^2A'$	.8689	-.0447	-224.5074	14.96
10M5R	$1^2A'$	.8815	-.0392	-224.7160	9.29
10M5R	$2^2A'$	.8663	-.0458	-224.5395	14.09
10M5R	$3^2A'$	.8745	-.0430	-224.5319	14.30
10M5R	$4^2A'$	.8685	-.0442	-224.5016	15.12
10M5R*	$8^2A'$	.6848	-.1035	-224.4480	16.58
8M6R	$1^2A'$	.8823	-.0391	-224.7189	9.21
8M6R	$2^2A'$	.8063	-.0748	-224.5599	13.54
8M6R	$3^2A'$	.8652	-.0463	-224.5412	14.04
8M6R	$4^2A'$	.8662	-.0458	-224.5035	15.06
8M6R	$5^2A'$	.8686	-.0442	-224.5013	15.13
8M6R	$6^2A'$	.8019	-.0702	-224.4936	15.34
5M4R	$1^2A''$	.8838	-.0358	-224.7271	8.71
5M4R	$2^2A''$	.8627	-.0441	-224.6872	10.07
5M4R	$3^2A''$	.8063	-.0658	-224.5662	13.37
5M4R	$4^2A''$	.7761	-.0814	-224.5053	15.02

/Cont'd...

Table 14 (Cont'd)

No. of reference Configurations	State	Σcoefficient^2	Correction/ a.u.	CI Energy/a.u.	I.P./eV
9M5R	$1^2A''$	.8859	-.0353	-224.7393	8.65
9M5R	$2^2A''$	.8668	-.0427	-224.6906	9.98
9M5R	$3^2A''$	.8551	-.0464	-224.5574	13.60
9M5R	$4^2A''$	.5828	-.1379	-224.5088	14.93
9M5R	$5^2A''$	.7123	-.0984	-224.4808	15.69
9M6R	$1^2A''$	.8884	-.0344	-224.7386	8.67
9M6R	$2^2A''$	.8739	-.0405	-224.6939	9.89
9M6R	$3^2A''$	.8511	-.0484	-224.5581	13.59
9M6R	$4^2A''$	.8207	-.0618	-224.5014	15.13
9M6R	$5^2A''$	.7758	-.0793	-224.4954	15.29
9M6R	$6^2A''$	.8214	-.0621	-224.4546	16.40

* failed to find root 5

† repeated a root, i.e. failed to find the desired root.

Table 15 Calculated Ionisation Potentials for Imidazole

State	I.P./eV	Excitation Process	Table No.
$1^2A''$	8.67	$-3a''$	17a
$1^2A'$	9.21	$-15a'$	18a
$2^2A''$	9.89	$-2a''$	17b
$2^2A'$	13.54	$[-15a' + (3a'' \rightarrow 4a'')]$	18b
$3^2A''$	13.59	$-1a'' + [-3a'' + (3a'' \rightarrow 4a'')]$	17c
$3^2A'$	14.04	$-14a$	18c
$4^2A'$	15.06	$-12a'$	18d
$5^2A'$	15.13	$-13a'$	18e
$4^2A''$	15.13	$-1a'' + [-3a'' + (3a'' \rightarrow 4a'')]$	17d
$5^2A''$	15.29	$[-3a'' + (3a'' \rightarrow 5a'')] + [-2a'' + (3a'' \rightarrow 4a'')]$	17e
$6^2A'$	15.34	$[-15a' + (3a'' \rightarrow 5a'')]$	18f
$6^2A''$	16.40	$[-2a'' + (3a'' \rightarrow 4a'')]$	17f

Table 16 Imidazole X^1A'

Coefficient^2	6a'-15a'	1a"	2a"	3a"	4a"	5a"
.9003M	20	2	2	2	-	-
.0054M	20	2	2	-	2	-
.0046M	20	2	1	1	1	1

Table 17a Imidazole $1^2A''$

Coefficient[2]	6a'-15a'	1a"	2a"	3a"	4a"	5a"	7a"
.8752M	20	2	2	1	-	-	-
.0001M	20	1	2	2	-	-	-
.0003M	20	2	1	2	-	-	-
.0002M	20	2	2	-	1	-	-
.0014M	20	2	2	-	-	1	-
.0005M	20	2	-	2	1	-	-
.0030M	20	2	-	2	-	1	-
.0039M	20	2	1	1	1	-	-
.0037M	20	2	1	1	-	1	-

Table 17b Imidazole $2^2A''$

Coefficient[2]	6a'-15a'	1a"	2a"	3a"	4a"	5a"	7a"
.0002M	20	2	2	1	-	-	-
.0009M	20	1	2	2	-	-	-
.8512M	20	2	1	2	-	-	-
.0007M	20	2	2	-	1	-	-
.0043M	20	2	2	-	-	1	-
.0001M	20	2	-	2	1	-	-
.0067M	20	2	-	2	-	1	-
.0017M	20	2	1	1	1	-	-
.0081M	20	2	1	1	-	1	-

Table 17c Imidazole $3^2A''$

Coefficient[2]	6a'-15a'	1a"	2a"	3a"	4a"	5a"	7a"
.0004M	20	2	2	1	-	-	-
.5592M	20	1	2	2	-	-	-
.0009M	20	2	1	2	-	-	-
.1889M	20	2	2	-	1	-	-
.0052M	20	2	2	-	-	1	-
.0424M	20	2	-	2	1	-	-
.0063M	20	2	-	2	-	1	-
.0358M	20	2	1	1	1	-	-
.0118M	20	2	1	1	-	1	-

Table 17d Imidazole $4^2A''$

Coefficient[2]	6a'-15a'	1a"	2a"	3a"	4a"	5a"	7a"
.0015M	20	2	2	1	-	-	-
.1270M	20	1	2	2	-	-	-
.0017M	20	2	1	2	-	-	-
.5782M	20	2	2	-	1	-	-
.0212M	20	2	2	-	-	1	-
.0053M	20	2	-	2	1	-	-
.0001M	20	2	-	2	-	1	-
.0277M	20	2	1	1	1	-	-
.0581M	20	2	1	1	-	1	-
.0132	20	2	2	-	-	-	1

Table 17e Imidazole $5^2A''$

Coefficient^2	6a'-15a'	1a"	2a"	3a"	4a"	5a"	7a"
.0090M	20	2	2	1	-	-	-
.0008M	20	1	2	2	-	-	-
.0056M	20	2	1	2	-	-	-
.0000M	20	2	2	-	1	-	-
.4831M	20	2	2	-	-	1	-
.0008M	20	2	-	2	1	-	-
.0021M	20	2	-	2	-	1	-
.2561M	20	2	1	1	1	-	-
.0183M	20	2	1	1	-	1	-
.0139	20	2	2	-	-	-	1
.0183	20	20	1	-	1	1	-

Table 17f Imidazole $6^2A''$

Coefficient^2	6a'-15a'	1a"	2a"	3a"	4a"	5a"	7a"
.0029M	20	2	2	1	-	-	-
.0553M	20	1	2	2	-	-	-
.0006M	20	2	1	2	-	-	-
.0073M	20	2	2	-	1	-	-
.0581M	20	2	2	-	-	1	-
.0069M	20	2	-	2	1	-	-
.0223M	20	2	-	2	-	1	-
.6405M	20	2	1	1	1	-	-
.0275M	20	2	1	1	-	1	-

Table 18a Imidazole $1^2A'$

Coefficient[2]	6a'-11a'	12a'	13a'	14a'	15a'	1a"	2a"	3a"	4a"	5a"
.8355M	12	2	2	2	1	2	2	2	-	-
.0013M	12	1	2	2	2	2	2	2	-	-
.0002M	12	2	1	2	2	2	2	2	-	-
.0000M	12	2	2	1	2	2	2	2	-	-
.0114M	12	2	2	2	1	2	1	2	1	-
.0256M	12	2	2	2	1	2	1	2	-	1
.0021M	12	2	2	2	1	2	2	1	1	-
.0062M	12	2	2	2	1	2	2	1	-	1

Table 18b Imidazole $2^2A'$

Coefficient[2]	6a'-11a'	12a'	13a'	14a'	15a'	1a"	2a"	3a"	4a"	5a"	6a"	8a"
.0002M	12	2	2	2	1	2	2	2	-	-	-	-
.0011M	12	1	2	2	2	2	2	2	-	-	-	-
.0001M	12	2	1	2	2	2	2	2	-	-	-	-
.0001M	12	2	2	1	2	2	2	2	-	-	-	-
.0190M	12	2	2	2	1	2	1	2	1	-	-	-
.0003M	12	2	2	2	1	2	1	2	-	1	-	-
.7812M	12	2	2	2	1	2	2	1	1	-	-	-
.0034M	12	2	2	2	1	2	2	1	-	1	-	-
.0105	12	2	2	2	1	1	2	2	-	1	-	-
.0125	12	2	2	2	1	2	2	1	-	-	1	-
.0115	12	2	2	2	1	2	2	1	-	-	-	1
.0183	12	2	2	2	1	2	1	1	2	-	-	-
.0277	12	2	2	2	1	2	1	1	1	1	-	-

Table 18c Imidazole $3^2A'$

Coefficient^2	6a'-11a'	12a'	13a'	14a'	15a'	1a"	2a"	3a"	4a"	5a"
.0001M	12	2	2	2	1	2	2	2	-	-
.0021M	12	1	2	2	2	2	2	2	-	-
.0004M	12	2	1	2	2	2	2	2	-	-
.8621M	12	2	2	1	2	2	2	2	-	-
.0000M	12	2	2	2	1	2	1	2	1	-
.0001M	12	2	2	2	1	2	1	2	-	1
.0001M	12	2	2	2	1	2	2	1	1	-
.0003M	12	2	2	2	1	2	2	1	-	1

Table 18d Imidazole $4^2A'$

Coefficient^2	6a'-11a'	12a'	13a'	14a'	15a'	1a"	2a"	3a"	4a"	5a"
.0027M	12	2	2	2	1	2	2	2	-	-
.8469M	12	1	2	2	2	2	2	2	-	-
.0044M	12	2	1	2	2	2	2	2	-	-
.0023M	12	2	2	1	2	2	2	2	-	-
.0002M	12	2	2	2	1	2	1	2	1	-
.0056M	12	2	2	2	1	2	1	2	-	1
.0039M	12	2	2	2	1	2	2	1	1	-
.0001M	12	2	2	2	1	2	2	1	-	1

Table 18e Imidazole $5^2A'$

Coefficient^2	6a'-11a'	12a'	13a'	14a'	15a'	1a"	2a"	3a"	4a"	5a"
.0003M	12	2	2	2	1	2	2	2	-	-
.0046M	12	1	2	2	2	2	2	2	-	-
.8598M	12	2	1	2	2	2	2	2	-	-
.0003M	12	2	2	1	2	2	2	2	-	-
.0012M	12	2	2	2	1	2	1	2	1	-
.0002M	12	2	2	2	1	2	1	2	-	1
.0017M	12	2	2	2	1	2	2	1	1	-
.0005M	12	2	2	2	1	2	2	1	-	1

Table 18f Imidazole $6^2A'$

Coefficient^2	6a'-11a'	12a'	13a'	14a'	15a'	1a"	2a"	3a"	4a"	5a"	8a"	10a"
.0002M	12	2	2	2	1	2	2	2	-	-	-	-
.0002M	12	1	2	2	2	2	2	2	-	-	-	-
.0001M	12	2	1	2	2	2	2	2	-	-	-	-
.0005M	12	2	2	1	2	2	2	2	-	-	-	-
.0032M	12	2	2	2	1	2	1	2	1	-	-	-
.0149M	12	2	2	2	1	2	1	2	-	1	-	-
.0246M	12	2	2	2	1	2	2	1	1	-	-	-
.7582M	12	2	2	2	1	2	2	1	-	1	-	-
.0127	12	2	2	2	1	1	2	2	1	-	-	-
.0221	12	2	2	2	1	2	2	1	-	-	1	-
.0134	12	2	2	2	1	2	2	1	-	-	-	1
.0131	12	2	2	2	1	2	1	1	-	2	-	-
.0112	12	2	2	2	1	2	1	1	1	1	-	-

Table 19 Assignment of the Imidazole PE Spectrum

Vertical I.P./eV	State	Table No.
8.78	$1^2A"$	17a
10.3	$1^2A'$	18a
10.3	$2^2A"$	17b
13.7	$2^2A'$ #	18b
13.7	$3^2A"$ #	17c
14.0	$3^2A'$	18c
14.7	$4^2A'$	18d
15.3	$5^2A'$	18e
	#$4^2A"$	17d
	#$5^2A"$	17e
	#$6^2A'$	18f

Shake up state

Table 20 SCF Eigenvalues for Pyrazole

Eigenvalue/eV	Symmetry	Bond Centres
-22.03	10a'	N1C2C3H3C4H4N5
-20.45	11a'	N5N1H1C2H2H3C4
-16.91	12a'	N1H1N5C4H4 - C3 - C2
-16.80	1a"	N1C2C3C4C5
-16.19	13a'	C2H2N1B5C4H4 - C3H3
-15.62	14a'	C2H2C3C4H4
-12.45	15a'	LPN
-10.25	1a"	C3C4N5 - N1
-9.68	2a"	N5 - C3C2

Table 21 Summary of Previous Calculations on Pyrazole

	Eigenvalue/eV			
Orbital	Kaufman [12]	Berthier [20]	Tae Kyu Ha [18]	Palmer [14]
10a'	-21.94	-22.71	-22.00	-24.07
11a'	-20.37	-21.22	-20.57	-22.79
12a'	-16.81	-18.82	-16.96	-19.24
13a'	-16.12	-17.13	-16.24	-18.59
14a'	-15.55	-16.80	-15.75	-17.58
15a'	-12.41	-12.73	-12.50	-13.84
1a"	-16.71	-18.49	-16.84	-19.15
2a"	-10.16	-12.39	-10.41	-13.01
3a"	-9.62	-11.07	-9.81	-11.32

Table 22 Summary of Results for Pyrazole

No. of reference Configurations	State	Σ coefficient^2	Correction/a.u.	CI energy/a.u.	I.P./eV
3M1R	GS	.9100	-.0263	-225.0469	-
5M3R	$1^2A'$	.8812	-.0402	-224.6797	9.99
5M3R	$2^2A'$	.8624	-.0469	-224.5285	14.11
5M3R	$3^2A'$	.8692	-.0439	-224.4966	14.97
6M4R	$1^2A'$	.8717	-.0429	-224.6706	10.24
6M4R	$2^2A'$	.8594	-.0484	-224.5334	13.97
6M4R	$3^2A'$	.8685	-.0443	-224.5007	14.86
6M4R	$4^2A'$	.8637	-.0464	-224.4765	15.52
8M5R	$1^2A'$	.8847	-.0372	-224.6773	10.06
8M5R	$2^2A'$	.8617	-.0475	-224.5344	13.94
8M5R	$3^2A'$	.8689	-.0439	-224.4980	14.94
8M5R	$4^2A'$	.8635	-.0464	-224.4762	15.53
8M5R	$5^2A'$	.8309	-.0575	-224.4694	15.71
5M4R	$1^2A''$	.8746	-.0394	-224 .7088	9.20
5M4R	$2^2A''$	.8692	-.0414	-224.6941	9.60
5M4R	$3^2A''$	.7955	-.0677	-224.5504	13.51
5M4R	$4^2A''$	.7424	-.0881	-224.4698	15.71
10M5R	$1^2A''$	.8825	-.0361	-224.7131	9.08
10M5R	$2^2A''$	.8796	-.0381	-224.6934	9.62
10M5R	$3^2A''$	.8483	-.0509	-224.5592	13.27
10M5R	$4^2A''$	.8513	-.0497	-224.4875	15.22
10M5R	$5^2A''$	.7488	-.0926	-224.4767	15.52

Table 23 Calculated Ionisation Potentials of Pyrazole

State	I.P./eV	Excitation Process	Table No.
$1^2A''$	9.08	-3a"	26a
$2^2A''$	9.62	-2a"	26b
$1^2A'$	10.06	-15a' (LPN)	25a
$3^2A''$	13.27	-1a" + [-3a" + (3a" → 4a")]	26c
$2^2A'$	13.94	-14a'	25b
$3^2A'$	14.94	-13a'	25c
$4^2A''$	15.22	-2a" + (3a" → 5a")	26d
$5^2A''$	15.52	-3a" + (3a" → 4a")	26e
$4^2A'$	15.53	-12a'	25d
$5^2A'$	15.71	[-15a' + (3a" → 4a")] + [-15a' + (2a" → 4a")]	25e

Table 24 Pyrazole GS X^1A'

Coefficient^2	6a'-15a'	1a"	2a"	3a"	4a"	5a"
.8990M	20	2	2	2	-	-
.0060M	20	2	2	-	2	-
.0051M	20	2	1	1	1	1

Table 25a Pyrazole $1^2A'$

Coefficient[2]	6a'-11a'	12a'	13a'	14a'	15a'	1a"	2a"	3a"	4a"	5a"	10a"
.8292M	12	2	2	2	1	2	2	2	-	-	-
.0000M	12	1	2	2	2	2	2	2	-	-	-
.0000M	12	2	1	2	2	2	2	2	-	-	-
.0024M	12	2	2	1	2	2	2	2	-	-	-
.0024M	12	2	2	2	1	2	1	2	1	-	-
.0313M	12	2	2	2	1	2	2	1	1	-	-
.0135M	12	2	2	2	1	2	2	1	-	1	-
.0057M	12	2	2	2	1	2	2	1	-	-	1

Table 25b Pyrazole $2^2A'$

Coefficient[2]	6a'-11a'	12a'	13a'	14a'	15a'	1a"	2a"	3a"	4a"	5a"	10a"
.0042M	12	2	2	2	1	2	2	2	-	-	-
.0004M	12	1	2	2	2	2	2	2	-	-	-
.0018M	12	2	1	2	2	2	2	2	-	-	-
.8484M	12	2	2	1	2	2	2	2	-	-	-
.0020M	12	2	2	2	1	2	1	2	1	-	-
.0018M	12	2	2	2	1	2	2	1	1	-	-
.0029M	12	2	2	2	1	2	2	1	-	1	-
.0002M	12	2	2	2	1	2	2	1	-	-	1

Table 25c Pyrazole $3^2A'$

Coefficient[2]	6a'-11a'	12a'	13a'	14a'	15a'	1a"	2a"	3a"	4a"	5a"	10a"
.0000M	12	2	2	2	1	2	2	2	-	-	-
.0001M	12	1	2	2	2	2	2	2	-	-	-
.8612M	12	2	1	2	2	2	2	2	-	-	-
.0020M	12	2	2	1	2	2	2	2	-	-	-
.0033M	12	2	2	2	1	2	1	2	1	-	-
.0013M	12	2	2	2	1	2	2	1	1	-	-
.0010M	12	2	2	2	1	2	2	1	-	1	-
.0000M	12	2	2	2	1	2	2	1	-	-	1

Table 25d Pyrazole $4^2A'$

Coefficient[2]	6a'-11a'	12a'	13a'	14a'	15a'	1a"	2a"	3a"	4a"	5a"	10a"
.0001M	12	2	2	2	1	2	2	2	-	-	-
.8619M	12	1	2	2	2	2	2	2	-	-	-
.0000M	12	2	1	2	2	2	2	2	-	-	-
.0003M	12	2	2	1	2	2	2	2	-	-	-
.0003M	12	2	2	2	1	2	1	2	1	-	-
.0001M	12	2	2	2	1	2	2	1	1	-	-
.0006M	12	2	2	2	1	2	2	1	-	1	-
.0000M	12	2	2	2	1	2	2	1	-	-	1

Table 25e Pyrazole $5^2A'$

Coefficient[2]	6a'-11a'	12a'	13a'	14a'	15a'	1a"	2a"	3a"	4a"	5a"	10a"
.0036M	12	2	2	2	1	2	2	2	-	-	-
.0004M	12	1	2	2	2	2	2	2	-	-	-
.0002M	12	2	1	2	2	2	2	2	-	-	-
.0003M	12	2	2	1	2	2	2	2	-	-	-
.2182M	12	2	2	2	1	2	1	2	1	-	-
.5886M	12	2	2	2	1	2	2	1	1	-	-
.0116M	12	2	2	2	1	2	2	1	-	1	-
.0079M	12	2	2	2	1	2	2	1	-	-	1
.0133	12	2	2	2	1	2	1	2	-	1	-

Table 26a Pyrazole $1^2A''$

Coefficient[2]	6a'-15a'	1a"	2a"	3a"	4a"	5a"
.8180M	20	2	2	1	-	-
.0006M	20	1	2	2	-	-
.0509M	20	2	1	2	-	-
.0010M	20	2	2	-	1	-
.0000M	20	2	-	2	1	-
.0008M	20	2	-	2	-	1
.0063M	20	1	2	1	1	-
.0022M	20	2	1	1	-	1
.0004M	20	1	1	1	2	-
.0022M	20	2	1	-	1	1
.0098	20	2	1	1	-	1

Table 26b Pyrazole $2^2A''$

Coefficient[2]	6a'-15a'	1a"	2a"	3a"	4a"	5a"
.0503M	20	2	2	1	-	-
.0011M	20	1	2	2	-	-
.8175M	20	2	1	2	-	-
.0001M	20	2	2	-	1	-
.0000M	20	2	-	2	1	-
.0049M	20	2	-	2	-	1
.0070M	20	1	2	1	1	-
.0002M	20	2	1	1	-	1
.0001M	20	1	1	1	2	-
.0002M	20	2	1	-	1	1

Table 26c Pyrazole $3^2A''$

Coefficient^2	6a'-15a'	1a"	2a"	3a"	4a"	5a"
.0009M	20	2	2	1	-	-
.5721M	20	1	2	2	-	-
.0009M	20	2	1	2	-	-
.1365M	20	2	2	-	1	-
.0645M	20	2	-	2	1	-
.0036M	20	2	-	2	-	1
.0001M	20	1	2	1	1	-
.0678M	20	2	1	1	-	1
.0006M	20	1	1	1	2	-
.0013M	20	2	1	-	1	1
.0100M	20	1	2	1	-	1

Table 26d Pyrazole $4^2A''$

Coefficient^2	6a'-15a'	1a"	2a"	3a"	4a"	5a"
.0072M	20	2	2	1	-	-
.0004M	20	1	2	2	-	-
.0015M	20	2	1	2	-	-
.0479M	20	2	2	-	1	-
.1086M	20	2	-	2	1	-
.0387M	20	2	-	2	-	1
.0191M	20	1	2	1	1	-
.5995M	20	2	1	1	-	1
.0173M	20	1	1	1	2	-
.0112M	20	2	1	-	1	1

Table 26e Pyrazole $5^2A''$

Coefficient[2]	6a'-15a'	1a"	2a"	3a"	4a"	5a"
.0012M	20	2	2	1	-	-
.0980M	20	1	2	2	-	-
.0001M	20	2	1	2	-	-
.5476M	20	2	2	-	1	-
.0510M	20	2	-	2	1	-
.0128M	20	2	-	2	-	1
.0020M	20	1	2	1	1	-
.0346M	20	2	1	1	-	1
.0010M	20	1	1	1	2	-
.0042M	20	2	1	-	1	1
.0178	20	-	2	2	1	-
.0540	20	2	1	1	-	1
.0179	20	1	1	2	1	-

Table 27 Theoretical Assignment of the Pyrazole PE Spectrum

Experimental Vertical I.P./eV	Assignment	Table No.
9.15	$1^2A''$	26a
9.88	$2^2A''$	26b
10.7	$1^2A''$	25a
13.6	$\#\ 3^2A''$	26c
	$2^2A'$	25b
14.7	$3^2A'$	25c
15.1	$\#\ 4^2A''$	26d
	$\#\ 5^2A''$	26e
	$4^2A'$	25d
	$\#\ 5^2A'$	25e

\# Shake up state

Table 28 SCF Eigenvalues for 1,2,4 Triazole 1-H tautomer

Eigenvalue/eV	Orbital	Bond Centres
-22.59	10a'	N4C5N1N2C3
-20.82	11a'	N1, N2C3N4C5
-17.50	12a'	N4C5, N1N2
-17.04	1a'	N1N2C3N4C5
-16.54	13a'	N2C3N4C5
-13.73	14a'	LP N2 + N4
-12.30	15a'	LP N2 - N4
-11.48	2a"	N1N2 - C3N4C5
-10.63	3a"	N1C5 - N2C3N4

Table 29 Summary of Results for 1,2,4 Triazole 1-H tautomer

No. of reference Configurations	State	Σcoefficient^2	Correction/ a.u.	CI Energy/a.u.	I.P./eV
5M1R	X^1A'	.8995	-.0348	-241.0972	-
4M4R	$1^1A'$	.8424	-.0660	-240.7215	10.22
4M4R	$2^1A'$	.8467	-.0618	-240.6638	11.79
4M4R	$3^1A'$	.7594	-.1073	-240.5766	14.16
4M4R	$4^1A'$	.8516	-.0602	-240.5462	14.99
6M2R	$1^1A'$	.8658	-.0529	-240.7215	10.22
6M2R	$2^1A'$	.8630	-.0544	-240.6755	11.47
10M5R	$1^1A'$	.8655	-.0526	-240.7215	10.22
10M5R	$2^1A'$	.8658	-.0528	-240.6768	11.44
10M5R	$3^1A'$	.8357	-.0689	-240.5580	14.67
10M5R	$4^1A'$	.8528	-.0597	-240.5470	14.97
10M5R	$5^1A'$	.7638	-.1016	-240.5408	15.14
4M2R	$1^1A''$	.8746	-.0463	-240.7152	10.39
4M2R	$2^1A''$	.8640	-.0519	-240.7082	10.58
8M4R	$1^1A''$	.8719	-.0474	-240.7208	10.18
8M4R	$2^1A''$	.8623	-.0527	-240.7114	10.43
8M4R	$3^2A''$	.8544	-.0568	-240.5849	13.88
8M4R	$4^1A''$	.7878	-.0930	-240.5437	15.00
8M5R	$1^1A''$	.8708	-.0481	-240.7237	10.16
8M5R	$2^2A''$	.8609	-.0535	-240.7141	10.42
8M5R	$3^1A''$	.8524	-.0566	-240.5776	14.14
8M5R	$4^1A''$	.7871	-.0909	-240.5308	15.41
8M5R	$5^1A''$	.7419	-.1083	-240.5048	16.12

Table 30 Calculated Ionisation Potentials of 1,2,4 Triazole 1-H

State	Excitation Process	I.P./eV	Table No.
$1^2A''$	-3a"	10.16	33a
$1^2A'$	-15a'	10.22	32a
$2^2A''$	-2a"	10.42	33b
$2^2A'$	-14a	11.44	32b
$3^2A''$	-1a" + [-2a" + (3a"→ 4a")] + [-2a" + (2a"→ 5a")]	14.14	33c
$3^2A'$	[-15a' + (3a"→ 4a")]	14.67	32c
$4^2A'$	-13a'	14.97	32d
$5^2A'$	[-15a' + (3a"→ 5a")]	15.14	32e
$4^2A''$	[-3a" + (3"→ 4a")] + [-2a" + (3a" →4a")]	15.41	33d
$5^2A''$	[-2a" + (3a" →4a")] + [-2a" + (3a" →5a")]	16.12	33e

Table 31 1,2,4 Triazole 1-H Ground State X^1A'

Coefficient	$6a_1$-$15a_1$	1a"	2a"	3a"	4a"	5a"
.8830M	20	2	2	2	-	-
.0026M	20	2	-	2	-	2
.0067M	20	2	2	-	2	-
.0039M	20	1	2	1	1	1
.0032M	20	2	1	1	1	1

Table 32a 1,2,4 Triazole $1^2A'$

Coefficient^2	6a'-12a'	13a'	14a'	15a'	1a"	2a"	3a"	4a"	5a"	6a"	7a"	9a"
.8350M	14	2	2	1	2	2	2	-	-	-	-	-
.0004M	14	1	2	2	2	2	2	-	-	-	-	-
.0008M	14	2	1	2	2	2	2	-	-	-	-	-
.0011M	14	2	2	1	1	2	2	-	1	-	-	-
.0097M	14	2	2	1	2	1	2	1	-	-	-	-
.0123M	14	2	2	1	2	-	2	-	1	-	-	-
.0006M	14	2	2	1	2	2	1	1	-	-	-	-
.0002M	14	2	2	1	2	2	1	-	1	-	-	-
.0000M	14	2	2	1	2	1	1	2	-	-	-	-
.0054M	14	2	1	2	2	2	1	1	-	-	-	-

Table 32b 1,2,4 Triazole 1-H $2^2A'$

Coefficient^2	6a'-12a'	13a'	14a'	15a'	1a"	2a"	3a"	4a"	5a"	6a"	7a"	9a"
.0012M	14	2	2	1	2	2	2	-	-	-	-	-
.0011M	14	1	2	2	2	2	2	-	-	-	-	-
.8267M	14	2	1	2	2	2	2	-	-	-	-	-
.0001M	14	2	2	1	1	2	2	-	1	-	-	-
.0002M	14	2	2	1	2	1	2	1	-	-	-	-
.0106M	14	2	2	1	2	-	2	-	1	-	-	-
.0131M	14	2	2	1	2	2	1	1	-	-	-	-
.0054M	14	2	2	1	2	2	1	-	1	-	-	-
.0001M	14	2	2	1	2	1	1	2	-	-	-	-
.0074M	14	2	1	2	2	2	1	1	-	-	-	-

Table 32c 1,2,4 Triazole $3^2A'$

Coefficient[2]	6a'-12'	13a'	14a'	15a'	1a"	2a"	3a"	4a"	5a"	6a"	7a"	9a"
.0003M	14	2	2	1	2	2	2	-	-	-	-	-
.0001M	14	1	2	2	2	2	2	-	-	-	-	-
.0010M	14	2	1	2	2	2	2	-	-	-	-	-
.0145M	14	2	2	1	1	2	2	-	1	-	-	-
.0238M	14	2	2	1	2	1	2	1	-	-	-	-
.0010M	14	2	2	1	2	-	2	-	1	-	-	-
.7052M	14	2	2	1	2	2	1	1	-	-	-	-
.0516M	14	2	2	1	2	2	1	-	1	-	-	-
.0138M	14	2	2	1	2	1	1	2	-	-	-	-
.0243M	14	2	1	2	2	2	1	1	-	-	-	-
.0127	14	2	2	1	2	2	1	-	-	-	1	-
.0182	14	2	2	1	2	1	1	1	1	-	-	-

Table 32d 1,2,4 Triazole $4^2A'$

Coefficient[2]	6a'-12a'	13a'	14a'	15a'	1a"	2a"	3a"	4a"	5a"	6a"	7a"	9a"
.0006M	14	2	2	1	2	2	2	-	-	-	-	-
.8466M	14	1	2	2	2	2	2	-	-	-	-	-
.0020M	14	2	1	2	2	2	2	-	-	-	-	-
.0054M	14	2	2	1	1	2	2	-	1	-	-	-
.0000M	14	2	2	1	2	1	2	1	-	-	-	-
.0001M	14	2	2	1	2	-	2	-	1	-	-	-
.0001M	14	2	2	1	2	2	1	1	-	-	-	-
.0005M	14	2	2	1	2	2	1	-	1	-	-	-
.0021M	14	2	2	1	2	1	1	2	-	-	-	-
.0008M	14	2	1	2	2	2	1	1	-	-	-	-

Table 32e 1,2,4 Triazole 1-H $5^2A'$

Coefficient[2]	6a'-12a'	13a'	14a'	15a'	1a"	2a"	3a"	4a"	5a"	6a"	7a"	9a"
.0002M	14	2	2	1	2	2	2	-	-	-	-	-
.0011M	14	1	2	2	2	2	2	-	-	-	-	-
.0002M	14	2	1	2	2	2	2	-	-	-	-	-
.0073M	14	2	2	1	2	1	2	1	-	-	-	-
.0170M	14	2	2	1	2	-	2	-	1	-	-	-
.0594M	14	2	2	1	2	2	1	1	-	-	-	-
.6487M	14	2	2	1	2	2	1	-	1	-	-	-
.0068M	14	2	2	1	2	1	1	2	-	-	-	-
.0225M	14	2	1	2	2	2	1	1	-	-	-	-
.0201	14	2	2	1	2	2	1	-	-	1	-	-
.0125	14	2	2	1	2	2	1	-	-	-	-	1
.0435	14	2	1	2	2	2	1	-	1	-	-	-

Table 33a 1,2,4 Triazole 1-H $1^2A"$

Coefficient[2]	6a'-15a'	1a"	2a"	3a"	4a"	5a"
.8142M	20	2	2	1	-	-
.0005M	20	1	2	2	-	-
.0441M	20	2	1	2	-	-
.0000M	20	2	2	-	1	-
.0012M	20	2	-	2	1	-
.0005M	20	2	-	2	-	1
.0018M	20	2	1	1	1	-
.0085M	20	2	1	1	-	1

Table 33b 1,2,4 Triazole 1-H $2^2A''$

Coefficient^2	6a'-15a'	1a"	2a"	3a"	4a"	5a"
.0434M	20	2	2	1	-	-
.0015M	20	1	2	2	-	-
.7997M	20	2	1	2	-	-
.0001M	20	2	2	-	1	-
.0008M	20	2	-	2	1	-
.0091M	20	2	-	2	-	1
.0054M	20	2	1	1	1	-
.0009M	20	2	1	1	-	1

Table 33c 1,2,4 Triazole 1-H $3^2A''$

Coefficient^2	6a'-15a'	1a"	2a"	3a"	4a"	5a"
.0000M	20	2	2	1	-	-
.6389M	20	1	2	2	-	-
.0020M	20	2	1	2	-	-
.0598M	20	2	2	-	1	-
.0341M	20	2	-	2	1	-
.0102M	20	2	-	2	-	1
.0921M	20	2	1	1	1	-
.0153M	20	2	1	1	-	1

Table 33d 1,2,4 Triazole 1-H $4^2A''$

Coefficient[2]	6a'-15a'	1a"	2a"	3a"	4a"	5a"
.0044M	20	2	2	1	-	-
.0103M	20	1	2	2	-	-
.0000M	20	2	1	2	-	-
.6088M	20	2	2	-	1	-
.0035M	20	2	-	2	1	-
.0004M	20	2	-	2	-	1
.1070M	20	2	1	1	1	-
.0527M	20	2	1	1	-	1
.0112	20	2	2	-	-	1
.0133	20	1	2	1	1	-
.0122	20	1	2	1	-	1

Table 33e 1,2,3 Triazole 1-H $5^2A''$

Coefficient[2]	6a'-15a'	1a"	2a"	3a"	4a"	5a"
.0069M	20	2	2	1	-	-
.0879M	20	1	2	2	-	-
.0033M	20	2	1	2	-	-
.07270M	20	2	2	-	1	-
.0181M	20	2	-	2	1	-
.0092M	20	2	-	2	-	1
.5341M	20	2	1	1	1	-
.0959M	20	2	1	1	-	1
.0409	20	2	2	-	-	1
.0098	20	2	-	1	1	1
.0129	20	1	1	2	1	-

Table 34 Theoretical Assignment of the PE Spectrum of 1,2,4 Triazole

Vertical

I.P./eV [14]	State	Table No.
10.0	$1^2A''$	33a
10.56	$2^2A''$	33b
11.1	$1^2A'$	32a
12.15	$2^2A'$	32b
14.6	# $3^2A''$	33c
	# $3^2A'$	32c
15.1	$4^2A'$	32d
	# $5^2A'$	32e
	# $4^2A''$	33d
16.0	# $5^2A''$	33e

Shake up state

Table 35 Summary of Results for 1,2,3 Triazole 1H

No. of reference Configurations	State	Σcoefficient^2	Correction/ a.u.	C.I. Energy/ a.u.	I.P./eV
1M1R	GSX'A'	.8810	-.0420	-241.0525	-
4M4R	1^2A'	.8384	-.0660	-240.6812	10.10
4M4R	2^2A'	.8221	-.0742	-240.6318	11.45
4M4R	3^2A'	.8529	-.0588	-240.4937	15.20
4M4R	4^2A'	.8507	-.0595	-240.4767	15.67
7M5R	1^2A'	.8469	-.0616	-240.6898	9.86
7M5R	2^2A'	.8415	-.0635	-240.6426	11.15
7M5R	3^2A'	.8529	-.0587	-240.4949	15.17
7M5R	4^2A'	.8499	-.0599	-240.4802	15.57
7M5R	5^2A'	.3289	-.2283	-240.5504	13.66
3M3R	1^2A"	.8608	-.0512	-240.6984	9.64
3M3R	2^2A"	.8471	-.0580	-240.6682	10.45
3M3R	3^2A"	.7271	-.1109	-240.5468	13.76
8M4R	1^2A"	.8638	-.0498	-240.7031	9.51
8M4R	2^2A"	.8592	-.0525	-240.6699	10.41
8M4R	3^2A"	.8410	-.0595	-240.5515	13.63
8M4R	4^2A"	.7962	-.0841	-240.5031	14.95

Table 36 1,2,3 Triazole 1H Calculated Ionisation Potentials

State	Excitation Process	I.P./eV	Table No.
$1^2A''$	-3a"	9.51	38a
$1^2A'$	-15a'	9.86	37a
$2^2A''$	-2a"	10.41	38b
$2^2A'$	-14a'	11.15	37b
$3^2A''$	-1a" +[-3a" + (3a" → 4a")] + [-2a" + (3a" → 4a")]	13.63	38c
$4^2A''$	-3a" + [(3a" → 4a")] [-2a" + (3a" → 4a")]	14.95	38d
$3^2A'$	-13a'	15.17	37c
$4^2A'$	-12a'	15.57	37d

Table 37a 1,2,3 Triazole 1H $1^2A'$

Coefficient^2	6a'-10a'	11a'	12a'	13a'	14a'	15a'	1a"	2a"	3a"	4a"	5a"
.8303M	10	2	2	2	2	1	2	2	2	-	-
.0000M	10	1	2	2	2	2	2	2	2	-	-
.0003M	10	2	1	2	2	2	2	2	2	-	-
.0000M	10	2	2	1	2	2	2	2	2	-	-
.0016M	10	2	2	2	1	2	2	2	2	-	-
.0133M	10	2	2	2	2	1	2	1	2	-	1
.0017M	10	2	2	2	1	2	2	2	1	1	-

Table 37b 1,2,3 Triazole 1H $2^2A'$

Coefficient^2	6a'-10a'	11a'	12a'	13a'	14a'	15a'	1a"	2a"	3a"	4a"	5a"
.0019M	10	2	2	2	2	1	2	2	2	-	-
.0024M	10	1	2	2	2	2	2	2	2	-	-
.0006M	10	2	1	2	2	2	2	2	2	-	-
.0005M	10	2	2	1	2	2	2	2	2	-	-
.7998M	10	2	2	2	1	2	2	2	2	-	-
.0042M	10	2	2	2	2	1	2	1	2	-	1
.0321M	10	2	2	2	1	2	2	2	1	1	-

Table 37c 1,2,3 Triazole 1H $3^2A'$

Coefficient^2	6a'-10a'	11a'	12a'	13a'	14a'	15a'	1a"	2a"	3a"	4a"	5a"
.0000M	10	2	2	2	2	1	2	2	2	-	-
.0002M	10	1	2	2	2	2	2	2	2	-	-
.0000M	10	2	1	2	2	2	2	2	2	-	-
.8498M	10	2	2	1	2	2	2	2	2	-	-
.0008M	10	2	2	2	1	2	2	2	2	-	-
.0007M	10	2	2	2	2	1	2	1	2	-	1
.0013M	10	2	2	2	1	2	2	2	1	1	-

Table 37d 1,2,3 Triazole $4^2A'$

Coefficient^2	6a'-10a'	11a'	12a'	13a'	14a'	15a'	1a"	2a"	3a"	4a"	5a"
.0005M	10	2	2	2	2	1	2	2	2	-	-
.0000M	10	1	2	2	2	2	2	2	2	-	-
.8447M	10	2	1	2	2	2	2	2	2	-	-
.0000M	10	2	2	1	2	2	2	2	2	-	-
.0012M	10	2	2	2	1	2	2	2	2	-	-
.0005M	10	2	2	2	2	1	2	1	2	-	1
.0031M	10	2	2	2	1	2	2	2	1	1	-

Table 38a 1,2,3 Triazole 1H $1^2A''$

Coefficient^2	6a'-15a'	1a"	2a"	3a"	4a"	5a"
.8428M	20	2	2	1	-	-
.0009M	20	1	2	2	-	-
.0104M	20	2	1	2	-	-
.0022M	20	2	2	-	1	-
.0002M	20	2	2	-	-	1
.0006M	20	2	-	2	1	-
.0050M	20	1	2	1	1	-
.0017M	20	2	1	1	1	-

Table 38B 1,2,3 Triazole 1H $2^2A''$

Coefficient^2	6a'-15a'	1a"	2a"	3a"	4a"	5a"
.0100M	20	2	2	1	-	-
.0009M	20	1	2	2	-	-
.8264M	20	2	1	2	-	-
.0007M	20	2	2	-	1	-
.0078M	20	2	2	-	-	1
.0010M	20	2	-	2	1	-
.0099M	20	1	2	1	1	-
.0025M	20	2	1	1	1	-

Table 38c 1,2,3 Triazole 1H $3^2A''$

Coefficient^2	6a'-15a'	1a"	2a"	3a"	4a"	5a"
.0030M	20	2	2	1	-	-
.5819M	20	1	2	2	-	-
.0001M	20	2	1	2	-	-
.0987M	20	2	2	-	1	-
.0181M	20	2	2	-	-	1
.0377M	20	2	-	2	1	-
.0042M	20	1	2	1	1	-
.0974M	20	2	1	1	1	-

Table 38d 1,2,3 Triazole 1H $4^2A''$

Coefficient^2	6a'-15a'	1a"	2a"	3a"	4a"	5a"
.0061M	20	2	2	1	-	-
.0032M	20	1	2	2	-	-
.0038M	20	2	1	2	-	-
.5289M	20	2	2	-	1	-
.0001M	20	2	2	-	-	1
.0062M	20	2	-	2	1	-
.0288M	20	1	2	1	1	-
.1900M	20	2	1	1	1	-
.0202	20	2	1	1	-	1
.0112	20	1	1	1	2	-

Table 39 SCF Eigenvalues for 1,2,3 Triazole 2H

Eigenvalue/eV	Symmetry	Bond Centres
-22.56	$4b_2$	N2, C1C5, N3C4
-20.17	$7a_1$	N1N2N3C4C5
-17.35	$8a_1$	N1C5C4N3 - N2
-17.18	$1b_1$	N1N2N3C4C5
-17.04	$5b_2$	N1N2N3
-13.76	$9a_1$	LP_N^+
-12.94	$6b_2$	LP_N^-
-11.11	$1a_2$	N1C5 - N3C4
-10.72	$2b_1$	N2 - C4C5

Table 40 Summary of the results for 1,2,3 Triazole 2-H

No. of reference Configurations	State	Σcoefficient	Correction/ a.u.	C.I. Energy/ a.u.	I.P./eV
1M1R	GSX $^1A_1$	.8739	-.0406	-241.0770	-
8M3R	GSX $^1A_1$	.8830	-.0409	-241.0876	-
8M3R	1^1A_1	.8747	-.0471	-240.8860	5.49
8M3R	2^1A_1	.8050	-.0802	-240.7819	8.32
4M4R	1^2A_1	.8347	-.0709	-240.6574	11.71
4M4R	2^2A_1	.8466	-.0626	-240.5006	15.97
4M4R	3^2A_1	.8011	-.0839	-240.4800	16.54
4M4R	4^2A_1	.8020	-.0801	-240.4309	17.87
10M4R	1^2A_1	.8545	-.0594	-240.6767	11.18
10M4R	2^2A_1	.8565	-.0608	-240.5217	15.40
10M4R	3^2A_1	.8601	-.0561	-240.5142	15.60
10M4R	4^2A_1	.8350	-.0656	-240.4614	17.04
1M1R	1^2A_1	.8423	-.0664	-240.6448	12.05
1M1R	1^2A_2	.8572	-.0545	-240.6910	10.79
4M2R	1^2A_2	.8715	-.0478	-240.6991	10.57
4M2R	2^2A_2	.8117	-.0790	-240.5247	15.32
7M3R	1^2A_2	.8781	-.0450	-240.6998	10.55
7M3R	2^2A_2	.8579	-.0541	-240.5184	15.49
7M3R	3^2A_2	.8177	-.0737	-240.4469	17.43
1M1R	1^2B_1	.8567	-.0555	-240.7121	10.22
2M2R	1^2B_1	.8559	-.0563	-240.7164	10.10
2M2R	2^2B_1	.7590	-.1023	-240.5585	14.40
6M4R	1^2B_1	.8662	-.0511	-240.7251	9.87
6M4R	2^2B_1	.8497	-.0573	-240.5685	14.12
6M4R	3^2B_1	.7829	-.0916	-240.4933	16.17

/Cont'd....

Table 40 (Cont'd)

No. of reference Configurations	State	Σcoefficient	Correction/ a.u.	C.I. Energy/ a.u.	I.P./eV
10M4R	1^2B_1	.8792	-.0448	-240.7238	9.90
10M4R	2^2B_1	.8693	-.0483	-240.5660	14.19
10M4R	3^2B_1	.8396	-.0635	-240.4740	16.70
10M4R	4^2B_1	.7038	-.0921	-240.3832	19.17
1M1R	1^2B_2	.8395	-.0680	-240.6793	11.11
2M2R	1^2B_2	.8402	-.0679	-240.6801	11.09
2M2R	2^2B_2	.8485	-.-623	-240.5106	15.70
6M3R	1^2B_2	.8613	-.0546	-240.6953	10.68
6M3R	2^2B_2	.8542	-.0591	-240.5190	15.47
6M3R	3^2B_2	.6706	-.1489	-240.5598	14.36
9M4R	1^2B_2	.8585	-.0556	-240.6980	10.60
9M4R	2^2B_2	.8495	-.0595	-240.5317	15.13
9M4R	3^2B_2	.8488	-.0629	-240.5224	15.38
9M4R	4^2B_2	.8448	-.0630	-240.4761	16.64
10M4R	1^2B_2	.8598	-.0549	-240.7004	10.53
10M4R	2^2B_2	.8473	-.0607	-240.5356	15.02
10M4R	3^2B_2	.8555	-.0588	-240.5229	15.37
10M4R	4^2B_2	.7915	-.0859	-240.4824	16.47

Table 41 1,2,3 Triazole 2H Calculated Ionisation Potentials

State	Excitation Process	I.P./eV	Table No.
1^2B_1	$-2b_1$	9.90	44a
1^2A_2	$-1a_2$	10.55	46a
1^2B_2	$-6b_2$	10.60	43a
1^2A_1	$-9a_1$	11.18	45a
2^2B_1	$-1b_1 + [-2b_1 + (2b_1 \rightarrow 3b_1)]$	14.19	44b
2^2B_2	$-6b_2 + [(2b_1 \rightarrow 3b_1)]$	15.13	43b
3^2B_2	$-5b_2$	15.38	43c
2^2A_1	$-7a_1 + [-9a_1 + (2b_1 \rightarrow 3b_1)]$	15.40	45b
2^2A_2	$-1a_2 + (2b_1 \rightarrow 3b_1)$	15.49	46b
3^2A_1	$-8a_1$	15.60	45c
4^2B_2	$-9a_1 + (1a_2 \rightarrow 3b_1)$	16.64	43d
3^2B_1	$[-2b_1 + (2b_1 \rightarrow 3b_1)] + [-1a_2 + (1a_2 \rightarrow 3b_1)]$	16.70	44c
4^2A_1	$-7a_1 + [-9a_1 + (2b_1 \rightarrow 3b_1)]$	17.04	45d
3^2A_2	$[-1a_2 + (2b_1 \rightarrow 3b_1)] + [-1a_2 + (1a_2 \rightarrow 2a_2)]$	17.43	46c

Table 42 1,2,3 Triazole 2H grand state X^1A_1

Coefficient^2	$4a_1$-$9a_1$	$1b_1$	$2b_1$	$3b_2$-$6b_2$	$1a_2$	$3b_1$	$2a_2$
.8633M	12	2	2	8	2	-	-
.0023M	12	2	-	8	2	2	-
.0093M	12	2	2	8	-	2	-
.0015M	12	2	2	8	-	-	2
.0009M	12	2	1	8	-	1	2
.0001M	12	2	2	8	1	-	1
.0003M	12	1	1	8	2	2	-
.0054M	12	2	1	8	1	1	1

Table 43a 1,2,3 Triazole 1^2B_2

Coefficient^2	$4a_1$-$8a_1$	$9a_1$	$1b_1$	$2b_1$	$1a_2$	$3b_2$-$4b_2$	$5b_2$	$6b_2$	$3b_1$	$2a_2$	$6b_1$
.8160M	10	2	2	2	2	4	2	1	-	-	-
.0013M	10	2	2	2	2	4	1	2	-	-	-
.0060M	10	2	2	2	-	4	2	1	2	-	-
.0000M	10	2	2	2	-	4	1	2	2	-	-
.0008M	10	2	2	1	2	4	2	1	1	-	-
.0115M	10	2	2	2	1	4	2	1	-	1	-
.0005M	10	1	2	1	2	4	2	2	-	1	-
.0226M	10	1	2	2	1	4	2	2	1	-	-
.0009M	10	1	2	2	1	4	2	2	-	-	1
.0000M	10	1	2	1	1	4	2	2	2	-	-

Table 43b 1,2,3 Triazole 2H 2^2B_2

Coefficient^2	$4a_1$-$8a_1$	$9a_1$	$1b_1$	$2b_1$	$1a_2$	$3b_2$-$4b_2$	$5b_2$	$6b_2$	$3b_1$	$2a_2$	$6b_1$
.0001M	10	2	2	2	2	4	2	1	-	-	-
.0062M	10	2	2	2	2	4	1	2	-	-	-
.0001M	10	2	2	2	-	4	2	1	2	-	-
.0001M	10	2	2	2	-	4	1	2	2	-	-
.8122M	10	2	2	1	2	4	2	1	1	-	-
.0073M	10	2	2	2	1	4	2	1	-	1	-
.0065M	10	1	=	1	2	4	2	2	-	1	-
.0006M	10	1	2	2	1	4	2	2	1	-	-
.0000M	10	1	2	2	1	4	2	2	-	-	1
.0144M	10	1	2	1	1	4	2	2	2	-	-
.0111	10	2	2	1	2	4	2	1	-	-	1
.0101	10	2	2	1	1	4	2	1	1	1	-

Table 43c 1,2,3 Triazole 2H 3^2B_2

Coefficient^2	$4a_1$-$8a_1$	$9a_1$	$1b_1$	$2b_1$	$1a_2$	$3b_2$-$4b_2$	$5b_2$	$6b_2$	$3b_1$	$2a_2$	$6b_1$
.0022M	10	2	2	2	2	4	2	1	-	-	-
.8316M	10	2	2	2	2	4	1	2	-	-	-
.0001M	10	2	2	2	-	4	2	1	2	-	-
.0078M	10	2	2	2	-	4	1	2	2	-	-
.0100M	10	2	2	1	2	4	2	1	1	-	-
.0001M	10	2	2	2	1	4	2	1	-	1	-
.0001M	10	1	2	1	2	4	2	2	-	1	-
.0003M	10	1	2	2	1	4	2	2	1	-	-
.0001M	10	1	2	2	1	4	2	2	-	-	1
.0002M	10	1	2	1	1	4	2	2	2	-	-

Table 43d 1,2,3 Triazole 2H 4^2B_2

Coefficient^2	$4a_1$-$8a_1$	$9a_1$	$1b_1$	$2b_1$	$1a_2$	$3b_2$-$4b_2$	$5b_2$	$6b_2$	$3b_1$	$2a_2$	$6b_1$
.0025M	10	2	2	2	2	4	2	1	-	-	-
.0000M	10	2	2	2	2	4	1	2	-	-	-
.0028M	10	2	2	2	-	4	2	1	2	-	-
.0000M	10	2	2	2	-	4	1	2	2	-	-
.0051M	10	2	2	1	2	4	2	1	1	-	-
.0002M	10	2	2	2	1	4	2	1	-	1	-
.0160M	10	1	2	1	2	4	2	2	-	1	-
.7440M	10	1	2	2	1	4	2	2	1	-	-
.0132M	10	1	2	2	1	4	2	2	-	-	1
.0076M	10	1	2	1	1	4	2	2	2	-	-
.0561	10	2	1	2	2	4	2	1	1	-	-

Table 44a 1,2,3 Triazole 1^2B_1

Coefficient^2	$4a_1$-$9a_1$	$1b_1$	$2b_1$	$3b_2$-$6b_2$	$1a_2$	$3b_1$	$2a_2$
.0025M	12	1	2	8	2	-	-
.0006M	12	-	2	8	2	1	-
.8481M	12	2	1	8	2	-	-
.0002M	12	1	2	8	-	2	-
.0000M	12	2	-	8	2	1	-
.0000M	12	2	2	8	-	1	-
.0092M	12	2	1	8	-	2	-
.0112M	12	1	1	8	2	1	-
.0011M	12	1	2	8	1	-	1
.0062M	12	2	1	8	1	-	1

Table 44b 1,2,3 Triazole 2H 2^2B_1

Coefficient^2	$4a_1$-$9a_1$	$1b_1$	$2b_1$	$3b_2$-$6b_2$	$1a_2$	$3b_1$	$2a_2$
.5819M	12	1	2	8	2	-	-
.0002M	12	-	2	8	2	1	-
.0022M	12	2	1	8	2	-	-
.0094M	12	1	2	8	-	2	-
.1375M	12	2	-	8	2	1	-
.1124M	12	2	2	8	-	1	-
.0014M	12	2	1	8	-	2	-
.0017M	12	1	1	8	2	1	-
.0087M	12	1	2	8	1	-	1
.0139M	12	2	1	8	1	-	1

Table 44c 1,2,3 Triazole 2H 3^2B_1

Coefficient^2	$4a_1$-$9a_1$	$1b_1$	$2b_1$	$3b_2$-$6b_2$	$1a_2$	$3b_1$	$2a_2$
.0009M	12	1	2	8	2	-	-
.0401M	12	-	2	8	2	1	-
.0013M	12	2	1	8	2	-	-
.0030M	12	1	2	8	-	2	-
.3037M	12	2	-	8	2	1	-
.3982M	12	2	2	8	-	1	-
.0069M	12	2	1	8	-	2	-
.0106M	12	1	1	8	2	1	-
.0160M	12	1	2	8	1	-	1
.0590M	12	2	1	8	1	-	1

Table 45a 1,2,3 Triazole 2H 1^2A_1

Coefficient^2	$4a_1$-$6a_1$	$7a_1$	$8a_1$	$9a_1$	$1b_1$	$2b_1$	$1a_2$	$3b_2$-$5b_2$	$6b_2$	$3b_1$	$2a_2$
.8155M	6	2	2	1	2	2	2	6	2	-	-
.0041M	6	1	2	2	2	2	2	6	2	-	-
.0013M	6	2	1	2	2	2	2	6	2	-	-
.0000M	6	2	1	2	2	2	-	6	2	2	-
.0009M	6	2	2	1	2	1	2	6	2	1	-
.0043M	6	2	2	1	2	2	1	6	2	-	1
.0009M	6	1	2	2	2	1	2	6	2	1	-
.0001M	6	2	1	2	2	1	2	6	2	1	-
.0274M	6	2	2	2	2	2	1	6	1	1	-
.0000M	6	2	2	2	2	1	1	6	1	2	-

Table 45b 1,2,3 Triazole 2H 2^2A_1

Coefficient^2	$4a_1$-$6a_1$	$7a_1$	$8a_1$	$9a_1$	$1b_1$	$2b_1$	$1a_2$	$3b_2$-$5b_2$	$6b_2$	$3b_1$	$2a_2$
.0026M	6	2	2	1	2	2	2	6	2	-	-
.0053M	6	1	2	2	2	2	2	6	2	-	-
.8323M	6	2	1	2	2	2	2	6	2	-	-
.0085M	6	2	1	2	2	2	-	6	2	2	-
.0019M	6	2	2	1	2	1	2	6	2	1	-
.0027M	6	2	2	1	2	2	1	6	2	-	1
.0035M	6	1	2	2	2	1	2	6	2	1	-
.0011M	6	2	1	2	2	1	2	6	2	1	-
.0019M	6	2	2	2	2	2	1	6	1	1	-
.0000M	6	2	2	2	2	1	1	6	1	2	-

Table 45c 1,2,3 Triazole 2H 3^2A_1

Coefficient^2	$4a_1$-$6a_1$	$7a_1$	$8a_1$	$9a_1$	$1b_1$	$2b_1$	$1a_2$	$3b_2$-$5b_2$	$6b_2$	$3b_1$	$2a_2$
.0067M	6	2	2	1	2	2	2	6	2	-	-
.3162M	6	1	2	2	2	2	2	6	2	-	-
.0058M	6	2	1	2	2	2	2	6	2	-	-
.0002M	6	2	1	2	2	2	-	6	2	2	-
.3711M	6	2	2	1	2	1	2	6	2	1	-
.0095M	6	2	2	1	2	2	1	6	2	-	1
.0087M	6	1	2	2	2	1	2	6	2	1	-
.0080M	6	2	1	2	2	1	2	6	2	1	-
.1157M	6	2	2	2	2	2	1	6	1	1	-
.0146M	6	2	2	2	2	1	1	6	1	2	-

Table 45d 1,2,3 Triazole 2H 4^2A_1

Coefficient^2	$4a_1$-$6a_1$	$7a_1$	$8a_1$	$9a_1$	$1b_1$	$2b_1$	$1a_2$	$3b_2$-$5b_2$	$6b_2$	$3b_1$	$2a_2$
.0043M	6	2	2	1	2	2	2	6	2	-	-
.3271M	6	1	2	2	2	2	2	6	2	-	-
.0040M	6	2	1	2	2	2	2	6	2	-	-
.0002M	6	2	1	2	2	2	-	6	2	2	-
.4282M	6	2	2	1	2	1	2	6	2	1	-
.0095M	6	2	2	1	2	2	1	6	2	-	1
.0085M	6	1	2	2	2	1	2	6	2	1	-
.0028M	6	2	1	2	2	1	2	6	2	1	-
.0349M	6	2	2	2	2	2	1	6	1	1	-
.0154M	6	2	2	2	2	1	1	6	1	2	-

Table 46a 1,2,3 Triazole 1^2A_2

Coefficient^2	$4a_1$-$9a_1$	$1b_1$	$2b_1$	$1a_2$	$3b_2$-$6b_2$	$2a_2$	$3b_1$	$6b_1$
.8434M	12	2	2	1	8	-	-	-
.0080M	12	2	2	-	8	1	-	-
.0054M	12	2	-	2	8	1	-	-
.0147M	12	1	2	1	8	-	1	-
.0037M	12	2	1	1	8	-	1	-
.0004M	12	1	1	1	8	-	2	-
.0025M	12	2	1	-	8	1	1	-

Table 46b 1,2,3 Triazole 2^2A_2

Coefficient^2	$4a_1$-$9a_1$	$1b_1$	$2b_1$	$1a_2$	$3b_2$-$6b_2$	$2a_2$	$3b_1$	$6b_1$
.0083M	12	2	2	1	8	-	-	-
.0006M	12	2	2	-	8	1	-	-
.0208M	12	2	-	2	8	1	-	-
.0159M	12	1	2	1	8	-	1	-
.7746M	12	2	1	1	8	-	1	-
.0210M	12	1	1	1	8	-	2	-
.0165M	12	2	1	-	8	1	1	-
.0114M	12	2	1	1	8	-	-	1

Table 46c 1,2,3 Triazole 2H 3^2A_1

Coefficient^2	$4a_1$-$9a_1$	$1b_1$	$2b_1$	$1a_2$	$3b_2$-$6b_2$	$2a_2$	$3b_1$	$6b_1$
.0025M	12	2	2	1	8	-	-	-
.0788M	12	2	2	-	8	1	-	-
.0040M	12	2	-	2	8	1	-	-
.0051M	12	1	2	1	8	-	1	-
.6864M	12	2	1	1	8	-	1	-
.0278M	12	1	1	1	8	-	2	-
.0131M	12	2	1	-	8	1	1	-

Table 47 Assignment of the PE Spectrum of 1,2,3 Triazole

Vertical IP/eV [14]	State	Table No.
10.06	1^2B_1	44a
10.9	1^2A_2	46a
	1^2B_2	43a
12.1	1^2A_1	45a
15.0	$\#2^2B_1$	44b
	$\#2^2B_2$	43b
	3^2B_2	43c
15.6	$\#2^2A_1$	45b
	$\#2^2A_2$	46b
	3^2A_1	45c
	$\#4^2B_2$	43d
	$\#3^2B_1$	44c
17.6	$\#4^2A_1$	45d
	$\#3^2A_1$	46c

\# indicates shake up state

Table 48 SCF Eigenvalues for 2H Tetrazole

Eigenvalue/eV	Orbital	Bond Centres
-23.68	10a'	N4N1N2N3
-21.08	11a'	N1N2N3C5N4
-18.17	1a"	N1N2N3C5N4
-18.08	12a'	H1N1N4C5H5
-15.71	13a'	LP N4 + N2N3
-13.92	14a'	LP N4 - N2N3
-13.24	15a'	LP N4,N2,N3
-12.48	2a"	N1N4 - C5N3N2
-11.69	3a"	N1N2 -N3C5N4

Table 49 Calculated Ionisation Potentials for 1H Tetrazole

State	No. of reference Configurations	Excitation Process	coefficient^2	CI energy/a.u.	IP/eV
$1^2A'$	3M3R	-15a'	.8476	-256.6370	10.40
$2^2A'$	3M3R	-14a'	.8471	-256.6089	11.16
$3^2A'$	3M3R	-13a'	.8341	-256.5426	12.97
$1^2A"$	3M3R	-3a"	.8631	-256.6095	11.15
$2^2A"$	3M3R	-2a"	.8548	-256.5818	11.90
$3^2A"$	3M3R	-1a"	.7403	-256.4338	15.93

Table 50 Summary of Results for 2H Tetrazole

No. of reference Configurations	State	Σcoefficient^2	Correction/ a.u.	C.I. Energy/ a.u.	I.P./eV
1M1R	GS X'A'	.8726	-.0497	-257.0567	-
4M1R	GS X'A'	.8809	-.0450	-257.0645	-
3M3R	1^2A"	.8503	-.0619	-256.6624	10.94
3M3R	2^2A"	.8423	-.0652	-256.6369	11.63
3M3R	3^2A"	.7401	-.1175	-256.5188	14.85
5M4R	1^2A'	.8377	-.0730	-256.6636	10.91
5M4R	2^2A'	.8339	-.0740	-256.6271	11.90
5M4R	3^2A'	.8184	-.0821	-256.5749	13.32
5M4R	4^2A'	.8454	-.0671	-256.4560	16.55
9M5R	1^2A'	.8503	-.0637	-256.6548	11.15
9M5R	2^2A'	.8303	-.0755	-256.6388	11.58
9M5R	3^2A'	.8387	-.0709	-256.5881	12.96
9M5R	4^2A'	.8132	-.0859	-256.5076	15.15
9M5R	5^2A'	.8069	-.0858	-256.5044	15.24
7M4R	1^2A'	.8478	-.0655	-256.6565	11.10
7M4R	2^2A'	.8328	-.0738	-256.6335	11.72
7M4R	3^2A'	.8337	-.0741	-256.5882	12.96
7M4R	4^2A'	.8089	-.0844	-256.4997	15.37
9M5R	1^2A"	.8558	-.0589	-256.6610	10.98
9M5R	2^2A"	.8561	-.0591	-256.6390	11.58
9M5R	3^2A"	.8443	-.0657	-256.5337	14.44
9M5R	4^2A"	.8039	-.0849	-256.4563	16.55
9M5R	5^2A"	.7033	-.1275	-256.4568	16.53
7M5R	1^2A"	.8509	-.0615	-256.6637	10.90
7M5R	2^2A"	.8437	-.0648	-256.6385	11.59
7M5R	3^2A"	.8296	-.0704	-256.5240	14.71
7M5R	4^2A"	.7932	-.0878	-256.4432	16.90
7M5R	5^2A"	.7611	-.1022	-256.4034	17.99

(Cont'd)...

Table 50 (Cont'd)

No. of reference configurations	State	$\Sigma_{coefficient^2}$	Correction/ a.u.	C.I. Energy/ a.u.	I.P./eV
11M5R	$1^2A''$	.8576	-.0580	-256.6590	11.03
11M5R	$2^2A''$	.8650	-.0548	-256.6457	11.39
11M5R	$3^2A''$	.8457	-.0634	-256.5208	14.79
11M5R	$4^2A''$	.8097	-.0860	-256.4812	15.87
11M5R	$5^2A''$	.7852	-.0969	-256.4509	16.69

Table 51 Calculated Ionisation Potentials for 2H Tetrazole

State	Excitation Process	I.P./eV	Table No.
$1^2A''$	-3a"	11.03	54a
$1^2A'$	-15a'	11.15	53a
$2^2A''$	-2a"	11.39	54b
$2^2A'$	-14a	11.58	53b
$3^2A'$	-13a'	12.96	53c
$3^2A''$	-1a" + [-2a" + (3a" → 4a")]	14.79	54c
$4^2A'$	-15a' + (2a" → 3a")	15.15	53d
$5^2A'$	-12a' + [-14a' + (3a" → 4a")] + [-14a' + (2a" → 4a")]	15.24	53e
$4^2A''$	[-3a" + (3a" → 4a")]	15.87	54d
$5^2A''$	[-3a" + (3a" → 5a")] + [-2a" + (2a" → 4a")]	16.69	54e

Table 52 Tetrazole Ground State X^1A'

Coefficient^2	6a'-10a'	11a'	12a'	13a'	14a'	15a'	1a"	2a"	3a"	4a"	5a"
.8701M	10	2	2	2	2	2	2	2	2	-	-
.0047M	10	2	2	2	2	2	2	-	2	2	-
.0038M	10	2	2	2	2	2	2	2	-	2	-
.0023M	10	2	2	2	2	2	2	2	-	-	2

Table 53a Tetrazole $1^2A'$

Coefficient[2]	6a'-10a'	11a'	12a'	13a'	14a'	15a'	1a"	2a"	3a"	4a"	5a"
.8232M	10	2	2	2	2	1	2	2	2	-	-
.0000M	10	2	1	2	2	2	2	2	2	-	-
.0002M	10	2	2	1	2	2	2	2	2	-	-
.0000M	10	2	2	2	1	2	2	2	2	-	-
.0097M	10	2	2	2	2	1	2	1	2	-	1
.0111M	10	2	2	2	2	1	2	2	1	1	-
.0009M	10	2	2	2	2	1	2	1	1	2	-
.0038M	10	2	2	2	1	2	2	1	2	1	-
.0013M	10	2	2	2	1	2	2	2	1	1	-

Table 53b Tetrazole $2^2A'$

Coefficient[2]	6a'-10a'	11a'	12a'	13a'	14a'	15a'	1a"	2a"	3a"	4a"	5a"
.0000M	10	2	2	2	2	1	2	2	2	-	-
.0000M	10	2	1	2	2	2	2	2	2	-	-
.0026M	10	2	2	1	2	2	2	2	2	-	-
.8245M	10	2	2	2	1	2	2	2	2	-	-
.0001M	10	2	2	2	2	1	2	1	2	-	1
.0024M	10	2	2	2	2	1	2	2	1	1	-
.0000M	10	2	2	2	2	1	2	1	1	2	-
.0001M	10	2	2	2	1	2	2	1	2	1	-
.0003M	10	2	2	2	1	2	2	2	1	1	-

Table 53c Tetrazole $3^2A'$

Coefficient[2]	6a'-10a'	11a'	12a'	13a'	14a'	15a'	1a"	2a"	3a"	4a"	5a"
.0002M	10	2	2	2	2	1	2	2	2	-	-
.0033M	10	2	1	2	2	2	2	2	2	-	-
.7984M	10	2	2	1	2	2	2	2	2	-	-
.0032M	10	2	2	2	1	2	2	2	2	-	-
.0070M	10	2	2	2	2	1	2	1	2	-	1
.0010M	10	2	2	2	2	1	2	2	1	1	-
.0001M	10	2	2	2	2	1	2	1	1	2	-
.0077M	10	2	2	2	1	2	2	1	2	1	-
.0177M	10	2	2	2	1	2	2	2	1	1	-

Table 53d Tetrazole $4^2A'$

Coefficient[2]	6a'-10a'	11a'	12a'	13a'	14a'	15a'	1a"	2a"	3a"	4a"	5a"
.0003M	10	2	2	2	2	1	2	2	2	-	-
.0000M	10	2	1	2	2	2	2	2	2	-	-
.0000M	10	2	2	1	2	2	2	2	2	-	-
.0008M	10	2	2	2	1	2	2	2	2	-	-
.0016M	10	2	2	2	2	1	2	1	2	-	1
.7787M	10	2	2	2	2	1	2	2	1	1	-
.0181M	10	2	2	2	2	1	2	1	1	2	-
.0000M	10	2	2	2	1	2	2	1	2	1	-
.0073M	10	2	2	2	1	2	2	2	1	1	-
.0156M	10	2	2	2	2	1	2	1	1	1	1

Table 53e Tetrazole $5^2A'$

Coefficient[2]	6a'-10a'	11a'	12a'	13a'	14a'	15a'	1a"	2a"	13a"	4a"	5a"
.0000M	10	2	2	2	2	1	2	2	2	-	-
.1219M	10	2	1	2	2	2	2	2	2	-	-
.0023M	10	2	2	1	2	2	2	2	2	-	-
.0000M	10	2	2	2	1	2	2	2	2	-	-
.0008M	10	2	2	2	2	1	2	1	2	-	1
.0069M	10	2	2	2	2	1	2	2	1	1	-
.0051M	10	2	2	2	2	1	2	1	1	2	-
.2523M	10	2	2	2	1	2	2	1	2	1	-
.4238M	10	2	2	2	1	2	2	2	1	1	-
.0104	10	2	2	2	1	2	2	1	2	-	1

Table 54a Tetrazole $1^2A"$

Coefficient[2]	6a'-10a'	11a'	12a'	13a'	14a'	15a'	1a"	2a"	3a"	4a"	5a"
.0795M	10	2	2	2	2	2	2	2	1	-	-
.0020M	10	2	2	2	2	2	1	2	2	-	-
.0490M	10	2	2	2	2	2	2	1	2	-	-
.0001M	10	2	2	2	2	2	2	2	-	1	-
.0032M	10	2	2	2	2	2	2	2	-	-	1
.0001M	10	2	2	2	2	2	2	-	2	1	-
.0044M	10	2	2	2	2	2	2	-	2	-	1
.0013M	10	2	2	2	2	2	2	1	-	2	-
.0003M	10	2	2	2	2	2	2	1	-	-	2
.0017M	10	2	2	2	2	2	2	1	1	-	1
.0110	10	2	2	2	2	2	1	1	2	1	-

Table 54b Tetrazole $2^2A''$

Coefficient[2]	6a'-10a'	11a'	12a'	13a'	14a'	15a'	1a"	2a"	3a"	4a"	5a"
.0498M	10	2	2	2	2	2	2	2	1	-	-
.0004M	10	2	2	2	2	2	1	2	2	-	-
.7792M	10	2	2	2	2	2	2	1	2	-	-
.0018M	10	2	2	2	2	2	2	2	-	1	-
.0007M	10	2	2	2	2	2	2	2	-	-	1
.0041M	10	2	2	2	2	2	2	-	2	1	-
.0015M	10	2	2	2	2	2	2	-	2	-	1
.0058M	10	2	2	2	2	2	2	1	-	2	-
.0039M	10	2	2	2	2	2	2	1	-	-	2
.0035M	10	2	2	2	2	2	2	1	1	1	-
.0142M	10	2	2	2	2	2	2	1	1	-	1
.0151	10	2	2	2	2	2	1	2	1	1	-

Table 54c Tetrazole $3^2A''$

Coefficient[2]	6a'-10a'	11a'	12a'	13a'	14a'	15a'	1a"	2a"	3a"	4a"	5a"
.0019M	10	2	2	2	2	2	2	2	1	-	-
.6219M	10	2	2	2	2	2	1	2	2	-	-
.0002M	10	2	2	2	2	2	2	1	2	-	-
.0017M	10	2	2	2	2	2	2	2	-	1	-
.0172M	10	2	2	2	2	2	2	2	-	-	1
.0012M	10	2	2	2	2	2	2	-	2	1	-
.0171M	10	2	2	2	2	2	2	-	2	-	1
.0005M	10	2	2	2	2	2	2	1	-	2	1
.0007M	10	2	2	2	2	2	2	1	-	-	2
.1804M	10	2	2	2	2	2	2	1	1	1	-
.0029M	10	2	2	2	2	2	2	1	1	-	1

Table 54d Tetrazole $4^2A''$

Coefficient[2]	6a'-10a'	11a'	12a'	13a'	14a'	15a'	1a"	2a"	3a"	4a"	5a"
.0051M	10	2	2	2	2	2	2	2	1	-	-
.0018M	10	2	2	2	2	2	1	2	2	-	-
.0051M	10	2	2	2	2	2	2	1	2	-	-
.6944M	10	2	2	2	2	2	2	2	-	1	-
.0260M	10	2	2	2	2	2	2	2	-	-	1
.0384M	10	2	2	2	2	2	2	-	2	1	-
.0001M	10	2	2	2	2	2	2	-	2	-	1
.0041M	10	2	2	2	2	2	2	1	-	2	1
.0081M	10	2	2	2	2	2	2	1	-	-	2
.0164M	10	2	2	2	2	2	2	1	1	1	-
.0155M	10	2	2	2	2	2	2	1	1	-	1
.0126	10	2	2	2	2	2	1	1	1	2	-

Table 54e Tetrazole $5^2A''$

Coefficient[2]	6a'-10a'	11a'	12a'	13a'	14a'	15a'	1a"	2a"	3a"	4a"	5a"
.0023M	10	2	2	2	2	2	2	2	1	-	-
.0000M	10	2	2	2	2	2	1	2	2	-	-
.0064M	10	2	2	2	2	2	2	1	2	-	-
.0013M	10	2	2	2	2	2	2	2	-	1	-
.4850M	10	2	2	2	2	2	2	2	-	-	1
.1154M	10	2	2	2	2	2	2	-	2	1	-
.0254M	10	2	2	2	2	2	2	-	2	-	1
.0081M	10	2	2	2	2	2	2	1	-	2	1
.0080M	10	2	2	2	2	2	2	1	-	-	2
.0131M	10	2	2	2	2	2	2	1	1	1	-
.0021M	10	2	2	2	2	2	2	1	1	-	1
.0143	10	2	2	2	2	2	1	2	1	-	1
.0101	10	2	2	2	2	2	2	1	-	1	1
.0215	10	2	2	2	2	2	1	1	1	1	1

Table 55 Theoretical Assignment for the PE spectrum of Tetrazole

Vertical I.P./eV	State	Table No.
11.3	$1^2A''$	54a
	$1^2A'$	53a
12.1	$2^2A''$	54b
	$2^2A'$	53b
13.63	$3^2A'$	53c
16.1	$3^2A''$	54c
	$4^2A'$	53d
	$5^2A'$	53e
	$4^2A''$	54d
	$5^2A''$	54e

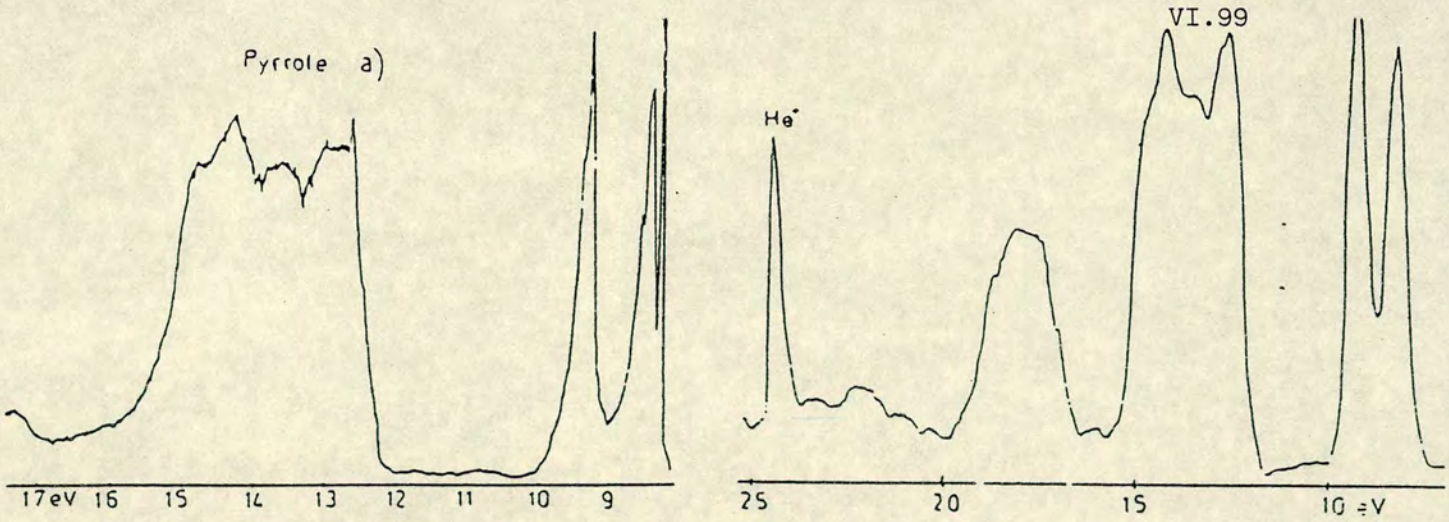

FIGURE (1) PE SPECTRUM OF PYRROLE

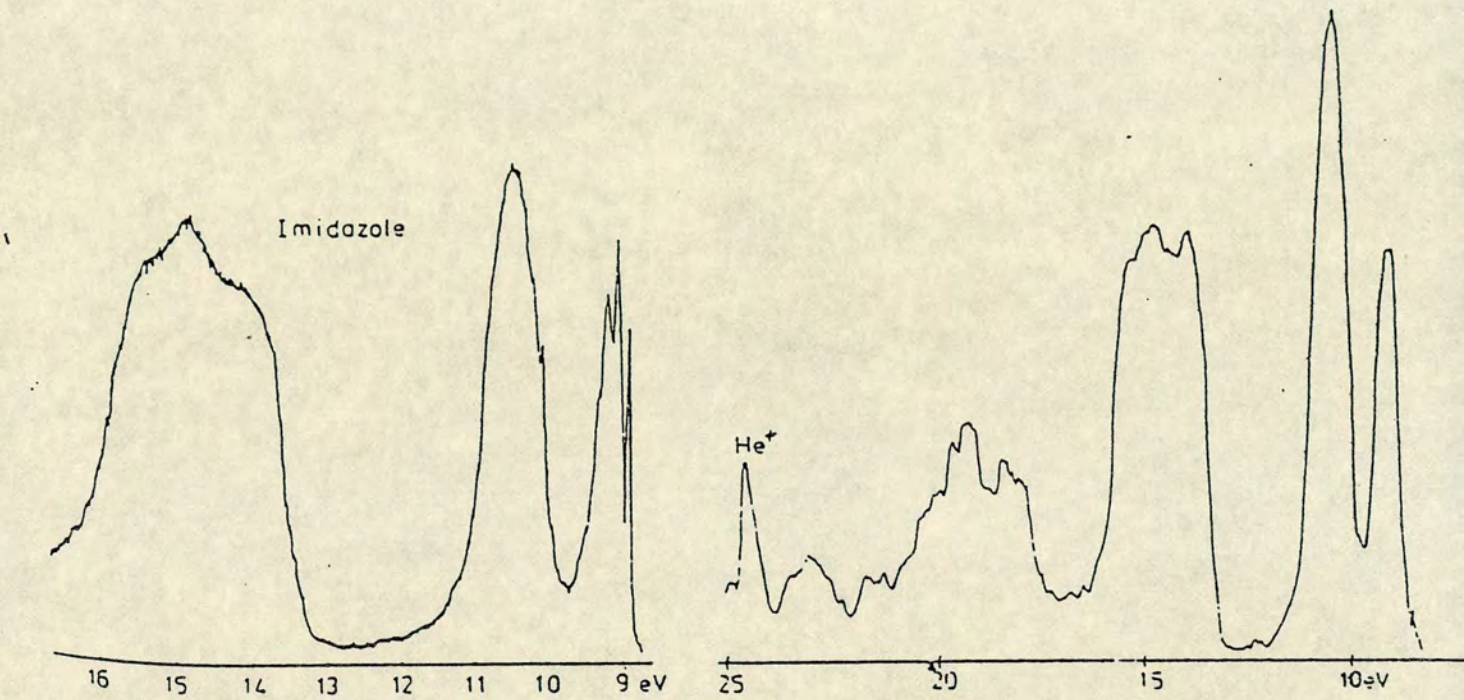

FIGURE (2) PE SPECTRUM OF IMIDAZOLE

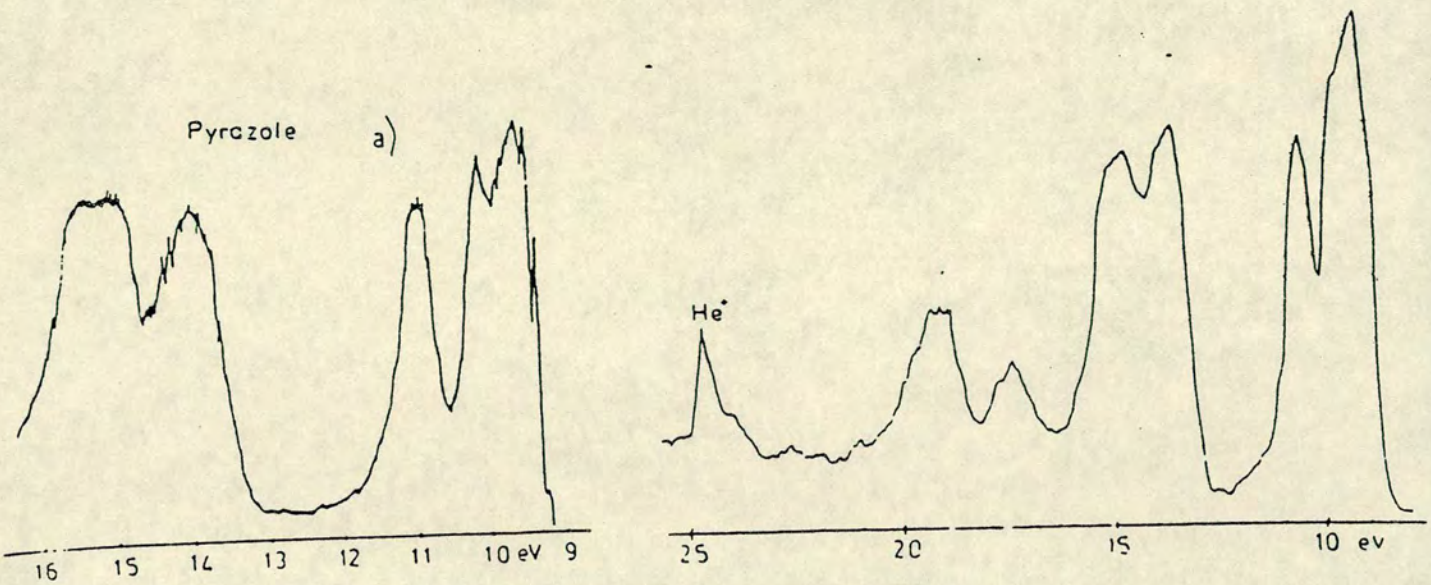

FIGURE (3) PE SPECTRUM OF PYRAZOLE

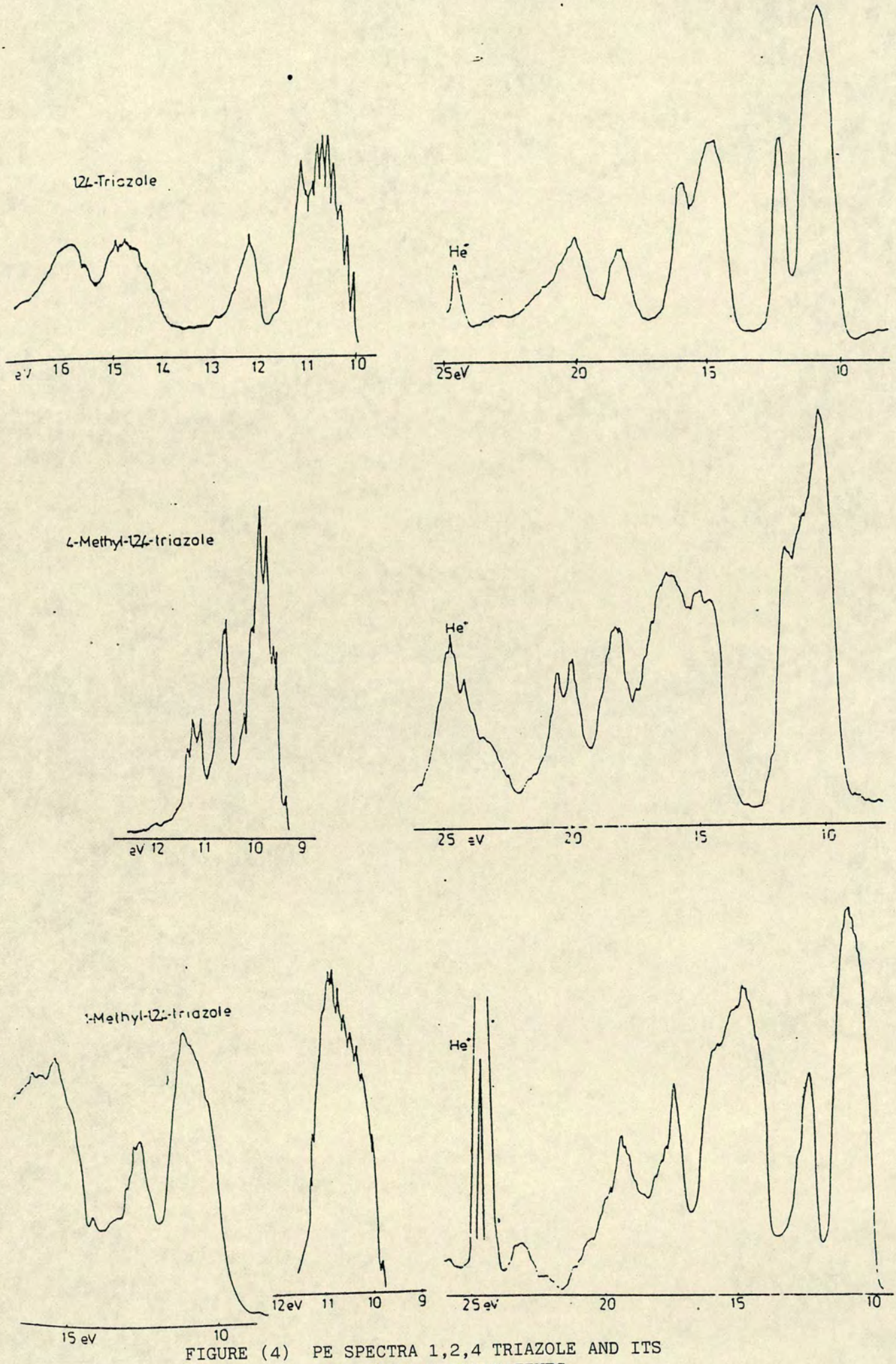

FIGURE (4) PE SPECTRA 1,2,4 TRIAZOLE AND ITS
1- AND 4-METHYL DERIVATIVES

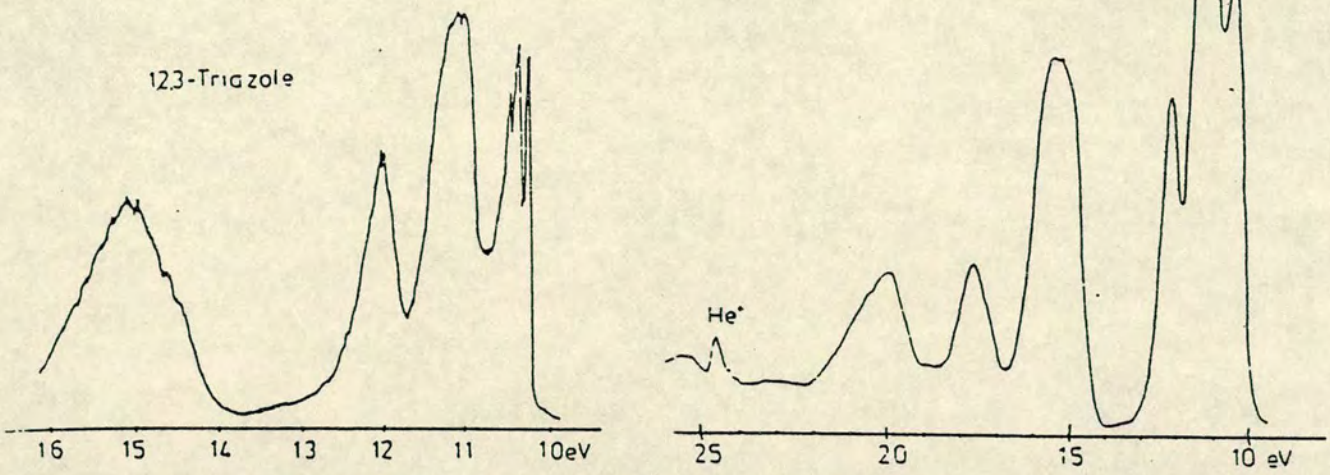

FIGURE (5) PE SPECTRUM OF 1,2,3 TRIAZOLE

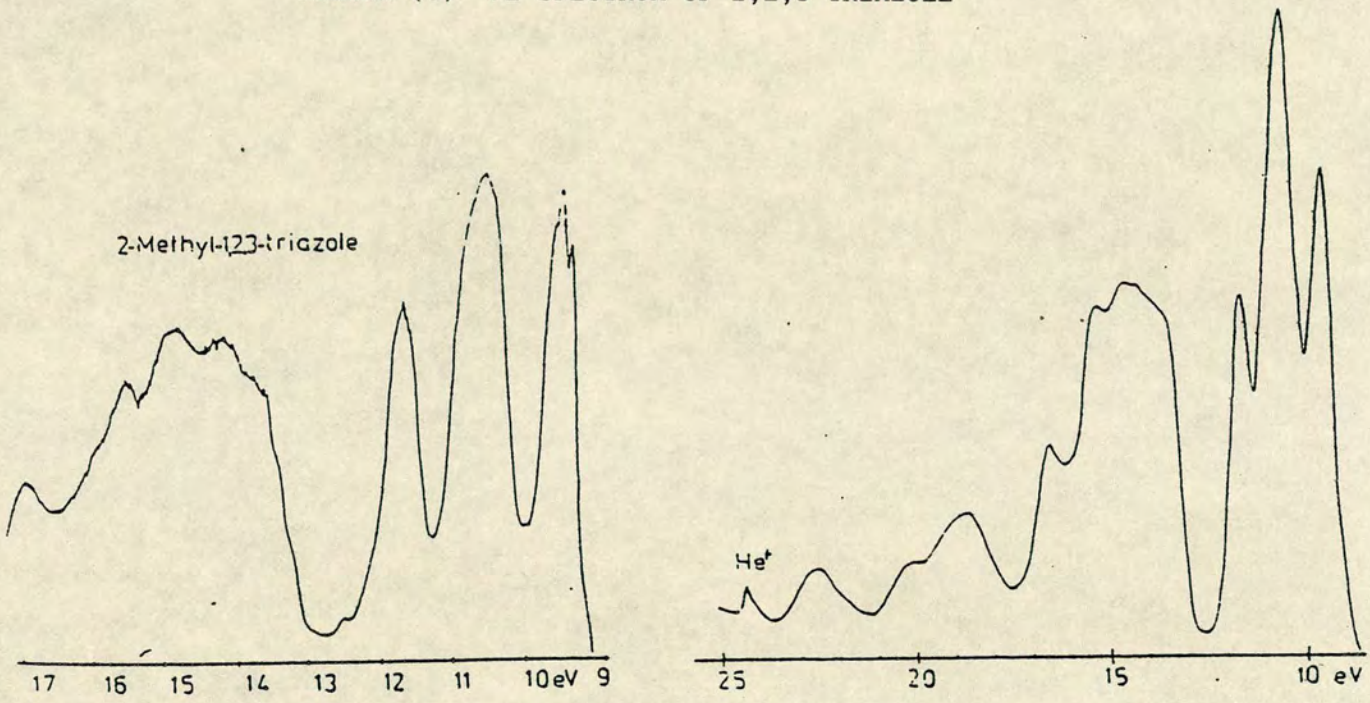

FIGURE (6) PE SPECTRUM OF 2 METHYL 1-1,2,3 TRIAZOLE

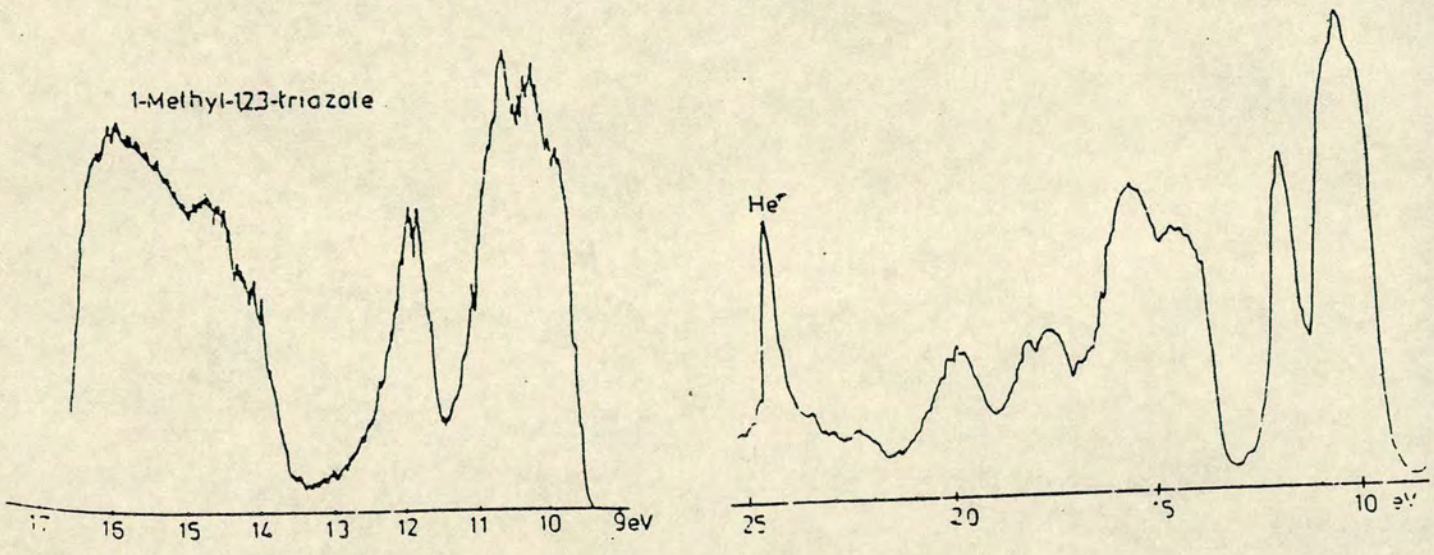

FIGURE (7) PE SPECTRUM OF 1-METHYL-1,2,3 TRIAZOLE

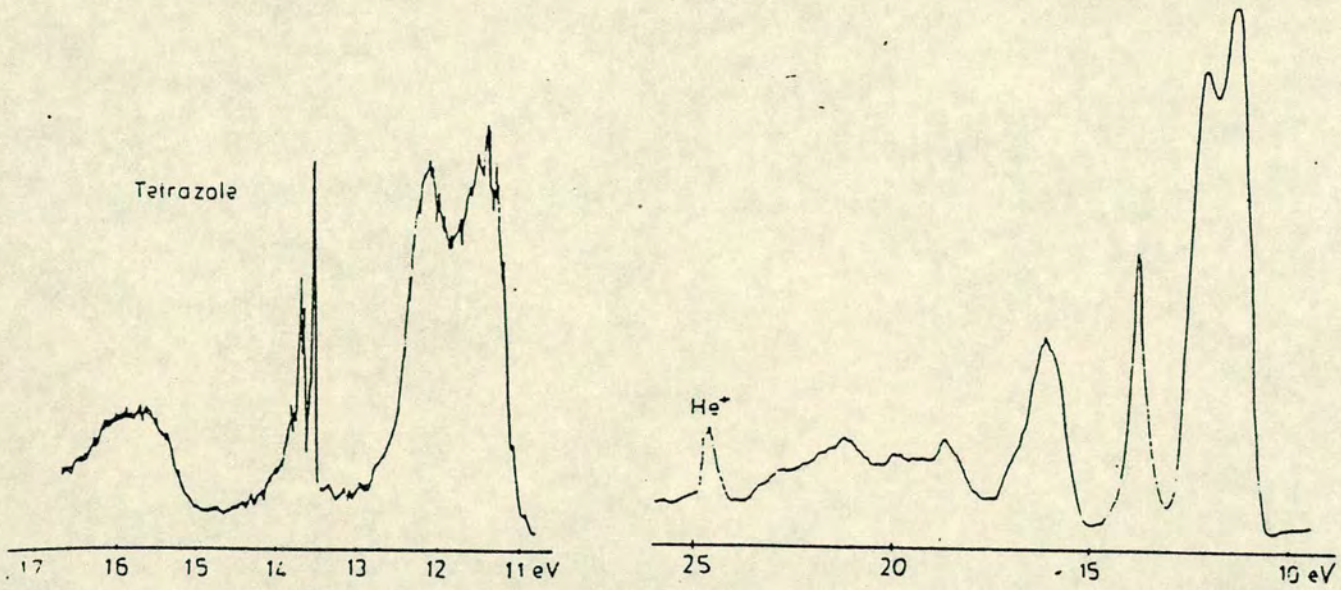

FIGURE (8) PE SPECTRUM OF TETRAZOLE

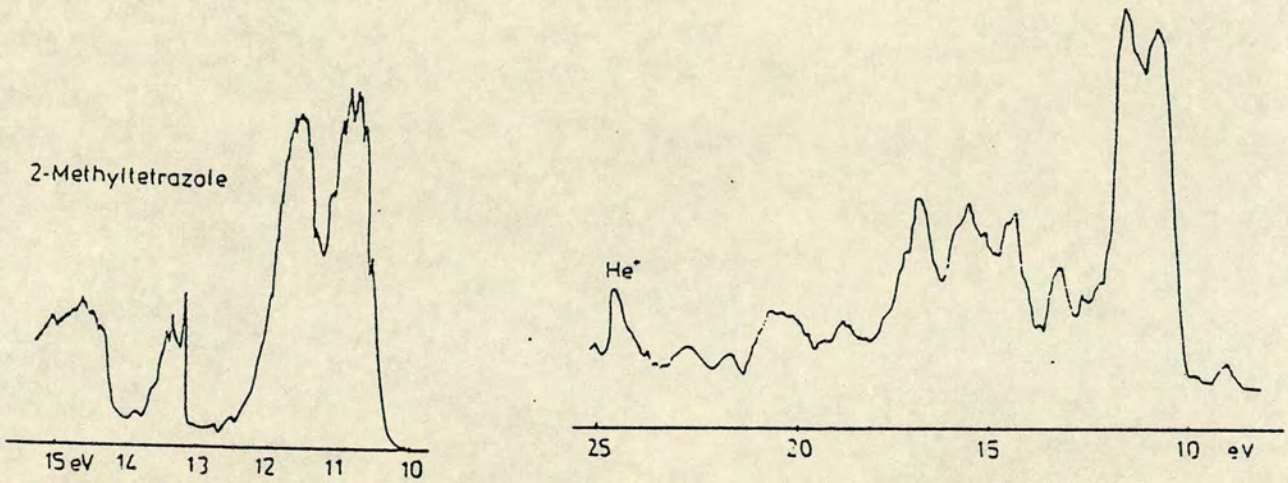

FIGURE (9) PE SPECTRUM OF 2 METHYL TETRAZOLE

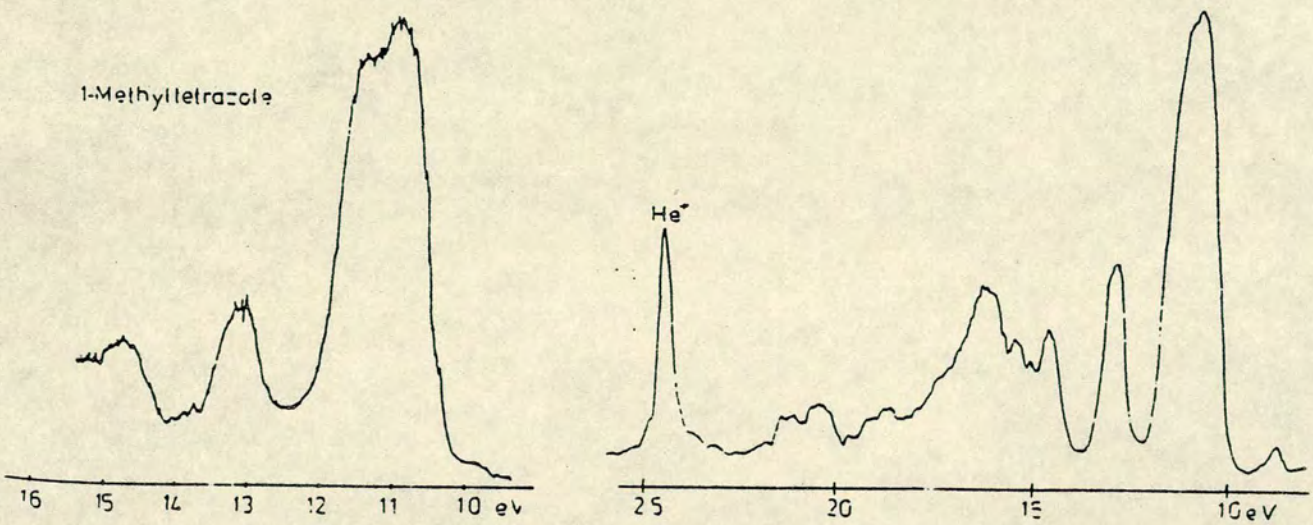

FIGURE (10) PE SPECTRUM OF 1 METHYL TETRAZOLE